

JOM

**OLYMPIC
MATERIALS:
Faster,
Higher,
Stronger**

A publication of The Minerals, Metals & Materials Society

FEBRUARY 2010
www.tms.org/jom.html



MECHANICAL PROPERTIES

- Aluminum
- Nanocomposite Materials
- Bulk Metallic Glasses

FRAY INTERNATIONAL SYMPOSIUM



Prof. Derek J. Fray

On Metals and Materials Processing in a Clean Environment :

- Principles
- Technologies
- Industrial Practice
- Environment/Health, Energy & Policies

Incorporating 3 International Symposiums:

- Advanced Sustainable Iron and Steel Making
- Sustainable Non-Ferrous Smelting in 21st Century
- Molten Salts and Ionic Liquids 2011

**Hilton Cancun Golf & Spa Resort
CANCUN, MEXICO**

4 - 7 December 2011

**Industry
driven and
organized**

**More
than 160
Sponsors
worldwide**

**Abstracts
limit date:
October 1st
2010**

This symposium honors the very distinguished work and lifetime achievements of Professor Fray. He is a well known figure in metals and materials extraction and processing world for its deeply original impact in several fields such as non-ferrous, ferrous and recycling, in various processing routes such as pyrometallurgy (sulphide and metallic smelting), hydro-metallurgy and electro-chemistry and in several investigating techniques such as experimental measurements and physical modelling. He is Fellow of some of the most prestigious professional organizations, author of almost 400 scientific papers and inventor of approximately 179 patents arising from 62 families of patents. Reflecting his rich activity the symposium will cover the equally important areas of principles, technologies and industrial practice with special emphasis on a globally sought clean environment of 21 century.



Florian Kongoli
Chair / FLOGEN
Canada / USA



Maurits Van Camp
Co-Chair / UMICORE
Belgium



R. Vasant Kumar
Co-Chair / U. Cambridge
United Kingdom



Hongmin Zhu
Co-Chair / USTB
China



S. Komar Kawatra
Co-Chair / MTU
USA



Mario Sanchez
Co-Chair / U. Concepcion
Chile



M. Gaune-Escard
Co-Chair / Polytechnique
France



George Z. Chen
Co-chair / U. Nottingham
United Kingdom

**Web site: www.flogen.com/FraySymposium Contact information: Dr. Florian Kongoli (fkongoli@flogen.com)
Phone: 1-514-344-8786 ext. 220 Toll-Free (N. America): 1-877-2-FLOGEN Fax: 1-514-344-0361**

ALUMINUM

- 23:** Aluminum Recycling—An Integrated, Industrywide Approach: Subodh K. Das, John A.S. Green, J. Gilbert Kaufman, Daryoush Emadi, and M. Mahfoud
- 27:** Aluminum Industry and Climate Change—Assessment and Responses: Subodh K. Das and John A.S. Green
- 32:** Adaptive Control of Feed in the Hall–Héroult Cell using a Neural Network: K.D. Boadu and F.K. Omani
- 37:** The Hot Formability of an Al–Cu–Mg–Fe–Ni Forging Disk: M. Aghaie-Khafri and A. Zargaran
- 42:** The Use of Friction Stir Welding for Manufacturing Small-scale Structures: T. Hirata and K. Higashi

NANOCOMPOSITE MATERIALS

- 49:** Nanocomposite Materials—Leading the Way in Novel Materials Design: Jonathan E. Spowart
- 50:** Fatigue and Fracture Toughness of Epoxy Nanocomposites: I. Srivastava and N. Koratkar

- 58:** The Current Activated Pressure Assisted Densification Technique for Producing Nanocrystalline Materials: J.E. Alaniz, J.R. Morales, and J.E. Garay

- 63:** Nanostructured Metal Composites Reinforced with Fullerenes: Francisco C. Robles-Hernández and H.A. Calderon

BULK METALLIC GLASSES

- 69:** Bulk Metallic Glasses: Overcoming the Challenges to Widespread Applications: Peter K. Liaw, Gongyao Wang, and Judy Schneider
- 70:** Understanding the Properties and Structure of Metallic Glasses at the Atomic Level: T. Egami
- 76:** Mechanical Response of Metallic Glasses: Insights from In-situ High Energy X-ray Diffraction: Mihai Stoica, Jayanta Das, Jozef Bednarčík, Gang Wang, Gavin Vaughan, Wei Hua Wang, and Jürgen Eckert
- 83:** Amorphous Metals for Hard-tissue Prosthesis: Marios D. Demetriou, Aaron Wiest, Douglas C. Hofmann, William L. Johnson, Bo Han, Nikolaj Wolfson, Gongyao Wang, and Peter K. Liaw

- 93:** Metallic Glasses: Gaining Plasticity for Microsystems: Yong Yang, Jianchao Ye, Jian Lu, Yanfei Gao, and Peter K. Liaw

FEATURES

- 13:** TMS: An Essential Connection to an Evolving Profession: George T. “Rusty” Gray
- 14:** The Journal Talks with 2009 TMS President Ray Peterson
- 17:** Advanced Materials Are a Game Changer in the Winter Olympics: Lynne Robinson

ALSO IN THIS ISSUE

insert: *Member News*

insert: *The Young Leader*

insert: *Professional Preface*

2: In the Final Analysis

3: News & Update

99: Meetings Calendar

101: Materials Resource Center: Jobs, Consultants, Marketplace

104: End Notes: “Global Innovations Symposium Flies High at TMS 2010”

About the Cover: The 2010 Vancouver Winter Olympics will be occurring a little less than 200 kilometers from the 2010 TMS Annual Meeting in Seattle, Washington, February 14–18. In recognition of this, the *JOM* feature on page 17 looks at the role that advanced materials technology will play in several Olympic events. Skis are among the most complex pieces of winter sports equipment as demonstrated by Tim Kelley, U.S. Ski Team, as he trains slalom in Saas Fee, Switzerland. (Photo courtesy of Adam Perreault/U.S. Ski Team.)

Oftentimes, we look at commercials as unwanted breaks in wanted activities. Me, if I'm watching television, I want to see what Jack Bauer is about to do next, not a string of commercials for automobiles and big-box stores; if I'm listening to the radio, I want to hear Muse or U2, not a pitch for some lite beer; if I'm browsing the web, I don't want to be assaulted with Flash highjacks and pop-up windows for mortgage companies.

But, if I'm at a conference, I want to see the program *and* the sponsoring organizations. And, in many cases, I want to see the exhibition most of all. A conference exhibition is nothing like TV ads . . . it's like shopping at a specialty mall that exists at one place on earth for three days only and that is built just for you. For those of you reading this editorial while ensconced at the TMS 2010 Annual Meeting in Seattle, that mall is here, and those three days are now.

Exhibitions are a trove of potential delights: Will someone who I want to visit be hosting a booth? Will I see some neat stuff demonstrated? Will there be irresistible new widgets? Will there be food? Will there be gotta-have souvenirs? Most importantly, will I find something that is going to make my workplace more efficient, competitive, and (dare I hope?) fun?

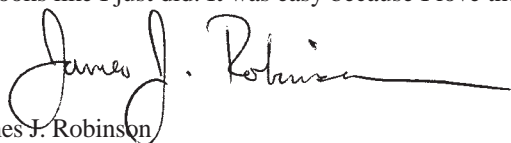
I'm ancient enough to recall the first TMS Annual Meeting Exhibition. It was held during 1987 in Denver and debuted in complement to festivities celebrating the centennial of the Hall-Héroult process. The exhibition was heavily light metals oriented back then and has tracked that way for two decades. In recent years, however, the profile has started to evolve, with aluminum still playing a prominent role, but with all points of the materials tetrahedron now taking on greater profile on the exhibit floor.

TMS's director of partner relations, Trudi Dunlap, leads our effort to make sure that there is something for everyone in the exhibition mall, err, hall. The effort includes input from the recently formed TMS Exhibitors Council—exhibitors who offer suggestions on how to improve and grow the event and provide a better experience for exhibitor and attendee alike. Trudi believes this effort important for many reasons, not the least of which is her astute observation that the exhibit hall is home to the suppliers that make the technologies presented in the session rooms and in journals like *JOM* possible. Exhibitors represent the infrastructural backbone of the community. She told me, for example, that . . .

- Software vendors Thermo-Calc (booth 100), CompuTherm (booth 428), and Sente (booth 414) produce and distribute tools used by computation materials science and engineering professionals as described in the October 2009 issue.
- Cutting-edge testing equipment manufacturers like Hysitron (booth 400), Agilent (booth 404), and CSM Instruments (booth 239) help scientists know how small volumes of materials deform and help everyone more easily understand the physical behavior of materials, which are common topics in any issue of the journal.
- Two of the top aluminum producers in the world, Rio Tinto Alcan (booth 309) and Hydro Aluminium Hycast (booth 608), participated in a special roundtable on Challenges for Sustainable Growth in the Aluminum Industry, as described in the November 2009 issue.

Good stuff and all true. . . . Just a minute. . . . I think that Trudi shared her thoughts in hopes that I might mention the exhibition in an upcoming editorial.

Looks like I just did. It was easy because I love the exhibition!



James J. Robinson
Publisher

JOM

184 Thorn Hill Road,
Warrendale, PA 15086, USA

Telephone: (724) 776-9000

Fax: (724) 776-3770

Web: www.tms.org/jom.html

E-Mail: jom@tms.org

PUBLISHER

James J. Robinson

FEBRUARY ADVISORS

Aluminum

Aluminum Committee

Pierre Homsí, Consultant,
retired from Rio Tinto Alcan

Nanocomposite Materials

Composite Materials Committee

Jonathan E. Spowart, U.S. Air Force
Research Laboratory

Bulk Metallic Glasses

Mechanical Behavior of Materials Committee

Peter K. Liaw, University of Tennessee

EDITORIAL STAFF

Maureen Byko, Editor

Cheryl M. Geier, Senior Graphic Designer

Shirley A. Litzinger, Production Editor

Elizabeth Rossi, Web Developer

PARTNER RELATIONS AND ADVERTISING STAFF

Trudi Dunlap, Director

Colleen Leary, Sales Representative

JOM (ISSN 1047-4838) is published monthly by Springer Sciences & Business Media, LLC (Springer) 233 Spring St., New York, NY 10013 in cooperation with The Minerals, Metals & Materials Society (TMS).

DISCLAIMER: The opinions and statements expressed in *JOM* are those of the authors only and are not necessarily those of TMS or the editorial staff. No confirmations or endorsements are intended or implied.

SUBSCRIPTIONS, ORDERS, AND OTHER FULFILLMENT INQUIRIES: *In the Americas*, contact Journals Customer Service, P.O. Box 2485, Secaucus, NJ 07096, USA; telephone (800) 777-4643 (in North America) or (212) 460-1500 (outside North America); e-mail journals-ny@springer.com. *Outside the Americas*, contact Journals Customer Service, Springer Distribution Center, Haberstr. 7, 69126 Heidelberg, Germany; telephone 49-6221-345-4303; e-mail subscriptions@springer.com.

TMS MEMBERS: Access this and back issues of *JOM* on-line at no charge via members.tms.org

POSTMASTER: Send address changes to: *JOM*, Springer, 233 Spring Street, New York, NY 10013, USA. Periodicals postage paid at New York, NY, and additional mailing offices.

12 Teams Step Up to the 2010 Materials Bowl Challenge

In a test of materials science knowledge and competitive resolve, 12 student teams are slated to participate in the TMS 2010 Materials Bowl, sponsored by Alcoa, on Sunday, February 14 at the TMS 2010 Annual Meeting. Three intense rounds of questions will focus on such broad topics as Energy Materials, Materials and Society, TMS and JOM, Seattle's Best (materials questions related to the TMS 2010 Annual Meeting city), Recycle Bin (questions from previous Materials Bowls), and Potpourri. In addition to bragging rights, the winning team will receive a cash prize and take home the traveling Materials Bowl Trophy. The final championship round, which will take place at 8:30 p.m. on February 14, will also feature the unveiling of the winner of the TMS, MSE & Me video contest.

TMS members are welcomed and encouraged to take a few moments to cheer on this year's Materials Bowl contestants, representing the following schools: Boise State University; California Polytechnic State University; Florida International University; Georgia Institute of Technology; Indian Institute of Technology, Kanpur; Iowa State University; University of British Columbia; University of Idaho; University of Minnesota, Twin Cities; University of Tennessee; University of Washington; Washington State University.

TMS2010

139th Annual Meeting & Exhibition



2010 TMS HONORS AND AWARDS RECIPIENTS

TMS and its divisions honor outstanding members annually for various achievements in their field and on behalf of the Society. TMS congratulates the following individuals who have received awards and honors this year and will be recognized at the TMS 2010 Annual Meeting in Seattle, Washington. To learn more about each award or how to nominate a colleague for an award, visit <http://www.tms.org/society/tmsawards.aspx>.

Fellow—Class of 2010: *The highest honor bestowed by TMS, the honorary class of Fellow was established in 1962. To be inducted, a candidate must be recognized as an eminent authority and contributor within the broad field of metallurgy, with a strong consideration of outstanding service to the Society. The maximum number of living Fellows cannot exceed 100.*

Jeff DeHosson: For his outstanding contributions to structure-property relationships in materials. Says DeHosson, "I consider the Fellow Award as a major honor in the international community of materials science and an important milestone in my career. TMS played a crucial role in my scientific life since the Society provided me a forum for the dissemination of my scientific accomplishments. Most importantly, the award is based on the recognition by my peers, i.e. my outstanding colleagues whose critical opinion I value most. Thanks are due to my research group, to the Zernike Institute for Advanced Materials-Groningen, and the Netherlands Materials Innovation Institute for their continuous support."

James W. Evans: For his pioneering and seminal work in extractive/process metallurgy and his reputation as a leader in this field worldwide. Says Evans, "My years of membership in TMS, since the late 70s, have taught me much that has been valuable in my career and given me the opportunity to interact with my colleagues in the Society to my great benefit. The Fellows of TMS are a highly distinguished group of people and I am deeply honored by this award."

Easo P. George: For his outstanding contributions to understanding deformation and fracture in intermetallic and metallic alloys and to designing new materials and functional use. "It is indeed a great pleasure to be elected TMS Fellow," says George. "I joined TMS as a student, shortly after which I went to my first technical meeting, giving a talk and making my first outside scientific contacts, and was hooked. The impact of TMS on my professional development—through meetings, publications, and friends made along the way—is immeasurable, and I am profoundly grateful for it."

Richard G. Hoagland: For outstanding contributions in fracture mechanics and atomistic modeling of dislocation mechanisms of deformation and fracture in a broad range of materials. Says Hoagland, "Well, this is really something! If I have done anything to deserve this recognition, it is because I have had the mighty broad shoulders of colleagues and mentors to stand on, and the help of the best students and postdocs anyone could hope for. Some are listed among the TMS Fellows alumni. But many others are, or have been, at places like Battelle, Ohio State University, McMaster University, Washington State University, and Los Alamos National Lab. TMS meetings have been important to me because they have provided a forum where I can meet these friends again, for exchanging new results with them and others and for learning new things. And, learning is what it is all about, isn't it?"

Philip J. Mackey: For the development of new metallurgical processes for the production of non-ferrous metals, long service to the metallurgical community and, in particular, for bridging copper metallurgists of the two Americas. "TMS has always been an exciting and important organization for me," says Mackey. "Throughout my career, it has played an important role in my professional life. Through TMS, I have met and worked with leaders in the industry. I first joined TMS in 1996 and it remains as relevant today as back then. It is a great honor and privilege to be recognized as a recipient of the 2010 TMS Fellow Award."

American Institute of Mining, Metallurgical, and Petroleum Engineers (AIME) Honorary Member: *AIME Honorary Membership is one of the highest honors that the Institute can bestow on an individual. It is awarded in appreciation of outstanding service to the Institute or in recognition of distinguished scientific or engineering achievements in the fields embracing the activities of AIME and its member societies.*

Y. Austin Chang

AIME Robert Earll McConnell Award: *This award recognizes beneficial service to society through significant contributions which tend to enhance a nation's standard of living or replenish its natural resources.*

Diran Apelian

AIME James Douglas Gold Medal: *This award recognizes distinguished achievement in non-ferrous metallurgy, including both the beneficiation of ores and the alloying and utilization of non-ferrous metals.*

James C. Williams

William Hume-Rothery Award: *The William Hume-Rothery Award was established in 1972 by the Institute of Metals Division of TMS and recognizes outstanding scholarly contributions to the science of alloys. The award includes an invitation to the recipient to be the honored lecturer at the William Hume-Rothery Memorial Symposium during the TMS Annual Meeting.*

Didier DeFontaine: Lecture: "How Hume-Rothery's Work Led to Computational Thermodynamics." "When I was a metallurgical engineering student in my native Belgium at the Catholic University of Louvain, the instructor taught the physical metallurgy course out of a textbook by William Hume-Rothery," says DeFontaine. "As a result, I learned about the great Oxford physicist/metallurgist Hume-Rothery very early on and his excellent textbook played no small role in the orientation of my career. Hume-Rothery was a hero in undergraduate school, but of course, I could not even dream that some day my name would be associated with that of the great man himself."

Institute of Metals Lecturer & Robert Franklin Mehl Award: *The Institute of Metals Lecture, established in 1921, recognizes an outstanding scientific leader who is selected to present a lecture at the TMS Annual Meeting. The Robert Franklin Mehl Award was established in 1972.*

Robert Ritchie: Lecture: "Nature-Inspired Structural Materials." Says Ritchie, "I have been a member of TMS for well over 30 years, and can remember with clarity listening to the great Mehl Award lectures of many years ago by such luminaries as Jack Christina, Mike Ashby, Peter Haasen, and Bill Nix. I am honored, yet humbled, to be the 2010 recipient of the TMS Robert Franklin Mehl Award and only hope that I am worthy enough to be included with this elite group of individuals."

Application to Practice Award: *The Application to Practice Award, established in 1986, recognizes an individual who has demonstrated outstanding achievement in transferring research results or findings into commercial production and practical use.*

Carol Handwerker: "For decades, TMS has played a major role in nurturing the discussion of the materials science and engineering of electronic interconnects," says Handwerker. "In the transition from Sn-Pb solders to Pb-free electronics, TMS has been *the* forum for the community to disseminate its newest results, discuss open issues, and debate the tradeoffs between different alloys with a serious focus on applications. I am very grateful to TMS for conferring on me the TMS Application to Practice Award for my work on Pb-free solder and for continuing to provide an open, exciting scientific forum where materials scientists and engineers can address problems of national concern."

John Bardeen Award: *The John Bardeen Award, established in 1994, recognizes an individual who has made outstanding contributions and is a leader in the field of electronic materials.*

Eugene Haller: Says Haller, "Winning the 2010 John Bardeen Award of TMS is a great honor and a much appreciated recognition of the research contributions that my collaborators, students, postdocs, and I have made. The award carries the name of one of my greatest heroes in the sciences, John Bardeen. I was fortunate to speak with John Bardeen on a few occasions and was always impressed by his friendly and low-key style of discussing science. As a young postdoctoral fellow at the Rad Lab in Berkeley, now the Lawrence Berkeley National Laboratory, I discussed our ultra-pure germanium research and development with John Bardeen, who at the time was reviewing our work for the Atomic Energy Commission, now the U.S. Department of Energy. He listened carefully with an approving smile!"

Bruce Chalmers Award: *The Bruce Chalmers Award was established in 1989 by the Materials Processing & Manufacturing Division of TMS and is named for Bruce Chalmers, widely acknowledged as a father of modern solidification science. The award recognizes outstanding contributions in the field of solidification science.*

(Continued on page 6.)

Special Lectures Examine Key Industry Issues and Developments

Distinguished experts will challenge TMS 2010 Annual Meeting attendees to consider, discuss, and explore a broad range of topics during the special lectures scheduled throughout the event. These include:

- **Extraction & Processing/Materials Processing & Manufacturing Joint Division Luncheon Lecture:** "Titanium: Its Attributes, Characteristics, and Applications," Rod Boyer, Boeing Commercial Planes (Tuesday, February 16). This presentation will focus on the desirable and unique attributes of this alloy system, as well as provide a general overview of some of the approaches being taken to reduce the cost—some of which could impact non-aerospace industries.
- **Extraction & Processing Division Distinguished Lecture:** "Alloy Formation during Electrochemical Cementation Reactions," J. Brent Hiskey, associate dean, University of Arizona (Tuesday, February 16). Metal displacement (cementation) reactions have been important to many hydrometallurgical processes for centuries. For the most part, these reactions involve rather straightforward electrochemical steps and the deposition of unique alloys by this technique has been reported for several systems. This presentation describes these systems and provides an explanation for this phenomenon.
- **Light Metals Division Luncheon Lecture:** "Aluminum—Are We There Yet?" Wayne Hale, executive vice president and CEO, Century Aluminum (Wednesday, February 17). With the global recession and the associated impact on commodities, industry consultants and pundits continually prognosticate the future of the aluminum industry. This presentation offers a review of the industry's current position, as well as the necessary milestones and potential bumps along the way, in addressing the vexing question, "Are we there yet?"

Also highlighting the Annual Meeting

is an array of symposia keynotes:

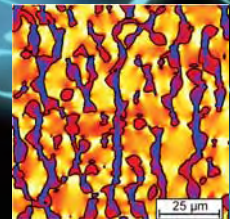
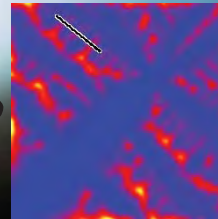
- **Institute of Metals/Robert Franklin Mehl Award Lecture:** "Nature-Inspired Structural Materials," Robert Ritchie, Chua Distinguished Professor of Engineering, University of California (Tuesday, February 16).
- **William Hume-Rothery Award Lecture:** "How Hume-Rothery's Work Led to Computational Thermodynamics," Didier DeFontaine, Professor Emeritus, University of California (Monday, February 15).
- **JIM International Scholar Award Lecture:** "Development of Coherent X-Ray Diffraction Microscopy and Its Application in Materials Science," Yukio Takahashi, Osaka University (Wednesday, February 17).
- **Vittorio de Nora Award Lecture:** "Designing Crushing and Grinding Circuits for Improved Energy Efficiency," Zeljka Pokrajcic, Worley-Parsons Services Pty Ltd—Minerals and Metals, Australia (Wednesday, February 17).

microstructure evolution simulation software



Simulation of microstructure evolution
in technical alloys:

- solidification
- recrystallization
- grain growth
- solid state transformations
- coupling to thermodynamic / mobility data



www.micress.de
support@micress.de
www.access-technology.de

Ever wonder where new ideas come from?

Out of the blue.

From its beginning, Permotech has been innovating. Indeed, it was founded to create an entirely new product in the casting industry— asbestos-free, pre-cast refractory components. Created as it was to pioneer a new idea, the company didn't stop there. In the nearly four decades since, Permotech has introduced one new idea after another. Even now, we're working on what's next.

PERMATECH®

SHAPING THE FUTURE OF REFRACTORY TECHNOLOGY

Graham, NC • permatech.net • 336.578.7728

Honors and Awards (Continued from page 4.)

Cristoph Beckermann: “The Bruce Chalmers award is a great honor and recognition by my peers that my research has had some impact in the field of solidification. It is mainly through TMS meetings that I learned about the many fascinating aspects of solidification, from both scientific and industrial perspectives. TMS also allowed me to make the connections that are necessary to work in this interdisciplinary field. I would like to share this award with all of my former graduate students and collaborators.”

Educator Award: *The Educator Award, established in 1986, recognizes an individual who has made outstanding contributions to education in metallurgical engineering and/or materials science and engineering.*

John Moore: Says Moore, “I am very honored to be nominated and awarded the 2010 Educator Award. I have been a member of TMS since 1979 and consider TMS to be the ‘professional home’ of metallurgical and materials engineers worldwide. TMS has provided me with the communication, networking, and professional interaction that I have needed for the past 30 years and also provides excellent support and interaction for materials in higher education.”

Robert Lansing Hardy Award: *Established in 1955, the Robert Lansing Hardy Award recognizes outstanding promise for a successful career in the broad field of metallurgy by a metallurgist under the age of 35. In addition, the winner receives a \$500 stipend from the Ford Motor Company.*

Diana Lados: “It is a great honor to receive this recognition and join a most distinguished group of materials scientists and engineers,” says Lados. “It is my intent to continue the tradition of research excellence established by this award and engage the younger generation in materials science and TMS. TMS is an excellent career development platform that facilitates valuable personal interactions. It is rewarding to be part of the TMS family and contribute to the exciting future of our field.”

Leadership Award: *The Leadership Award, established in 1986, recognizes an individual who has demonstrated outstanding leadership in the field of metallurgy and materials.*

Donald Gubser: “To be chosen as the recipient of the 2010 TMS Leadership award is a special honor to me. It provides recognition from a very prestigious professional society that my science leadership has been judged by my peers to be of high quality,” says Gubser. “It is especially gratifying to know that this award basically emanates from those with whom I have worked closely, both from within my own organization, as well as within the larger scientific community through professional activities and duties. To be appreciated and valued by those I have worked with for many years, and by the members of TMS, is indeed a very high and humbling honor.”

Champion H. Mathewson Award: *The Champion H. Mathewson Award, established in 1933, is awarded to an author(s) of a paper or series of closely related papers which represents the most notable contribution to metallurgical science during the period under review.*

Guillaume Reinhart: Paper Title: “In-Situ and Real-Time Analysis of the Formation of Strains and Microstructure Defects during Solidification of Al-3.5 Wt Pct Ni Alloys.” Says Reinhart, “This award represents the achievement of several years of work between the IM2NP (formerly L2MP) laboratory in Marseille where I did my Ph.D. and the European Synchrotron Radiation Facility where the experiments were performed. I’m very grateful for this nomination, which also motivates my research group even more to keep on contributing to metallurgical and materials science.”

Early Career Faculty Fellow Award: *Established in 2006, the Early Career Faculty Fellow Award honors an assistant professor for accomplishments that have advanced the academic institution where employed, as well as recognizes his or her abilities to broaden the technological profile of TMS.*

Xingbo Liu: Lecture: “Energy Materials—Past, Present, and Future.” Says Liu, “Since I became a member in 2002, TMS has played a critical role in my career development. Through attending and organizing symposia and participating in different committees, I have had the valuable opportunity to interact with scientists and engineers in the field of high-temperature materials for energy conversion from all over the world. I am thrilled to be the recipient of the TMS 2010 Early Career Faculty Fellow Award and will exert more of my efforts in contributing to the TMS community.”

Shri Ram Arora Award: *The Shri Ram Arora Award for Materials Science and Engineering Education was established in 2001 to recognize, encourage, and support the quest for knowledge within the materials science and engineering community.*

Sponsors Ensure Convenience, Comfort at TMS Annual Meeting

Making sure that the TMS 2010 Annual Meeting is a positive, productive experience down to the last detail are the sponsors who have underwritten an array of events and amenities. For instance, Fives Solios has once more been named the meeting’s Premier Green Sponsor, actively supporting TMS in its efforts to make the Annual Meeting environmentally sound by helping to eliminate waste, encourage recycling, and conserve energy. A supporter of the TMS Annual Meeting for more than 20 years, Fives Solios will provide canvas messenger bags to all full conference registrants and is flagging the recycling containers in the Washington State Convention Center with its name and logo. Headquartered in St. Germain En Laye, France, Fives Solios designs and supplies processing equipment and turnkey plants for aluminum producers worldwide, particularly in the reduction areas of gas treatment centers and bath processing plants.

Keeping Annual Meeting participants connected to home and work has been made possible by Wahl Refractory Solutions, Inc., which has underwritten the cost of the free Wi-Fi made available in the Annual Meeting Exhibit Hall. Stellar Materials is also sponsoring the Exhibit Hall’s Cyber Center—computer pods which can be accessed by all attendees and exhibitors. Helping meeting attendees stay on track and informed throughout the event is the Information Booth sponsor, Harbison-Walker Refractories, as well as B&P Processing, which is sponsoring the Annual Meeting



The annual meeting exhibit hall, with its displays of materials-related products and processes, is a popular gathering spot.

and Exhibit Hall entrance, and Pamas & Company, the 2010 Annual Meeting lanyard sponsor.

A complete list of Annual Meeting sponsors can be found on the TMS 2010 Annual Meeting Web site.

Women in Science Breakfast Lecture Highlights ADVANCE Initiative

An overview of the successes and challenges experienced by the ADVANCE Center for Institutional Change at the University of Washington will be the focus of the annual Women in Science Breakfast Lecture, to be held February 15, from 7 to 8 a.m. at the Sheraton Seattle. Eve A. Riskin, Washington's associate dean of academic affairs, professor of electrical engineering, and center director, will discuss the program's outcomes since its inception in 2001 and strategies it has used to enhance recruitment, retention, and leadership development of its female faculty. She will also share interventions that can support success of female faculty in the science, technology, engineering, and mathematics (STEM) disciplines. An initiative of the National Science Foundation, ADVANCE seeks to improve the climate for success of women in STEM at universities in the United States. The Women in Science Breakfast Lecture is free to all Annual Meeting attendees.

Lamborghini Revs Up TMS 2010 Exhibition

The TMS 2010 Exhibition will be the epicenter of networking activity when it opens for business at the Washington State Convention Center at noon on Monday, February 15. New this year is the TMS Lunch and Learn Session, "Carbon Fiber Composites Research and Development at Automobili Lamborghini," scheduled to begin at 12:30 p.m. in the exhibit area on February 15. In addition to hearing first-hand how Lamborghini, the University of Washington, and Boeing have partnered to advance excellence in carbon fiber composite technology, program attendees will get a chance to see a Lamborghini *Murciélago LP 670-4 SuperVeloce* up close. (The *Murciélago* will be on display in the exhibit hall for the duration of the exhibition.)

TMS 2010 Annual Meeting attendees

Apu Sarkar: "It is a great honor to receive the prestigious Shri Ram Arora award. This award will help me gain international recognition, while encouraging me and boosting my confidence to work on new and challenging research problems," says Sarkar.

Vittorio de Nora Prize for Environmental Improvements in Metallurgical Industries: *New for 2010, the de Nora Prize recognizes outstanding materials science research and development contributions to the reduction of environmental impacts as applied in global metallurgical industries, with a particular focus on extractive processing.*

Zeljka Pokrajcic: Lecture: "Designing Crushing and Grinding Circuits for Improved Energy Efficiency." Says Pokrajcic, "I am both honored and excited to be the first recipient of the Vittorio de Nora Prize. It is a prestigious and coveted award from an equally highly regarded organization. The award will significantly lift the profile of environmental improvements and increased energy efficiency in the energy-intensive minerals industry. I hope that my contribution through the research already undertaken and the work planned as a result of the prize will further contribute to environmental improvements in metallurgical industries."

Alexander Scott Distinguished Service Award: *Since 1994, TMS has recognized a member for outstanding contributions to the Society with the Distinguished Service Award.*

Brajendra Mishra: "The membership of TMS is a privilege to me," says Mishra. "It helped me shape my career not only as a student, but also as a practicing materials engineer. The leadership opportunities provided to me by TMS have been most beneficial, along with the chance to serve the profession. Recognition of my service to TMS through this Distinguished Service Award is an honor that I shall forever proudly cherish."

Electronic, Magnetic & Photonic Materials Distinguished Service Award: *This award recognizes an individual whose continuous service to the TMS Electronic, Magnetic & Photonic Materials Division (EMPMD) has clearly facilitated the Society's capability to serve its electronic, magnetic, and photonic materials-oriented members and their supporting organizations.*

Elizabeth Holm: "I am honored to accept this award for service to TMS and the EMPMD. However, I must admit that I have received much more from my TMS membership than I have given back," says Holm. "TMS has supported my scientific and professional advancement since I was a student. I hope to reciprocate by continuing to serve the Society throughout my career."

Electronic, Magnetic & Photonic Materials Distinguished Scientist/Engineer Award: *This award recognizes an individual for research excellence in one or more areas related to electronic, magnetic, and photonic materials science.*

Brent Fultz: "TMS meetings have been a home for me since my days as a graduate student, consistently offering a stimulating environment for the exchange of new ideas. Over the years, my TMS colleagues and friends were some of the best for discussing ideas about the vibrational entropy of materials, and studies of entropy by inelastic scattering methods. These discussions helped me optimize the research that is recognized by this award."

Extraction & Processing Distinguished Service Award: *This award recognizes an individual who has demonstrated outstanding long-term service to industries served by the Extraction & Processing Division.*

Patrick Taylor: "It is an honor to receive the 2010 TMS EPD Distinguished Service Award. I attended my first TMS meeting in 1975 and gave my first professional presentation. Over these past 34 years I have truly benefited, professionally and personally, from my participation in TMS EPD. The many hours that I have devoted to help TMS and EPD has been paid back, many times, through the positive impact of this society on my professional career and the friends that I have made."

Extraction & Processing Distinguished Lecture Award: *This award recognizes an eminent individual in the field of extraction and processing of nonferrous metals with an invitation to present a comprehensive lecture at the TMS Annual Meeting.*

J. Brent Hiskey: Lecture: "Alloy Formation during Electrochemical Cementation Reactions."

Extraction & Processing Science Award: *This award, established in 1955, recognizes a paper that represents notable contributions to the scientific understanding of the extraction and processing of nonferrous metals.*

Stanko Nikolic, Peter C. Hayes, Hector Henao, and Eugene Jak: Paper Title: "Advantages of Continuous Copper Fire Refining in a Packed Bed."

Extraction & Processing Technology Award: *This award recognizes a paper containing notable contributions to the advancement of technology related to the extraction and processing of nonferrous metals.*

Gabriel Riveros, Andrzej Warczok, Daniel Smith, and Ariel Balocchi: Paper Title: "Phase Equilibria in Ferrous Calcium Silicates, Parts I-IV."

Light Metals Distinguished Service Award: *This award, established in 1995, recognizes an individual whose continuous service to the TMS Light Metals Division has clearly facilitated the Society's capability to serve its light metals-oriented members and their supporting organizations.*

Neale Neelameggham: "It is an honor and pleasure to receive the Distinguished Service Award from the Light Metals Division of TMS. I have been a member of TMS for over 35 years and actively engaged in the different committees during the past ten years. I appreciate the confidence my co-volunteers and peers from the Magnesium Commit-

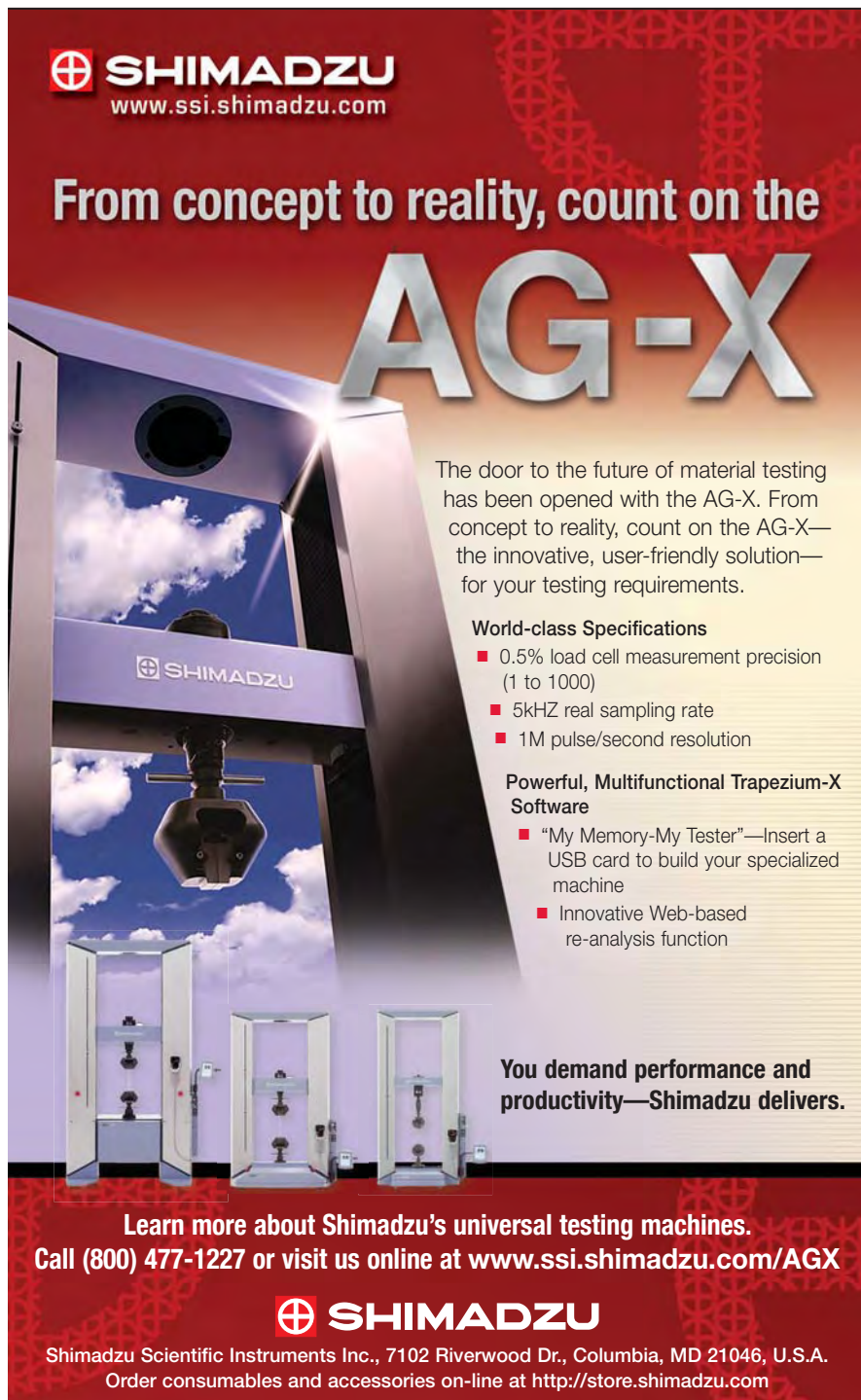
tee will also have ample opportunity to learn about the latest technologies, products, and services from approximately 100 exhibitors covering the spectrum of materials science and engineering. These include long-time exhibition supporters Rio Tinto Alcan, Outotec, Dubai Aluminium, Hydro Aluminum Hycast, Fives Solios, and Gillespie+Powers, Inc. In addition, TMS is welcoming a number of new exhibitors to this year's event, such as Big C, Agilent Technologies, CIMM Group, Farra Engineering Ltd., Magnesium Elektron, Major, Momentum Press, Oli Systems, and SunStone.

NIST Technology Innovation Program Selects New Projects

The U.S. National Institute of Standards and Technology (NIST) announced on December 15 that it will provide up to \$71 million through its Technology Innovation Program (TIP) for 20 new projects that support innovative, high-risk research in new technologies. The new projects include developing unmanned, hovering aircraft for bridge inspections, a high-speed sorting system for recycling aerospace metals, and nanomaterials for advanced batteries. The awards will be matched by other funding sources to achieve nearly \$150 million in new research over the next two to five years. The projects were selected from a TIP competition announced on March 26, 2009. A complete list of these initiatives can be accessed at http://www.nist.gov/public_affairs/releases/20091215_tip_awards.htm.

TIP is a merit-based, competitive program that provides cost-shared funding for research projects by single small- or medium-sized businesses or by joint ventures that may include universities, non-profit research organizations, and national laboratories. The intent of the program is to support and accelerate innovation in the United States through high-risk, high-reward research in areas of critical national need.

TIP also announced that it is currently seeking comments on white papers prepared by its staff and posted on the TIP Web site. These white papers articulate the goals and scope of technical challenges that could be addressed in future TIP competitions. The white papers can be accessed at http://www.nist.gov/tip/wp_cmts/index.html.



SHIMADZU
www.ssi.shimadzu.com

From concept to reality, count on the AG-X

The door to the future of material testing has been opened with the AG-X. From concept to reality, count on the AG-X—the innovative, user-friendly solution—for your testing requirements.

World-class Specifications

- 0.5% load cell measurement precision (1 to 1000)
- 5kHz real sampling rate
- 1M pulse/second resolution

Powerful, Multifunctional Trapezium-X Software

- "My Memory-My Tester"—Insert a USB card to build your specialized machine
- Innovative Web-based re-analysis function

You demand performance and productivity—Shimadzu delivers.

Learn more about Shimadzu's universal testing machines.
Call (800) 477-1227 or visit us online at www.ssi.shimadzu.com/AGX

SHIMADZU
Shimadzu Scientific Instruments Inc., 7102 Riverwood Dr., Columbia, MD 21046, U.S.A.
Order consumables and accessories on-line at <http://store.shimadzu.com>

One Source One Partner

1
One Source
One Partner



for Leading Brand Solutions & Expertise in Bauxite Mining
& Refining, Calcination, and Smelting

High Performance for Alumina Handling Systems

Every day, worldwide, our equipment crushes, conveys, grinds, digests, clarifies, precipitates, stores, and calcinates bauxite to produce alumina. Combining the respected brand names of MÖLLER, KOCH-MVT, FULLER-TRAYLOR, EIMCO, DORR-OLIVER, KREBS, and ABON, FLSmidth offers a broad range of equipment and processes while increasing recoveries, lowering energy consumption, and providing proven reliability.

FLSMIDTH

www.FLSmidthMinerals.com

Please visit us at TMS 2010 booth 227.



SUPERIOR PRODUCTS CUSTOM ENGINEERED
FOR YOUR DEMANDING APPLICATIONS

Our innovative WalMaxXx™ refractories offer maximum protection at extreme temperatures against:

- Oxidation
- Erosion
- Aluminum

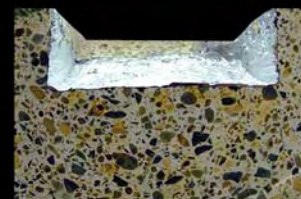
WalMaxXx™ can be installed as:

- MegaBrix™ precast furnace lining
- Castable
- Gunnite

To discuss your application, contact us at 800-837-WAHL.

Please visit www.wahlref.com or email us at sales@wahlref.com for additional information on our products for the aluminum industry including SIFCA™ door perimeters, troughing, impellers and skim tools.

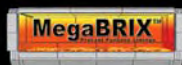
No Aluminum Penetration



WalMaxXx™ Aluminum Cup Test



No Aluminum Adhesion
after 12 months of
service life in a batch
operating scrap melter



PROVIDED BY:
Wahl Refractory Solutions
767 State Route 19 South
Fremont, OH 43420

JOM READER POLL

To vote, go to
www.tms.org/jomsurvey.html.

Last month's question:

In the 2009 salary survey by the American Association of Engineering Societies, the median pay for materials engineers with 35+ years since earning their baccalaureate degrees was \$119,224. This month, *JOM* asks, how would you characterize materials engineers' salaries?

Last month's answers:

Inadequate **59.46%**

Fair **24.32%**

Generous **16.22%**

This month's question:

This issue contains a cover story about the use of advanced materials in the Olympic games (which will be held in Vancouver, just hours away from the TMS 2010 Annual Meeting in Seattle, Washington), and notes the controversy that can result when athletes are too reliant on technology to improve their performances. This month, *JOM* asks, what effect has materials science had on the competitive spirit of the Olympics?

This month's answers:

- Little impact: Superior athletes will prevail regardless of the equipment they used.
- Moderate impact: Technology can provide the push needed for a good athlete to become a winner.
- Significant impact: Advanced materials have given an unfair edge to the teams that can afford the best technology.

tee, the Energy Committee, LMD Council, and other committees have had with my contribution in conferring this award. My humble thanks to them."

Light Metals Technology Award: *This award recognizes an individual who has demonstrated outstanding long-term service to the light metals industry by consistently providing technical and/or operating knowledge that has enhanced the competitiveness of the industry.*

Douglas Granger: "To be chosen by ones peers to receive the prestigious Light Metals Technology Award is a great honor that I truly appreciate," says Granger. "At the same time, it is a humbling experience to be joining a roster that includes so many distinguished scientists and technologists. Throughout my more than 30-year career in light metals research and development, TMS has been of immense importance to me. Much of what I have accomplished would not have occurred without the stimulating discussions and thoughtful guidance provided by my TMS colleagues."

Light Metals Award: *This award, established in 1983, is conferred upon the author(s) of a paper, presented in the preceding year in a Light Metals Division sponsored session at the Annual Meeting, which notably exemplifies the solution of a practical problem.*

Anthimos Xenidis, Charalabos Zografidis, Ioannis Kotsis, and Dmitrios Boufounos: Paper Title: "Reductive Roasting and Magnetic Separation of Greek Bauxite Residue for its Utilization in the Iron Ore Industry." Says Xenidis, "My collaborators and I feel deeply honored to be the recipients of the 2010 Light Metals Best Paper Award of TMS. This is recognition of the quality of the research work we carry out at the National Technical University of Athens. Rightly so, it fills us with pride. However, this award is not just a valued distinction, but also a high level standard for which we will have to strive in our future endeavors."

Light Metals Division JOM Best Paper Award: *This award, established in 1994, is presented to the author(s) of a paper published in an issue of the preceding volume year of JOM under a light-metals-related topic.*

Barry Welch, Martin Iffert, and Maria Skyllas-Kazacos: Paper Title: "Applying Fundamental Data to Reduce the Carbon Dioxide Footprint of Aluminum Smelters."

Materials Processing & Manufacturing Division Distinguished Scientist/Engineer Award: *This award recognizes an individual who has made a long-lasting contribution to the design, syntheses, processing, and performance of engineering materials with significant industrial applications.*

Yuntian Zhu: "It is a great honor to be recognized with this award by colleagues," says Zhu. "For my entire academic career, TMS has provided me with essential and great opportunities for academic growth, service, and networking with colleagues. The importance of membership in TMS cannot be overstated for professionals in materials science and engineering."

Materials Processing & Manufacturing Division Distinguished Service Award: *This award recognizes an individual whose dedication and commitment to the Materials Processing & Manufacturing Division has made a demonstrable difference to the objectives and capabilities of the division and the Society.*

John Smugeresky

Structural Materials Distinguished Materials Scientist/Engineer Award: *This award, established in 1996, recognizes an individual who has made a long-lasting contribution to the fundamental understanding of microstructure, properties, and performance of structural materials for industrial applications.*

Reinhold Dauskardt: "I am delighted that I am receiving this award and recognition from TMS," says Dauskardt. "I have been a long-standing member of TMS and have been very impressed at how the Society has embraced new and non-traditional areas of materials and biomaterials research. This has kept the society scientifically and technologically relevant and the reason that I enjoy attending the annual meetings."

Structural Materials Division Distinguished Service Award: *This award recognizes an individual whose dedication and commitment to the Structural Materials Division has made a demonstrable difference to the objectives and capabilities of the division and the Society.*

Dallis Hardwick

Structural Materials Division JOM Best Paper Award: *This award, established in 2007, is presented to the author(s) of a paper published in an issue of the preceding volume year of JOM under a structural-materials-related topic.*

Marc A. Meyers, Sirirat Traiviratana, V.A. Lubarda, David J. Benson, and Eduardo M. Bringa: Paper Title: "The Role of Dislocations in the Growth of Nanosized Voids in Ductile Failure of Metals."

WASHINGTON NEWS



From Betsy Houston,
Federation of Materials Societies

Science and Engineering Indicators 2010: Declaring that the state of the science and engineering enterprise in the United States is strong but slipping, the National Science Board released the biennial Science and Engineering Indicators report at a briefing at the White House on January 15. The report, mandated by law, provides information on the scope, quality and vitality of America's sci-

ence and engineering enterprise. This year, it stressed the nation's position in the global economy. Over the past decade, R&D intensity—how much of a country's economic activity or gross domestic product is expended on R&D—has grown considerably in Asia, while remaining steady in the United States. Annual growth of U.S. R&D expenditures has averaged five to six percent, while Asian countries have skyrocketed to double, triple, or even four times that. Other key indicators include intellectual research outputs; patents; the globalization of capability; funding; performance and portfolio of U.S. R&D trends; and the composition of the U.S. science and engineering workforce. The report is prepared by the National Science Foundation's (NSF) Division of Science Resources Statistics (SRS) on behalf of the National Science Board (NSB). Both the extensive final report and a more easily usable Digest are online at www.nsf.gov/news.

Science and Technology Agenda: Rep. Bart Gordon's tenure as Chairman of the House Science and Technology Committee has been marked by an aggressive schedule of hearings and successes in getting bills passed in the House. The Committee won't slow down this year, even though Rep. Gordon (D-TN) has announced his retirement from Congress at the end of the term. The signature piece will be reauthorization of the America COMPETES Act which expires at the end of FY 2010, keeping the National Science Foundation (NSF), the National Institute of Standards and Technology (NIST), and the Office of Science within the Department of Energy (DOE) on the path to doubling their research and development budgets. Chairman Gordon's plan is to get a multi-year COMPETES reauthorization drafted and through the House by Memorial Day. In addition to its current provisions, the bill is also likely to include new programs and policy direction at NSF, NIST, and other agencies. Also by the end of May, the committee expects to draft and report out a multi-year reauthorization of NASA. In energy, the committee intends to draft legislation to authorize a broad research and development program on nuclear energy at the DOE. The new program is expected to address enrichment, reprocessing, generation, and the storage of spent fuel. The committee also will spur development of new energy technologies through targeted, stand-alone bills.

Energy Information Hub Funding: Three Energy Innovation Hubs, to be funded at up to \$122 million over five years, will be established in FY 2010. The three hubs will focus on:

- Production of fuels directly from sunlight
- Improving energy-efficient building systems design
- Computer modeling and simulation for the development of advanced nuclear reactors

Universities, national laboratories, nonprofit organizations, and private firms are eligible to compete for an award and are encouraged to form partnerships. Further information is available at www.energy.gov/hubs.

Public Access to Research Results: The Scholarly Publishing Roundtable convened last summer by the House Science and Technology Committee, in collaboration with the White House Office of Science and Technology Policy. In mid-January, it released its report, calling on federal agencies that fund research to develop and implement policies ensuring free public access to research results "as soon as possible after those results have been published in a peer-reviewed journal." The Roundtable identified a set of principles viewed as essential to a robust scholarly publishing system, including the need to preserve peer review, the necessity of adaptable publishing business models, the benefits of broader public access, the importance of archiving, and the interoperability of online content. The group also affirmed the high value of the "version of record" for published articles and of all stakeholders' contributions to sustaining the best possible system of scholarly publishing. The report can be found at www.aau.edu.

Thermodynamic Calculation And Kinetic Simulation



CompuTherm, LLC

Software • Databases • Consulting

SOFTWARE

Pandat, PanEngine and Winphad

- Multi-component multi-phase thermodynamic and phase equilibrium calculation
- User friendly interface
- Automatic calculation
- Dynamic-link library for custom applications such as *Solidification, Heat Treatment, Diffusion, Casting, Welding, Corrosion and More*

DATABASES

For commercial Al-, Cu-, Mg-, Fe-, Ni-, Ti-based and solder alloys

CONSULTING

Multi-component phase equilibria, thermal stability, thermodynamic compatibility, weldability, castability and more

Please visit us at TMS 2010 booth 428.

Contact us

CompuTherm, LLC Tel: (608)274-1414
437 S. Yellowstone Dr. Fax: (608)274-6045
Suite 217 www.computherm.com
Madison, WI 53719 USA info@computherm.com

NETZSCH



Instruments & Testing Services

Thermal Analysis

- High Temperature & Classical DSC, DTA, TGA, DSC-TGA
- High Accuracy Specific Heat
- Coupling to FTIR & MS

Conductivity & Flash Diffusivity

- -125 to +2000°C
- New Guarded Hot Plate

Dilatometers

- CTE & Sintering to +2800°C

Contract Testing Services

NETZSCH Instruments

37 North Ave.

Burlington, MA 01803

Call (781) 272-5353

Fax (781) 272-5225

e-mail: NIB-Sales@Netzsch.com

www.e-Thermal.com



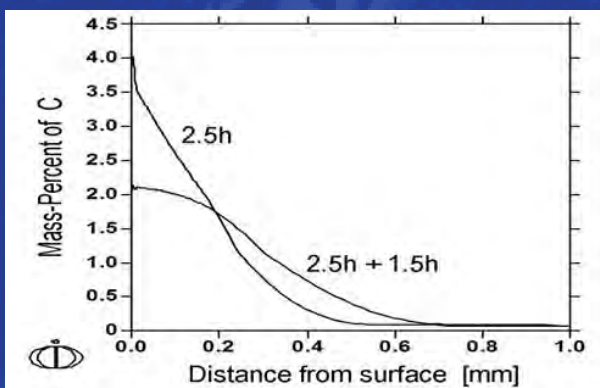
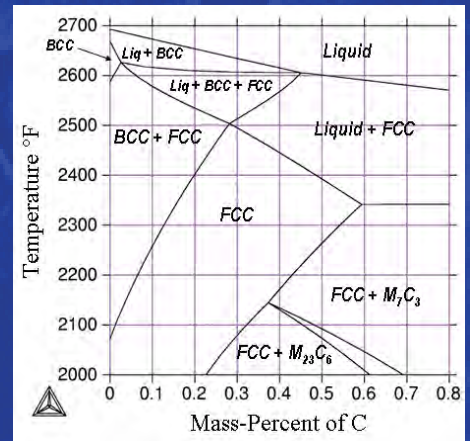
Thermo-Calc Software

Thermodynamic and Diffusion Simulation Software

Thermo-Calc

Thermo-Calc: powerful software for thermodynamic calculations for multi-component multi-phase systems. Thermo-Calc can be used for a wide range of applications including:

- ✓ Calculating stable and meta-stable phase equilibria
- ✓ Predicting amounts of phases (mass, volume and mole fractions) and their compositions
- ✓ Liquidus and solidus temperatures, Scheil solidification
- ✓ Thermochemical data such as enthalpies, heat capacity, and activities
- ✓ Predicting driving forces and transformation temperatures
- ✓ Phase diagrams (isothermal, isoplethal sections for multi-component multi-phase systems)
- ✓ Databases for Fe-, Ni-, Al-, Ti-, Mg- based alloys, solders, refractory oxides, slags and more...
- ✓ Alloy design: Modifying chemistry to improve properties or reduce costs
- ✓ Amount and composition of phases varying with temperature or composition of the alloy
- ✓ Quality control: How phase balance and certain properties vary within in-tolerance compositional variation



DICTRA

A unique engineering tool for simulating various types of diffusion-controlled phase transformations in multi-component systems. DICTRA provides valuable information on the time evolution of the microstructure. Applications include:

- ✓ Homogenization
- ✓ Diffusion controlled phase transformation kinetics
- ✓ Carburizing & Decarburizing
- ✓ Nitriding and carbonitriding
- ✓ Microsegregation during solidification
- ✓ Coarsening / Dissolution of precipitates
- ✓ Interdiffusion
- ✓ Databases for Fe-, Al- and Ni- based alloys

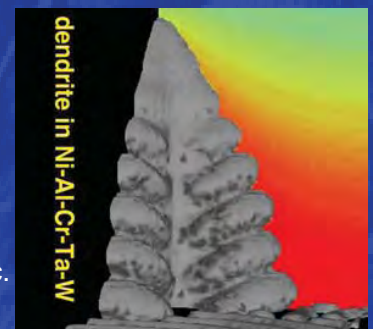
Thermo-Calc Programming Interfaces

Thermo-Calc Programming Interfaces are available for users who wish to integrate many of the Thermo-Calc functions and utilize the thermodynamic databases directly from their own in-house written software.

TQ-Interface: For programming in Fortran

TC-API: For programming in C++, Java, Microsoft Visual Basic and Excel etc.

TC-Matlab toolbox: For accessing Thermo-Calc from Matlab™.



Calculated using MICRESS® in conjunction with the TQ-Interface.

TCC (Ver. S) / TCW (Ver. 5) / DICTRA 25 now available

USA, Canada and Mexico:
Email: Paul@thermocalc.com
Phone: (724) 731 0074
Fax: (724) 731 0078
www.thermocalc.com

Please visit us at
TMS 2010 booth 100.

Rest of the World:
Email: info@thermocalc.se
Phone: +46-8-545 959 30
Fax: +46-8-673 37 18
www.thermocalc.com

TMS: An Essential Connection to an Evolving Profession

George T. “Rusty” Gray III



It is with excitement and a great sense of honor that I accept the Presidency of The Minerals, Metals & Materials Society for 2010–2011. Let me introduce myself. My name is George Thompson Gray III, but no one calls me that.

To family, friends, and the materials community, I’m “Rusty;” a nickname given to me by my grandfather.

My education includes a B.S. and M.S. from the South Dakota School of Mines, a Ph.D. from Carnegie-Mellon University, and a three year postdoctoral fellowship at the Technical University in Hamburg-Harburg, Germany. Today, I’m a Laboratory Fellow at Los Alamos National Laboratory, where I have pursued both fundamental and applied research for the last 25 years.

When not at work, I enjoy a number of activities outside of materials science including bee-keeping, weaving baskets, and designing and building stained glass lamps. I also have a passion for volunteering to help those less fortunate. For each of the last eight years, for example, I’ve spent a week in Mexico as site-boss for 50–80 high school students there to help build houses.

I have been supported in all of these activities, in more ways than I can name, by my wife Altana and our two children, Alex and Krista.

As a professional, I have been an active member of TMS since 1986. As a young professional, TMS served as my primary conduit of materials science knowledge and the principle place for me to present and receive technical feedback on my research. Within TMS, I have served on the Programming, Ti-

tanium, and Mechanical-Behavior committees and served two terms on the TMS Board of Directors—first as chair of the Structural Materials Division and then as the Director of Publications.

As is undoubtedly the case with many of you, TMS has been—and is—my central networking tie into the evolving world of materials and a welcoming venue to meet twice a year with research colleagues and friends.

My goals as TMS president are to work with you, the volunteers, along with TMS staff, to maximize the value of TMS to its membership by strongly supporting our core strengths. These include maintaining TMS as:

- The preferred source of and dissemination venue for leading-edge technical information and knowledge for its members
- The home society for the manufacturing, engineering, research, and materials education communities and cultures, bridging science and engineering technologies critical to industry, research, and academia
- The society dedicated to excellence and growth in supporting the evolving field of materials science and engineering through education, and the application of materials to benefit societal needs

As president I hope to positively impact TMS’s value to members in three specific areas: international liaisons, leadership development, and the society’s value proposition.

A focus on international liaisons is critical because TMS must remain agile in the rapidly changing materials field; one avenue is through international teaming initiatives. This year’s jointly organized conference with the Brazilian Metallurgical, Materials, and Mining Society (ABM) builds on the TMS Al-

liance of the Americas initiative aimed at working with society partners from South America and Canada. To the north, initiatives are underway with the Metallurgical Society of the Canadian Institute of Mining, Metallurgy and Petroleum, especially with our participation on Lead-Zinc 2010 during their Conference of Metallurgists.

Next, leadership development is key because leaders within strong, enduring organizations don’t happen by chance; they are sought, most often through informal and personal contacts and thereafter developed and nurtured on an ongoing basis. While staff can help coach the process, the volunteers are best positioned to influence members’ engagement in committees, boards, etc.

Finally, the focus on our “value” proposition: TMS is committed to demonstrating its ability to remain relevant to meet the ever-changing needs of our diverse membership through innovations in our technical meetings and exhibits, publications, information technologies and content, and member services while continuing to focus on fostering an inclusive environment for the very diverse community that is materials science and engineering.

As TMS continues to develop and grow new initiatives in many of these areas, it is you, the membership, who I challenge to both support our society and our materials community. Seize any opportunity to mentor a new engineer or scientist, promote your field through organizing a symposium, volunteer in your local schools promoting science and math, or join a TMS committee.

We’ll all be richer for the effort.

George T. Gray III is Laboratory Fellow in the Dynamic Materials Properties Section at Los Alamos National Laboratory, Los Alamos, New Mexico and the 2010 TMS president.

The Journal Talks with 2009 TMS President Ray Peterson

TMS President Ray D. Peterson will complete his term as president of the society at the TMS 2010 Annual Meeting this month. Peterson is director of technology for Aleris International, a global leader in the production and sale of aluminum rolled and extruded products, recycled aluminum, and specification alloys. Peterson is Past Chair of the TMS Light Metals Division, and has also chaired the Aluminum Committee and the Recycling Committee. He has been a member of TMS since 1985. As Peterson neared the end of his term, JOM interviewed him to reminisce about the challenges and accomplishments of his year as president.



Q. 2009 was a year of worldwide financial instability. How has TMS emerged from the downturn, and what strategies were employed to keep the organization on track financially?

A. 2009 was a difficult year, and TMS, like so many businesses worldwide, felt the effects of the downturn. For example, participation at the annual meeting dropped off when employers imposed travel restrictions to control costs and some of our usual attendees had to cancel due to the economic crisis. That impacted our revenue side for the meeting, which is significant because the annual meeting is one of our big income sources. But Executive Director Warren Hunt and his staff really worked hard on reducing costs through the rest of year through careful management. As the recession dragged on, we cancelled several small conferences and eliminated one in-person board of directors meeting

and replaced that meeting with phone and web conferences. Some resources were reallocated and sadly, we even had to freeze staff salaries to keep our economics in order.

More importantly for the long term, though, because we can't save ourselves into prosperity we put more effort this year into working on the income side for the future. In particular, we looked at what we can do to grow our income, and concluded that we need to make some long-term changes to encourage growth, particularly in new areas, which we will talk about more a little later on. I see these changes as being very positive for TMS in the coming years.

Q. The board of directors decided in late 2009 to build on TMS's technical strengths with its initiative to "Grow TMS" in the areas of computational materials science and engineering, micro- and nanostructure processing and property relationships, and materials and energy. How do you see this plan changing the future profile of TMS?

A. The materials field is not static; new areas are constantly developing and evolving. For an organization it's sometimes easy to maintain the status quo but TMS can't—and won't—do that. We have to nurture our core areas so they remain strong but we have to grow new areas, as well. We're not going to abandon our traditional areas, but we have members who may be moving from the traditional areas TMS serves into newer disciplines such as micro- and nanostructuring, computational materials science and engineering, and materials and energy. These are all growing areas, and we want to be part of that growth. So I guess you might say that as your interest in careers changes, TMS is going to

be there to foster your development and interchange. We're going to grow with our members.

As to the long-term future of TMS, we're a multifaceted, very broad organization, and we're going to be adding new areas of concentration around the periphery as the field of materials science expands. We're going to become more inclusive, covering a larger field. Growing in these new directions should make us stronger without taking anything away from our core strengths.

Q. One of your broad goals, stated a year ago, was to encourage greater participation of members in TMS and its many benefits. What improvements have you seen in member involvement?

A. First I want to say I thought TMS staff really took this challenge to heart, and I was very impressed by that. Our members have access to a great deal of content on-line, such as the *AIME Transactions* archive, electronic subscriptions to *Metallurgical and Materials Transactions A and B*, new resources for consultants, an e-mentoring program, the Job and Financial Resources Center, the TMS e-library—so many options for members are now on-line that in the past weren't. Not everybody has access to a university library, so these expanded on-line offerings are beneficial, especially to members employed outside of academia.

And to help members feel more personally connected, in *JOM* and on-line we've begun to provide a monthly focus on our members, looking at them outside of their profession. We're learning about their hobbies and their interests, and how that makes them who they are.

A little bit peripheral to this, we've been working on improving the exhibit at the annual meeting. We've taken into

consideration the comments and suggestions of both exhibitors and members to foster the best opportunities for exchange on the exhibit floor. At the same time, we understand that not everyone can attend the annual meeting, so we continue looking for ways to provide members more value with on-line products and other services.

In the end we have to look at ourselves as being just like any other seller of services or goods. If we don't provide the services that somebody wants they'll go elsewhere. It's a competitive world and we have to realize our members are also customers.

Q. Another goal of yours was to take a close look at the TMS honors and awards program and identify areas for improvement. In December the board agreed to adjust the awards program to better fit the current TMS membership, as discussed in your December 2009 JOM article. How will TMS members benefit from the changes to this program?

A. That was an area I took a personal interest in and spent a lot of time and effort on because, when we reviewed the honors and awards program, we could see that our system seemed to be out of date with the current field. As a result, many of our accomplished members were not being recognized—we have a lot of talented people but they may not be eligible for recognitions under the existing system. After some study we concluded that there were several reasons for this. First, it was rather hard to nominate people, and perhaps some people found the process too intimidating and time consuming. Also, not all members had awards to aspire to. If you were in one of the newer areas of materials science, our old awards may not have matched up to what you were doing. A key finding was that many of our awards were really geared to our senior members, which is nice, but we have other people who should be receiving awards who are not at the end of their career. This led us to develop new categories of awards: a mid-career award and awards for processes, structure, and properties, which would be open to anybody within the materials science field.

We also worked at strengthening the divisional awards for all technical divisions, and really tried to streamline the

whole process for our awards system. Unfortunately, it will be a year and a half before anyone sees the output of this program update, because the nominations process for 2011 is just now finishing up. That's another area of improvement—where the awards process used to take 18 months from nomination to presentation, the cycle will be shortened to 10 months. We're really compressing the schedule, but that won't happen until after the 2011 meeting.

With these improvements, I believe we've made it easier to recognize our best and brightest members. And that's really one of the key functions of a professional society.

Q. The TMS Foundation announced a new initiative to support materials science and engineering service outside the classroom or lab, through a collaboration with Engineers Without Borders USA. What about the Engineers Without Borders program made it a good fit for TMS support?

A. In 2009 our Materials and Society Committee was authorized and became active, and their emphasis was how we, as engineers and scientists, can make a positive impact on society, both locally and globally. This Engineers Without Borders project was a direct outgrowth of that committee. The project was ideal because we involved our Material Advantage chapters. We've found that students at this level are enthusiastic supporters of the kinds of concepts Engineers Without Borders emphasizes, so it was a natural fit between extending our outreach and involving our student chapters. This is a one-year trial, but we're very hopeful that it will be something we can continue to support through the Foundation.

Q. What are the key achievements of the TMS Board of Directors during your term?

A. In no particular order, our accomplishments include the honors and awards update; keeping the society financially strong even through the economic downturn; and planning for the future growth of TMS.

We created and approved the Women in Materials Science and Engineering Committee, and completed the update of our bylaws and administration policy. That process started almost two years

ago, and granted, may not be very exciting but it is very important we had our bylaws in place. We continued to work on membership rules, and how to keep members involved, even holding our membership dues constant for 2010.

The continuation of the Alliance of the Americas was fruitful in 2009. We met with the Metallurgical Society of the Canadian Institute of Mining, Metallurgy and Petroleum (MetSoc) at their annual meeting in Canada, and have been very active with the Brazilian Metallurgical, Materials and Mining Association (ABM), with a joint conference scheduled for 2010. We hope this will be the first step in continued collaborations among the Alliance of Americas societies.

We also worked at intersociety cooperation in the area of extractive processing, coordinating meeting scheduling to reduce conflicts between the Society for Mining, Metallurgy, and Exploration (SME) and MetSoc.

In the areas of advocacy, undergraduate education, and K-12 education we continued to work at better coordination with all the different materials societies. We explored new technologies like YouTube and Facebook to keep our members connected. Again we're not giving up on our old ways of doing things but trying to find new ways to meet the needs of our society, and, where possible, save money as well.

Q. What was the greatest challenge of serving as TMS president?

A. A big challenge was understanding the breadth of activities that go on within TMS. Even though I was active with the board of directors for five years prior to coming into the presidency, I've learned many new things about TMS activities since I became president, which is just amazing to me.

Also a challenge, frankly, was the demand on my time, I knew this position would require a lot of time, and the job is fun and exciting, but I still have a regular job that demands my presence. As president, you just have to figure out how you're going to fit these other things into everyday life. I want to thank my employer, Aleris, for permitting me to do this and giving me a little bit of a break. It's a very demanding job and it's not all fun and glory, but very satisfying in the end.



Your Professional Partner for Career Advancement

Introducing 4 more reasons to renew your TMS membership in 2010!

- 1.** E-mentoring – Designed to assist colleagues at every career level with professional development.
- 2.** Consultant Resources – A compendium of tools, templates, and tips to ensure your business infrastructure is sound.
- 3.** TMS On Reserve– An anthology of 12 newly-digitalized, library archive volumes of foundational documents and select conference proceedings from the American Institute of Mining, Metallurgy, and Petroleum Engineers (AIME).
- 4.** OneMine – A collaborative effort among societies to create a single global resource for mining and minerals research. TMS members receive a special subscription rate.

Enjoy these and the numerous other TMS benefits you've come to value by accessing our sleek, redesigned Members Only Web pages.

Discover how all of your TMS professional essentials are just a click away!

<http://members.tms.org>

LEARN • NETWORK • ADVANCE

www.tms.org





Updates on friends and colleagues in the materials community

TMS e-Mentor Program Continues to Grow



Ben Poquette



Nitin Chopra

Two additional TMS members are offering their insights on career development strategies as TMS e-Mentors. Providing an industry perspective is Ben Poquette, president of Keystone Materials LLC. Nitin Chopra, assistant professor at the University of Alabama, can advise on career questions related to the academic sector. They join the inaugural TMS e-Mentor team of Thomas Battle, senior metallurgist, Midrex Technologies and current chair of the TMS Extraction & Processing Division Council; Chandler Becker, materials research engineer at the U.S. National Institute of Standards and Technology (NIST); Jeffrey Fergus, professor at Auburn University; and Robert D. Shull, group leader of the Magnetic Materials Group at NIST and 2007 TMS President.

Launched in November 2009, the TMS e-Mentor program is a new member benefit designed to meet the career development needs of students and young professionals, while also providing an additional networking opportunity to those more established in their careers. The latest addition to the suite of resources available through the TMS Job and Financial Security Resource Center, the TMS e-Mentor program offers the opportunity to conveniently and confidentially pose questions to an experienced TMS member on day-to-day or long-term career issues.

To begin using the TMS e-Mentoring Program, log on to the Members Only home page and select “e-Mentor Program.”

TMS Welcomes New Members

At its October meeting, the TMS Board of Directors approved a slate of 34 new members representing 11 countries and an array of materials science and engineering disciplines. Please join us in congratulating these individuals as they begin to explore the many personal and professional growth opportunities offered to them as full members of TMS:

- Thomas L. Aldrich: ASARCO LLC, Tucson, Arizona.
- Iyad Talal Alzaharah: KFUPM, Dhahran, Saudi Arabia.
- Lynn H. Baldwin: Fort Worth, Texas.
- Richard S. Bradley Jr.: CQE Systems, Inc., Wheaton, Illinois.
- Renee Downie: The Equity Engineering Group, Inc., Houston, Texas.
- Michael Driver: McKeesport, Pennsylvania.
- Oladapo O. Eso: ATI Engineered Products, Huntsville, Alabama.
- Janardhan Gangojirao: Shimoga Karnataka, India.
- Jicheng Gong: University of Oxford, United Kingdom.
- Isaias Almaguer Guzman: Servicios Indust Penoles SA CV, Torreón, Mexico.
- Eugene E. Haller: University of California, Berkeley.
- Vincent H. Hammond: Army Research Labs.
- Xiaohua Hu: McMaster University, Ontario, Canada.
- Mitsuo Ishii: Nippon Steel Corporation, Tokyo, Japan.
- Jagannadham Kasichainula: North Carolina State University, Raleigh.
- James E. Krzanowski: University of New Hampshire, Durham, New Hampshire.
- Fiona Levey: Northborough, Massachusetts.
- Xiping Liang: GCL Holding Company Ltd.
- Freddy O. Martinez: KB Alloys LLC, Robards, Kentucky.
- Nelida Mingolo: Universidad de

Buenos Aires, Argentina.

- Peter D. Moran: Michigan Technological University, Houghton, Michigan.
- Renee Pedrazzani: University of Rochester, New York.
- Mihriban O. Pegguleryuz: McGill University, Montreal, Canada.
- Charles A. Pitzer: Pitzer Consulting, El Segundo, California.
- Siba P. Ray: Alcoa, New Kensington, Pennsylvania.
- Rodney G. Riek: Harley Davidson Motor Co., Wauwatosa, Wisconsin.
- Ralph R. Sawtell: Alcoa, Cleveland, Ohio.
- Tania M. Slawewski: The Pennsylvania State University, University Park.
- Oleksandr Vasylyev: Institute for Problems of Materials Science, Kyiv, Ukraine.
- Hakon Viumdal: Tel-Tek, Porsgrunn, Norway.
- Hong Nguyen Vu: Institute of Chemical Technology, Prague 6, Czech Republic.
- Mingxu Xia: BCAST, London, United Kingdom.
- Hideyuki Yasuda: Osaka University, Japan.
- Jiaming Zhang: Ann Arbor, Michigan.

Jeffrey Wadsworth Receives 2009 National Materials Advancement Award

Jeffrey Wadsworth, Battelle Memorial Institute president and chief executive officer and TMS Fellow, received the 2009 National Materials Advancement Award from the Federation of Materials Societies at a reception on December 9. The award was conferred on Wadsworth for the major role that he has played in national science and technology policy, with a particular emphasis on the role and contributions of materials science and engineering.



TMS Member Profiles

Meet a Member: Xingbo Liu: TMS' "Energetic" 2010 Early Career Faculty Fellow

By Lynne Robinson

Xingbo Liu's career path was revealed to him in the blink of an eye.

He was on a high school field trip to the Institute of Metal Research, about a mile from his home in Shenyang, northeastern China, when he peered through a transmission electron microscope (TEM) for the first time. "I remember seeing materials down to the atom scale and thinking, 'That's so cool.' Then, I thought, 'I want to do that,'" he recalled. "It was amazing to see something so tiny."

It was little wonder that Liu was taken with the view through the TEM. With his father's being a mechanical engineer and his mother a metallurgist, the lure of materials science was almost a genetic predisposition. His pursuit of "the cool" initially took him to the University of Science and Technology, Beijing, where he was ultimately drawn to research superalloys for jet engine turbines. "It was just really exciting for me to be able to help make something that could fly," he said.

Now an assistant professor in the Mechanical and Aerospace Engineering Department at West Virginia University, Liu has turned his attention to something that he finds not only exciting, but also urgently needed—the development of sustainable sources of

energy. Since joining TMS in 2002, he has worked diligently to "broaden awareness of new materials in new areas, such as renewable energy sources and fuel cells." Currently the JOM advisor for the Energy Committee, Liu is also vice chair of the High Temperature Alloys Committee and was a founding member of the TMS Energy Conversion and Storage Committee. This year marks two new milestones in his TMS involvement. He is a lead symposium organizer for the first time at the TMS 2010 Annual Meeting, namely for Materials in Clean Power Systems V: Clean Coal-, Hydrogen Based-Technologies, Fuel Cells, and Materials for Energy Storage. And, he was named the 2010 TMS Early Career Faculty Fellow.

As a requirement of the Early Career Faculty Fellow award, Liu is presenting the TMS Young Leader Tutorial Luncheon Lecture at the Annual Meeting and, not surprisingly, his topic is "Energy Materials—Past, Present, and Future." Said Liu, "I'm going to make this fun. I plan to present a picture about how energy use has evolved, from ancient India, to the invention of the steam engine, to the impact of high temperature, nickel-based alloys and the development of high efficiency

fuel cells. I want to encourage broad interest in the topic so that the audience will want to learn the details on their own."

As for the Materials in Clean Power Systems V symposium, Liu said that he is particularly pleased that this year's program features a strong energy storage component, focused primarily on energy conversion and generation.

The larger context for Liu's scientific interests is currently shaped by his 18-month-old son, Ethan—"My new inspiration," he notes. An avid reader of philosophical works, Liu is particularly intrigued by the contributions of Bertrand Russell, considered a founder of analytic philosophy. "To me, philosophy is like reading a review paper about the universe," he said. "Every time I study it, I find something new. It challenges me and keeps me from just focusing on what is going on today."

Occasionally, Liu also finds time to play tennis, although since Ethan's birth, he admits to "playing more Wii tennis." His wife, Li Zhao, first taught him the sport in China in the late 1990s. "I started playing tennis with my friends and they became frustrated with me because I was a beginner and they wanted to play more competitive games. They said, 'We know someone who is more patient who can teach you,' and that's how I met my wife. She taught me for half a year and then we started dating. Then she lost her patience.

"She never did teach me how to serve."

Lynne Robinson is a news and feature writer for TMS.



Figure 1: Liu with his son, Ethan—"My new inspiration"—as they hike Mary's Peak on the Oregon Coast.

Each month, *JOM* profiles a TMS member and his or her activities both in and out of the realm of materials science and engineering. To suggest a candidate for this feature, contact Maureen Byko, *JOM* editor, at mbyko@tms.org.

the YOUNG LEADER

Volume 5, Number 1

The Newsletter of the TMS Young Leaders Committee

MEET A YOUNG LEADER: BEN POQUETTE ON BUILDING A BUSINESS

Ben Poquette can personally attest to the challenges of moving a new technology from the laboratory to successful commercial application as president of Keystone Materials LLC, a company he founded with the other inventors of the patent pending GraphiMetal™ coating process. (A detailed case study on GraphiMetal™ is posted in the Established Materials Community archive of Materials Technology@TMS.) Poquette offered the following perspectives and advice on building a technology business.



Q. How did Keystone Materials begin?

A. While still a PhD candidate at Virginia Tech, I was asked to co-advise a senior design team with my faculty advisor, Stephen Kampe. The team's project eventually focused on highly adherent metal coatings on graphite foam. By graduation, the students had submitted the application for a provisional patent. Roughly a year later, I joined Dr. Kampe to create Keystone Materials in an effort to scale up the GraphiMetal™ coating process and make it available for commercial and defense applications.

Q. What have been some of the key challenges in developing your business?

A. Having a technical background, the key challenge to me personally was the realization that the majority of our efforts would be

consumed by business considerations, such as marketing and safety.

Q. What accomplishments with Keystone Materials are you proudest of so far?

A. We were able to bring our GraphiMetal™ coatings technology from laboratory to pilot scale manufacturing within the first 12 months of our existence with strictly private funding. Also, the ability of GraphiMetal™ coatings to facilitate high quality solder joining to graphite foam, using traditional solder fluxes and alloys, has generated significant interest from the private sector.

Q. What TMS resources have you found to be particularly helpful?

A. Networking, networking, networking. Even as an undergraduate student, I realized that the TMS membership is populated by great people, and being involved is your ticket to meeting those people.

Q. What advice would you give to others who are considering their own business?

A. Put together a solid team. Your product or idea may be outstanding, but it takes a great team to bring real success. It may be tempting to pull together a group of friends or even a group made up of strictly technical folks. However, both of these approaches can be a recipe for failure. Ideally, the team has members who trust each other, work well together, and have a complimentary mix of backgrounds and contacts. This, coupled with a strong leader, can make nearly any product successful.

LESSONS LEARNED FROM THE EMERGING LEADERS ALLIANCE

Preparing future engineering leaders for the challenges that they will face in advancing their organizations is the intent of the Emerging Leaders Alliance, launched in 2008. A joint venture of leading engineering societies, the Alliance offers a comprehensive leadership development experience culminating in a three-day Capstone Program.

As a partner organization of the Alliance, TMS was proud to send three of its young leaders to the Capstone Program in October 2009 (Figure 1). Said one of them, Don Siegel, University of Michigan, "The most valuable aspect of my experience was learning how to acknowledge the varied social styles of my peers."

Amy Clarke, Los Alamos National Laboratory, who also participated, said, "I am more aware of my leadership strengths and weaknesses and have identified areas for improvement that will result in personal growth, improve my ability to work effectively with others, and expand my future career opportunities."

"Participating in the Emerging Leaders Alliance truly exceeded my expectations," echoed TMS' third participant, Michele Manuel, University of Florida. "I know that the relationships that were fostered at this meeting will result in long-term professional partnerships."

Applications for the 2010 program start being accepted in the spring. For more information, go to the Emerging Leaders Alliance Web site at www.emergingleadersalliance.org.

THE YOUNG LEADER

A Young Leader is any TMS professional member in good standing age 35 or under. The goals of the TMS Young Leaders Committee are to recognize young professionals, develop in them an appreciation and awareness for TMS activities, provide services specifically tailored to young members, and encourage networking with TMS leaders and prominent society members. For more on TMS Young Leader activities, visit www.tms.org/YoungLeaders/YoungLeaders.html.

TMS YOUNG LEADER COMMITTEE OFFICERS

Gregory Thompson, Chair

Alpesh Shulka, Vice Chair

Ben Poquette, Secretary

Subhadarshi Nayak, Past Chair



Figure 1. TMS' representatives at the 2009 Emerging Leaders Alliance Capstone Program (left to right): Michele Manuel, Don Siegel, and Amy Clarke.

TMS ANNOUNCES 2010 YOUNG LEADER PROFESSIONAL DEVELOPMENT AWARD WINNERS

Congratulations to the ten young professionals selected to receive the 2010 TMS Young Leader Professional Development Award. Chosen from each of the five TMS technical divisions, the winners receive support from the TMS Foundation to attend two TMS technical conferences and are provided with opportunities to become more involved with the Society and to network with TMS leadership.



Frank Balle
Light Metals Division

A junior scientist at the Center for Mathematical and Computational Modeling, University of Kaiserslautern, Germany, Frank Balle is currently researching innovative solid state joining techniques for light metals, as well as ultrasonic techniques for characterization of the monotonic and cyclic deformation behavior of composites.

He holds a M.Sc. in mechanical engineering and a Ph.D. in materials science from the University of Kaiserslautern.



Weisheng Cao
Structural Materials Division

As a materials scientist with CompuTherm LLC, Weisheng Cao is researching the development of integrated computational tools for multi-component phase diagram calculation and materials property simulation, as well as thermodynamic, kinetic, and processing modeling for potential applications in industry. He

holds both M.S. and Ph.D. degrees in materials science and engineering from the University of Wisconsin-Madison.



Nitin Chopra
Electronic, Magnetic, & Photonic Materials Division

Nitin Chopra is an assistant professor in the Metallurgical and Materials Engineering Department at the University of Alabama. His current research interests include nano/microfabrication, nanostructure growth, and nanoscale heterostructures. Chopra earned a B.S. degree

in materials and metallurgical engineering from the Indian Institute of Technology and a Ph.D. in materials science and engineering from the University of Kentucky.



Rachel DeLucas
Extraction & Processing Division

Rachel DeLucas is a process engineer in the melting operations and SGQ plant at H.C. Starck. She holds an M.S. in manufacturing engineering from Boston University and a B.S. in archeology and materials from the Massachusetts Institute of Technology.



Sandip Harimkar
Materials Processing & Manufacturing Division

An assistant professor at Oklahoma State University, Sandip Harimkar holds a Ph.D. in materials science and engineering from the University of Tennessee and an M.S. in metallurgical engineering from the Indian Institute of Science. His research interests encompass the processing and characterization of advanced materials.



Paul Ohodnicki
Electronic, Magnetic, & Photonic Materials Division

Paul Ohodnicki is a research and development engineer with the vacuum coatings group at PPG Industries, where he works on new product development of large area glass coatings. He received a B.S. in both engineering physics and economics at the University of Pittsburgh and earned his Ph.D. in materials science and engineering at Carnegie Mellon University.



Andre Phillion
Light Metals Division

An assistant professor with the School of Engineering at the University of British Columbia, Andre Phillion previously worked as a post-doctoral fellow with the Computational Materials Laboratory at the Ecole Polytechnique Fédérale de Lausanne, Switzerland. His current research interests include developing new experimental and mathematical modeling tools to understand the relationships between microstructure and physical properties of multi-phase materials during phase transformations.



Doug Spearot
Materials Processing & Manufacturing Division

Doug Spearot is an assistant professor in the Department of Mechanical Engineering, University of Arkansas, where his research focuses on computational materials science, nanoscale material behavior, and multiscale structure-property relationships. He holds a B.S. in mechanical engineering from the University of Michigan and earned his M.S. and Ph.D. in mechanical engineering, with a focus on computational materials science, from the Georgia Institute of Technology.



Kinga Unocic
Structural Materials Division

Kinga A. Unocic is using advanced characterization techniques to study high temperature thermal barrier coatings and thermally grown oxides on metallic alloys as a research staff scientist with the Corrosion Science and Technology Group at Oak Ridge National Laboratory. She received her M.S. degree in metallurgical engineering from AGH-University of Science and Technology in Krakow, Poland, and her Ph.D. in materials science and engineering from Ohio State University.



James Yurko
Extraction & Processing Division

James Yurko is the co-founder, process development manager, and chief engineer of Electrolytic Research Corporation LLC. He received his B.S. in materials science and engineering from the University of Michigan and holds a Ph.D. in metallurgy, with a minor in business, from the Massachusetts Institute of Technology.

PROFESSIONAL PREFACE

Volume 17, Number 1

The Newsletter for Student Members of The Minerals, Metals & Materials Society



GRADUATE STUDENT SPOTLIGHT: PENN STATE AND CASE WESTERN RESERVE UNIVERSITIES

Last fall, TMS established a Graduate Student Advisory Council to address the professional needs of graduate students within the society. The council held an initial meeting at the Materials Science and Technology 2009 conference in Pittsburgh, Pennsylvania, last October and will reconvene at the TMS 2010 Annual Meeting in Seattle, Washington, this month to further look at ways that TMS can meet the unique needs of graduate students.

On campus, many schools have their own organizations to serve these students. This edition of *Professional Preface* looks at the activities of the on-campus graduate student groups at Pennsylvania State University and Case Western Reserve University.

Pennsylvania State University

In the summer, when most undergraduates head home, student activities on campus often come to a halt. Last year, the graduate students at Pennsylvania State University (Penn State) decided to take advantage of this downtime to plan a lecture series geared toward their own needs, according to James Saal, a doctoral student in Penn State's materials program and vice chair of the TMS Graduate Student Advisory Council.

The graduate students organized a lecture series that featured talks by faculty members and alumni from the materials science and engineering department and focused on post-graduate career options for students. The lecture series also incorporated presentations from faculty members in other disciplines, including a talk by one of Penn State's business professors on entrepreneurship. The summer series ended with a tour of a steel plant outside Harrisburg, Pennsylvania.

For the plant tour, it made sense, Saal said, to coordinate the trip with the undergraduate students at Penn State in order to benefit as many students as possible and to help defray the cost of the trip. The undergraduate and graduate groups are mostly separate organizations, but there is a lot of coordination among the different materials groups on campus. Last year, Penn State's graduate group participated in the American Cancer Society's Relay for Life. In 2010, they plan to participate again in this competitive fundraising event and may even challenge the undergraduate Material Advantage club at their school to form their own team.

Other plans for Penn State's graduate students in 2010 include activities as varied as movie nights and etiquette dinners. The graduate students also plan to arrange meetings and luncheons that encourage student interaction with the distinguished speakers who regularly visit the campus as part of the materials department's seminar series.

Case Western Reserve University

In 2009, the Graduate Materials Society (GMS) at Case Western Reserve University added a new event to its annual line-up: a graduate student research colloquium. In November, the GMS sponsored an event in which three students gave 15-minute presentations on their research.

It was a volunteer-based activity just for graduate students, according to Lisa Deibler, treasurer of the GMS and secretary of TMS's Graduate Student Advisory Council. The goal was to create a casual environment where graduate students could share their

2010 STUDENT AWARD WINNERS

Each year, the TMS Foundation and TMS technical divisions fund scholarships and awards to help students pursue their academic goals. The application deadline for 2011 scholarships and awards is March 15, 2010. Scholarship applications and submission requirements can be accessed through www.tms.org/Students/Awards.html. The following student members received this year's awards.



1. TMS J. Keith Brimacombe Presidential Scholarship

"I feel incredibly honored and privileged to receive the J. Keith Brimacombe Presidential Scholarship Award. This award will generously help fund my final year of undergraduate education, and give me the opportunity to attend the TMS conference to network with professionals in my field and further develop my research interests."

Kelsey Stoerzinger, Northwestern University



2. TMS Outstanding Student Paper, Graduate Division, First Place

"TMS has been and will continuously be a very important part in my career development since it was firstly introduced to me by my advisor, Dr. Xinghang Zhang, in 2005. I am very delighted and honored to be the recipient of this prestigious award. I would like to express my sincere gratitude to TMS for providing various good opportunities not only for me, but also for many other young scientists."

Engang Fu, Texas A&M University



3. TMS Outstanding Student Paper, Graduate Division, Second Place

"It is a great honor for me to be recognized by an outstanding society such as TMS with this award. I would like to dedicate this award to my family and my advisors, Profs. Peter K. Liaw and Hahn Choo, for their invaluable support and guidance throughout my Ph.D. study. I would also like to thank TMS for their continuous support to student members. This award has already boosted my confidence and has encouraged me to continue to pursue and achieve my education and career goals."

Soo Yeol Lee, University of Tennessee



4. Electronic, Magnetic & Photonic Materials Division Gilbert Chin Scholarship

"I'm so honored to be the recipient of the EMPMD Gilbert Chin Scholarship. I have dedicated many hours to extracurricular research, and am so pleased to see that it has paid off. This scholarship also encourages me to continue my education and remain an active part of TMS in the future. Thank you EMPMD of TMS!"

Sarah Miller, Washington State University



5. Extraction & Processing Division Scholarship

"I am extremely grateful to be a recipient of the generous EPD Scholarship for the 2009-2010 school year. It is nice to have the backing of such a great organization, as TMS is, to help me get through my final year in college."

(CONT. ON NEXT PAGE)

(CONT. ON NEXT PAGE)

2010 STUDENT AWARD WINNERS (CONTINUED)



The financial, academic, and multiple other resources TMS has provided me with are above and beyond what would normally be expected from a student's standpoint. Thank you once again for your generous gift.
Eric Young, South Dakota School of Mines

6. Extraction & Processing Division Scholarship

"I feel very fortunate for the opportunities I have received as a metallurgical engineering student and as a member of TMS. I am grateful for the scholarship I have received from TMS and the ability to continue studying and being a part of the up and coming technology that is currently being developed."

Ryan Morrison, University of Utah



7. Extraction & Processing Division Scholarship

"It is a great honor for my efforts to be recognized by the TMS. This award will help me to pursue graduate studies in metallurgy."

Kalen Jensen, University of Alberta



8. Extraction & Processing Division Scholarship

"Thank you so much for the opportunity you have provided me by choosing me as the recipient for the Extraction & Processing Division Scholarship Award. I am very grateful to receive this award. Not only will this scholarship help to provide financial assistance for the upcoming school year, it also gives me great encouragement for my future in the materials science field. I will strive to do the very best I can and I hope to be an important asset to the study of metallurgy and materials science."

Erin Diedrich, Washington State University



9. Light Metals Division Scholarship

"It is truly an honor to receive the TMS Light Metals Division Scholarship. This scholarship will help to alleviate the cost of attending The Pennsylvania State University and to further my education in the field of materials science and engineering. My research with magnesium and aluminum has helped me to understand the importance of light metals and I hope to contribute to this specific area of metallurgical sciences. The Department of Materials Science and Engineering at Penn State and my research advisor, Dr. Zi-Kui Liu, have greatly helped me to fully embrace the field of materials. I am proud to be recognized by TMS and appreciate the encouragement to pursue excellence in the fascinating field of materials science and engineering."

Laura Jean Lucca, Pennsylvania State University



10. Light Metals Division Scholarship

"I am very honored to receive such a prestigious award from one of the largest materials science and engineering societies in the world. I am truly grateful to TMS for their generosity and encouragement. The provided financial support will help me pursue my studies and research and attend future conferences. I would also like to thank the students and professors of the Materials Engineering Department of McGill University for their passion and enthusiasm."

Dmitri Nassyrov, McGill University



11. Light Metals Division Scholarship

"This scholarship gives me the funds to continue my education. It allows me to take the 18 credits I want to, instead of working at a minimum wage job. This scholarship will allow me to devote more time to my classes, meaning I will not only continue my education but I will receive a better, more complete education because of this scholarship. And for that, I thank you."

Michael Fank, University of Wisconsin



12. Materials Processing & Manufacturing Division Scholarship

"I am honored to be a recipient of the MPMD Scholarship and to join the prestigious list of others who have received this award before me. As a second year recipient, I feel that the previous support of TMS is making me better all the time. Thanks to the support of TMS, my future is looking brighter all the time."

Eric Young, South Dakota School of Mines



13. Materials Processing & Manufacturing Division Scholarship

"I am exceedingly grateful to TMS and the Materials Processing & Manufacturing Division for honoring me with the MPMD Scholarship. This award is a valuable contribution to my materials education, and it encourages me to pursue greater endeavors in education, professional development, and materials research. I would also like to thank the fantastic faculty at Washington State University for their unwavering support."

Whitney Patterson, Washington State University



14. Structural Materials Division Scholarship

"As a student, I am extremely thankful for the commitment of TMS in developing the next generation of professional engineers. The organization is not only a great technical resource, but it also provides me the opportunity to interact with and learn from other people within the materials community."

David Cole, University of Cincinnati



15. Structural Materials Division Scholarship

"I would like to thank you for awarding me the Structural Materials Division Scholarship. This scholarship has given me the opportunity to continue to excel in my field of study. It has assisted me in funding my education. Given this scholarship I will be able to focus more on my academics and continue to strive to keep my scholarship and to be honored for more scholarships. This will help me in my achievements and provide encouragement to be more successful. I appreciate this scholarship very much, and thank you for the support."

Mohamad Zbib, Washington State University

GRADUATE STUDENT SPOTLIGHT (CONTINUED)

research progress with their colleagues. The three presenters represented various stages of the process, from the beginning stages of master's degree research to a nearly finished doctoral project.

While some of Case Western's GMS activities are exclusively for graduate students, Deibler thinks that coordination with their undergrad counterparts is also valuable.

"Undergraduates have a different focus," Deibler said, explaining the need for separate groups. "But it's good to do things together, too, so they can see what it's like to be a grad student."

The two groups come together for a weekly department lunch, an event typically attended by 20–30 people. Everyone pitches in a few dollars, and students take turns preparing lunch. Other GMS social and community activities in 2009 included a Grad Student Night Out at a local billiard hall, barbeques, and participation in the American Cancer Society's Relay for Life fundraising project.

For 2010, the Case Western GMS is planning to repeat its successful research colloquium and other events, but also is developing new activities. One new project encourages materials students to share their favorite hobbies. Students will meet regularly to take turns teaching their fellow students about their outside interests, opening these grad students to a whole new set of skills that can't be found in a materials classroom.

Enhanced for the Web

This article appears on the JOM web site (www.tms.org/jom.html) in html format and includes links to additional on-line resources.

Advanced Materials Are a Game Changer in the Winter Olympics

Lynne Robinson

It starts with a push.

Propelled by the strength and collective will of four powerful sprinters gripping its sides, an Olympic bobsled launches from a frozen start ramp, accelerating from a standstill to 40 kilometers an hour in less than five seconds. At about 50 meters into the race, the team hops into the sled one by one, with the pilot already preparing to hit the first of 16 turns built into the ice-encased track of the Whistler Sliding Centre, site of the bobsleigh competitions for the 2010 Vancouver Winter Olympics. Like a fiberglass bullet, the sled shoots down a vertical drop of 152 meters, subjecting its crew to crushing G-force and bruising jolts around the curves, while attaining speeds of nearly 150 kilometers an hour. Victory at the end is measured in hundredths of a second, with almost imperceptible factors deciding the difference between a medal run and a disappointing finish.

For the 2010 Olympics, the Swiss Bobsleigh Federation (SBSV) wanted to make sure that those factors had nearly nothing to do with the construction of the sled. Under the project name CITIUS—which echoes the Olympic motto, “Citius, Altius, Fortius (faster, higher, stronger)—SBSV marshaled the talents and resources of the Swiss Federal Institute of Technology (ETH



Figure 1. “A bobsled is a fascinating vehicle,” notes Ulrich Suter, professor in ETH Zurich’s Department of Materials and CITIUS project coordinator. “It has no engine and derives its kinetic energy solely from the gravitational acceleration in the ice channel and the initial thrust by the crew before they board the sled.” (Courtesy ETH Zurich)



Figure 2. SBSV athletes and the CITIUS endure the wind tunnel test, where the sled was challenged to withstand a 150 kilometer per hour headwind. (Courtesy ETH Zurich)

Figure 3. Dany Heatley, who will play for Team Canada at the 2010 Winter Olympics, puts the high-performance fiber composites in his equipment to the test. The adoption of advanced composite materials has revolutionized hockey stick design, both in terms of weight and performance. Since a composite structure is a laminate of individual layers, there is much greater control over a stick’s stiffness and mass distribution, as well as the strength and toughness profile, according to Travis Downing of Easton Hockey. The anisotropy of fiber also enables the freedom to control the strength, stiffness, and torsion characteristics of a stick based on fiber orientation in each layer of the laminate. (Courtesy Easton Hockey)



Zurich), a consortium of industrial partners, and current and former bobsleigh athletes to work on “building a better bob” (Figure 1).

THE SCIENCE OF THE SLED

“An initial question we asked ourselves was ‘what slows down a bobsled?’” said Ulrich Suter, professor in ETH Zurich’s Department of Materials and CITIUS project coordinator. “After a careful analysis, we decided to break the problem into a number of simpler tasks. Aerodynamics is clearly important, especially in the very fast track at Whistler. The shape and surface structure of the runners are also very relevant. The hull and chassis materials, as well as the dynamics within the system, play a crucial role in the mechanical dissipation of energy in the bobsled. And, above all, safety is paramount—the sled must survive a crash at full speed and protect the crew. We numerically simulated all key aspects of the sleds and tried to isolate the most important factors, and then experimentally tested our assumptions to optimize the design.”

A particular challenge for CITIUS was developing a state-of-the-art bobsled in accordance with the rules for construction and design enforced by the Fédération Internationale de Bob-sleigh et de Tobogganing (FIBT), the governing organization for competitive bobsledding. The runners, for instance, have to be constructed from a rigidly defined steel procured from a prescribed source, with any type of modifying treatments “forbidden, including those which even cause only a local variation of the physical characteristics and/or of the composition and/or structure of the material.” Steels used elsewhere on the sled are more generally described

as “an alloy of iron and carbon with an iron content of more than 50 percent,” while “rubber or rubber-like material” can be incorporated into the sled for the purpose of damping vibrations. Hulls have no prescribed material at all. Suter said he was surprised, actually, at “how many unspecified areas were left in a seemingly very complete—some might say overly complete—book of rules.”

Working within these parameters, a team of more than 20 ETH Zurich scientists and engineers from a wide range of disciplines applied their specific expertise to different aspects of the CITIUS bobsled. A battery of tests revealed the sources and nature of vibrations, which forces were exerted where on the chassis, and the specific stiffness and strength of certain materials. “Our simulations indicated that several apparent inefficiencies of the sleds might be avoided with an appropriate choice of materials,” said Suter. “However, almost all standard elastomeric materials were inadequate to the demands of the sport. And, many tested adhesives proved insufficient under the (dynamic) mechanical and thermal stresses of bobsled racing.”

To address these issues, the research team created elastomeric damping materials specifically for the CITIUS, while also developing a composite hull strengthened with long-fiber reinforcement. Once the components were assembled into prototype sleds, athletes from the SBSV tested the CITIUS in the wind tunnel at the Audi works in Ingolstadt, Germany (Figure 2). The real moment of truth for the project occurred when, bristling with sensors to measure forces, driving dynamics, and aerodynamic properties, the CITIUS hurtled down an ice track for the first time near Innsbruck, Austria. Although highly guarded about revealing details of the CITIUS’ development and performance, the research team was pleased with the results, according to

the CITIUS Dossier posted on the ETH Zurich Web site.

A WEIGHTY MATTER

Whether smoothing the performance of a bobsled careening down the Whistler ice track, or giving an aerials skier an extra bounce into the Canadian sky, advanced materials technologies like those used in the CITIUS project will be on prominent display at this year’s Winter Olympics. The quest for a competitive edge through advancements in engineering isn’t limited to these elite athletes, however. Said Travis Downing, a materials engineer in research and development at Easton Hockey, California, “Once full composite hockey sticks were introduced onto the market about ten years ago, they immediately became the ‘must have’ stick among professional players. Subsequently, amateur players were quick to jump on that trend, as well. The fact that it is nearly impossible to find a wooden hockey stick anymore speaks volumes to the adoption rate of composite sticks” (Figure 3).

A key advantage of composite hockey sticks over wooden ones, said Downing, is weight. Wooden sticks routinely tip the scales at more than 650 grams, while modern composite sticks can be as low as 400 grams. By being lighter, composite sticks are easier to control and provide for greater swing velocity. Downing said that composite hockey sticks have also been found to be superior to wooden ones in storing and rapidly releasing strain energy, which enables players to boost their shot velocity. From a manufacturing standpoint, composites make it possible to reproduce a hockey stick’s properties exactly each time, while the organic nature of wood tends to introduce inconsistencies from stick to stick (Figure 4).

“For most sports, lowering the weight of the equipment without re-

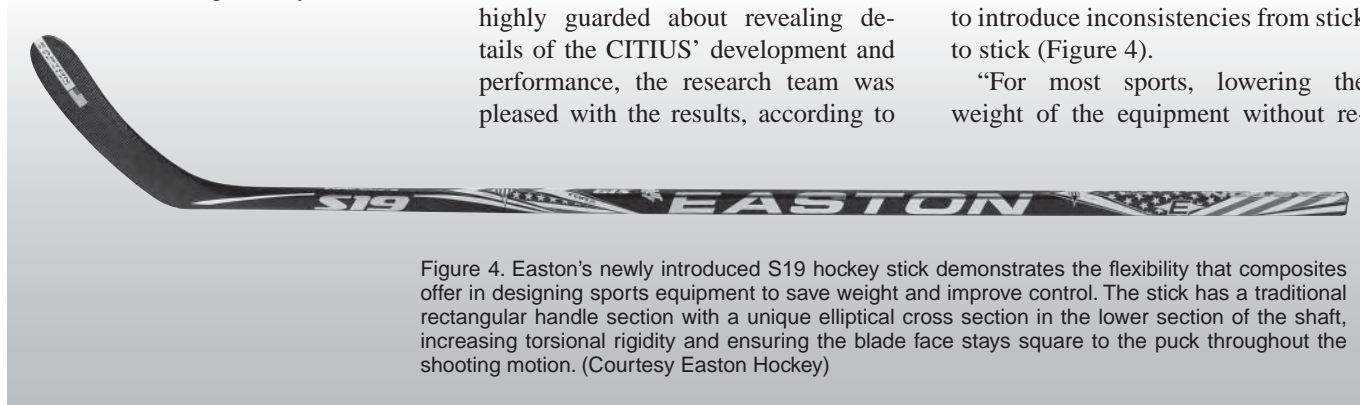


Figure 4. Easton’s newly introduced S19 hockey stick demonstrates the flexibility that composites offer in designing sports equipment to save weight and improve control. The stick has a traditional rectangular handle section with a unique elliptical cross section in the lower section of the shaft, increasing torsional rigidity and ensuring the blade face stays square to the puck throughout the shooting motion. (Courtesy Easton Hockey)

ducing performance is highly desirable,” said Katharine Flores, an associate professor at Ohio State University and TMS member who was tapped by NBC to contribute to its Science of the Olympic Winter Games educational series. “This can be addressed both by improved materials and improved processing technologies. Beyond that, the design really depends on the sport. With skis, for instance, the most important consideration is probably stiffness. If the ski deflects or twists a lot, that steals kinetic energy—and speed—from the skier” (Figure 5).

“Perhaps the most interesting thing about sports equipment is what doesn’t drive change—cost,” Flores continued. “Even recreational users are willing to pay more for perceived improvements in performance.”

Many of the advancements in sporting equipment owe their origins to the aerospace industry, particularly in the application of composites and lightweight alloys. Said Downing, “The entire sports equipment spectrum—from baseball and softball bats, to tennis rackets, to golf shafts, to bicycle and motorsports structures—uses essentially the same carbon fiber and two-part epoxy that was originally developed for military and aerospace applications.”

Even with space age technology, the quest for optimum performance in sporting equipment can be challenging. “Because hockey is such a fast-paced sport with frequent collisions, it becomes crucial to have the proper balance of performance and durability in a stick,” said Downing. “The unfortunate reality is those factors are largely in opposition to one another, given the desire to maintain the lightest structure possible. Composite suppliers tend to address the problem by adjusting the epoxy formulation, with variation in fiber properties also factoring into the equation through alteration of tensile modulus, strength, and elongation to failure.”

TECHNOLOGY VS. TECHNIQUE

The next big advancement in sports materials technology may be launched by the power of small. Easton-Bell



Figure 5. Skis have evolved from simple wooden slats to complex systems of layered materials, customized to a specific use. Stiffness is a highly desired characteristic for downhill skiers, who depend on it for control as they fly down a slope. Joey Discoe, seen here in moguls training, needs a more flexible ski to execute the jumps, flips, and spins required in this competition. Specialty alloys, carbon fiber, and even piezo-ceramics for vibration damping have been incorporated into modern ski design. (Courtesy Todd Shirman, U.S. Ski Team)

Sports, of which Easton Hockey is part, has already had initial success adding functionalized multi-wall carbon nanotubes (CNTs) to strengthen epoxy resin for bat, bicycle, and hockey applications. “It has been difficult to realize the full promise that single-wall CNTs has shown in the lab, because the processing technology needed to exploit their full potential has not reached maturity,” said Downing. “The next few years, however, will see additional leaps forward in nanostructured composites for sports applications.”

As exciting and anticipated as these potential advancements may be, Flores noted that concerns about technology overshadowing technique in the elite sports world beg to be addressed, fueled by such recent controversies as the Speedo® LZR Racer™ suit worn by Michael Phelps in the 2008 Beijing Olympics.

“There are some important ethical considerations at work in the use of advanced materials and technological advancements in general,” she said. “The Olympics, in particular, are supposed to be about reaching for the pinnacle of human athletic achievement, with ‘hu-

man’ being the operative word. A lot of people feel that it really shouldn’t be about who has the latest and greatest gadget. There is a fine line between engineering the equipment to highlight the capabilities of the athlete—freeing him or her from various physical constraints—and engineering the equipment to artificially improve the performance of the athlete.

“For the recreational athlete, however, I think these ethical considerations go away,” she continued. “There’s nothing wrong with making equipment that improves the performance and, as a result, the experience of recreational players so they will enjoy the game more and stick with it.”

ACKNOWLEDGEMENT

JOM would like to acknowledge Francis H. (Sam) Froes, retired director and department head, Materials Science and Engineering Department, University of Idaho, and TMS member for the insights and background information he contributed to this article.

Lynne Robinson is a news and feature writer with TMS.



Magnesium Elektron

SERVICE & INNOVATION IN MAGNESIUM



By Land, Sea or Air Magnesium Elektron Alloys are there....

Magnesium Elektron is a world leader in the production of high performance magnesium alloys and products. Magnesium Elektron began production of magnesium in 1936 and subsequently developed a wide range of magnesium alloy systems and products. Over time, Magnesium Elektron has patented 21 magnesium alloys for a wide variety of applications. New magnesium alloys recently developed by Magnesium Elektron include Elektron®21 and Elektron®675, as well as Elektron®WE43 now offered in rolled form.

Magnesium Elektron has 7 manufacturing sites located in US, Canada, United Kingdom and Czech Republic, all dedicated to producing high performance alloys in cast, wrought and powder form. In addition, Magnesium Elektron operates a fully integrated magnesium engraving plate business, while also producing zinc, brass and copper engraving plates and support chemicals which serve the Graphic Arts industry.

The company is part of the Luxfer Group, an international manufacturer of high performance engineering materials including magnesium alloys, zirconium products and high pressure lightweight gas cylinders. Magnesium Elektron personnel will be presenting 5 technical papers at TMS 2010 139th Annual Meeting and Exhibition. Please visit us at Booth #437 on the exhibition floor of the Washington State Conference Center. Also visit our website at www.magnesium-elektron.com for contact information.

Magnesium Elektron North America
1001 College Street PO Box 258
Madison, IL 62060
Phone: 800-851-3145
Web: www.magnesium-elektron.com

Please visit us at TMS 2010 booth 437.



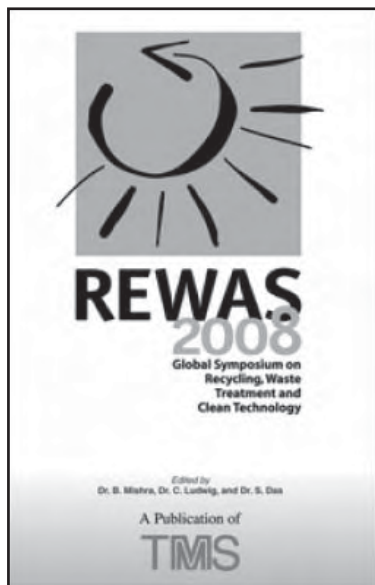
SIMPLIFIND

Tap into the incredible network of The Minerals, Metals & Materials Society with The Minerals, Metals & Materials Society Marketplace. Powered by MultiView, the Guide gives materials and metallurgy professionals a faster and easier way to find great vendors.

Simplifind your search today at tmsmarketplace.com.



Visit the Knowledge Resource Center to reserve your copy today!



REWAS 2008: Global Symposium on Recycling, Waste Treatment and Clean Technology

by B. Mishra, C. Ludwig, and S. Das, editors

The 2008 Global Symposium on Recycling, Waste Treatment and Clean Technology (REWAS 2008) is the third in a series of international conferences to address the continuing globalization of environment protection through progress in recycling technology, re-engineering of the production system, and clean technologies. The conference incorporates the Fifth International Symposium on Recycling of Metals and Engineered Materials and R'08 - the World Congress on the Recovery of Materials and Energy for Resource Efficiency. Technical topics covered in the conference proceedings include:

- Aluminum By-product Recovery and Secondary Production
- Automotive Recycling
- Case Studies in the Development of Waste Treatment Technologies
- Clean Technology and Re-engineering of Current Processes
- Composite Materials
- Design and Engineering of Waste Treatment Plants
- Economic Evaluation of Waste Treatment Strategies
- Electronic Waste
- Environmental Issues Related to Waste Storage and Recycling
- Ferrous Metals
- General Recycling and Solid Waste Processing
- Heavy-Metal Containing Waste
- Nonferrous Metals
- Precious and Rare Metals
- Radioactive Waste
- Refractory Metals
- Remediation of Contaminated Soil and Industrial Sites
- Resources, Monitoring and Characterization of Waste
- Treatment of Liquid and Gaseous Effluents
- Waste Conversion and Reutilization

TMS Member price \$64

TMS Student Member price \$49

To order these or related publications, contact TMS:

E-mail publications@tms.org • Phone (724) 776-9000, ext. 256 • Fax (724) 776-3770

Aluminum Recycling—An Integrated, Industrywide Approach

Subodh K. Das, John A.S. Green, J. Gilbert Kaufman, Daryoush Emadi, and M. Mahfoud

The aluminum industry is a leading proponent of global sustainability and strongly advocates the use of recycled metal. As the North American primary aluminum industry continues to move offshore to other geographic areas such as Iceland and the Middle East, where energy is more readily available at lower cost, the importance of the secondary (i.e., recycled metal) market in the U.S. will continue to increase. The purpose of this paper is to take an integrated, industry-wide look at the recovery of material from demolished buildings, shredded automobiles, and aging aircraft, as well as from traditional cans and other rigid containers. Attempts will be made to assess how the different alloys used in these separate markets can be recycled in the most energy-efficient manner.

INTRODUCTION

In his recent book *Aluminum Recycling*,¹ Mark Schlesinger points out that in traditional extractive metallurgy, the raw material used to produce a metal is mined from the earth and then is separated from other gangue minerals and impurities. In aluminum recycling, however, the ore body consists of scrap metal found on the ground rather than in it. He further notes that scrap comes with its own variety of gangue and impurities such as paint coatings and metal attachments, as well as dirt and other contaminants. So, while the recycling process still requires some refinement and expenditure of energy, the amounts of effort and energy involved are much less than those in refining mined ores.

The aluminum industry "Vision" document,² published in 2001, notes that the electrical energy embedded in metallic aluminum can be considered to be an "energy bank" because

it can be essentially recovered during recycling. Thus, from a sustainability viewpoint, aluminum recycling is tapping into a convenient "urban mine" of material that enables reuse while saving energy and reducing environmental impacts. This urban mine analogy is becoming increasingly real as the amount of aluminum in vehicles continues to increase in order to improve performance, reduce weight, increase fuel efficiency, and enhance safety.

See the sidebar for background on aluminum recycling.

How would you...

...describe the overall significance of this paper?

This paper introduces the concept and suggests several implementable ideas to design and commercialize recycle-friendly aluminum alloys for key market sectors.

...describe this work to a materials science and engineering professional with no experience in your technical specialty?

Most of the aluminum alloys used in the commerce today have been designed and sold commercially using primary and pure aluminum, pure alloying elements, and sometimes special elements to meet perceived customers needs. This practice is not economically and environmentally sustainable as it leads to a larger carbon footprint and lower recycling rates for the aluminum industry products.

...describe this work to a layperson?

In order to achieve the sustainability goals of a manufacturing industry, each of the commercially sold product(s) to its intermediate or ultimate customer(s), must be designed and processed keeping the recyclability in mind during the entire phase of its product life cycle.

MODELING THE URBAN ALUMINUM MINE

Modeling, together with some life cycle assumptions, has also been used to explore the impact of recycling on the overall U.S. metal supply.¹⁰ This "urban mine" model assumes that the amount of scrap that will become available in a given time frame can be predicted based on the amount of material sold into specific markets and the typical life cycle of material in these markets. For instance, building components, automobiles, and beverage cans have useful lives that are, respectively, ~50, ~15, and ~0.2 years, and the amount of metal that is sold to these markets is known and can be forecast into the future with some assurance.

Existing industry data has been used for the model. The model inputs include primary production data from 1893, secondary production data from 1913, and imports from 1911. These data are merged with market information for the last 40 or 50 years in order to project future U.S. metal supplies. The model also projects information based upon the market size and growth rates from 1990 to 2000. Specifically the percentage of the overall market and the average growth rate over the decade were, respectively: transportation (37%, 9.8%), containers and packaging (23%, 0.3%), consumer durables (8%, 4.8%), building and construction (15%, 2.6%), electrical (8%, 3.0%), machinery and equipment (7%, 4.8%), and others (2%, 1.7%).

Considerable insight has been gained from the macro-model of the urban mine.¹⁰ A major conclusion is that the automotive area, driven by the number of vehicles (~15 million per

year) and the growing amount of aluminum used per vehicle, will dominate the future scrap source picture.

RECYCLING CHALLENGES BY MARKET APPLICATION

Capturing the metal in the recycling process represents only a part of the overall recovery process. A more significant challenge is preserving the economic value of the alloying ingredients by recycling specific wrought alloys into the same or similar wrought alloys. The ideal is to recycle a specific alloy back to the identical alloy, as with beverage cans; the value of the alloy is maximized.

Transportation Recycling—The Major Recycling Opportunity

As noted in the Modeling section and in Reference 10, the transportation area is the biggest market for aluminum and the scrap generated from used autos and trucks now exceeds that from recycled beverage cans. Specifically, according to the *Aluminum Statistical Report*¹¹ the transportation market sector consumes ~8.7 million pounds or 33.9% of North American production. Over the period 2001–2005, the annual growth rate of aluminum in this market has been 5.4%. This growth is driven by the need to save weight, increase fuel efficiency, and enhance safety. The

drive toward “sustainable mobility” is increasing, and the aluminum recycling potential from the automotive sector is enormous.

Automotive recycling is relatively complex due to the large number of alloys used. In a parallel paper,¹² the authors have explored an ideal automotive recycling scenario addressing these issues. Among the alloys widely used are Al-Cu (2xxx) alloys 2008 and 2010 for body sheet; Al-Mg (5xxx) alloys 5022 and 5754 for body sheet; Al-Mg-Si (6xxx) alloys 6111 for body sheet and 6063 for structural components, including frames; and Al-Zn-Mg (7xxx) alloys like 7029, 7116, and 7129 for bumpers. Casting alloys like A356.0, 360.0, and A380.0 are used for engine and other mounting components. It is apparent from an examination of the compositions of these alloys¹² that the high-Zn 7xxx alloys are not compatible with the other alloys, and the relatively high Cu in the 2xxx alloys will not fit well with the 5xxx and 6xxx alloys

Thus the potential importance of pre-shred dismantling becomes clear. Ideally, all vehicles would be recycled and would be subject to a pre-shred disassembly process where large components of known alloy composition (i.e., wheels, bumpers, engine blocks, perhaps body sheet components like hoods, deck lids, and door panels) would be removed and segregated for remelting. Hand-held chemical analyzers could aid preliminary separation and sorting of alloys. As one example, the batching of all bumpers together—grouping alloys 7029, 7116, and 7129—would probably yield a melt that could be directly reused for bumpers as a 7xxx alloy.¹² The remainder of the auto hulk would be shredded, subjected to laser-induced breakdown spectroscopy (LIBS) sorting,^{8,9} and remelted, using the most efficient processes to reduce dross losses and maximize recovery. Of course, if/when shredding technology develops to the point where individual alloys can be identified and separated, pre-shred disassembly may not be warranted.

Another option is to revisit the idea of developing some single versatile “unalloy” that could meet many of the requirements for a large number of automotive components, thus simplifying

BENEFITS OF AND BACKGROUND ON ALUMINUM RECYCLING

The conventional benefits that are cited for aluminum recycling are energy savings, emissions reductions, and the elimination of landfill wastes. A comprehensive life cycle analysis conducted by the industry under USCAR guidance, and which involved analysis of 15 unit processes in 213 plants worldwide, verified these savings.³ Specifically, it was shown that the production of primary aluminum, when all electrical generation, transmission losses, and transportation fuels are accounted for, requires ~45 kWh of energy and emits ~12 kg of CO₂ for each kilogram of metal. On the other hand, the recycling of aluminum requires only ~2.8 kWh of energy and emits only ~0.6 kg of CO₂ for each kilogram of metal. Thus, ~95% of the energy and ~95% of the environmental emissions are saved when the metal is recycled. The energy banked in the metal during the initial melting process is recovered, with minor losses, each time the material is recycled.

A newer and more critical benefit of aluminum recycling is that it helps to maintain a viable North American aluminum fabrication industry. With the declining aluminum primary industry, the secondary industry based upon recycling now provides the bulk of domestic metal to the downstream fabrication industry.

Historically, since the start of the aluminum industry in 1888, some amount of recycling has always occurred. It has been estimated that ~70% of all the aluminum that has ever been made is still in active use.⁴ But, it was not until the advent of the aluminum can in 1965 and the buy-back programs of the Reynolds Metals Company that recycling became part of the public awareness. The success of the beverage can spawned the secondary, or recycling, industry. The large number (~10,000) of recycling centers that emerged nationwide during the 1970s and 1980s has given way to fewer but more active recycling companies with curbside collection of all recyclables that go to municipal recycling facilities (MRFs). There are now some 300 MRFs representing more than half the U.S. population and this phenomenon has generated a subsidized dealer market for aluminum cans, along with other recyclable items.

For the U.S. market, an increase of 1% in aluminum can collection is equivalent to a saving of \$12 million, so renewed effort is being put in that direction. For example, the Aluminum Association and the Can Manufacturing Institute have formed the Aluminum Can Council to develop educational and promotional programs. Other groups have also been active in this effort, notably Secat, Inc., the Center of Aluminum Technology at the University of Kentucky, and the Sloan Industry Center for a Sustainable Aluminum Industry to focus on recycling issues. This consortium has already addressed some of the cultural and societal factors that influence recycling.⁵⁻⁷

Another new development has been the advent of the industrial shredder. The shredding of large industrial scrap such as automobiles, refrigerators, freezers, and other large machinery has been complemented by the developments by Huron Valley Steel Corporation^{8,9} of color sorting and laser induced breakdown spectroscopy, making it possible to analyze the emitted plasma light from a scrap sample and determine its chemical composition. In the future, it should be economically feasible to separate and sort aluminum scrap on an alloy-by-alloy basis by virtue of the developments on an industrial scale.

the scrap stream. This has proven difficult to achieve because of the diverse performance requirements of different components. However, some progress has been made, as companies like Toyota use alloy 6022 for both inner (-O temper, greater formability) and outer (-T4 temper, greater dent resistance) body components.

Building and Construction— A Hidden Opportunity

The third largest market sector for aluminum, after transportation and containers/packaging, is the building and construction (B&C) market that also includes highway structures (e.g., lamp posts, signs, bridge decks). This market has not received much attention in regard to recycling, primarily because the life cycles of buildings and highway structures are so long, ~30–50 years, plus the smaller amounts of aluminum previously used in B&C applications. Newer architectural designs, however, have emphasized the value of aluminum to make buildings more energy efficient through the use of sun screens, cladding and shades, curtain wall construction and advanced window designs, and the potential value of recycling. The aluminum components have increased.

Recent studies at the Technical University of Delft¹³ have provided a comprehensive evaluation of recycling during the demolition of nine types of buildings located in six countries in Europe. In this study, conducted under EU regulations and employing ISO-certified protocols and contractors, the deconstruction and demolition of the buildings was closely monitored and comprehensive data were collected.

The following conclusions were among those drawn from the Delft study, all supporting the recycling of aluminum components from B&C structures:¹³

- The average aluminum collection rate for all nine buildings was 95.7%.
- Even though the aluminum content of the buildings was <1%, there was still a substantial mass of aluminum available for recovery.
- Much of the aluminum in a building is on the periphery (e.g., air conditioners, sun shades and awnings, etc.) and is easy to recover.
- Non-residential high-rise buildings

Table I. Nominal Compositions of Potential New Recycling Friendly Alloys Resulting from B&C Product Sorting and Remelting

Alloy	Al,%	Si	Fe	Cu	Mn	Mg	Cr	Zn	Ti
505X	~96.0	0.4	0.4	0.15	0.6	2.5	0.15	0.25	0.1
606X	~96.0	0.5	0.5	0.2	0.12	0.8	0.15	0.15	0.12

and factories contain much more aluminum, by 1–2 orders of magnitude, than residential buildings.

- Residential construction in warm climates contains ~20 times more aluminum than in cold climates (i.e., sun shades, reflectors). Future architectural designs are anticipated to increase this amount.
- Recovery is enhanced when a subcontractor is involved who wishes to reuse some components (i.e., windows), directly.

An examination of the *2005 Aluminum Statistical Review*¹¹ indicates that the 3.7 billion pounds of metal in this market is almost equally divided between extruded shapes and sheet products. The workhorse alloys for B&C extrusions are Al-Mg-Si alloys 6061 and 6063.^{14,15} Alloy 6061 provides the best combination of strength, cost, weldability, and corrosion resistance, while alloy 6063 is more readily extrudable with lower strength and lower cost. By contrast, for B&C sheet and plate, the most widely used alloys are the Al-Mg 5xxx series, ranging from 5050 with ~1.5% Mg to 5456 with ~4.5% Mg. These alloys are characterized by excellent corrosion resistance, toughness, weldability, and moderate strength. While the 5xxx and 6xxx alloys can usefully be remelted together, it is clearly desirable to separate the 5xxx alloys from the 6xxx alloys prior to melting to most efficiently reuse the alloying constituents.

It is fortuitous that the 6xxx alloys are primarily extrusions and the 5xxx alloys are primarily sheet and plate. Thus a rudimentary sorting of 5xxx from 6xxx alloys can be achieved by merely separating structural extrusions from sheet and plate materials at the demolition site.¹⁶

It is useful to speculate upon the alloy content likely to result if the approach of separating the sheet and plate components from the extrusions components is adopted. Table I illustrates two potential output compositions from remelting these two separations, designated 505X and 606X. These are speculative illus-

trations; a mass balance based upon the expected inputs by alloy and product would lead to more precise projections.

The projected average 505X composition in Table I is similar to a 5052-type alloy, with higher Si and Zn impurities, plus a higher Mn content (0.6% vs. a max. of 0.1 for 5052). Based upon the known performance of commercial 5xxx alloys, all of these three variances may be acceptable for direct reuse of this composition in many products. The Si and Zn impurities are not likely to be troublesome, and the high Mn content may lead to slightly higher strength. It would be practical to define a new alloy based upon the likely output from B&C recycled sheet and plate that could be reused directly in B&C applications, as well as others perhaps.

Similarly, the 606X-type represents a melding of 6061 and 6063 compositions, with variation to be expected based upon the mix of the two at a given time, which also appears potentially directly reusable; it would have useful structural strength when heat treated and aged and would be rather readily extrudable.

Thus, if component pre-sorting based upon separating rolled and extruded products is adopted during demolition, it seems likely that both output remelt compositions could be directly reused in B&C applications, including highway structures, with no further processing.

Recycling Aerospace Alloys— An Overlooked Opportunity

For decades, thousands of obsolete aircraft have been sitting in the southwest desert “graveyards,” while the demand for recycled aluminum increases. The discarded aircraft provide a large potential source of valuable metal. However cost-effective recycling of aircraft alloys is complex because aircraft alloys are typically relatively high in alloying elements like Cu (2xxx series) and Zn (7xxx series), and may contain low levels of minor elements to optimize fracture toughness.

Again it would seem that dismantling

Table II. Potential Compositions of Some Recycled Aircraft Alloys Assuming Pre-Sorting

Alloy	Al	Cu	Fe	Mg	Mn	Si	Zn	Others
R2xxx	~93	4.4	0.5	1.0	0.7	0.5	0.1	0.2
R7xxx	~90	2.0	0.4	2.5	0.2	0.2	6.0	0.2

and presorting would aid in maximizing the value of recycled aircraft aluminum.¹⁷ One technique would be to dismantle aircraft into certain logical component groups, as these typically are made of alloys of the same series. As examples, landing gears, engine nacelles, tail sections, and flaps could be presorted, and wings separated from fuselages. Such separations may be desirable anyway to permit removal of non-aluminum components before shredding.

Guidance in dismantling and presorting would be available from aircraft manufacturers who can identify the alloys used in various components. If/when such information is not available, it may be possible to identify the various alloys with hand-held mobile spectrometers. Non-aluminum components may also be readily identified using this technique. If a useful level of discrimination and separation of 2xxx and 7xxx series alloys is feasible, the compositions of recycled metal are likely to represent something like those shown in Table II.

Based upon this hypothesis, there would appear to be opportunities for direct reuse of the recycled metal in new 2024-like and 7075-type alloys. Upon solution heat treatment and precipitation aging, the properties of these remelt alloys are likely to be similar to those of 2024 and 7075. Subject to more thorough performance evaluation, there is reason to conclude that such metal might be utilized in non-fracture-critical aerospace components or in other structural market application. If, on the other hand, 2xxx and 7xxx alloys cannot be sorted before remelting, the combination of Cu and Zn is likely to require some type of beneficiation of the remelt before being very useful, even in non-aerospace applications.

Two other factors should be noted at this stage.

- First, at least small quantities of several other wrought aluminum alloys like 2219 and 6061 and cast alloys like 201.0, A356.0, and A357.0 may go into any such recycle mix.
- Second, aircraft alloys typically

have grain-refining elements such as Cr, Zr, and V present in small quantities (~0.1% or less), and the potential buildup of such elements in addition to Fe, Mg, and Si needs to be the subject of further study. This second factor will become increasingly important as newer aircraft alloys such as 2124, 2048, 7050, 7055, and 7085 enter the recycle mix.

CONCLUSIONS

In several major product areas, opportunities to enhance the recycled metal stream have been identified.

First, the potential secondary metal supply in the automotive vehicle market dwarfs all other product streams. The vehicle recycling process is complex because of the large number of both wrought and cast alloys involved. The primary opportunities to increase the value of recycled automotive aluminum arises from the ability to dismantle as many components of known alloy classes (e.g., bumpers, wheels, body sheet, castings) prior to shredding, and segregate them before remelting. Without such strategies, the recycled metal stream will be limited to the production of casting alloys, much of it overseas.

Next, in the area of building and construction, the aluminum components of buildings being demolished are readily recoverable for recycling, and can readily be sorted by extruded or rolled products, effectively separating Al-Mg-Si (6xxx) alloys from Al-Mg (5xxx) series alloys. Remelting these as segregated lots will provide compositions suitable for direct reuse in B&C applications.

Finally, if aircraft structures can be dismantled and presorted by Al-Cu (2xxx) and Al-Zn (7xxx) alloys, the segregated remelt compositions may be directly reusable in non-fracture-critical components.

More in-depth analysis and mass flow balances are needed to more precisely determine the likely compositions of recycled metal from each of these product

areas to more precisely determine the realistic opportunities and likely remelt compositions. Secat has proposed to undertake such studies collaboratively with organizations such as HVSC and other interested market leaders.

ACKNOWLEDGEMENTS

The authors acknowledge the partial support of Qatar National Research Fund through a grant from College of the North Atlantic-Qatar, Doha, Qatar.

References

1. Mark E. Schlesinger, *Aluminum Recycling* (Boca Raton, FL: CRC Press, Taylor & Francis Group, 2007), p. 9.
2. *Aluminum Industry Vision – Sustainable Solutions for a Dynamic World* (Arlington, VA: The Aluminum Association, 2001), p. 17.
3. Roy F. Weston, *Life Cycle Inventory Report for the North American Aluminum Industry, AT-2 Report* (Arlington, VA: The Aluminum Association, November 1998).
4. *Alcoa 2004 Sustainability Report* (Pittsburgh, PA: Alcoa, 2004), p. 10; www.alcoa.com/global/en/about_Alcoa/sustainability_report_2004/images/sr_online_final.pdf.
5. S.K. Das, *Light Metals 2006*, ed. T.J. Galloway (Warrendale, PA: TMS, 2006), pp. 911–916.
6. John Green and Michael Skillingberg, *Light Metal Age* (August 2006), p. 33.
7. Fred W. Morgan and Margaret V. Hughes, *JOM*, 58 (8) (2006), p. 32.
8. Adam Gesing et al., *Aluminum 2001*, ed. S.K. Das, J.G. Kaufman, and T.J. Lienert (Warrendale, PA: TMS, 2001), pp. 31–42.
9. Adam Gesing et al., *Aluminum 2002*, ed. S.K. Das and M.H. Skillingberg (Warrendale, PA: TMS, 2002), pp. 3–17.
10. William T. Choate and John A.S. Green, *Light Metals 2004*, ed. A.T. Taberoux (Warrendale, PA: TMS, 2004), pp. 913–918.
11. *Aluminum Statistical Review for 2005* (Arlington, VA: The Aluminum Association, 2005).
12. S.K. Das, J.A.S. Green and J.G. Kaufman, *JOM*, 59 (11) (2007), pp. 47–51.
13. *Collection of Aluminum from Buildings in Europe*, Delft University of Technology (Brussels, Belgium: European Aluminum Association, 2004), www.eaa.net.
14. J. Randolph Kissell and Robert L. Ferry, *Aluminum Structures—A Guide to Their Specifications and Design* (New York: John Wiley & Sons, Inc., 1995), p. 33.
15. J. Gilbert Kaufman, *Introduction to Aluminum Alloys and Tempers* (Materials Park, OH: ASM International, 2000), pp. 87–118.
16. S.K. Das and J. Green, *Light Metals 2008*, ed. David H. DeYoung (Warrendale, PA: TMS, 2008), pp. 1113–1118.
17. S.K. Das and J. Gilbert Kaufman, *Light Metals 2007*, ed. Morten Sorlie (Warrendale, PA: TMS, 2007), pp. 1161–1165.

Subodh K. Das, John A.S. Green, and J. Gilbert Kaufman are with Phinix, LLC, P.O. Box 11668, Lexington, KY 40577-1668; Daryoush Emadi is with Qatar University, Doha, Qatar; and M. Mahfoud is with the College of the North Atlantic-Qatar, Doha, Qatar. Dr. Das can be reached at skdas@phinix.net.

Aluminum Industry and Climate Change—Assessment and Responses

Subodh K. Das and John A.S. Green

It is now possible to assess the impact of the production processes of aluminum on the environment and to describe some of the ongoing responses and opportunities for improvement. This is compared with the benefits of aluminum in transportation, where the growing usage in various forms of transport due to its low density, high strength, and ability to be recycled enables reduced mass, increased fuel efficiency, reduced emissions and increased safety. It is the purpose of this paper to compare and contrast the emissions generated in the production of aluminum with the benefits accruing from its increased use in transportation.

INTRODUCTION

Aluminum is a latecomer to the suite of industrial metals. It was only relatively recently, in 1886, when commercial application of the metal began following the discovery of the Hall-Héroult reduction process. By contrast, metals like copper, tin, lead, zinc, and iron have been known for centuries. However, by virtue of its light weight and other unique properties, aluminum has now surpassed most metals in terms of global production and is second only to iron (steel). A survey of primary aluminum smelters of the world lists a total global capacity of about 41 million metric tons, although some 7% of this amount has been shut down on a temporary basis.¹ With this large global production, it is logical to ask about the impact of the metal on the global environment.

The industry first began a comprehensive accounting of the energy used, and the emissions generated, during all facets of production in the mid-1990s. This initial effort was undertaken by

the Aluminum Association when the industry was challenged by the automotive producers, under the United States Automotive Materials Partnership (USAMP) initiative, to develop a life cycle inventory (LCI) for the metal. The results of the LCI were first published in 1998,² and now have been incorporated into an ASM International Sourcebook.³

While the domain of this initial

study was the North American industry, since it included the chain of plants that supply the big automotive companies, it was in fact global in nature, as it included data from 213 plants located in Australia, Africa, Brazil, and Jamaica as well as from many operations in North America.

The responsibility for continuing this database and extending it globally to Asia and the Far East has now been passed to the International Aluminum Institute (IAI);³ see Chapter 3 for details of the initial LCI study; see Chapter 4 for more recent IAI surveys and information; see Chapters 5 and 6 for discussions of materials flow modeling of aluminum based on this information; see Chapter 7 for discussion about the beneficial impact of recycling; and lastly see Chapter 10 and related appendices for information about carbon dioxide and other emissions. For current information about industry progress and goals, see the IAI Web site.⁴

With this body of information, it is now possible to assess the impact of the production processes of aluminum on the environment and to describe some of the ongoing responses and opportunities for improvement. This is compared with the benefits of aluminum in transportation, where the growing usage in various forms of transport due to its low density, high strength, and ability to be recycled enables reduced mass, increased fuel efficiency, reduced emissions, and increased safety. It is the purpose of this paper to compare and contrast the emissions generated in the production of aluminum with the benefits accruing from its increased use in transportation.

See the sidebar for background on assessing aluminum production emissions.

How would you...

...describe the overall significance of this paper?

Consistent with earlier predictions, this assessment of the aluminum industry suggests that the reduction of carbon dioxide emissions through the use of aluminum in transportation are growing at a rate greater than the emission generated by increased production. Thus the industry will have a negative carbon footprint likely by 2020.

...describe this work to a materials science and engineering professional with no experience in your technical specialty?

This paper describes the actions being taken by the global industry to decrease its environmental footprint such as process efficiency improvements and recycling and contrasts with emission savings through its use in transportation (i.e., automobiles). The paper outlines the life cycle flow model being used to assess the situation.

...describe this work to a layperson?

This paper assesses the response of the aluminum industry to environmental challenges and climate changes. Overall, it is suggested that the use of aluminum is beneficial to the environment, especially through its use in the transportation industry, where its light weight makes vehicles more fuel efficient.

FIVE INDUSTRY RESPONSES

Process Efficiency Improvements

The process technology of the industry is continuing to evolve, especially in the regions of low-cost energy. An obvious means to further reduce the CO₂ footprint of the industry is to use energy from the most efficient generating plants and to use a greater proportion of renewable energy. Recently, both Alcoa and Century Aluminum have established smelters in Iceland, where hydro and geothermal power is available. Additional sources of hydro power are being developed in China and Brazil and this trend is expected to continue.

With regard to existing plants in the United States and globally, plants are being upgraded with new technology. For example, in some alumina refineries, the older rotary calcinations tech-

nology is being upgraded to the more energy efficient fluid bed technology. In the area of smelter technology, the cell amperage is being increased and, in development activities, cells to operate at 500,000 A are being explored. Higher cell amperages proportionally increase the productivity of the cell. Along with increasing amperage, the use of slotted anodes better enables the escape of the CO₂ gas from the spacing between the electrodes, and improves operation of the cell. Also, better cell controls, the use of magnetic compensation to stabilize cell operation, and the adoption of alumina point feeders all have helped to increase efficiency of cell operations. Using these and other developments over the last 50 years, the average amount of electricity needed to make a pound of aluminum has been reduced from ~12 kWh to ~7 kWh. These significant improvements are expected to continue to gradually improve cell efficiency.

More radical energy efficiency improvements have been limited by the extremely corrosive and aggressive cell environment and by the lack of materials to withstand exposure to the cryolite electrolyte at the operating temperature of ~950°C. Two significant cell design improvements have been pursued intermittently with limited success by various companies over the past three decades, but the costs and operating lifetime of available materials has limited their economic effectiveness. These technologies are the use of wettable / drained cathodes and the use of inert anodes. Both of these technologies promise to improve efficiency by reducing the ohmic resistance within the anode cathode distance (ACD) in the cell. The ACD is typically 4–5 cm and constitutes about 40% of the overall cell resistance. For a more complete discussion of these electrode systems and the complex issues involved see Reference 5.

ASSESSMENTS OF ALUMINUM PRODUCTION EMISSIONS

The energy to produce aluminum in the United States has been reduced by 64% over the past 45 years. This reduction has come about by technical progress (22%) and by the growth of recycling (42%). Globally, these energy saving trends are similar, and in some countries the energy savings may be accentuated because newer technology smelters with better energy efficiency are being built overseas.

Despite this significant progress, aluminum remains one of the energy-intensive materials to produce. The U.S. aluminum industry directly consumes 42.3×10^9 kWh of electricity annually, or 1.1% of all the electricity consumed by the residential, commercial, and industrial sectors of the U.S. economy.⁵

The energy values discussed in this paper are tacit energy values; in other words they include the value for the fuel to create the energy in the first place as well as the value for the actual energy used in the process itself. Many different fuels are used in the overall production process throughout the world depending on the region—for an extensive discussion on fuel usage, see Reference 6. In all cases, the industry has sought to use hydro power where available and the carbon footprint of hydro power is generally considered to be zero. Currently, the industry use of hydro power in the United States is ~40% and globally is ~50%. Nuclear power also has a low carbon footprint, but its use by the industry in the United States is less than 2%.

Specifically, the most energy intensive phases of aluminum production are the electrolysis or reduction step, followed by the anode preparation for the reduction process, and then the alumina production process. In total, it requires 60.5 kWh/kg to produce primary metal ingot whereas it only requires 2.8 kWh/kg to produce secondary, or recycled metal. Thus, ~95% of the energy embedded in the metal during the reduction process is saved when the metal is recycled. Also, virtually the same proportion of process emissions is eliminated by recycling.

There are two significant emissions from the fuel used in the process. In alumina calcination, the fuel used is combusted to carbon dioxide. In anode preparation, the fuel and the excess carbonaceous material within the coke and pitch likewise is eventually converted to CO₂. In fact, in most anode baking furnaces, the fuel residual in the pitch is fully utilized in the process to assist with heating the baking furnace and minimize the need for additional fuel. Again, the process offgas is eventually lost as CO₂.

In the smelter cell itself, the cell reaction produces oxygen which reacts with the carbon anode and generates a mixture of mostly CO₂ with a small amount of carbon monoxide. There is also some additional burning of the anode materials, independent of the electrochemical reaction, which also yields CO₂. All cell gases are captured and treated in a gas handling system but CO₂ is eventually released to the atmosphere.

Other gases, called perfluorocarbons (PFC), are released from the cell during upset conditions when the supply of alumina is depleted in the cell and an alternative anode reaction becomes dominant. These gases are tetrafluoromethane (CF₄) and to a much less extent hexafluoroethane (C₂F₆). These gases are significant since they have considerable global-warming potential and are equivalent to 6,500 and 9,200 times that of CO₂, respectively. In other words, 1 kg of CF₄ released to the atmosphere is equivalent in its warming capacity to 6,500 kg of CO₂. On average, in a modern cell the PFC emissions account for 2.2 kg CO₂ / kg Al (see Table D4 in Reference 3).

The industry has been proactive in seeking a reduction of the PFC emissions. In fact, while worldwide production of aluminum has increased ~24% since 1990, the emissions of PFCs have declined ~39% from the 1990 baseline. This is due to better cell control and the introduction of point feeder systems that enable a more precise addition of the amount of alumina that is added to the cell. This beneficial trend is expected to continue.

The carbon cathode is made “wetable” by the addition of small quantities of titanium diboride which is baked into the cathode. TiB_2 is expensive and is slowly consumed during the process which is a further drawback. However, it is estimated that a wettable cathode can improve the cell performance by ~15% and it is thought that several companies are currently testing this technology. The combination of a wettable cathode, together with an inert anode, which would enable a decrease, and more precise control of the ACD, is estimated to improve cell performance by ~20%. Alcoa, Hydro, and Moltech are companies known to be exploring inert anode technology.⁷

From the environmental viewpoint, the inert anode is the Holy Grail of the industry at present since its use would eliminate the need for carbon anodes and the related anode baking completely, and would generate oxygen, instead of CO_2 , as the cell off gas. This would have a huge impact on the industry, eliminating more than 60% of its CO_2 footprint. Of course, it would cost some energy to make the inert anodes but this is difficult to estimate since it is not known whether the best electrode material will be ceramic, metallic or cermet. Regardless, the beneficial impact would be huge.

Finally, if these electrode materials can be proven on an industrial scale, it is a relatively easy step to visualize additional improvements in cell design from the exclusively horizontal electrode assembly used in industry today to a more compact, energy-dense, vertical electrode assembly. However, this is probably some two or three decades in the future. Thus, there are many options for future improvements, though the best options still require extensive research and development.

Recycling

As stated previously, recycling of aluminum saves ~95% of the energy and emissions as compared to primary production. While the industry always has been proactive in emphasizing the need for recycling (i.e., in the case of used beverage cans (UBC), the need now is to reemphasize recycling of UBC but in addition to push for all other types of recycling, especially of

automotive aluminum).

With regard to UBC material, the rate of recycling in the United States is a lackluster 52% as compared to rates of ~95% for Brazil and Norway. This means that the balance is being lost in landfills around the country. It has been estimated that there is an accumulated total of 20 million tons of UBC material in the United States. This equals the annual production of three new aluminum smelters! This has led to the suggestion to mine the landfills to recover the buried cans.⁸ An attractive alternative is not to bury the material in the first place—possibly through the sorting of municipal waste prior to land filling. In this regard, it is noteworthy that Alcoa has now set a goal and called upon the industry to raise the UBC recycling rate to 75% by the year 2015.⁹

For the future, the more important area for recycling will be automotive aluminum, as the volume of recycled aluminum from automotive components exceeded the metal coming from UBC for the first time in 2005.¹⁰ With the growth of automotive aluminum for light weighting, fuel efficiency and safety considerations, this area is anticipated to become even more dominant, especially with the recent increases in fuel prices (see the next section).

With regard to processing of automotive wastes, the important recent development is the introduction of the industrial shredder. This has automated the process of vehicle recycling and, unlike the case of an individual beer or beverage can, it has taken the decision away from the hands of individual consumers. Virtually all used vehicles are shredded, and the U.S. Environmental Protection Agency (EPA) estimates that ~90% of all automotive aluminum is now recovered and recycled.

To capitalize on the benefits of the shredder, there is now a need to improve and extend the dismantling and presorting of vehicle components. A key issue in recycling is the control of the alloying additions and impurities to retain the value of the secondary metal. Some alloys can be recycled better than others. For example, the 3xxx, 5xxx, and 6xxx alloys generally used in automotive applications have similar alloying additions of magnesium and silicon and can be readily commingled for melting.

However, if a 7xxx alloy containing zinc and copper additions and normally used for high-strength aerospace applications is used as a bumper in a vehicle application, the zinc and copper alloy additions enormously complicate the recycling procedures and reduce the value of the metal. Different streams of recycled metal will be needed to fully benefit from the metal that is recovered.

There is a need to make automotive designers aware of the complexities of recycling and the impact that certain designs may have on the quality and economics of recycled metal. Also, there is a need to refine dismantling and presorting procedures prior to shredding and to refine separation and sorting of the non-magnetic metallic concentrate after shredding. The recent demonstration of laser based post-shredder sorting technology (e.g., LIBS) by the Huron Valley Steel Corporation¹¹ has been a great tool to sort material, but as yet it is just being used to beneficiate 3xxx alloy feedstock even though in concept it could enable individual alloy separation. Equipment cost and process time limit the application.

Further, there is a need to explore the development of recycle-friendly aluminum alloys for certain market segments of the industry. Conceptually, these alloys would have alloy additions and impurity contents that likely would fit recycle metal streams and would not require any, or at least a minimum, of post processing for reuse. These issues are discussed at length in Reference 10. Another way to improve the quality of recycled metal is to employ a rudimentary alloy separation during recycling. For example, most aluminum used in the building and construction market is either the 5xxx alloy, mostly in sheet form, or the 6xxx alloy, generally used as an extrusion. Accordingly, if the dismantlers segregate the different shapes at the job site an effective alloy separation can be achieved and the resultant secondary melt quality will be improved. These and other issues are detailed in Reference 12. Lastly, for the most efficient recycle process, it is important to adopt the best melting practice which limits the exposure of the molten metal to oxygen and reduces metal loss through dross formation.

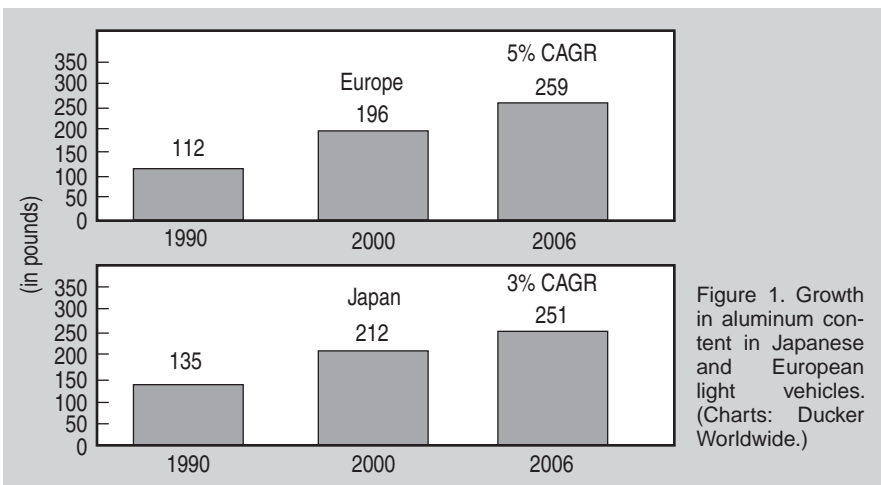


Figure 1. Growth in aluminum content in Japanese and European light vehicles. (Charts: Ducker Worldwide.)

Promote Aluminum Use in Transportation to Reduce Emissions

The unique properties of aluminum make it an ideal material to reduce the mass of transportation vehicles. Reduction of mass directly converts to a saving of fuel. This applies to all forms of transport such as aircraft, railcars, ships, and especially cars and trucks and buses. Less fuel usage in turn reduces CO₂ emissions.

Properties that are key are its light weight (roughly a third of the density of steel), high strength, and corrosion resistance. Light weighting of the vehicle structure reduces fuel requirements, and enables bigger, lighter structures with “crumple” zones and other features to improve passenger safety.

The growth of aluminum usage has been ongoing for more than 30 years and is a global trend (see Figure 1). Recent increases in the price of oil and gas and concerns for the carbon footprint of vehicles will almost certainly enhance this trend. In North America in 2007, the average light vehicle contained 327 lb. of aluminum and there are no obvious factors, other than the metal’s price, to constrain this trend (see Figure 2).

Earlier problems with the metal’s formability have been reduced as designers have become familiar with aluminum alloys and fabricators gain more experience with forming it. Future high-mileage vehicles will need to contain large quantities of light metals such as aluminum, magnesium, and titanium to attain their high-performance goals.

Two additional factors are important with regard to aluminum use in vehicles and directly follow from the extensive

life cycle inventory and materials flow modeling of the industry. First, each pound of aluminum replacing two pounds of traditional materials (iron or steel) in a vehicle can save a net 20 pounds of CO₂ emissions over the lifetime of the typical vehicle. Second, a fuel savings of 6–8% can be gained for every 10% weight reduction resulting in fewer greenhouse gas (GHG) emissions.

Further, according to the EPA, nearly 90% of automotive aluminum is recovered and recycled. It is estimated that about 57% of the aluminum content in North American vehicles was sourced from recycled material. The alloy specifications for cast aluminum alloys, used for items like engine blocks and motor housings, are quite tolerant of recycled material. For additional discussion, see Reference 13.

Carbon Trading

Although the outlines of a carbon trading scheme are not yet developed and far from clear, such a system probably would have a significant impact on the aluminum industry. For example, a little more than 0.4 kg of carbon anode

is consumed to make 1 kg of aluminum. Accordingly, a carbon trading scheme would strongly encourage development to make the technical breakthrough to achieve a viable inert anode material. Success here would eliminate the need for carbon anodes completely and have a huge impact on the greenhouse gas footprint of the industry for the reasons cited above.

Another result expected from a carbon trading scheme is that the recycling of aluminum (secondary production) would be favored over primary production. This follows from the fact that only 5% of the energy is required for recycling as compared to primary production and no carbon anodes are involved in the recycling process. An additional benefit is that recycling facilities (remelters) are smaller facilities and only require about 10% of the capital costs of a new smelter installation. Thus, carbon trading might favor more remelters construction in consumption-rich countries like China and India where the supply of scrap is more likely to be available. It is unlikely to modify production technology in the energy-rich areas of Iceland and the Middle East where scrap availability is limited.

ADDING IT ALL UP

Figure 3 illustrates a material flow model for the global aluminum industry throughout its life cycle that has been developed by IAI for the year 2004—for additional details, see Reference 3, p. 95. The values cited are in millions of metric tons.

The area of the circles illustrates the relative volume of the flows. The total products in use, an estimated 538 million metric tons, represent more than 70% of all of the aluminum that has ever

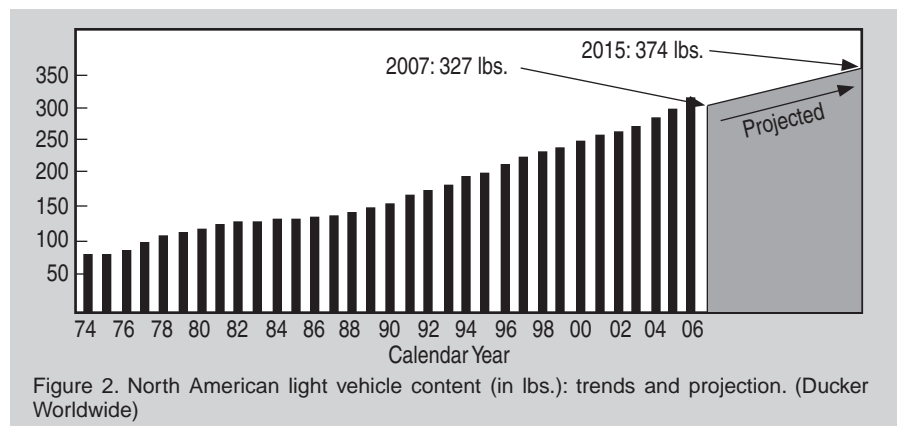


Figure 2. North American light vehicle content (in lbs.): trends and projection. (Ducker Worldwide)

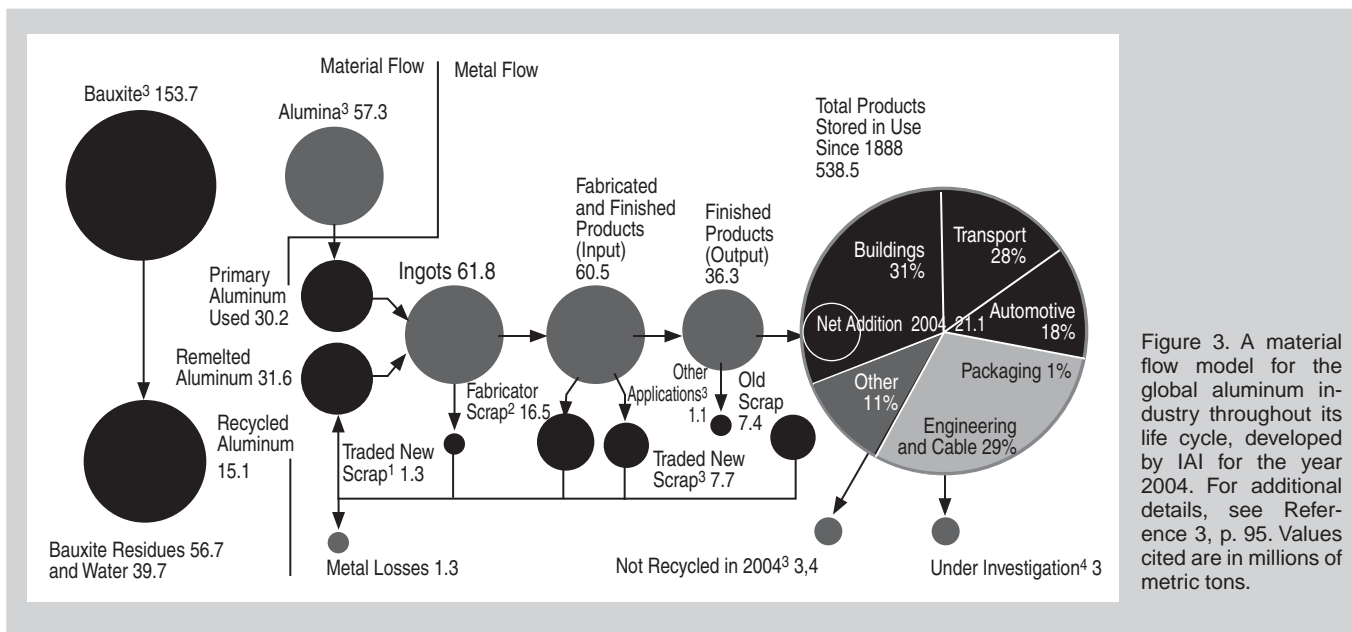


Figure 3. A material flow model for the global aluminum industry throughout its life cycle, developed by IAI for the year 2004. For additional details, see Reference 3, p. 95. Values cited are in millions of metric tons.

been produced. With this database it is possible to assess current energy and emissions intensity and project ahead for future years the energy use and GHG footprint of the industry.

Based on the growth of recycling and the reducing energy intensity of the primary production and the significantly lower PFC emissions, the CO₂ emissions footprint of the industry is decreasing on a per ton basis, although the industry continues to expand production. On the other hand, the savings of CO₂ emissions from the transportation use of aluminum are continuing to grow as more and more metal is used and the resultant fuel savings accumulate and the amount of recycled material is increased. Assuming the global industry can be updated to the best available technology as of 2003, the model indicates that the fuel efficiency and emissions savings due

to aluminum use in transportation will surpass the global industry's production emissions by 2020 (Reference 3, see Chapters 5&6). The 2007 Alcoa Annual Report contains the statement "the use of aluminum in planes, trains, and automobiles is projected to make the entire aluminum industry greenhouse gas neutral by the year 2025." Whatever the precise date, this is indeed an encouraging sign!

References

1. R.P. Pawlek, *Light Metal Age*, 66 (2) (2008), p. 6.
2. *Life Cycle Inventory Report for the North American Aluminum Industry*, Report AT-2 (Arlington, VA: Aluminum Association, 1998).
3. John A.S. Green, editor, *Aluminum Recycling and Processing for Energy Conservation and Sustainability*, ASM Sourcebook (Materials Park, OH: ASM International, 2007).
4. International Aluminum Institute, London, www.worldaluminium.org.
5. In Ref. 3, Chapter 10, p. 158.
6. In Ref. 3, pp. 71, 77, 160, 232, etc.

7. Ioan Galasiu, Rodica Galasiu, and Jomar Thons-tad, *Inert Anodes for Aluminum Electrolysis* (Düsseldorf, Germany: Aluminium-Verlag, 2007).

8. S. Das et al., "Recovering Aluminum from Used Beverage Cans—The Dilemma of 900,000 Annual Tons" (Paper presented at TMS 2007 Annual Meeting, Orlando, FL, February 25–March 1, 2007).

9. Alcoa Annual Report 2007 (Pittsburgh, PA: Alcoa, 2007), p. 18.


10. S.K. Das, J.A.S. Green, and J. Gilbert Kaufman, *JOM*, 59 (11) (2007), p. 47.

11. Adam Gesing et al., *Aluminum 2002*, ed. S.K. Das and M.H. Skillingberg (Warrendale, PA: TMS, 2002), pp. 3–15.

12. S. Das, J. Gilbert Kaufman, and J.A.S. Green, "Aluminum Recycling—An Integrated, Industry-Wide Approach," in this issue, pp. 23–26.

13. "Aluminum in Autos: Driving toward a Sustainable Environment" (Arlington, VA: The Aluminum Association, Aluminum Transportation Group Media Kit), www.autoaluminum.org.

Subodh K. Das is CEO and Founder of Phinix, LLC, P.O. Box 11668, Lexington, Kentucky, 40577-1668; and John A.S. Green, consultant, is retired from The Aluminum Association. Dr. Das can be reached at skdas@phinix.net.



**Your Materials Books
and More e-Store!**
<http://knowledge.tms.org>

**Visit the Knowledge
Resource Center to reserve
your copy today!**

Converter and Fire Refining Practices

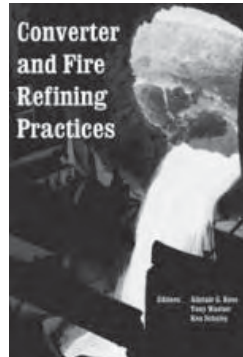
by Alistair Ross, Tony Warner, and Ken Scholey, editors

These proceedings will provide readers with an update on research, development, and operating practice in the fields of converting, fire refining, and casting in the base metal pyrometallurgy industry. Materials and supply vendors, service providers, and researchers and plant operators in the pyrometallurgy industry will find this book to be a valuable resource.

From the 2005 TMS Annual Meeting held in San Francisco, California, February 13–17, 2005.

**TMS Member price \$121; Non-member price \$173;
TMS Student Member price \$96**

To order these or related publications, contact TMS:
E-mail publications@tms.org • Phone (724) 776-9000, ext. 256 • Fax (724) 776-3770



Adaptive Control of Feed in the Hall-Héroult Cell using a Neural Network

K.D. Boadu and F.K. Omani

A linear neural network is proposed for estimating alumina concentration in an aluminum reduction cell. Bath resistance/alumina concentration data from a simulated 140 kA Center-Break Hall-Héroult cell were used as input vectors to train a two-layer neural network constructed with six constraints and six degrees of freedom. Results from simulated and real data tests using the derived estimation algorithm are presented. Also, neural network is compared with extended Kalman filter and shown to have a superior performance in the estimation problem. Finally, the paper claims robustness for the neural algorithm against changes in resistance due to cell events like tapping and anode change.

INTRODUCTION

In recent years several research papers have been published on the control of alumina concentration in the Hall-Héroult cell. Resistance slope calculations have been used with considerable success in the estimation of alumina concentration in the bath.^{1,2} In the search for improved accuracy in the prediction of concentration, other methods have been used and reported. These include the use of the ARMAX model,³ Runge-Kutta methods,⁴ and the extended Kalman filter.^{5,6}

The main focus of such research is to improve on the current and energy efficiencies of the Hall-Héroult process. The literature abounds with the relationship between the alumina concentration in an electrolytic cell and current and energy efficiencies. Low levels of alumina concentration often lead to an increase in the anode overpotential which increase anode effect frequency and thus lower the energy and production efficiencies of the cell.

High concentrations of alumina lead to sludge formation which lower metal production.⁷⁻¹¹ Therefore feed control strategies aim at maintaining the concentration of alumina in the bath within the limited range of 2.5 to 6 wt.%,¹² to avoid underfeeding or overfeeding.

The application of simple resistance

slope calculations to the estimation problem has proved inadequate in the face of a search for higher current efficiency. This is due to the noise in the resistance data that often causes false or belated anode effect alarms and thus causes overfeeding or underfeeding problems. More robust methods have, however, demanded impractical computing power from cell microcontrollers.

The extended Kalman filter solution applied to the estimation problem^{5,6} has been seen to have three major problems:

1. Convergence, stability, and optimality of the estimator cannot be guaranteed due to the nonlinear nature of the relationship between resistance and concentration.⁵
2. The algorithm is dependent on regular estimates of anode movements, to be compensated for independently, in order to provide stable estimates.¹
3. The continuous relinearization of the system at each sampling interval makes it difficult to obtain a steady Kalman gain. Thus in implementation, the Kalman gain has to be adapted on-line, giving rise to a more complicated algorithm. Consequently, the need to reset the covariance matrix after every feed leads to the Kalman filter detuning and giving rise to initial poor estimates, before subsequent convergence to more accurate estimates (see Figure 9).

In this paper we present a neural network approach to the estimation problem. A set of the five most recent measurements of cell resistance, and the previous estimate of alumina concentration, are presented to the network as input vectors for each mea-

How would you...

...describe the overall significance of this paper?

The overall significance of this paper is to increase the current, energy, and production efficiencies of an aluminum reduction cell. It simultaneously reduces gas emissions, and for that matter, environmental pollution by a reduction cell.

...describe this work to a materials science and engineering professional with no experience in your technical specialty?

The key to maximizing the efficiencies of the Hall-Héroult process for aluminum reduction is a good prediction of the alumina concentration. This paper proposes the use of a neural network as a model-free algorithm for the prediction problem. It abandons the usual model-based approaches due to the time-series, polynomial nature of the resistance-concentration curve in the reduction cell.

...describe this work to a layperson?

Aluminum reduction cell control computers need to keep a careful balance between under- and over-feeding a cell with alumina, the primary input in the production of aluminum. The aim is to maximize efficiency and reduce cell conditions which throw more than permitted gases out to pollute the atmosphere. This paper proposes neural networks as a better method for the control computers in predicting alumina concentration and maintain better control over alumina feed.

sured alumina concentration (provided as the trainer signal). The neural network learns the functional relationship between resistance and concentration. After the off-line training, the network is easily implemented on-line, using the parameters obtained through training to estimate the concentration of alumina.

In general, the approaches adopted so far to solve the estimation problem have depended on scientific rationalism to look for a tractable function relating bath resistance to the alumina concentration, through the use of models. "But how close can a low-order polynomial come to the time-series footprints left by a chaotic system?"¹³

We therefore wish to propose the approach of scientific empiricism (neural networks, in this case) to solving this estimation problem. In this approach, we let the resistance data tell their own story via model-free algorithms. Our simulated and real data test results show that the trained network has a superior performance to the extended Kalman filter.

NEURAL NETWORK THEORY

Neural networks are model-free estimators which employ numerical algorithms to transduce numerical inputs to numerical outputs. Fashioned after the "cognitive computations" of the human brain, albeit a gross abstraction, neural

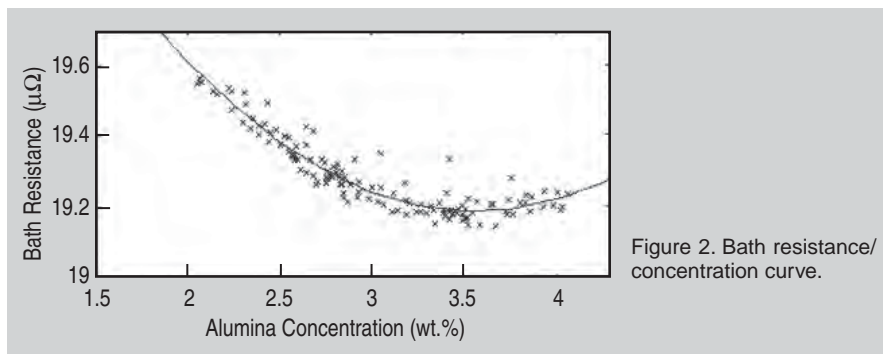


Figure 2. Bath resistance/concentration curve.

networks are constructed with many simple nonlinear summary junctions connected together by connections of varying strength to approximate unknown functions with raw sample data.¹⁴

The Adaline

The ADALINE (adaptive linear element) is a neural network which linearly combines its input to derive an output.

In training the ADALINE, an input pattern vector $\mathbf{R}_t = [r_0, r_1, r_2, r_3, \dots, r_n]^T$ and a desired response (trainer signal), d_t , are presented to the network at each iteration. Then the components of the input vector, \mathbf{R}_t , are weighted by the weight vector $\mathbf{W}_t = [w_0, w_1, w_2, w_3, \dots, w_n]^T$. The weighted inputs are then summed, the inner product $\mathbf{R}_t \mathbf{W}_t^T$, to produce a linear input for the output layer of the network, which is a transfer function that finally produces the net-

work output, X_t . The linear error is then given by $\epsilon_t = d_t - X_t$. For the next iteration, an adaptation algorithm adjusts \mathbf{W} in a way that minimizes ϵ_t^2 . Learning stops when the sum of the squared errors is less than an error goal^{15,16} (see Figure 1).

Neurocomputing is currently in use in the industry for solving problems in signal processing, speech recognition, visual perception, adaptive control, and robotics.

For this study we used supervised learning as a stochastic approximation of the error surface of the unknown resistance/concentration function. We applied the Widrow-Hoff learning rule (α -LMS) to an adaptation of the ADALINE which embodies the minimal disturbance principle. The unknown resistance/concentration function $f: \mathbf{X} \rightarrow \mathbf{Y}$ is estimated from observed random vector samples $(x_1, y_1), \dots, (x_m, y_m)$ by minimizing an unknown expected error functional.¹⁴⁻¹⁶

THE WIDROW-HOFF DELTA RULE (α -LMS)

The α -LMS was used as the weight adaptation algorithm due to the untractable nature of the problem of predicting alumina concentration in a chaotic system. The weight update equation can be written as:

$$W_{t+1} = W_t + \alpha \frac{\epsilon_t R_t}{|R_t|^2} \quad (1)$$

Where α is the network learning rate. It can be shown that the error is reduced by the factor α for each adaptation cycle, thus making α control stability and speed of convergence during learning.¹⁵

THE REDUCTION PROCESS

The nerve center of aluminum reduction is the electrolytic cell. The primary

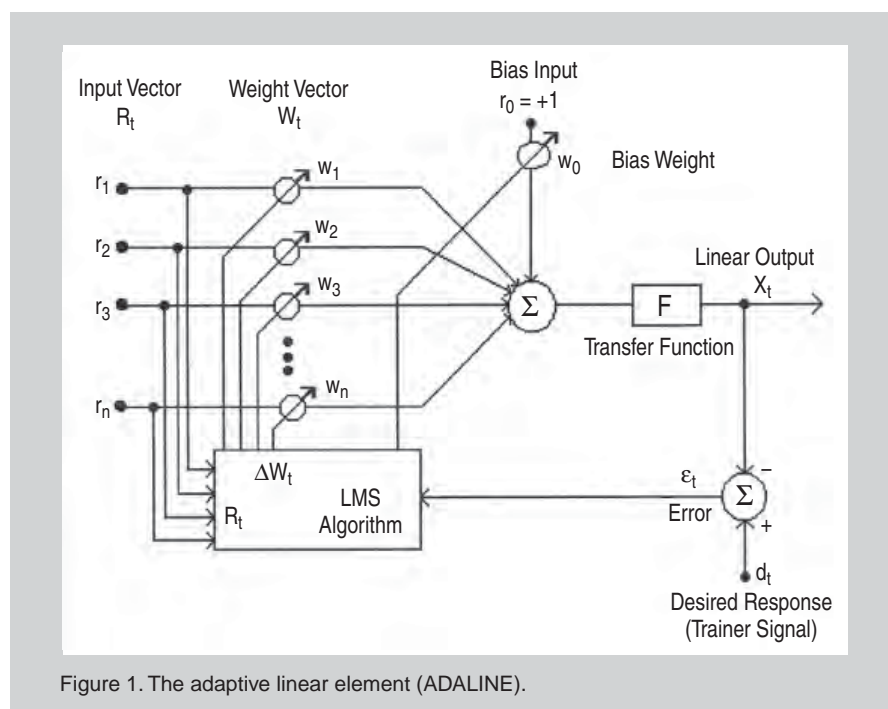
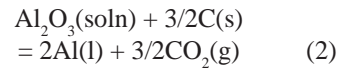
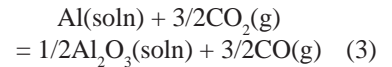


Figure 1. The adaptive linear element (ADALINE).

reaction in the cell can be represented by:



This reduction is carried out in cryolite bath using carbon electrodes, at a temperature around 960°C and at an efficiency ranging between 85 and 95% of Faraday's theoretical production rate of aluminum.^{5,7,9} The main loss in efficiency is caused by the reoxidation of the aluminum¹¹ through the reaction:



The process is quite chaotic because while the primary reaction is continuous, the removal of the aluminum produced (tapping) is discrete. Other noise inducing events in the course of the reaction include anode consumption and change, unstationary bath volume, interpolar distance and temperature, and unscheduled addition of alumina.

Resistance Concentration Curves

Recent studies (on both point-feeder and center-break cells) on the shape of the resistance-concentration curve¹⁷ typify the nonlinearities in the ohmic resistance reported in the literature. See Figures 2, 3, and 4.

It is clear from Figure 2 that the ohmic resistance does not identify the alumina concentration. However, a partial derivative of the resistance w.r.t. the alumina concentration (Figure 3) does.⁵ (This is the reason for the choice of the ADALINE since it obtains an implicit numerical differentiation of the resistance at the first layer synaptic junction.) The characteristic behavior of alumina concentration over time is also shown in Figure 4.

Rate of Alumina Dissolution

Alumina dissolution in cryolite melt has also been the subject of various research work in the industry. The main factors that impact the dissolution rate include the alumina concentration, bath temperature, feeding method,¹⁸ and cell operating conditions.¹⁹ The rate of dissolution is reported as 0.027 wt.%/min. for the center-break cells studied in Reference 17, and 0.0625 wt.%/min. for the point-feeder cells in the same study. The

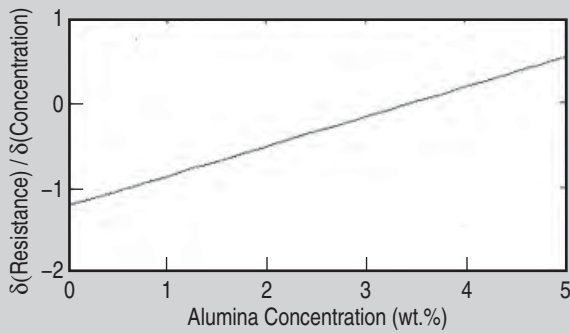


Figure 3. Partial derivative of resistance with respect to concentration/concentration curve.

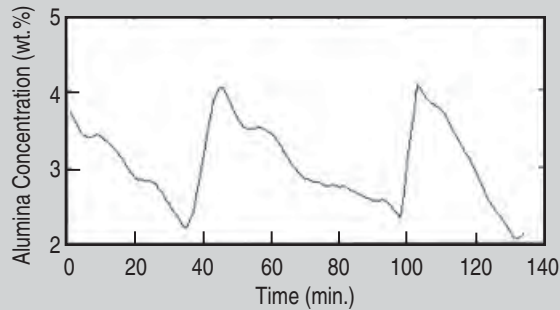


Figure 4. Bath concentration/ feed time curve.

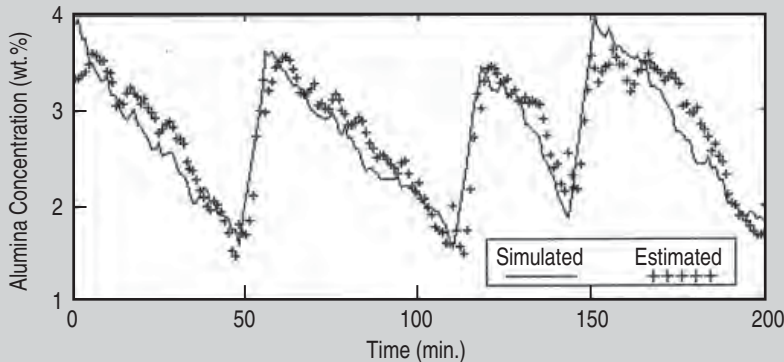


Figure 5. Simulated concentration and neural network estimated concentration curves (input pattern: R_t, \dots, R_{t-4}).

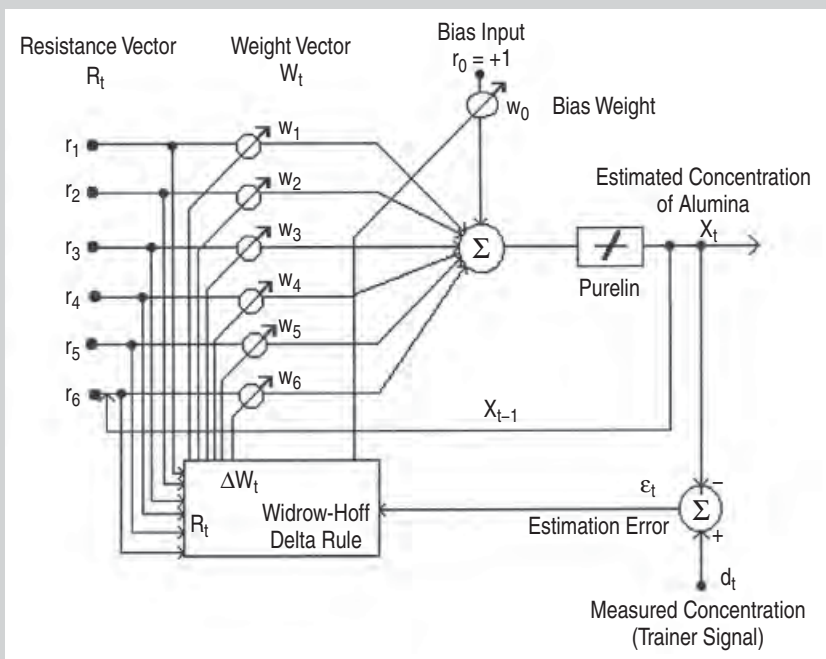


Figure 6. Optimal neural network learning machine.

rate of dissolution was needed for the present study in order to build a simulator to test the neural-based feed strategy developed. To get this value, the concentration-time curve (see Figures 7 and 8) derived from the real cell data collected from 2 center-break cells were differentiated. This yielded a dissolution rate of 0.0253 wt.%/min. which was used for the simulation in this paper.

The Learning Process

To train the neural network to learn the resistance/concentration relationship, a two-layer Widrow–Hoff supervised learning network was built. Data from a simulated 140 kA center-break cell⁶ was used for the training.

Resistance data was regressed as the input pattern vector using the five most recent resistances (\mathbf{R}). The Widrow–Hoff delta rule (α -LMS) was used to generate the weight vector (\mathbf{W}). A network bias was allowed (w_{0t}) with an input of unity (r_{0t}). The purelin transfer function¹⁶ was used, and for each iteration a trainer signal (d_t) was provided as the measured alumina concentration scalar at time t . The network output, $F(\mathbf{R}_t \mathbf{W}_t^T)$, was then the estimated concentration of alumina, given the resistance vector \mathbf{R} .

The estimation error is calculated as ε_t which is used via the Widrow–Hoff delta rule to adjust \mathbf{W} for the next iteration (see Figure 1).

SELECTING THE OPTIMAL NETWORK ARCHITECTURE

The basic concept adopted in this paper for the training of the network was a moving average input, to enhance effective resistance–concentration pattern recognition. Initial simulations were run

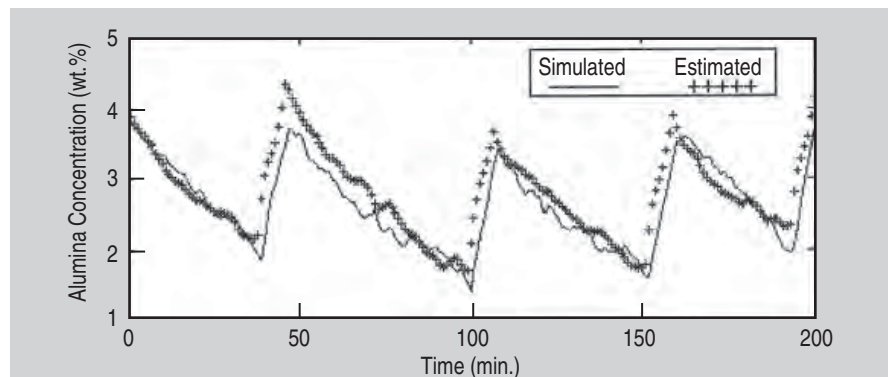


Figure 7. Simulated concentration and neural network estimated concentration curves (input pattern: $R_t, \dots, R_{t-4}, X_{t-1}$).

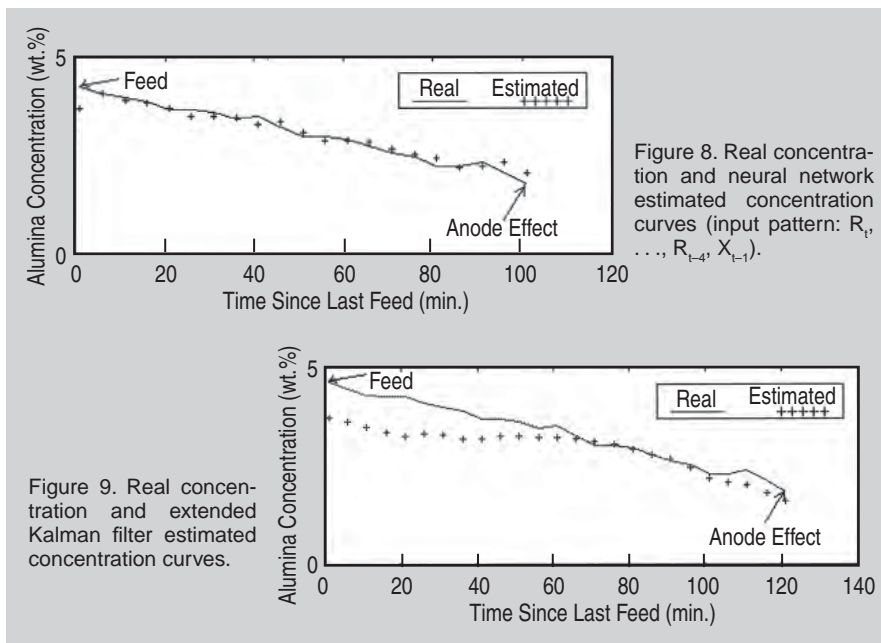


Figure 8. Real concentration and neural network estimated concentration curves (input pattern: $R_t, \dots, R_{t-4}, X_{t-1}$).

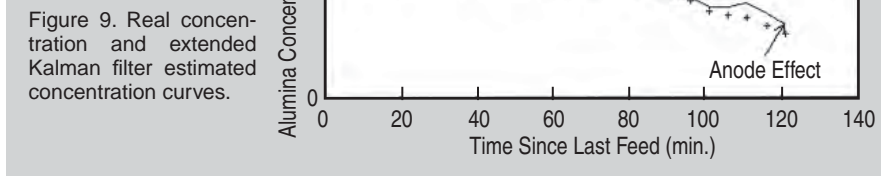


Figure 9. Real concentration and extended Kalman filter estimated concentration curves.

using the five most recent resistances (R_t, \dots, R_{t-4}) as the input. The network's performance looked good (Figure 5) but came up with an unacceptable sum squared error of 9.6317 (against a goal of 0.5) over a training cycle of 1,000 iterations. An auto-regressive-moving-average (ARMA)-type input pattern was therefore considered next ($R_t, \dots, R_{t-4}, X_{t-1}$). Then the performance of the network significantly improved (Figure 7), with a final sum squared error of 0.8770. Performance, however, started deteriorating on the next ARMA-type input of $R_t, \dots, R_{t-4}, X_{t-1}, X_{t-2}$. The optimal training input pattern was therefore selected as $R_t, \dots, R_{t-4}, X_{t-1}$ giving the final architecture (Figure 6) of:

$$X_t = F(\mathbf{R}_t \mathbf{W}_t^T + \text{Bias}) \quad (4)$$

where $\mathbf{R}_t = R_t, R_{t-1}, R_{t-2}, R_{t-3}, R_{t-4}, X_{t-1}$, and $\mathbf{W}_t = W_1, W_2, W_3, W_4, W_5, W_6$

THE ESTIMATION ALGORITHM

Over 1,000 iterations were run through the network using a 5×134 bath resistance data input matrix and a 1×134 measured alumina concentration vector (trainer signals), with each iteration changing the network weights to improve the estimation. Network learning ceased at the following output parameters: Weight Vector $\mathbf{W} = [-0.2564, -0.2046, -0.0537, +0.0919, +0.3402, +0.9646]$; Network Bias = +1.6799; Final sum squared error = 0.8770. Therefore the algorithm for estimating the concentration of alumina (X_t) in a cell, given the 5 most recent resistances (\mathbf{R}) is:

$$X_t = \sum_{k=1}^{n=5} R_{6-k} W_k + X_{t-1} W_{n+1} + 1.6793 + \delta_t \quad (5)$$

where δ_t = rate of alumina dissolution.

The neural algorithm defined in Equation 5 was tested on a 140 kA center-break simulated and real cell data. Results are shown in Figures 7 and 8. (The real cell data used for the test was collected with anode movements frozen.)

An extended Kalman filter algorithm⁶ was tested on the same set of data used for the neural network test in Figure 8. Performance of the neural network (Figure 8) was superior

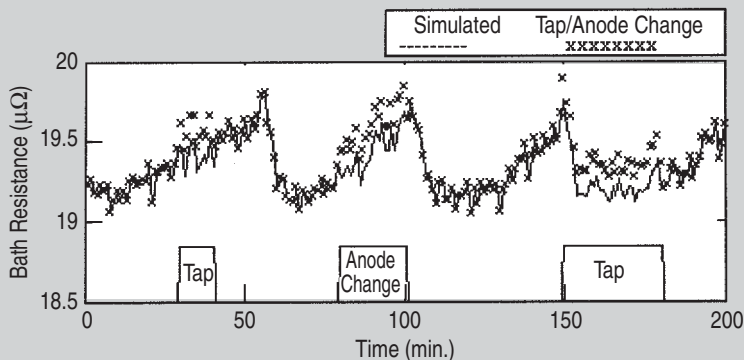


Figure 10. Simulated resistance and resistance vectors during tap/anode change simulation.

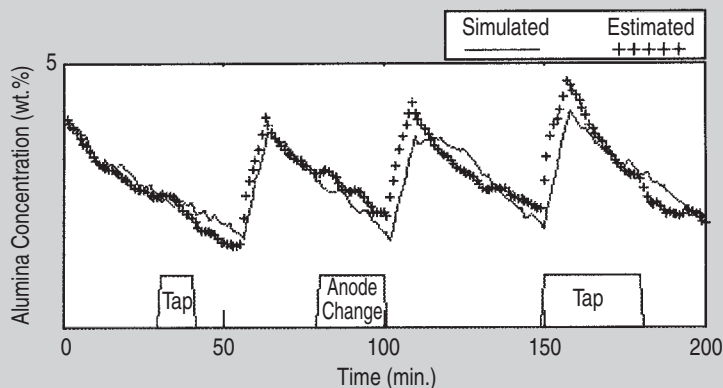


Figure 11. Simulated concentration and neural network estimated concentration curves (tapping and anode change simulated).

to that of the extended Kalman filter (Figure 9). Late convergence of the extended Kalman filter algorithm after each feed makes it unsuitable for use on short feed cycle cells (e.g., point feeders).

TEST FOR ROBUSTNESS

Finally, the neural algorithm was tested for robustness during a simulation of anode change and tapping by random increases in the cell resistance over random time ranges in the feed cycle. The estimated concentration of alumina continued to be correct during these simulations. This performance of the algorithm was in line with scientific expectation because of the network's numerical differentiation of the resistance w.r.t. concentration which linearizes the resistance input before the concentration is estimated. Figure 10 shows the changes in bath resistance during the simulated tapping/anode change period. Figure 11

shows the corresponding performance graph of the neural network algorithm, demonstrating the robustness of the algorithm during cell events like tapping and anode change.

CONCLUSION

Algorithms for estimating alumina concentration in the Hall-Héroult cell have been saddled with the search for a resistance/concentration model. This paper has shown that the model-free generalization mechanism employed in neural networks for pattern recognition can well be applied to the uncertain and imprecise environment in the cell, through the use of a black-box approximator from input to output. The estimation algorithm is very simple and yet robust, and can be used effectively in a feed control program to keep the concentration of alumina within preferred limits. The sense of mystery and beauty that characterize neurocomputing overwhelmed us in

no small way. In a bid to keep computations simple, the massively parallel topology of neural networks was not used. With more computing power, a fully connected single neuron, or more parallel neurons may be tried for still better performance in predicting alumina concentration in the cell for higher current and production efficiencies.

References

1. M. Farrow, *Journal of Metals*, 36 (11) (1984), pp. 33-34.
2. Y. Macaudiere, *Light Metals 1988*, ed. L.G. Boxall (Warrendale, PA: TMS, 1988), pp. 607-612.
3. T. Moen, J. Aalbu, and P. Borg, *Light Metals 1985*, ed. H.O. Bohner (Warrendale, PA: TMS, 1985), pp. 459-469.
4. Laszlo Tikasz et al., *Light Metals 1988*, ed. L.G. Boxall (Warrendale, PA: TMS, 1988), pp. 583-588.
5. Einar Arne Sørheim and Peter Borg, *Light Metals 1989*, ed. P.G. Campbell (Warrendale, PA: TMS, 1989), pp. 379-384.
6. Joan S. McKenna, F.K. Omani, and Thomas Nyadzie, *JOM*, 45 (11) (1993), pp. 44-47.
7. K. Grjotheim and B.J. Welch, *Aluminium Smelter Technology* (Düsseldorf, Germany: Aluminium-Verlag, 1988).
8. K. Grjotheim et al., *Aluminium Electrolysis* (Düsseldorf, Germany: Aluminium-Verlag, 1982).
9. R.A. Lewis, "Technical Fundamentals of the Aluminum Reduction Cell Process" (Foothill Ranch, CA: Kaiser Aluminum and Chemical Corporation, 1994).
10. Claude A. Wilson and Alton T. Tabereaux, *Light Metals 1983*, ed. E.M. Adkins (Warrendale, PA: TMS, 1983), pp. 479-493.
11. B. Lillebuen and Th. Møllerud, in Ref. 3, pp. 637-646.
12. K.R. Robilliard and B. Rolofs, in Ref. 5, pp. 269-273.
13. Bart Kosko, *Neural Networks for Signal Processing* (Englewood Cliffs, NJ: Prentice-Hall, 1992).
14. Bart Kosko, *Neural Networks and Fuzzy Systems* (Englewood Cliffs, NJ: Prentice-Hall, 1992).
15. Clifford Lau and Bernard Widrow, editors, *Special Issue on Neural Networks I* (Piscataway, NJ: The Institute of Electrical and Electronic Engineers (IEEE), September 1990).
16. Howard Demuth and Mark Beale, *Neural Network TOOLBOX* (Natick, MA: The MathWorks, Inc., 1992).
17. E.R. Owusu-Sechere, "Characteristics of Cell Resistance and Alumina Concentration in Bath (Mead & Tacoma Prebake Cells)" (Foothill Ranch, CA: Kaiser Aluminum and Chemical Corporation, DTC, 1994).
18. H. Maeda, S. Matsui, and A. Era, in Ref. 3, pp. 763-780.
19. G.I. Kuschel and B.J. Welch, in Ref. 5, pp. 299-305.

K.D. Boadu, formerly an automated systems programmer at Kaiser Aluminum & Chemical Corporation-Valco Works, Tema, Ghana, is currently the Chief Executive Officer of Arrow Network Systems, a wireless telecommunications company operating in West Africa. F.K. Omani is the Head of the Research, Consultancy & ICT Department of The Regional Maritime University, Accra, Ghana. Dr. Omani can be reached at fkomani@hotmail.com.

The Hot Formability of an Al-Cu-Mg-Fe-Ni Forging Disk

M. Aghaie-Khafri and A. Zargaran

The high temperature formability of AA2618-T61 forged disk was studied by means of tensile test over temperatures and strain rates ranging from 100 to 400°C and 3×10^{-5} – 3×10^{-3} s⁻¹, respectively. The constitutive equations of the material were calculated based on an Arrhenius-type equation and the ductility of the material was evaluated considering elongation and percent reduction of area. The results showed that both kinds of softening mechanisms, dynamic recovery and dynamic recrystallization, occurred during high temperature deformation of the alloy. Strain rate sensitivity of the material was evaluated in all the deformation conditions and the obtained values were used to calculate the apparent activation energy.

INTRODUCTION

Formability of a material is the extent to which it can be deformed in a particular process before the onset of failure. There are many variables that influence sheet metal formability, which can be broadly classified as process variables and material variables.¹ Process variables determine the nature of external loading on the work piece, whereas material variables determine the kind of response the material exhibits to that loading. Previous investigations have shown that hot formability of aluminum alloys are determined by process parameters, such as deformation temperature, strain rate, and strain degree. Softening mechanisms such as dynamic recovery and dynamic recrystallization are two important material variables controlling the hot formability of aluminum alloys.^{2–5}

AA2618 a heat-treatable Al-Cu-Mg-Fe-Ni forging alloy was developed originally to raise the temperature

How would you...

...describe the overall significance of this paper?

The high temperature formability of AA2618-T61 forged disk was studied by means of tensile test over different temperatures and strain rates. The main softening mechanism of the AA2618-T61 forged disk deformed at high Zener-Hollomon (Z) parameter value (100–200°C, s⁻¹) is dynamic recovery. Dynamic recrystallization is the primary softening mechanism when the alloy deformed at low Z value (350–400°C, s⁻¹). Dynamic recovery and dynamic recrystallization play a role at the same time at medium Z value (250°C, s⁻¹).

...describe this work to a materials science and engineering professional with no experience in your technical specialty?

AA2618, a heat-treatable AlCu-Mg-Fe-Ni forging alloy, was developed originally to raise the temperature limit of conventional 2000 alloys. This work evaluates the high temperature tensile formability of AA2618-T61 forging disk over a temperature range of 100–400°C. The influence of deformation temperature, strain rate and strain degree, and softening mechanisms such as dynamic recovery and dynamic recrystallization on the hot formability of AA2618-T61 are studied.

...describe this work to a layperson?

AA2618 is one of the aluminum alloys originally developed for aircraft components and automobile industries. This alloy was successfully used as the primary structure of the supersonic Concorde airplane. Fabrication of components is dependent on the mechanical properties of material such as strength, ductility, and formability. The aim of the present work is to study the mechanical properties of this alloy at high temperature.

limit of conventional 2000 alloys. The addition of a small amount of Fe and Ni enhances the microstructural stability of the alloy for applications involving high-temperature exposures up to 300°C.⁶ The presence of stable intermetallic particles, such as the Al₉FeNi particles, helps to control grain size and impede dislocation motion. The AA2618 alloy is widely used for the production of forged components such as engine parts for both automotive and aircraft applications.^{7,8} The conventional processing route consists of heating and maintaining the billet at the hot working temperature for a sufficiently long time followed by forging. Later, the component is solution-treated and artificially aged to produce the required balance of mechanical properties.⁹

The ageing sequence of this alloy and several aspects of its mechanical response at high temperature are well known.^{10–12} The warm formability of a solution-treated AA2618 aluminum alloy was investigated by means of torsion tests at temperatures between 150 and 300°C. Dynamic precipitation took place during deformation raising the flow stress and lowering ductility. The flow stresses were substantially higher than those observed by testing the same alloy in the as-extruded state.⁹

The hot and warm formability of AA2618 aluminum alloy, in the as-solutioned condition, was also investigated. The effect of the precipitation of second-phase particles, occurring during deformation, on the flow curve shape and on the stress level was evaluated.¹³ Other studies have analyzed the effect of high-temperature creep on the precipitate structure. Several concurring phenomena, such as the loss of coherency of precipitates, the change in particle size and distribution, and

the transformation of the metastable into the stable phase, can be strain-enhanced, and lead to the progressive softening of the structure during creep.¹⁴ To the best of authors' knowledge, there have been few reports on the high-temperature tensile properties of the AA2618-T61 forging disk. The aim of the present work is to study the influence of temperature on the tensile formability of AA2618-T61 forging disk over a temperature range of 100–400°C.

See the sidebar for experimental procedures.

RESULTS AND DISCUSSION

Stress-strain Curve and Microstructure

Figures 1 and 2 show the nominal stress-strain curves of the forging disk at various temperatures and strain rates which show the effects of deformation temperature and strain rate on the flow behavior of the material. At the low-temperature regime the stress-strain curves monotonically increase up to fracture; at intermediate temperatures

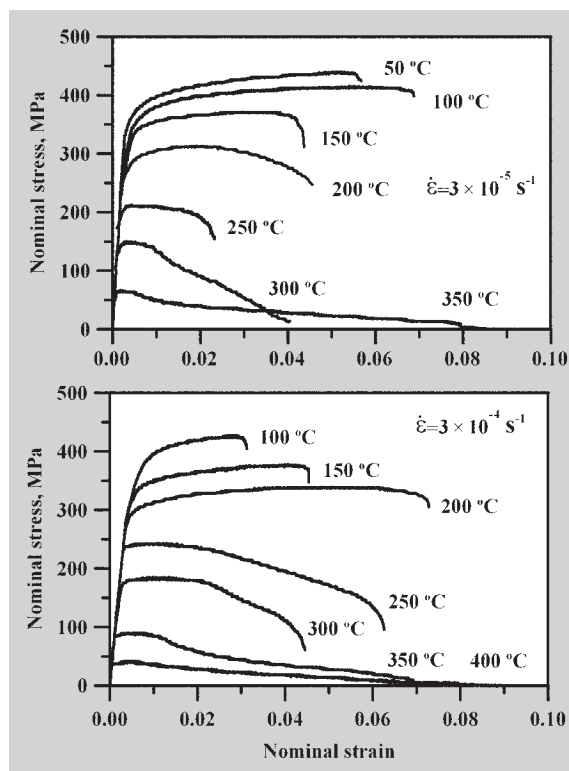


Figure 1. Nominal stress-strain curves of the AA2618-T61 forged disk at different strain rates and temperatures.

the curves increase up to the peak followed by a moderate decrease in nominal stress. At the high-temperature regime the decrease in stress becomes

more and more pronounced, and it transforms in a continuous reduction in stress, approaching zero.

The variations of flow stress with temperature for different strain rates are shown in Figure 3. It is clear that flow stress decreased with increasing temperature. However, the slope of the curves increased by increasing temperature and tends to a constant value at 400°C and strain rate of $3 \times 10^{-4} \text{ s}^{-1}$. The dependence of the flow stress on temperature can be evaluated by Seeger theory of flow stress.¹⁵ The stress required for deformation can be divided into two parts: σ^* , which is dependent on the temperature and σ_G , which is the athermal component of the flow stress:

$$\sigma = \sigma^* + \sigma_G \quad (1)$$

It can be seen that the athermal component of stress is $\sigma_G \approx 32 \text{ MPa}$ at a strain rate of $3 \times 10^{-4} \text{ s}^{-1}$.

Deformation at 100–250°C results in a microstructure with elongated grains, which are typical of dynamic recovery. One such microstructure is shown in Figure 4, which corresponds to a specimen deformed at 200°C and strain rate of $3 \times 10^{-3} \text{ s}^{-1}$. Figure 5 shows that the elongated grains decompose during high temperature deformation and some fine and equiaxed grains are ob-

EXPERIMENTAL PROCEDURE

The aluminum wrought alloy AA2618-T61 was delivered as forged disk with chemical composition of 0.3Si-1.06Fe-1.92Cu-1.18Mg-0.9Ni-0.07 Ti and Al balance (all values in wt.%). The optical micrograph of the material was shown in Figure A, which consists of uniformly distributed fine Al_2CuMg intermetallic particles and larger precipitates embedded in aluminum solid solution phase. In the present investigation the energy dispersive x-ray spectroscopy (EDX) point analysis of the particles confirmed that the large precipitates consist of Al_3FeNi intermetallic.

The specimens used in the tensile tests were cut in radial direction from the center of the forging and had a diameter of 4 mm and a length of 25 mm in the gauge-length section. Hot tensile testing was performed in a servo-hydraulic machine, Instron 8800, equipped with a three-zone split furnace. The tests were conducted in laboratory air environment over the temperature and initial strain rate range of 100–400°C and $3 \times 10^{-5} - 3 \times 10^{-3} \text{ s}^{-1}$, respectively. The temperature was controlled with the aid of a thermocouple fixed on the test specimen's surface. Maximum temperature variation was well within 2°C, of the set-point temperature over the entire duration of the test. Before each test, the specimen was maintained or soaked at the test temperature for 15 min, so as to achieve stability with the environment.

Samples for optical microscopy were sectioned from the gauge area, mounted, mechanically polished according to the standard procedure and then etched with a solution of 10 ml Hf, 5 ml HNO_3 and 85 ml H_2O .

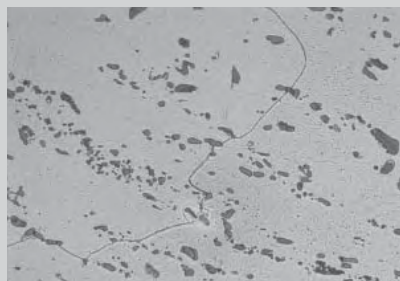


Figure A. Optical micrograph of the microstructure of AA2618-T61. The microstructure consists of uniformly distributed fine Al_2CuMg precipitates and larger intermetallic particles.

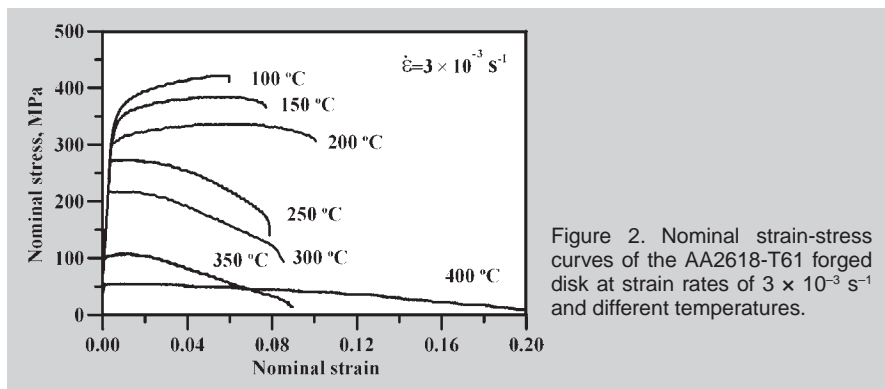


Figure 2. Nominal strain-stress curves of the AA2618-T61 forged disk at strain rates of $3 \times 10^{-3} \text{ s}^{-1}$ and different temperatures.

served along the big angle boundaries at 250°C with the strain rates of $3 \times 10^{-3} \text{ s}^{-1}$, illustrating that dynamic recrystallization occurs during tensile deformation at the deformation conditions. The microstructure of forged disk deformed at 300°C and $3 \times 10^{-4} \text{ s}^{-1}$ is shown in Figure 6, which exhibits typical dynamic recrystallization features and the absence of annealing twins.

High-temperature Ductility

The ductility of the forged disk in hot and warm conditions, measured as total elongation is shown in Figure 7. It can be observed ductility of the material increased over the temperature range of 100–200°C mainly due to dynamic recovery process. However, after an initial increase, the total elongation to fracture gradually decreased over a temperature range of 200–300°C followed by an abrupt increase at 400°C. Furthermore, in the case of higher strain rate, deformation proceeds to larger strains. Figure 8 shows the tension specimens deformed at 200 and 300°C. Although the elongation of the specimen deformed at 300°C decreased, the reduction of area severely increased with temperature (Figure 9).

In general, in several alloys dynamic recovery and dynamic recrystallization are the main softening mechanisms; however, in aluminum alloys softening mechanisms are characterized by the ability of dislocation to cross-glide or to climb easily, under annihilative attraction.⁹ The observed loss of ductility at 250°C is an expression of the low level of dynamic recovery which is a consequence of the dynamic nature of the precipitation processes occurring during high-temperature deformation. In this case, the microstructure does not depend only on applied stress, but

is the product of a complex interaction among the kinetics of generation and annihilation of dislocations, nucleation of new phases and zones, and growth of precipitates.⁹ Freshly nucleated fine particles very effectively pin dislocations, thus reducing recovery and lowering ductility. The interaction between particles and dislocations involves pinning and diffusion along dislocations. Such effect, if temperature is sufficiently high, provides sufficient driving force and accelerates the transition toward the dynamic recrystallization. Consequently, deformation in the

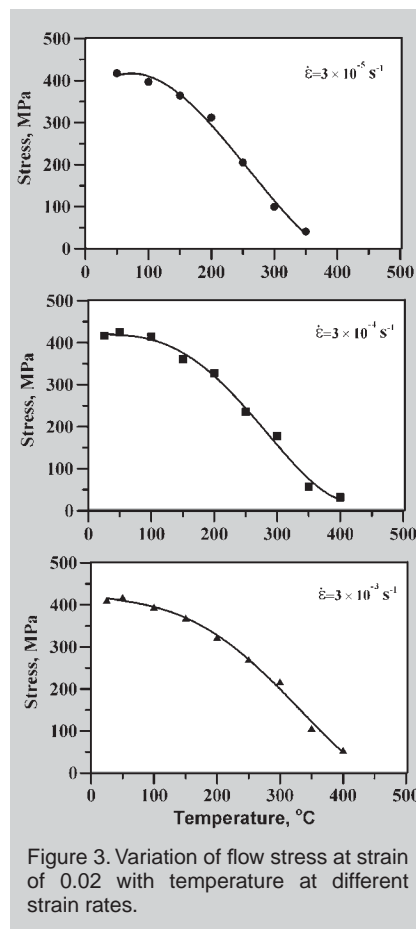


Figure 3. Variation of flow stress at strain of 0.02 with temperature at different strain rates.

partially recrystallized regions becomes unstable causing severe necking and subsequent ductile fracture observed at 300°C. The steep increase in ductility at higher temperatures (350–400°C) implies that a complete softening due to dynamic recrystallization has taken place, and the recovered structure, which is expected to be the cause of the observed premature failure, has been removed. Furthermore, at higher temperature metastable or stable precipitates coarsened and the precipitates become less and less effective in pinning dislocations; new dislocations are generated and recover in larger subgrains.⁹ It can be concluded that dynamic precipitation retards

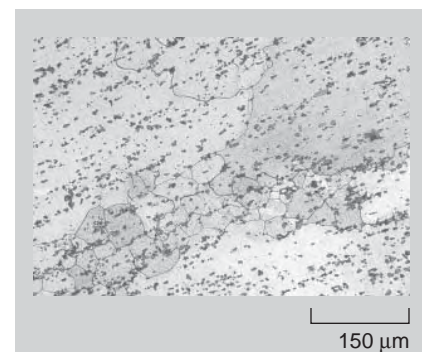


Figure 4. Microstructure of the sample deformed at temperature of 200°C and strain rate of $3 \times 10^{-3} \text{ s}^{-1}$.

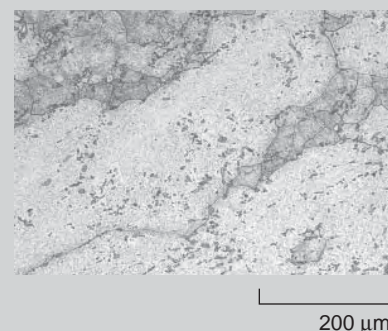


Figure 5. Microstructure of the sample deformed at temperature of 250°C and strain rate of $3 \times 10^{-3} \text{ s}^{-1}$.

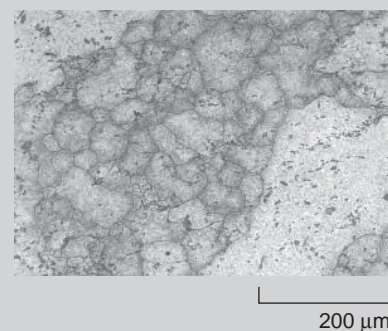


Figure 6. Microstructure of the sample deformed at temperature of 300°C and strain rate of $3 \times 10^{-4} \text{ s}^{-1}$.

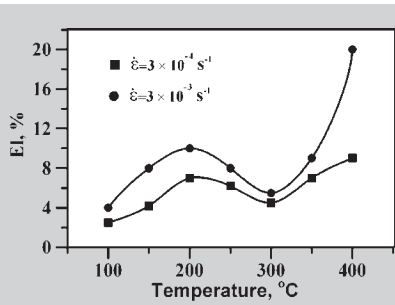


Figure 7. Variation of total elongation as a function of temperature at different strain rates.

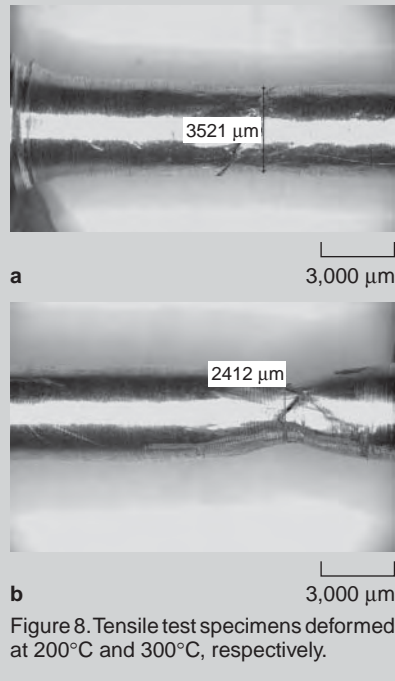


Figure 8. Tensile test specimens deformed at 200°C and 300°C, respectively.

recovery and stimulates subsequent dynamic recrystallization at the higher temperatures. The latter at sufficient high temperatures (350–400°C) promotes ductility.

Figure 10 shows the variation of flow stress with strain rate on a $\ln\text{-}\ln$ plot at different temperatures and at plastic strains of 0.02. The strain rate-flow stress profile is clearly linear between 150 and 400°C. Strain rate sensitivity coefficient (m) as an important material property can affect formability of metals and can be defined as:^{16,17}

$$m = \left. \frac{\partial \ln \sigma}{\partial \ln \dot{\epsilon}} \right|_{T, \epsilon} \quad (2)$$

The calculated strain rate sensitivity (m) at constant true plastic strain and temperature based on Equation 1 is shown in Figure 11. The m value is nearly constant up to 200°C and shows an abrupt increase at 250–300°C. As it is observed, the mean value of m changes

from 0.007 at 200°C to 0.2 at 350°C. The phenomenon can be attributed to the dynamic recrystallization at higher temperatures that produces higher strain rate sensitivity.¹⁸

Constitutive Equation

The hot and warm forming behavior of AA2618 aluminum alloys can be modeled by correlating flow stress to strain rate and temperature according to the well known constitutive equation:¹⁹

$$\sigma = B \dot{\epsilon}^m \exp\left(\frac{mQ}{RT}\right) = BZ^m \quad (3)$$

where $Z = \dot{\epsilon} \exp\left(\frac{Q}{RT}\right)$ is

the Zener–Hollomon parameter representing the temperature modified strain rate, Q is the activation energy related to the deformation mechanism taking place in the material during the process, R is the universal gas constant, T is the absolute temperature, $\dot{\epsilon}$ is the strain rate, m is strain rate sensitivity coefficient, and B is a material parameter. From Equation 3, the apparent activation energy Q , may be defined by:

$$Q = \left. \frac{R}{m} \frac{\partial \ln \sigma}{\partial (1/T)} \right|_{\dot{\epsilon}, \epsilon} \quad (4)$$

Plots of $\ln \sigma$ versus $1/T$ for a strain of 0.02 and different strain rates are shown in Figure 12. It is clear the two lines that were fitted to the experimental data represent two different softening mechanisms at low and high temperatures.

The calculated apparent activation energy decreased with temperature mainly due to greater values of strain rate sensitivity at higher temperatures, shown in Figure 13. The mean value of the apparent activation energy at high temperature region (247 ± 14 kJ/mol) is greater than the value of one calculated for self-diffusion in aluminum alloys (143.4 kJ/mol).²⁰ It is worth noting the activation energy determined from Equation 4 is ‘apparent’ because the microstructural and substructural changes accompanying deformation influence Q through their effect on σ and m . Thus, given the same deformation rate controlling mechanism, Q will vary depending on the microstructural

and substructural changes occurring during deformation.²¹ The unexpected value of activation energy in the present investigation is a consequence of the precipitation process occurring during high-temperature deformation. In this case, the microstructure does not depend only on applied stress, but is the product of a complex interaction among the kinetics of generation and annihilation of dislocations, dynamic recovery and dynamic recrystallization, nucleation and growth of precipitates. It can be concluded that dynamic precipitation restricts dislocation and grain boundary mobility and delays recovery. This leads to high values of apparent activation energy related to the deformation mechanisms taking place at high temperature.

The conventional procedure for calculating constitutive equations for high temperature deformation based

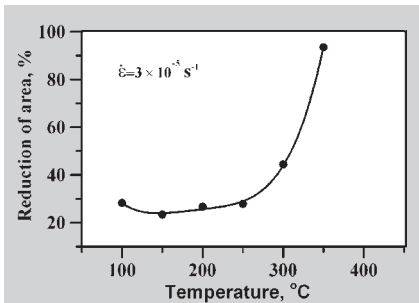


Figure 9. Variation of reduction of area as a function of temperature at strain rates of $3 \times 10^{-5} \text{ s}^{-1}$.

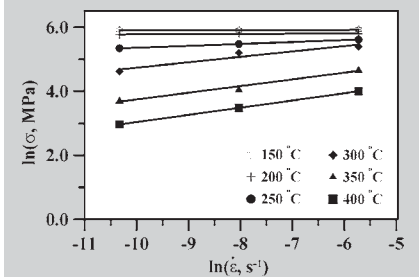


Figure 10. Variation of $\ln(\sigma)$ versus $\ln(\dot{\epsilon})$ at a strain of 0.02 and different temperatures.

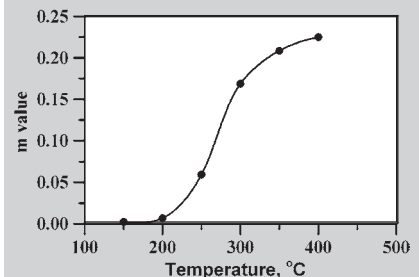


Figure 11. Plot of strain rate sensitivity versus temperature.

on Equation 3 assumes that, in steady state, the activation energy and m value of samples tested at different temperatures appear approximately identical for a fixed stress. Concerning these assumptions, if Equation 3 adequately represents the constitutive behavior of AA2618-T61 aluminum alloy, then a log-log plot of the flow stress versus the Zener–Hollomon parameter should yield a straight line with a slope of m . The mean value of apparent activation energy for high temperature region (247 ± 14 kJ/mol) was used to calculate the Zener–Hollomon parameter and is plotted versus the flow stress in Figure 14. This plot shows a good correlation between the flow stress and the Zener–Hollomon parameter which implies that the flow stress follows the expected trend with respect to strain rate and temperature.

CONCLUSIONS

Based on the present study on the high temperature formability of AA2618-T61 forging disk, the follow-

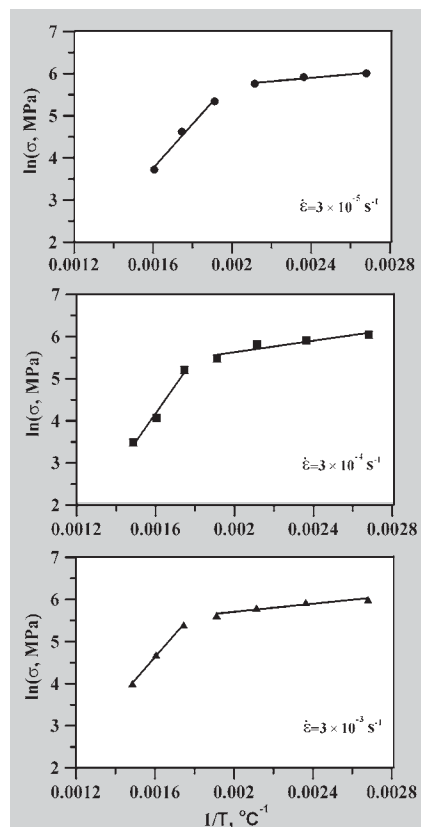


Figure 12. Plot of flow stress versus $1/T$ at a strain of 0.02.

ing conclusions can be made.

Strain rate sensitivity is believed to influence the post-uniform deformation of the material at high temperature deformation conditions. Maximum elongation and percent reduction of area about 18% and 98 %, respectively, was obtained at strain rate of $3 \times 10^{-3} \text{ s}^{-1}$ and 400°C , where the strain rate sensitivity (m) was at maximum of 0.22.

The main softening mechanism of the AA2618-T61 forged disk deformed at high Z value ($100\text{--}200^\circ\text{C}$, $3 \times 10^{-3} \text{ s}^{-1}$) is dynamic recovery. Dynamic recrystallization is the primary softening mechanism when the alloy deformed at low Z value ($350\text{--}400^\circ\text{C}$, $3 \times 10^{-5} \text{ s}^{-1}$). Dynamic recovery and dynamic recrystallization play the role at the same time at medium Z value (250°C , $3 \times 10^{-5} \text{--} 3 \times 10^{-3} \text{ s}^{-1}$).

The observed loss of ductility over a temperature range of $200\text{--}250^\circ\text{C}$ is believed to be an expression of the low level of dynamic recovery which is a consequence of the dynamic precipitation processes occurring during high-temperature deformation. Subsequent decrease in ductility at $250\text{--}300^\circ\text{C}$ is attributed to the severe strain localization at partially recrystallized regions.

Flow stress was found to increase monotonically at low temperature, while at the higher temperatures of the investigated range the stress–strain curves exhibited a peak, followed by softening.

The mean apparent activation energy for tensile deformation of the alloy is 247 ± 14 kJ/mol, which is higher than that one calculated for self-diffusion in aluminum alloys. The appreciate difference between the two activation energy values is a consequence of the dynamic precipitation process occurring during high-temperature deformation.

References

- G.E. Dieter, editor, *Workability Testing Techniques* (Metals Park, OH: American Society for Metals, 1984).
- H. Yamagata, *Scr. Met. Mater.*, 27 (2) (1992), pp. 201–203.
- B. Ren and J.G. Morris, *Met. Mater. Trans.*, 26A (1995), pp. 31–40.
- H.J. McQueen, *Mater. Sci. Eng.*, A387–389 (2004), pp. 203–208.
- H.E. Hu et al., *Mat. Sci. Eng.*, A488 (2008), pp.

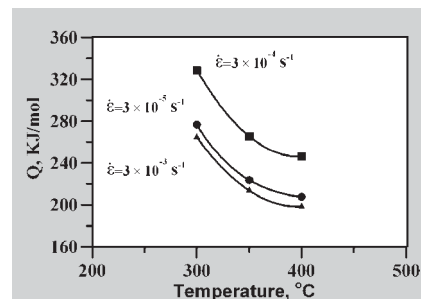


Figure 13. Variation of apparent activation energy as a function of temperature at different strain rates.

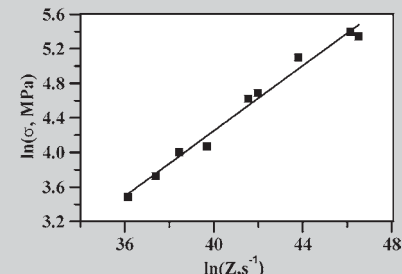


Figure 14. Variation of flow stress versus Zener–Hollomon parameter at a strain of 0.02 and temperature range of $300\text{--}400^\circ\text{C}$.

64–71.

- I. Özbek, *Mater. Charac.*, 58 (2007), pp. 312–317.
- J. Wang et al., *Mater. Charac.*, 59 (2008), pp. 965–968.
- J.C. Williams and E.A. Starke, *Acta Mater.*, 51 (2003), pp. 5775–5799.
- F. Bardi, M. Cabibbo, and S. Spigarelli, *Mater. Sci. Eng.*, A334 (2002), pp. 87–95.
- ASM Handbook vol. 2* (Materials Park, OH: American Society for Metals, 1990).
- K. Yu et al., *Mater. Sci. Eng.*, A368 (2004), pp. 88–93.
- D. Bobrow, A. Arbel, and D. Eliezer, *J. Mater. Sci.*, 26 (1991), pp. 2045–2049.
- P. Cavaliere, *J. Light Metals*, 2 (2002), pp. 247–252.
- R. Singer and W. Blum, *Z. Metallkde.*, 68 (1977), p. 328.
- A. Seeger, *Work Hardening*, vol. 46, ed. J.P. Hirth and J. Weertman (New York: TMS-AIME, 1968), pp. 27–63.
- M. Aghaie-Khafri and R. Mahmudi, *JOM*, 50 (11) (1998), pp. 50–52.
- M. Aghaie-Khafri and N. Golarzy, *Mater. Sci. Eng.*, A486 (2008), pp. 641–647.
- F. Monetteillet and J.J. Jonas, *Metall. Mater. Trans.*, 27A (1996), pp. 3346–3348.
- M. Aghaie-Khafri and N. Golarzy, *J. Mater. Sci.*, 43 (2008), pp. 3717–3724.
- O.D. Sherby, R.J. Klundt, and A.K. Miller, *Metall. Trans.*, 8A (1977), p. 843.
- C. Girish Shastry et al., *Mat. Sci. Eng.*, A465 (2007), pp. 109–115.

M. Aghaie-Khafri, Associate Professor, and A. Zargaran, graduate student, are with the Faculty of Mechanical Engineering, K.N. Toosi University of Technology, P.O. Box 19395-1999, Tehran, Iran. Prof. Aghaie-Khafri can be reached at +98 09123088389; fax +98 21 88674748; e-mail maghaei@kntu.ac.ir.

The Use of Friction Stir Welding for Manufacturing Small-scale Structures

T. Hirata and K. Higashi

Friction stir welding (FSW) is a relatively new joining process and is being used commercially in several industry sectors. In small and medium enterprises, however, this novel technology has not been applied despite its remarkable advantages because of the drawbacks of FSW. A database has been assembled and drawbacks have been analyzed then solved appropriately in the Industry-Government-Academia Collaboration Project. As an outgrowth, the optimum and individual know-how of practical FSW technology could be transferred to medium and small enterprises.

INTRODUCTION

Friction stir welding (FSW) is a relatively new joining process. It was developed initially for aluminum alloys, by The Welding Institute (TWI) of the United Kingdom.¹ In FSW, a cylindrical, shouldered tool with a profiled probe is rotated and slowly plunged into the joint line between two pieces of sheet or plate material, which are butted together. Frictional heat is generated between the wear-resistant welding tool and the material of the workpieces. This heat causes the latter to soften without reaching the melting point and allows traversing of the tool along the weld line. It leaves a solid phase bond between the two pieces. The advantages result from the fact that the FSW process takes place in the solid phase below the melting point of the materials to be joined. In addition, the process offers low distortion and is energy efficient, environmentally friendly, and versatile.

Friction stir welding is currently being used commercially in several sectors, such as the railway, automotive, and aerospace industries. However,

How would you...

...describe the overall significance of this paper?

In this paper, several approaches for developing practical friction stir welding (FSW) processes in medium and small enterprises are introduced. Friction stir welding has attracted a great deal of attention as a high-quality welding technology and is currently being used commercially in several industry sectors. However, practical use has not advanced in small and medium enterprises because of some technical problems. This article describes experiments to determine how practical FSW technology could be transferred to those medium and small enterprises.

...describe this work to a materials science and engineering professional with no experience in your technical specialty?

Friction stir welding (FSW) is a relatively new joining process. The process advantages result from the fact that the FSW process takes place in the solid phase below the melting point of the materials to be joined. However, this novel technology cannot be applied in small and medium enterprises because it is very difficult to make small products by using FSW. A new FSW system has been developed in this work so that practical FSW technology could be transferred to the medium and small enterprises.

...describe this work to a layperson?

Welding technology is important for manufacturing, with fusion welding the most popular technology in metal welding. Friction stir welding is a relatively new joining process that, like fusion welding, does not melt the materials. The process advantages are low distortion, energy efficiency, environmental friendliness, and versatility. In this work, research and development on FSW was carried out to promote the products upgrade and strengthen the price-competitive edge in the medium and small enterprises.

most applications of FSW are limited to major enterprises, and practical use has not been advanced in small and medium enterprises. This is because additional value is high even if an only linear weld is possible when large-scale structures are manufactured by major enterprises. However, the cost cannot be justified when small and medium enterprises make small products using FSW. In addition, it is very difficult for small and medium enterprises to conduct needed three-dimensional (3-D) welding by FSW.

The City Area Project—an industry-government-academia collaboration project at Osaka-East-Urban Area in Osaka Prefecture, by the Ministry of Education, Culture, Sports, Science and Technology Japan (MEXT) was established in 2004. This project mainly conducted research and development on FSW to promote product upgrades and strengthen the price-competitive edge of the major industries such as metalworking machinery in Osaka Prefecture. The schematic of the procedure used to carry out this project is shown in Figure 1.

A new FSW machine was developed during this project with two types of heads: a high-output linear head with two-axes movement (X and Y axes) and a 3-D drive head with five-axes movement (X, Y, Z, a, and c axes). Therefore, this machine is capable of welding a material in a wide range of shapes.

Several approaches were carried out to develop a practical FSW process for medium and small enterprises.^{2,3} The drawbacks that occurred during the FSW experiments were analyzed and solved appropriately. As a result, the optimum and individual know-how on practical FSW could be transferred to

medium and small enterprises. Images of the supply device of metallic parts and the water-cooling plate used in FSW are shown in Figure 2. It was possible to produce in less time and at low cost. In addition, the newly developed tool is shown in Figure 3. This tool is highly suitable for use in a 3-D FSW process. In this paper, a database constructed in this project is introduced, and several approaches for developing practical FSW processes for medium and small enterprises are introduced.

See the sidebar for details on the FSW database.

DEVELOPMENT APPROACH

Supply Device of Metallic Parts

The supply device of metallic parts and a schematic of the chassis of the device are shown in Figure 4. In the conventional method, the top and bottom of the column or the column and the base were connected by bolts. It is possible to reduce the number of modules, duration of the process, and cost if the supply device made of metallic

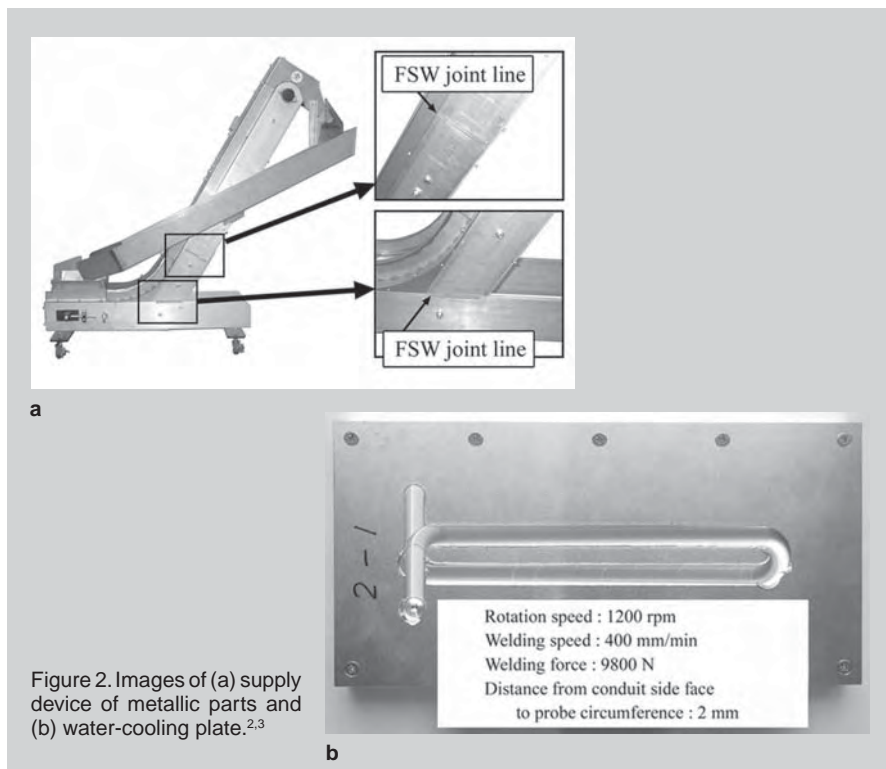


Figure 2. Images of (a) supply device of metallic parts and (b) water-cooling plate.^{2,3}

parts can be manufactured using FSW. In addition, it is expected to be able to manufacture products with a good design.

The material used was a 6063-T5 aluminum alloy sheet with a thickness of 10 mm. Single-pass friction stir butt welds were produced using an FSW tool with a shoulder diameter of 20 mm and a probe length of 9.8 mm. The cross section of the weld joint under the optimum FSW condition is shown in Figure 5. The weld did not exhibit cracks and porosity, indicating that the weld was of good quality. Moreover, the joint efficiency under the optimum FSW condition was approximately 70%. This value was considered to be very high because the 6063-T5 aluminum alloy was a heat-treated aluminum alloy.

During FSW, it is necessary to hold the material firmly in place. In particular, it is important to firmly hold the material along the direction vertical to the welding direction from the



Figure 3. The tool developed in this project.³

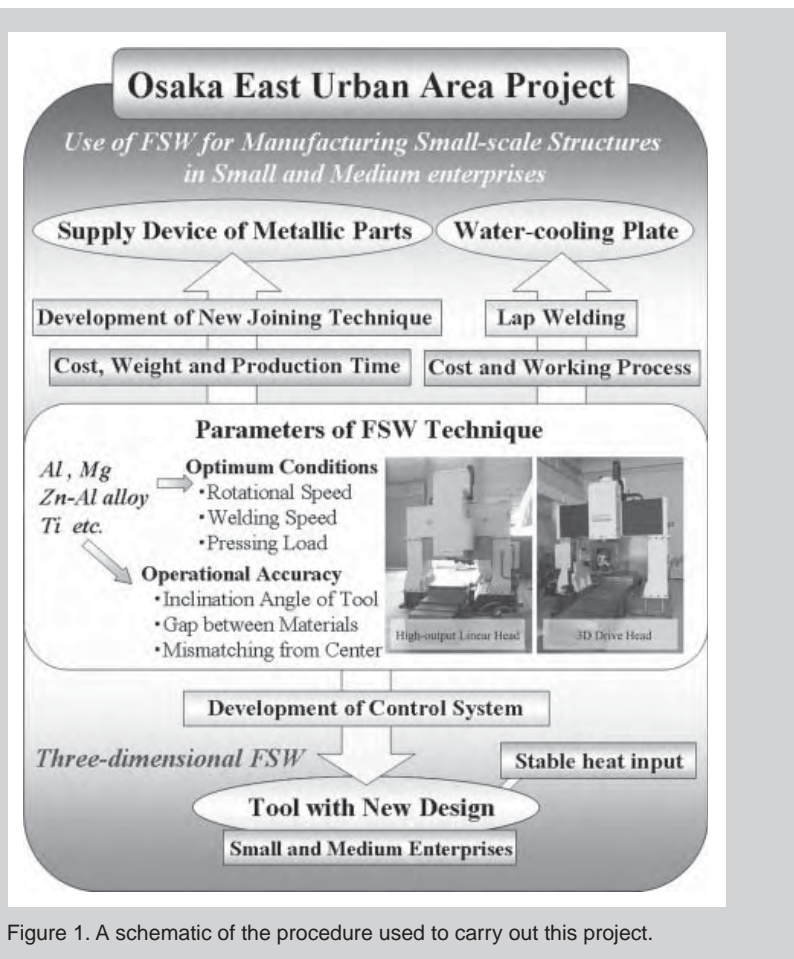


Figure 1. A schematic of the procedure used to carry out this project.

FRICTION STIR WELDING DATABASE

Friction stir welding (FSW) is considered by many to be the most significant development in metal joining in the last decade. In addition, friction stir processing (FSP) has been developed based on the basic principles of FSW. This technique is used to induce material modification. To put the FSW technique to practical use in medium and small enterprises, it is important to analyze various parameters. In this project, we investigated numerous parameters such as welding parameters, weld joint properties, and operation accuracy.

Aluminum and Magnesium Alloys

Table A lists the parameters of aluminum and magnesium alloys used in the study along with the welding conditions of the FSW (FSP) techniques.⁴⁻²⁵ It has been reported that 2000 and 7000 aluminum alloys have been joined using FSW because this technique has the ability to join materials that cannot be fusion welded. Friction stir welding conditions influence the properties of a weld joint. The relationship between the heat input parameter RtD^3/V and the grain size d in the stir zone of a 5083 aluminum alloy is shown in Figure A.⁷ Rt is the rotational speed; V , the welding speed; and D , the shoulder diameter of the tool. It is evident that RtD^3/V is closely related to d . Further, a refinement in the grain size of the weld zone improved the formability of the weld joint.⁷ Therefore, RtD^3/V was considered to be a key parameter in the manufacture of industrial machines using FSW.

Titanium

Titanium and its alloys, which have high specific strength, excellent corrosion resistance, and good biocompatibility, are widely used in aircrafts and artificial bones.²⁸ Unfortunately, since titanium and

its alloys have a high oxygen affinity, they cannot be welded easily; therefore, tungsten inert gas welding (TIG) is usually used for welding titanium alloys.²⁹ FSW is suitable for titanium and its alloys. In this study, a

pin tool was developed using relatively low-cost metallic materials such as heat-resistant alloys, with or without surface treatment.³⁰ An image of pure titanium welded using FSW is shown in Figure B. The maximum

Table A. Parameters of Aluminum and Magnesium Alloys used in This Study along with the Welding Conditions of the FSW (FSP) Techniques⁴⁻²⁵

Material (Thickness)	Tool		Welding Conditions		Ref.
	Shoulder Diameter (mm)	Probe Diameter (mm)	Rotational Speed (rpm)	Welding Speed (mm/min)	
1050-H24 (5t)	15	6	600 ~ 2,000	100 ~ 800	4
5052-O (3t)	9	3	2,000 ~ 4,000	1,000 ~ 2,000	5
5052-O (3t)	15	3	4,000	500 ~ 1,000	5
5083-O (1t)	9	3	250 ~ 1,600	130 ~ 350	6
5083-O (3t)	12	4	500 ~ 1,000	100 ~ 200	7
2017-T351 (5t)	15	6	1,500	25 ~ 200	8
2024-T351 (6t)	16	6	850	120	9
2024-T6 (6t)	16	6	850	120	9
2024-T351 (7t)	23	8.2	215 ~ 360	77 ~ 267	10
6061-T6 (6t)	15 ~ 21	6	1,200	75	11
6061-T6 (3.2t)	12.7	3.18	1,000	76	12
6056 (4t)	14	6	500 ~ 1,000	40 ~ 80	13
6082-T6 (3t)	10	3	715 ~ 1,500	71.5 ~ 200	14
7075-T6 (7t)	20	6.5	700	160	15
7075-T6 (6t)	18	6	350	120	16
7449-T3 (22t)	23	8	350	175 ~ 350	17
7449-T79 (22t)	23	8	350	175 ~ 350	17
AZ31B (0.64t)	19	6.3	800 ~ 1,000	60	18
AZ31B (4t)	12	4	375 ~ 2,250	20 ~ 375	19
AZ31B (1.9t)	13	5	1,400	300	20
AZ31-H24 (4.95t)	19.05	6.35	500 ~ 1,000	60 ~ 240	21
AZ61 (6.3t)	18	8	1,220	90	22
AM60B (2t)	19	6.3	2,000	120	23
AZ91D (2t)	8	3	800 ~ 1,800	90 ~ 750	24
LA141 (2t)	12	4	1,500	200	25

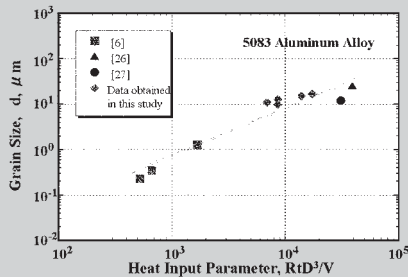


Figure A. Relationship between RtD^3/V and d in the stir zone of 5083 aluminum alloy.⁷



Figure B. Pure titanium welded using FSW.

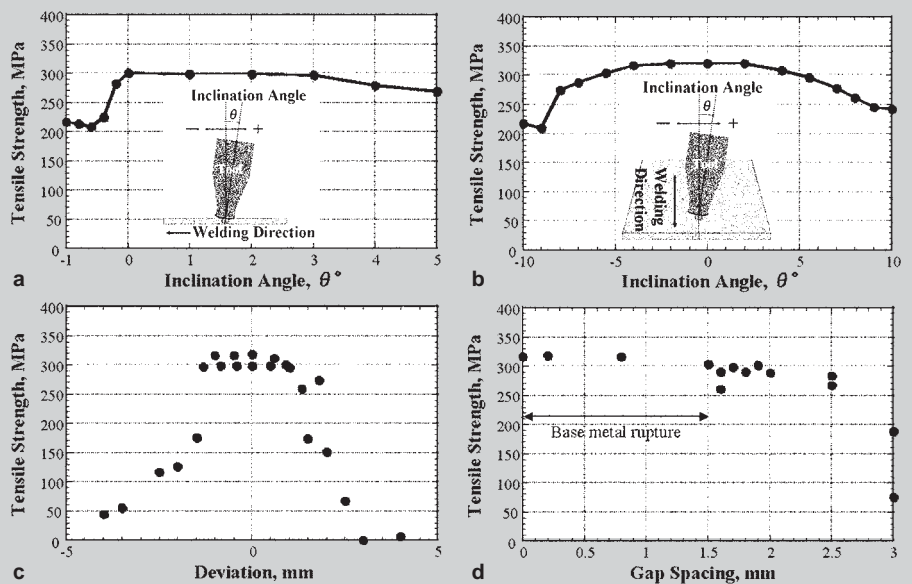


Figure C. Allowable operational deviation in (a) parallel inclination against direction of welding, (b) vertical inclination against direction of welding, (c) butt line/tool-travel line deviation, and (d) gap spacing.^{3,31,32} The material used was 5083 aluminum alloy.

joint efficiency was about 90%, and it was suggested that it could be welded using the low-cost pin tool.

Operational Accuracy

For three-dimensional (3-D) FSW, it is most important to improve operational accuracy.^{31,32} Therefore, the objective of this study is to elucidate the following: allowable deviation (deviation is defined as the misalignment of the butt and tool-travel lines); allowable gap spacing (gap spacing is defined as the separation between the butt faces); allowable tool angle (tool angle is defined as angle at which the tool is inclined in the parallel and perpendicular directions to the welding direction).

The allowable operational deviations are shown in Figure C. An FSW tool with a conventional shape, made of die steel, was used in this study. The butt line/tool-travel line was allowed to deviate up to half the probe diameter distance when the butt line was placed on the advancing side of the tool rotation. So we have the one-fourth of probe diameter allowance on both sides by setting the butt line from the probe center in a quarter of the probe diameter to advancing side. The allowable gap spacing was three-eighths of the probe diameter when the butt line was placed at the center of the tool-traveling line. In the case of the inclination angle, the plus and minus angles indicate the angles of advancing and retreating and of the right and left, respectively. The allowable tool inclination in the direction perpendicular to the welding direction is 2° in the right and left directions. The allowable tool inclination in the direction parallel to the welding direction is 3° of the advancing angle and 0.4° of the retreating angle, because material loss was significantly high and defects occurred on the surface of the weld line when the retreating angle was greater than 0.4° . These results were important as they were used for the development of a 3-D control system.³³ The samples produced by using this control system are shown in Figure D. In this way, this machine is capable of applying the weld to the materials in a wide range of the shapes by using this control system.

Friction Stir Processing

The microstructures of several materials change to fine-grained structures due to dynamic recrystallization during FSP. In this study, many FSPed materials were investigated.³⁴⁻³⁷ For example, FSP was used to effectively produce a Zn-22wt.%Al alloy with a very fine-grained microstructure. The initial texture of the Zn-rich phase became random due to FSP, as shown in Figure E. This microstructural evolution due to FSP

influenced the deformation behavior of the FSPed Zn-22Al alloy. Figure Fa and b shows the variations in flow stress and elongation to failure of the Zn-22Al alloy as a function of strain, respectively. The value of the elongation to failure was almost the same for all

materials at a low strain rate. However, at a high strain rate, the value of the elongation to failure of the FSPed material was higher than that of the base material. Therefore, FSP is considered to be suitable for improving the mechanical properties of materials.

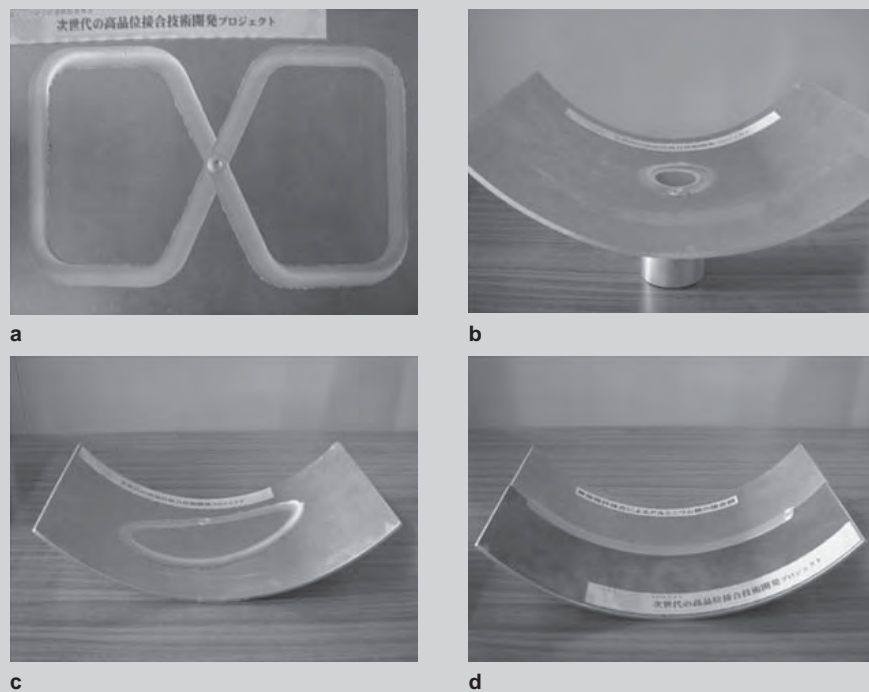


Figure D. Images of samples produced by using this control system.

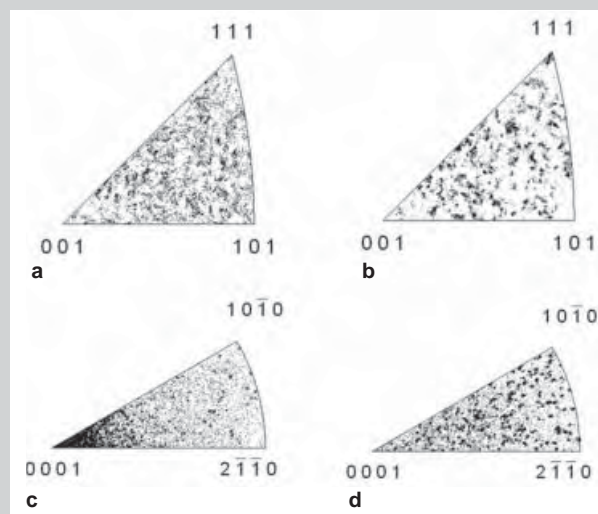


Figure E. Inverse pole figures of (a) Al-rich phase of base material, (b) Al-rich phase of friction-stir processed material, (c) Zn-rich phase of base material, and (d) Zn-rich phase of friction-stir processed material.³⁷

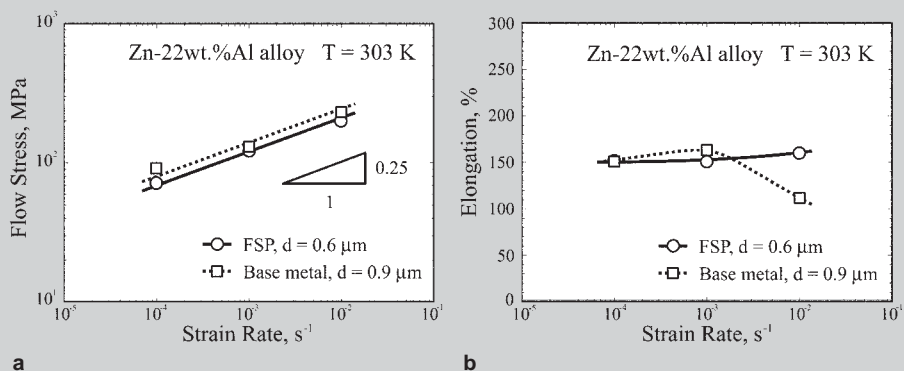


Figure F. Variations in (a) flow stress and (b) elongation-to-failure as a function of strain rate.³⁷

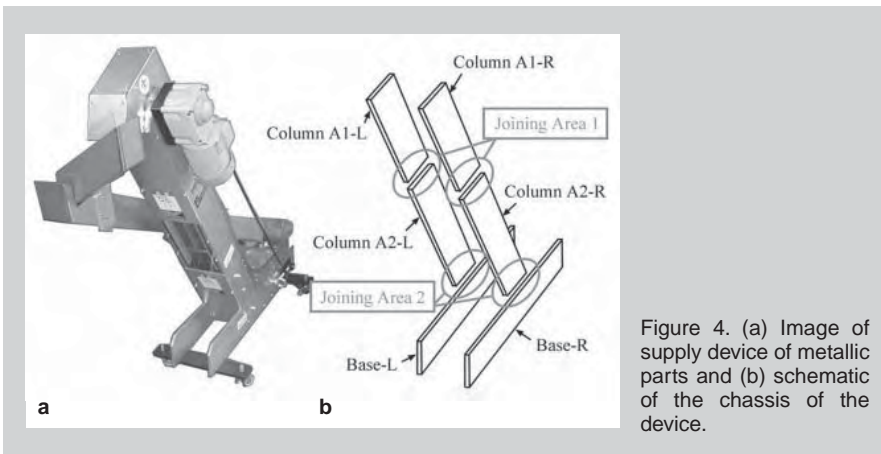


Figure 4. (a) Image of supply device of metallic parts and (b) schematic of the chassis of the device.

viewpoint of measurement accuracy. When applying FSW for manufacturing a large-sized product, large-scale structures are often linear welded for long distances. Therefore, both sides of the welded blank are often parallel, and it is comparatively easy to firmly hold the material along the direction vertical to the welding direction. However, when applying FSW for manufacturing a small-sized product in small and medium enterprises, it is predicted that both sides of the welded blank will often not be parallel. In other words, it is necessary to investigate the possibility of using another method for firmly holding the welded blank with a special shape in place. Therefore, another welding method was developed.

From the design considerations, the right and left side of the column of the welded surface must be placed inside the supply device of metallic parts. In

addition, considering the fact that distortion is caused after FSW, welded blanks and jigs were created, as shown in Figure 6. Columns A1 and A2 were fixed by blocks, and Column A1 was pushed by an air cylinder. Since one side of Column A2 was not parallel to the welding direction, it was difficult to push Column A2 from this side using the air cylinder. Therefore, it was assumed that Column A2 was held in a fixed position using a fixing pin. Further, it was easy to push the columns in a direction perpendicular to the welding direction, and the product was manufactured with high-dimensional accuracy.

The base and column were welded using the same approach as were the columns, as shown in Figure 7. Blocks were used for fixing the column; the base was pushed by the air cylinder. In addition, the column was fixed by using the fixing pin. Welding the base and column using the above-mentioned method resulted in the successful manufacture of the supply device of metallic parts at low cost, as shown in Figure 2a. Therefore, a technique employing the fixed pin was used in manufacturing structures with specific design considerations, and it was expected that this technique should be applied to manufacture other products.

Water-cooling Plate

The conventional method to develop a water-cooling plate made of aluminum alloy is shown in Figure 8. A gun drill was used to create holes in the aluminum block. Next, the holes were blocked in order to form a waterway. Therefore, the development of the water-cooling plate resulted in low work-

ability and high cost. If the waterway is formed in the aluminum block and the cover by aluminum board is welded at the edge of the waterway on the basis of a lap FSW design, a reduction in both the duration of the working process and production cost is expected.

Materials used to develop the water-cooling plate were 5052-H112 and 5052-H34 aluminum alloy sheets with thicknesses of 30 mm and 2 mm, respectively. The diameters of the probe and the shoulder of the FSW tool were 4 mm and 12 mm, respectively. The length of the probe was 2.9 mm. The macrosection of the water-cooling plate joined using lap welds under optimum FSW condition is shown in Figure 9. In the figure, the left and right sides represent the retreating (RS) and advancing sides (AS) of the weld, respectively. The weld did not exhibit cracks and

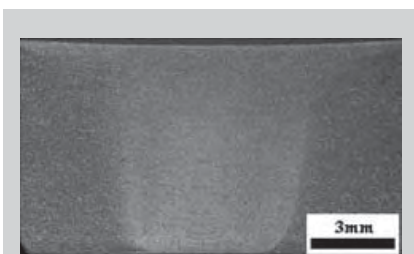


Figure 5. Cross section of the weld joint under optimum FSW conditions.^{2,3}

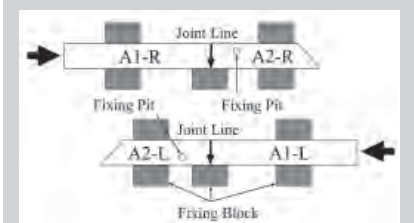


Figure 6. Method using FSW technique for welding columns.^{2,3}

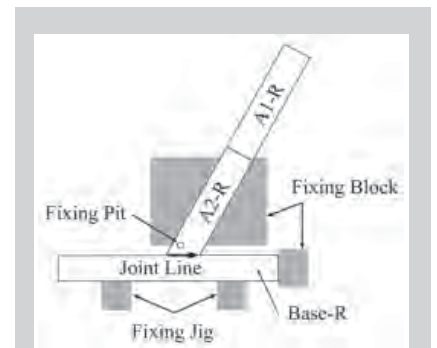


Figure 7. Method using FSW technique for welding the base and column.^{2,3}

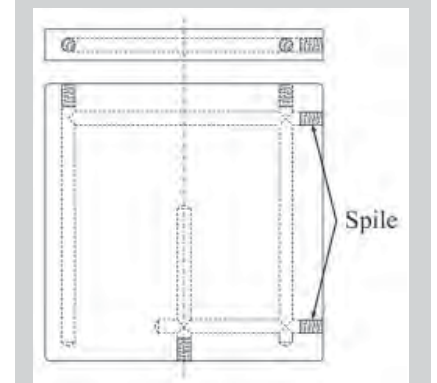


Figure 8. Conventional method for developing water-cooling plate.



Figure 9. Macrosection of the plate joined using lap welds under optimum FSW condition.³

voids, indicating that the weld was of good quality. However, the joint interface remained horizontal on the RS of the weld.

Specimens were extracted from welds, and shear tensile tests were performed on them under two welding conditions. Rotational speed of 1,200 rpm and welding speeds of 400 mm/min. and 100 mm/min. were maintained. The shape of the specimen is shown in Figure 10. Because the joint interface remains horizontal on the RS of the weld, welding was performed in directions A and B. Since all the specimens fractured at the upper board, it implied that weld joints were of very good quality. However, the strength of the joints varied, and the maximum shear strength was obtained at the rotational speed of 1200 rpm, welding speed of 400 mm/min., and in the welding direction B.

We challenged to develop a simple water-cooling plate. The schematic of the simple water-cooling plate is shown in Figure 11. This plate was developed under the optimum FSW condition. Further, the welding route with circular arc was partially employed from the viewpoint of practical use. Therefore, the 3-D drive head with five axes movement was used in the welding of the water-cooling plate. The image of the water-cooling plate is shown in Figure 2b. The plate could be welded ef-

fectively. In addition, the water-cooling plate successfully passed the air and pressure tightness tests. Therefore, it was possible to develop the water-cooling plate with lap weld and five axes movement using a rapid and inexpensive manufacturing process.

Tool for 3-D FSW

One of the features of FSW is that the tool used for welding is kept in a fixed position. The position of the tools used in the working and the FSW machines is shown in Figure 12. During cutting, the tools are kept in a fixed position. On the other hand, during FSW, the tools are inclined at the advancing angle along the direction vertical to the planar direction of the material. This is because it is easy to supply a steady heat input during FSW. In addition, it is possible to inhibit the occurrence of burrs, and a tool with a complex shape is not required. The welding quality is expected to deteriorate remarkably when FSW is performed using the conventional FSW tool, which is not inclined at the advancing angle. However, it is difficult to maintain the inclination of the tool at the advancing angle during 3-D FSW. Moreover, it is necessary to consider the geometric interference between the FSW machine and the tool, as shown in Figure 13. Therefore, not only the advancing angle but also the retreating angle is very important for

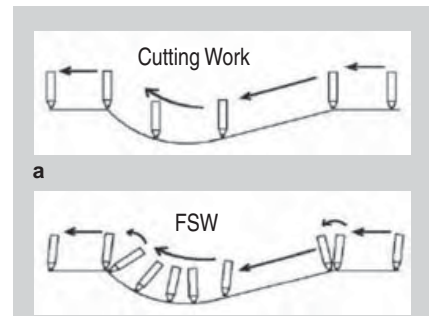


Figure 12. Position of tools used in (a) working machine and (b) FSW machine.

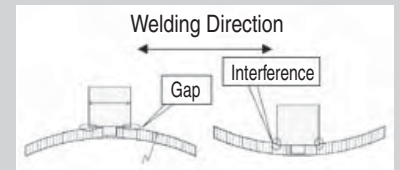


Figure 13. Geometric interference between the work machine and the tool.

3-D FSW, and the development of a tool which can weld in a wide range of inclination angles has been expected. Thus, the new tool required for 3-D FSW has been developed and is introduced in this section.

As shown in Figure C in the sidebar, a high joint strength was obtained along the range of the advancing angle; however, the joint strength decreased with an increase in the retreating angle when the conventional FSW tool was used. The joint strength decreased significantly when the retreating angle was greater than 0.4° , because material loss was very high and defects occurred on the surface of the weld line. Therefore, the development of a new tool was needed so FSW could be performed when the retreating angle was greater than 0.5° .

We have paid attention to a part of the shoulder for developing the new tool, and the design of the new tool has been discussed. The newly developed FSW tool is shown in Figure 3. The probe of the new tool was almost the same as that of the conventional tool. On the other hand, a unique design was adopted to develop the shoulder of the new tool, which differed from that of the conventional tool. FSW was performed using the new tool. The image of the tensile specimen extracted from the welds, and the mechanical properties of the weld joint are shown in Figure 14. 6063-T6 aluminum alloy was

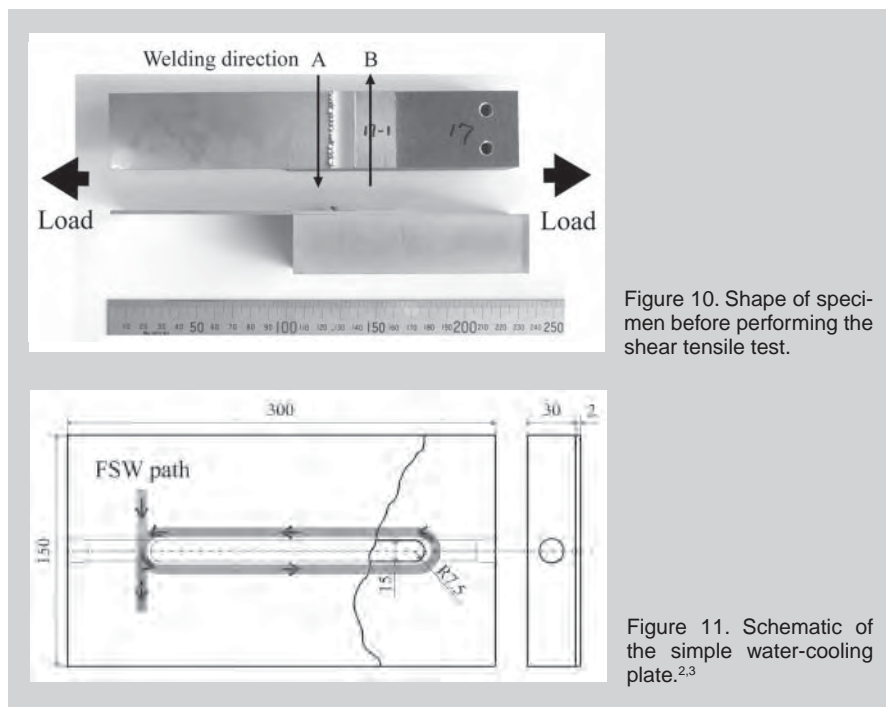


Figure 10. Shape of specimen before performing the shear tensile test.

Figure 11. Schematic of the simple water-cooling plate.^{2,3}

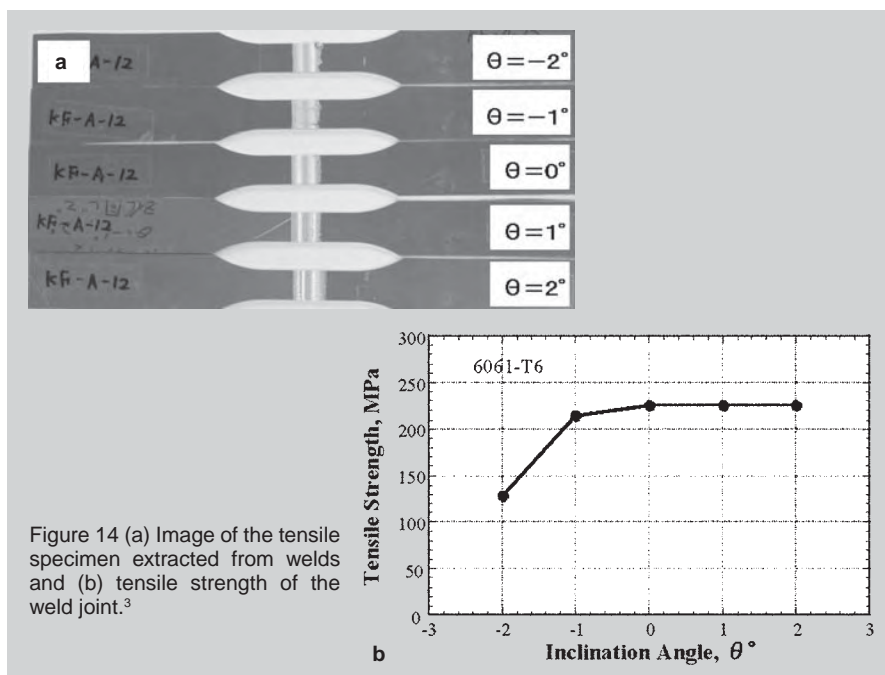


Figure 14 (a) Image of the tensile specimen extracted from welds and (b) tensile strength of the weld joint.³

used as the material. It was possible to perform welding in the range of the advancing angle without the occurrence of burrs. In addition, it was possible to perform welding in the range of the retreating angle range without penetrating the plate material, and a defect was not observed on the surface. Good welding quality was obtained until the retreating angle of 1° . The position of the tool used in FSW has an influence on various aspects. For example, the design of the 3-D FSW becomes simple if the tool inclination is not considered. In addition, the load on the machine is expected to reduce, especially when the tool is inclined in the range of the retreating angle. The miniaturization of the FSW machine is possible. Therefore, the development of the new tool is considered to be cost effective. From the above-mentioned results, it is apparent that this new tool is highly suitable for use in 3-D FSW, and the applicability of FSW employing this tool can be enhanced in the future.

CONCLUSION

Many problems remain in applying FSW for manufacturing products in small and medium enterprises. Moreover, it is very important to solve these problems to enhance the applicability of the FSW technique. In Osaka Prefecture, "Research Association for

Practical Use of Friction Stir Technology" (established by the Osaka Industrial Promotion Organization) was formed as a successor to the Urban Area Industry-Government-Academia Collaboration Project (2004–2007). We aim at enhancing the applicability of the FSW technique via this association in the future.

ACKNOWLEDGEMENT

This work is a part of the Osaka East Urban Area Industry-Government-Academia Collaboration Project on FSW "CITY AREA" sponsored by MEXT, 2004–2007. The authors would like to especially acknowledge Shimonishi Seisakusho Co., Ltd, Nakata Co., Ltd, and Isel Co., Ltd. They also would like to express their sincere appreciation to Associate Prof. Masato Tsujikawa, Prof. Sachio Oki, Prof. Masahiko Ikeda, Associate Prof. Yorinobu Takigawa, and Prof. Yoji Marutani. They would like to express their thanks to the parties concerned in Technology Research Institute of Osaka Prefecture.

References

1. C.J. Dawes and W.H. Thomas, *Weld. J.*, 75 (1996), pp. 41–45.
2. T. Tanaka et al., *J. Japan Inst. Light Metals*, 57 (2007), pp. 549–553 (Japanese).
3. T. Hirata et al., *J. JFJA*, 7 (2008), pp. 25–30 (Japanese).
4. H.J. Liu et al., *Sci. Tech. Weld. Join.*, 8 (2003), pp.

- 450–454.
5. Y.S. Sato et al., *Mater. Sci. Eng. A*, 369 (2004), pp. 138–143.
6. Y.S. Sato et al., *Mat. Sci. Eng. A*, 354 (2003), pp. 298–305.
7. T. Hirata et al., *Mater. Sci. Eng. A*, 456 (2007), pp. 344–349.
8. H.J. Liu et al., *J. Mater. Process. Tech.*, 142 (2003), pp. 692–696.
9. C. Genevois et al., *Acta Mater.*, 53 (2005), pp. 2447–2458.
10. M.A. Sutton et al., *Mater. Sci. Eng. A*, 354 (2003), pp. 6–16.
11. K. Elangovan and V. Balasubramanian, *Mater. Design*, 29 (2008), pp. 362–373.
12. D. C. Hofmann and K. S. Vecchio, *Mater. Sci. Eng. A*, 402 (2005), pp. 234–241.
13. P. Cavaliere et al., *J. Mater. Process. Tech.*, 180 (2006), pp. 263–270.
14. L. Fratini and G. Buffa, *Int. J. Machine Tools & Manufacture*, 45 (2005), pp. 1188–1194.
15. P. Cavaliere and A. Squillace, *Mater. Character.*, 55 (2005), pp. 136–142.
16. J.-Q. Su, T.W. Nelson, and C.J. Sterling, *Mater. Sci. Eng. A*, 405 (2005), pp. 277–286.
17. M. Dumont et al., *Acta Mater.*, 54 (2006), pp. 4793–4801.
18. J.A. Esparza et al., *J. Mater. Sci. Lett.*, 21 (2002), pp. 917–920.
19. W. Xunhong and W. Kuaishe, *Mater. Sci. Eng. A*, 431 (2006), pp. 114–117.
20. M.B. Kannan et al., *Mater. Sci. Eng. A*, 460–461 (2007), pp. 243–250.
21. N. Afrin et al., *Mater. Sci. Eng. A*, 472 (2008), pp. 179–186.
22. S.H.C. Park, Y.S. Sato, and H. Kokawa, *Scr. Mater.*, 49 (2003), pp. 161–166.
23. J.A. Esparza, W.C. Davis, and L.E. Murr, *J. Mater. Sci.*, 38 (2003), pp. 941–952.
24. S.H.C. Park, Y.S. Sato, and H. Kokawa, *J. Mater. Sci.*, 38 (2003), pp. 4379–4383.
25. M. Tsujikawa et al., *Mater. Trans.*, 47 (2006), pp. 1077–1081.
26. K. Colligan et al., *Proc. 3rd Int. FSW Symp.* (Cambridge, U.K.: The Welding Institute, 2001).
27. J.K. Kristensen et al., *Proc. 5th Int. FSW Symp.* (Cambridge, U.K.: The Welding Institute, 2004).
28. G. Luetjering and J.C. Williams, *Titanium* (Berlin: Springer, 2003).
29. M.J. Donachie Jr., *Titanium; A Technical Guide* (Metals Park, OH: ASM International, 1988), pp. 131–141.
30. M. Ikeda et al., *Proc. 6th Int. FSW Symp.* (Cambridge, U.K.: The Welding Institute, 2006).
31. S. Oki et al., *Mater. Sci. Forum*, 539–543 (2007), pp. 3838–3843.
32. S. Oki et al., *Proc. 6th Int. FSW Symp.* (Cambridge, U.K.: The Welding Institute, 2006).
33. Y. Okawa et al., *Welding Tech.*, 55 (2007), pp. 71–75 (Japanese).
34. M. Tsujikawa et al., *Mater. Trans.*, 46 (2005), pp. 3081–3084.
35. M. Tsujikawa et al., *Mater. Trans.*, 48 (2007), pp. 618–621.
36. J. Kobata et al., *Mater. Lett.*, 61 (2007), pp. 3771–3773.
37. T. Hirata et al., *Scr. Mater.*, 56 (2007), pp. 477–480.

T. Hirata is with the Metals and Machinery Department of the Technology Research Institute of Osaka Prefecture, 2-7-1 Ayumino, Izumi-city, Osaka 594-1157, Japan; K. Higashi is with the Graduate School of Engineering, Osaka Prefecture University, 1-1 Gakuen-cho, Sakai-city, Osaka 599-8531, Japan.

Nanocomposite Materials—Leading the Way in Novel Materials Design

Jonathan E. Spowart

Note: A nanocomposite is defined as a multiphase solid material where one of the phases has one, two, or three dimensions of less than 100 nm, or structures having nanoscale repeat distances between the different phases that make up the material.¹

The Nanocomposite Materials symposium which was held at the TMS 2009 Annual Meeting comprised around 70 technical presentations submitted from more than a dozen different countries. The resulting special emphasis topic should convey to *JOM* readers the breadth and depth of the technical efforts currently underway in this rapidly developing field. Included are three papers that represent this diversity both in material systems (metallic, polymeric, and ceramic) and applications (structural and/or multifunctional).



As the field of nanomaterials has matured, nanocomposites have emerged as a promising and practical path for novel materials design. Although the ability to combine different material classes to provide a useful balance of properties is nothing new—this is the basis of all rational composite materials design—the ability to combine disparate materials at the nanometer scale has led to a plethora of new materials with increased functionality beyond that predicted by the “rule of mixtures.” These effects can be attributed primarily to the size scale of the phases. At the nanometric scale—where surface and interfacial phenomena dominate over volume effects—material designers need to be aware of such quantities as specific surface area, surface energy, particle morphology, and particle spatial distribution. Accordingly, there has been a steady maturation in

the processing science needed to take full advantage of the continually widening materials design space. For example, two of the papers describe a promising emerging technique for nanocomposite material processing: spark-plasma sintering. The technique uses a combination of electric field, direct and/or indirect heating, and pressure to densify the material to increased levels compared with conventional sintering. Likewise, additional advances continue to be made in the area of materials characterization, both in terms of understanding of the underlying physics of nanoscale phenomena, and in the development of new experimental techniques. Scanning probe microscopy and high-resolution (scanning) transmission electron microscopy (TEM) are rapidly becoming the tools of choice for microstructural characterization, along with focused ion beam (FIB) milling for specimen preparation and micro-machining.

The first paper, “Fatigue and Fracture Toughness of Epoxy Nanocomposites,” by I. Srivastava and N. Koratkar provides a thorough overview and introduction to the major issues affecting fatigue and fracture toughness in a major class of structural nanocomposite materials. The addition of nanofillers to existing epoxy systems has been shown to enhance fatigue and fracture behavior, even at relatively low levels of reinforcement. The article reviews the major technological developments in the field, while describing the underlying, inter-related mechanisms responsible for the improvements in performance.

The second paper, “The Current Activated Pressure Assisted Densification Technique for Producing Nanocrystalline Materials” by J.E. Alaniz, J.R. Morales, and J.E. Garay, highlights some of their group’s ongoing work in tailoring

properties via control of nanocrystalline structure, through the successful use of an emerging processing technique. The materials of interest are oxide nanocomposites, designed to exhibit very different functional behaviors—magnetic and optical—therefore emphasizing the broad applicability of nanocomposites beyond structural materials.

The third paper, “Nanostructured Metal Composites Reinforced with Fullerenes” by F.C. Robles-Hernández and H.A. Calderon is an in-depth investigation of the synthesis and characterization of metallic-matrix structural nanocomposites. The paper gives insight into the application of standard techniques such as TEM, x-ray diffraction, and micro-indentation for characterizing microstructure–property relationships.

The future certainly looks bright for nanocomposite materials, with the joint ASM/TMS Composite Materials Committee of the Structural Materials Division of TMS recently deciding to organize biennial symposia along the same theme. However, one outstanding issue is raw material cost, which is related to quality and reliability of supply for large-scale synthesis. It is hoped that future TMS symposia will address these issues as well as emphasizing the technical aspects of nanocomposite materials research. Stay tuned.

Reference

1. P.M. Ajayan, L.S. Schadler, and P.V. Braun, *Nanocomposite Science and Technology* (Weinheim, Germany: Wiley VCH, 2003).

Jonathan E. Spowart is a Senior Materials Research Engineer and Research Leader within the Metals, Ceramics and NDE Division of the Materials and Manufacturing Directorate, Air Force Research Laboratory, Wright-Patterson Air Force Base, OH. He is also the secretary and current *JOM* Advisor for the joint ASM/TMS Composite Materials Committee.

Fatigue and Fracture Toughness of Epoxy Nanocomposites

I. Srivastava and N. Koratkar

The fatigue and failure mechanisms of epoxy composites have been researched extensively because of their commercial importance in fields demanding materials with high specific strength. Particulate, sheets, short and long fibers with dimensions in the micrometer and nanometer range are the major fillers which have been studied for enhancing the fatigue resistance of epoxies. The nano and micro scale dimensions of the fillers give rise to unexpected and fascinating mechanical properties, often superior to the matrix including fracture toughness and fatigue crack propagation resistance. Such properties are dependent on each other (e.g., the fatigue properties of the polymer composites have been found to be strongly influenced by its toughness). This article is a review of the various developments in this field and the underlying mechanisms which are responsible for performance improvements in such composites.

INTRODUCTION

Fatigue is a mode of progressive failure in solids under cyclic loading at stresses lower than the material's ultimate tensile stress.¹ Due to the increasing use of polymers and their composites in engineering applications, especially the aerospace industry, the fatigue properties of composites have inspired much work.²⁻⁵ The characterization of material behavior under cyclic loading is done either by fatigue life (S-N) measurement or by studying the fatigue crack propagation (FCP) rate in the material. The growth of a crack in the stable region under cyclic loading (Figure 1) is governed by the Paris law and is given by $\frac{da}{dN} = C(\Delta K)^n$.⁷ According to the Paris law, the crack

How would you...

...describe the overall significance of this paper?

The mechanical properties of epoxy nanocomposites have been extensively researched because of their commercial importance in fields demanding materials with high specific strength. Various fillers like nano-ceramic, nano-rubber, carbon nanotubes, and nano-clay sheets have been studied for enhancing the fatigue resistance and fracture toughness of epoxy composites. This article is a review of the significant developments to enhance fracture toughness and fatigue resistance of epoxy nano-composites.

...describe this work to a materials science and engineering professional with no experience in your technical specialty?

Thermoset polymers like epoxy are important for the aerospace and automobile industry due to their high specific strength. However, they lack damage tolerance, a critical attribute for advanced applications. Introduction of a second phase in the epoxy matrix may improve the mechanical properties, especially fracture toughness and fatigue resistance. Epoxy nanocomposites utilizing carbon nanotubes, nano-ceramics and nano-rubber exhibit superior properties compared to the matrix.

...describe this work to a layperson?

Epoxy composites have greatly influenced the aerospace and automobile industry by allowing new designs and innovations. Two important material properties critical for advanced applications are high fracture toughness and resistance to cyclic loading. Epoxy has poor crack propagation resistance because of low ductility and hence second phase nanoparticles are introduced in the epoxy matrix for improvements. This article describes how fillers of various geometries and chemical nature affect the matrix.

propagation rate per cycle (da/dN) is directly proportional to the stress intensity factor range ΔK and two constants, C and n , which depend on the testing parameters including moisture, temperature, loading frequency, and the stress ratio.⁸ The faster the rate of crack propagation, the lower the fatigue resistance. Smaller values of the Paris exponent signify high material resistance to FCP. The Paris exponent, and hence the fatigue properties of the material, have been found to be strongly influenced by their fracture toughness. An increase in toughness of the matrix has been associated with an increase in FCP resistance of the material.^{9,10}

The S-N curve is another classical approach used for studying fatigue behavior of a material. The curve gives an estimate of the material's fatigue life under controlled amplitude of cyclic stress. Hysteresis loss measurements are also utilized to determine the resistance of polymers to crack initiation and crazing.

The fatigue process has been traditionally divided into three stages: crack initiation, crack propagation, and final failure.¹¹ Surface flaws and inclusions are the most common sites for fatigue crack initiation. In most engineering materials cracks are inherently present on the component surface. Another area prone to crack generation is the second phase-matrix interface. Due to high local stress concentration and the discontinuity in mechanical properties at the particle-matrix interface crack initiation becomes easy. In polymer matrix composites (PMC), the failure mechanisms are not as well understood/defined as in metals. In the failure of a PMC multiple mechanisms might contribute, such as matrix crazing, shear yielding, delamination,

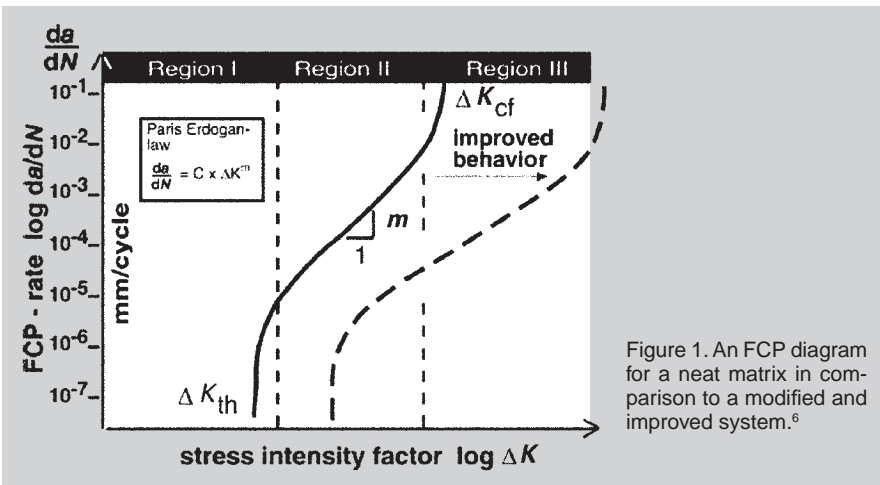


Figure 1. An FCP diagram for a neat matrix in comparison to a modified and improved system.⁶

ered silicate membranes,^{33,34} and their combinations.^{35,36}

FILLER PROPERTIES AFFECTING TOUGHNESS AND FATIGUE

The use of fillers like elastomers with lower modulus than that of the matrix results in composites with increased toughness³⁷ due to high ductility, but modulus of the composite decreases,¹⁸ whereas for inorganic fillers the modulus of the composite is observed to be more than that of the polymer matrix.^{38,39} The size of the fillers also plays a central role. Use of nano-fillers (NF) has proved more effective than micro-filler (MF) in enhancing the strength of the polymer matrix, without compromising ductility. The size of the NF (a few tens of nm in diameter) being smaller than the micro-sized filler reduces the stress concentrations in comparison to MF (a few tens of μm in diameter).⁴⁰ The high stress concentration at the surface makes MF more prone to cracking as compared to NF.

Another advantage of having nano-sized fillers is that for the same volume fraction of fillers added, the particle density will be higher for NF than for MF. Therefore, the distance between two neighboring particles will be

fiber breakage, debonding, plastic void growth, and matrix cracking.¹² Some scanning electron micrographs to convey a broad picture of failures in polymer composites are shown in Figure 2.

See the sidebar on page 52 for a description of polymer failure modes.

THERMOSETTING EPOXIES

Epoxy resin (two or more groups of epoxide per molecule) and a curing agent comprise an epoxy system. Epoxy composites are used for aircraft, automobiles, ship-building, resin casting, slide bearings, and many other applications because of their good chemical and corrosion resistance, high specific strength, and multiple curing options.² Despite these advantages epoxy lacks a crucial attribute: damage tolerance. Offering a fracture energy of less than 0.3 kJ/m^2 , they can be classified as highly brittle.¹⁸ As specified by Johnston,¹⁹ the fracture energy for a resin to be used in aircraft structures should lie in the range of $1.9\text{--}3 \text{ kJ/m}^2$. Epoxy possess aromatic rings, which increase the polymer chain stiffness and has high cross link density; hence the plastic deformation in front of the crack tip is highly localized. This extremely localized plastic deformation causes little absorption of energy leading to catastrophic brittle failure. Enhancement in strength and stiffness of the polymer matrix can be obtained by increasing the cross-link density, but it also increases the brittleness of the polymer leading to reduced toughness.²⁰ In order to control the toughness and hence the fatigue of

thermoset polymers, studies have been done on the introduction of a second phase in them. Since the toughening mechanism in thermoset polymers is not a well-understood phenomenon, it led to the study of various kinds of fillers to obtain optimum mechanical properties of the composite. Some of the second phases that have been studied are micro- and nano-size particulates like rubber (e.g., carboxyl terminated butadiene acrylonitrile (CTBN)),^{21,22} thermoplastics (e.g., polyethersulphone),^{23–26} ceramic particles (e.g., Al_2O_3),²⁷ some reactive diluents;²⁸ long and short fibers including carbon nanotubes;^{29,30} laminates of fibers^{31,32} in different orientations, lay-

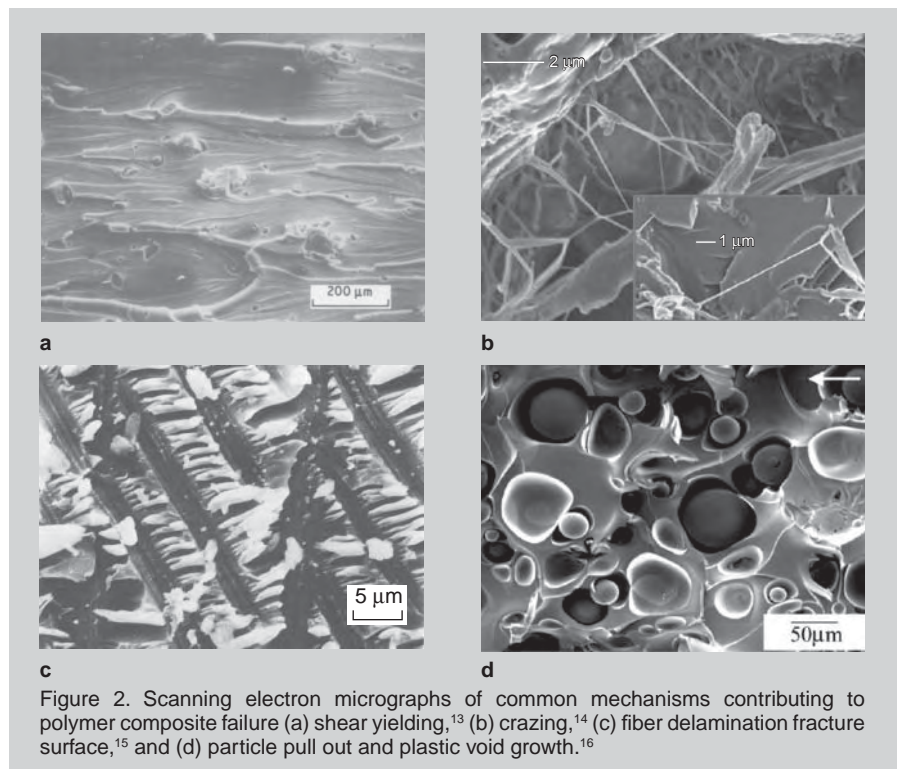


Figure 2. Scanning electron micrographs of common mechanisms contributing to polymer composite failure (a) shear yielding,¹³ (b) cracking,¹⁴ (c) fiber delamination fracture surface,¹⁵ and (d) particle pull out and plastic void growth.¹⁶

BASIC FAILURE MODES IN POLYMERS

Depending upon the chemistry and the curing agent used, the failure mode of the polymer matrix could be either ductile or brittle. The ductile mode is often identified by shear yielding. An increase in brittle nature of the polymer is seen as a shift from shear yielding to micro-voiding followed by crazing. In case of networked polymers like epoxy highly brittle failure without crazing is common.

Shear Yielding

Shear yielding is an energy absorption mechanism associated with polymer failure. It occurs when localized plastic flow starts in response to an applied stress at approximately 45° to the applied load. Such plastic flow might spread shear bands in the whole sample (Figure 2a) absorbing a significant quantity of energy or might lead to localized yielding resulting in isolated shear bands.

Crazing

Crazing is another common failure mode that is observed in glass and amorphous thermoplastic polymers.¹⁷ During crazing, microcracks form under tensile load and are held together by polymer fibrils called crazes (Figure 2b). Formation and plastic deformation of such crazes involves absorption of energy, which leads to enhanced toughness. When the applied stress is high enough to cause failure of the fibrils, the microcracks start growing.

smaller for nano-sized fillers, which is an important parameter in crack bowing and pinning. Lack of transparency is another issue associated with micrometer-sized fillers in polymer composites.⁴¹ Transparency of the composite is improved for nano-fillers as their size is less than the wavelength of light, especially when a good dispersion is achieved.⁴² The presence of fillers affects the crystallinity, mobility, and other structural aspects of polymer chains.⁵

Fillers also act as nucleating sites for crystallization of polymer chains.^{43,44} The effectiveness of load transfer between the polymer and the filler is a function of wettability and adherence.^{45,46} The two plots in Figure 3 demonstrate the difference in the static mechanical and fatigue properties of the neat epoxy, Al₂O₃ reinforced epoxy, and APTES (3-aminopropyltriethoxysilane) modified Al₂O₃ reinforced epoxy. The surface modification of fillers improves their dispersion, which could also be attained by physical means like ultrasonication.^{49,50}

Another significant filler property is the aspect ratio.⁵¹ Layered silicates, with thickness in nanometers and length and width in micrometers, and carbon nanotubes, with diameter in nanometers and length in micrometers, have much higher aspect ratios than particulates. This leads to a more ef-

ficient load transfer and the increased toughness of the composite.⁵²⁻⁵⁴

PARTICULATE-POLYMER COMPOSITE

Rubber – Thermoset

Around 1971, the Sultan and McGarry group initiated research on the effect of rubber in thermoset polymers.⁵⁵⁻⁵⁸

Reactive functional elastomers (e.g., CTBN (carboxyl terminated Butadiene),^{21,59-61} HTBN (hydroxyl terminated Butadiene),⁶² ATBN (amine terminated Butadiene),^{63,64} VTBN (Vinyl terminated Butadiene),⁶⁵ and ETBN (epoxy terminated Butadiene)^{66,67}) increased the fracture toughness of the polymer matrix when added between 5–20% weight fraction.¹⁸

To obtain rubber dispersion in epoxy, rubber is dissolved in epoxy resin followed by curing with appropriate hardener. After curing, a dispersed phase of rubber in epoxy matrix is observed. The degree of phase separation and the dispersion size can be controlled by controlling curing parameters and filler volume fraction.^{18,68} Elastomer addition by either phase separation at adequate temperature or through addition in the form of fine solid powder was found to improve the ductility of the thermoset, increasing its toughness to around 2–4 kJ/m².¹⁸ Shown in Figure 4a is a scanning electron micrograph of the dispersed phase of nano-rubber in epoxy. Treatment of rubber with silane coupling agents, plasma oxidation, and acid treatment has been found to enhance interfacial interaction, leading to an increase in fracture toughness.⁷⁰⁻⁷²

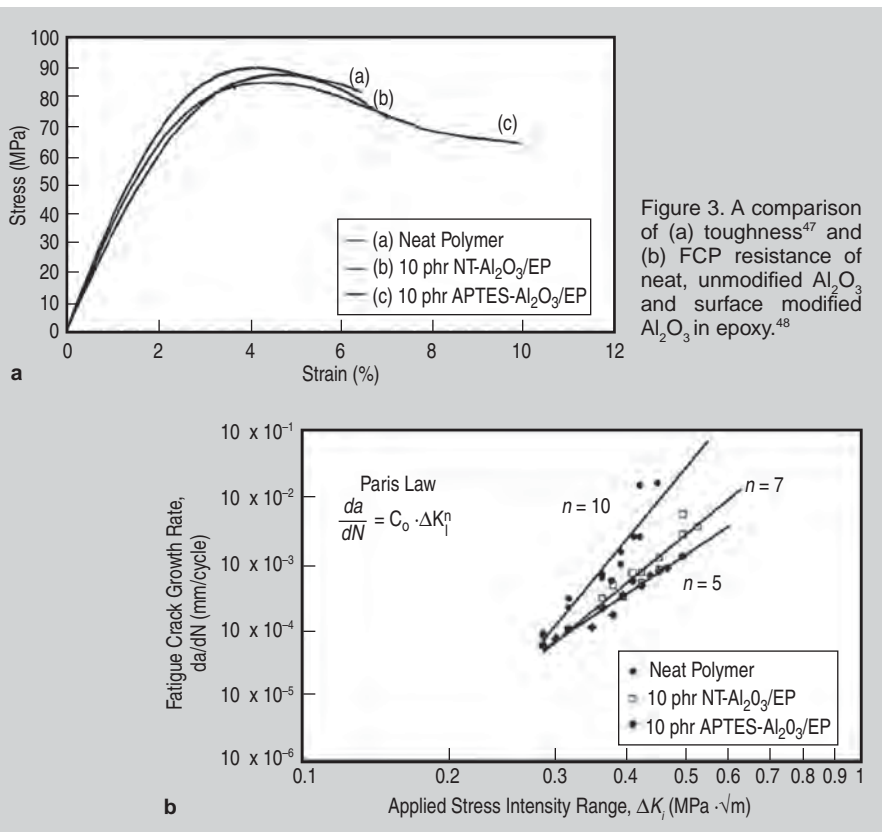


Figure 3. A comparison of (a) toughness⁴⁷ and (b) FCP resistance of neat, unmodified Al₂O₃ and surface modified Al₂O₃ in epoxy.⁴⁸

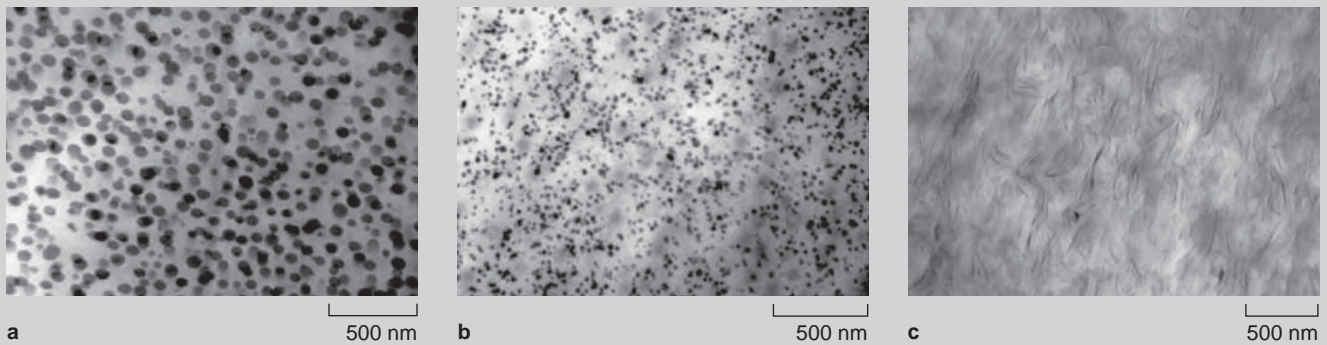


Figure 4. Transmission electron micrographs of dispersed phases: (a) nano-rubber, (b) nano-silica, and (c) organoclay C30B in nylon-6 matrix.⁶⁹

The crack propagation velocity in rubber-reinforced polymers has been measured⁷³ and it was observed that crack blunting in the rubber phase of the composite significantly decreased the crack propagation velocity. In the presence of rubber particles the crack tip blunts due to localized shear yielding around it. Figure 5a is a plot of FCP rate in rubber reinforced epoxy composite with increasing filler content.

The plot shows improvement in the fatigue resistance of the composite with increasing rubber phase fraction. Fatigue property studies of elastomer-epoxy composites have shown the early initiation of crazes around the rubber particles, proving useful in the late life of the material by improving the toughness of the polymer matrix via microcrazing, cavitation, and shear yielding.^{74,76} The rubber phase undergoes significant strain and finally acts as a ligament in the polymer craze.⁷⁷ However, this ductility is achieved at the cost of modulus, strength, and impact resistance of the matrix.^{18,71}

Ceramic – Thermoset

The reinforcement of epoxy using ceramic particles with materials such as glass beads,^{27,78} silica,^{79–81} and alumina,^{49,82} from micrometer to nanometer size, is found to increase the toughness of the matrix without compromising its rigidity. Surface-coated inorganic fillers have been found to improve mechanical properties of the composite under both tensile and cyclic load.^{49,83} In Figure 4b a scanning electron micrograph of the dispersed phase of nano-silica in epoxy matrix is shown. The fatigue studies of ceramic-filled polymer have shown significant improvement,^{50,83} increasing K_{IC} from $\sim 0.5 \text{ MPa}^{1/2}$ to $0.88 \text{ MPa}^{1/2}$ with

$\sim 20.2 \text{ wt.}\%$ of nano SiO_2 fillers, with an increase in elastic modulus from 2.96 GPa to 3.85 GPa.¹⁰

Numerous phenomena are associated with the toughness increase in particulate-reinforced composites, some of which are crack deflection, crack pinning, and debonding followed by plastic void growth. Crack deflection is the process of tilting and twisting of cracks in the matrix around the filler particles, as shown schematically in Figure 6a and b. During the deflection process the crack tip propagates under mixed I and II

mode and the fracture surface roughens (Figure 6c) as an outcome of increase in fracture toughness.^{85–87}

Theoretical models for such deflection studies have been analyzed by Faber and Evans.⁸⁴ Crack pinning is a process similar to pinning of dislocations by impurity or second phase particles in the matrix. First proposed by Lange,⁸⁸ the process describes the bending of the crack front in the presence of pinning elements, which obstruct its smooth motion. The crack pinning is studied by observing the bowing of the crack front,

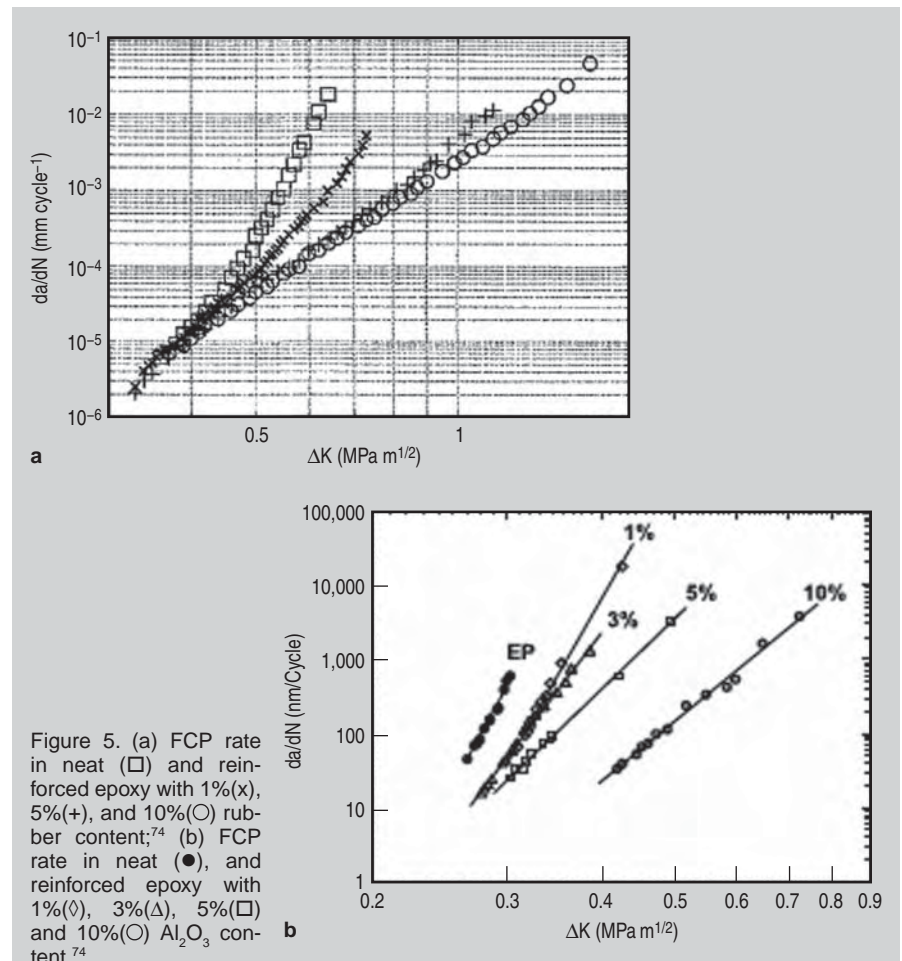


Figure 5. (a) FCP rate in neat (\square) and reinforced epoxy with 1% (x), 5% (+), and 10% (o) rubber content;⁷⁴ (b) FCP rate in neat (\bullet), and reinforced epoxy with 1% (\diamond), 3% (Δ), 5% (\square) and 10% (o) Al_2O_3 content.⁷⁴

as shown schematically in Figure 7a. Crack pinning is observed only when the filler size is greater than the crack-opening displacement; hence it is an effective pinning mechanism mostly for micrometer size fillers for epoxy matrix whose crack opening size has been calculated to be $\sim 1.7 \mu\text{m}$.⁸⁵ The crack front bows in between the particles, leaving behind tail-like structures (Figure 7b).

Particle debonding and local plastic

void growth is another phenomenon contributing to the fracture toughness increase of the polymer matrix infiltrated with micro- and nano-fillers (Figure 8). The debonding of the filler relaxes the stress state at the crack tip and causes deformation of polymer matrix by void growth process.⁸⁵

Plastic void growth of the polymer has been reported to be the major cause of toughening for nano-sized SiO_2 and

Al_2O_3 particles due to enhanced shear yielding of the polymer. Functionalized nano- Al_2O_3 fillers which had better adhesion with the epoxy matrix than untreated fillers, were found to have 39% higher strain to break as compared to the neat polymer, whereas unmodified nano- Al_2O_3 fillers showed only 6% increase at 10 phr (parts per hundred) filler concentration. It was realized that the plastic void growth mechanism is

FATIGUE BEHAVIOR IN COMPOSITES

Clay Nanosheet Polymers

Exfoliated clay sheet reinforced polymers have been considered for improved fatigue resistance of polymers. When the intercalation of clay layers through polymer chains is not possible, phase separation occurs and a micro-composite instead of nano-composite is obtained, making the dispersion of nano-clay in the polymer critical for composite properties. Dispersion of clay nano-sheet in polymer is difficult due to the hydrophilic nature of clays and hydrophobic nature of polymers. The dispersion barrier is overcome using organic surfactants like vinylbenzyltrimethylammonium chloride (VDAC), which makes the clay surface organophilic.⁸⁹ Forcing polymer chains through the exfoliated layers of clay sheets (a few nm thick) leads to a finely dispersed composite (Figure 4c).^{34,90-92} The high aspect ratio of exfoliated clay layers provides large interfacial contact area with the matrix.⁹³ Studies on the mechanical properties including fatigue of such nano-layer reinforced composites have shown improvement in neat and traditional fiber reinforced polymers. An addition of 5 wt.% nano silicate clay in polypropylene has been found to increase fatigue strength coefficient (true stress which causes failure in one reversal) by 13.3% with respect to the neat polymer and at the same time resulting in an increment in modulus and yield strength by 90% and 5%, respectively.⁹⁴ The stiffness and toughness of nano-

clay epoxy composite has been reported to increase with an increase in filler content.⁹⁵ The fracture surfaces of such composites have been found to be much rougher than plain epoxy, indicating higher energy absorption by the system prior to fracture. Crack deflection has been implied by the presence of steps and microcracking on the fracture surface.⁹⁶ The fracture toughness and FCP resistance of the composite have been found to increase by chemical modification of clay sheets like surface treatment of the clay layers with 3-aminopropyltriethoxysilane or long chain alkylammonium salt and using physical means like forcing polymer in between clay layers using a twin screw extruder.^{97,98}

Nanofibers

Nanofibers are whiskers with diameters in the range of a few hundred nanometers and lengths of a few hundred micrometers. Vapor grown carbon nanofibers (VGCNFs) obtained from chemical vapor deposition of hydrocarbons, have been used to reinforce the epoxy matrix due to its excellent mechanical properties.⁹⁹ Vapor grown carbon nanofibers consist of a few-nanometer-diameter carbon tubes surrounded by concentric circles of carbon layers increasing its outer diameter to around 50–200 nm.

Dispersion of the VGCNFs is difficult to achieve as the fibers get twisted and intertwined. Using surface treatments like functionalization and plasma treatment, better dispersion and interfacial ad-

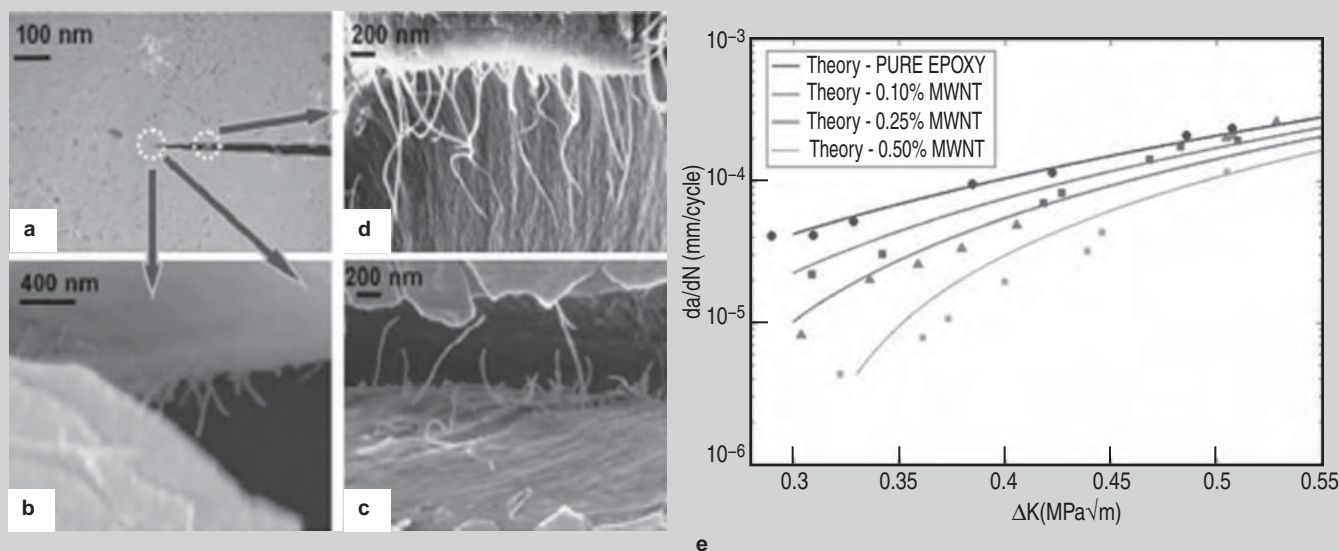


Figure A. (a) Scanning electron micrograph of the side view of the fatigue crack. The microstructure of the sample in the vicinity of the crack is shown. (b) Close to the crack tip, fiber bridging zone is shown, where the nanotubes are pulled out of the matrix but are effectively bridging the crack interface. (c) At a small distance behind the crack tip, some nanotubes are bridging the crack and some are pulled out of the matrix. (d) Far behind the crack tip, nanotubes are completely pulled out of the matrix. (e) Lowering of FCP rate in MWNT reinforced epoxy with increasing weight fraction of MWNT.²⁹

the main mechanism resulting in the rise in toughness.^{47,48} Figure 5b is a plot of FCP in Al₂O₃ epoxy composite with varying volume fraction of filler. See the sidebar for fatigue behavior in various composites.

THREE-PHASE COMPOSITES

Oriented fiber reinforced composites with excellent longitudinal prop-

erties have poor transverse properties due to lack of fibers in the thickness direction.¹⁰⁵ Lack of fibers through the thickness of the composite also leads to poor fatigue behavior. Weaving of fibers in the thickness direction (i.e., stitched composites) can be used to improve the transverse properties of laminated composites but only at the cost of longitudinal properties.^{106,107} Another approach to improve the properties of

these traditional composites is by using nanofillers like CNTs to improve the interlaminar strength of the composite.¹⁰⁸ The CNTs could either be randomly distributed or vertically oriented on the fibers.^{109–111} The effect of functionalization of the CNTs in such three phase composites was observed to further enhance the transverse and longitudinal toughness of traditional epoxy/fiber composites.^{112,113}

hesion between the polymer matrix and carbon nano-fibers (CNF) is achieved.¹⁰⁰ Since random dispersion of VGCF leads to isotropic properties in the composite, to obtain desired alignment extrusion¹⁰¹ and magnetic field¹⁰² are employed. Vapor grown carbon nanofibers have resulted in an increase in the fracture toughness of epoxy with increasing fiber content.¹⁰³ The fatigue life and the fatigue strength of nanofiber-reinforced epoxy were also found to improve substantially on introduction of ~2% VGCF.¹⁰⁴ The increase in fracture toughness is attributed to fiber debonding and the pull out mechanism.

Carbon Nanotube Polymers

Carbon nanotubes have been demonstrated to increase the fatigue life of PMCs. The fatigue crack propagation velocity is significantly reduced through the action of crack bridging by the CNTs and the subsequent dissipation of energy that occurs due to the frictional pull out of the bridging CNT fibers as shown in Figure Aa–d. In the low stress intensity factor amplitude regime a decrease in the crack propagation rate by over ten-fold is reported,³⁰ with strong dependence on the weight fraction of CNTs. Figure Ae shows the increase in resistance to fatigue crack propagation with an increase in the weight fraction of multiwalled carbon nanotubes (MWNTs) in the epoxy matrix. The amount of CNT required for such a reduction in FCP rate is less than 1% which is small in comparison to the amount of particulate nano-fillers (~5–10%).

For the case of CNT fillers, a substantial reduction in the fatigue suppression with increasing ΔK (Figure Ae) is observed. This is because in the case of CNTs the dominant toughening and fatigue

crack suppression mechanism is crack bridging. The fatigue crack is bridged by high aspect ratio nanotubes generating a fiber-bridging zone in the wake of the crack tip. As the crack advances energy is dissipated by the frictional pull-out of the bridging nanotubes from the epoxy matrix which slows the crack propagation speed. However this crack bridging effect loses effectiveness at high ΔK due to progressive shrinkage in the size of the fiber-bridging zone as ΔK is increased.²⁹ The fact that such behavior is not observed in nanoparticle filled epoxy composites indicates that crack bridging phenomena are not playing a dominant role in the fracture and fatigue of nanoparticle filled polymer systems. Reducing the CNT diameter and increasing its length has been shown to increase the effectiveness (Figure B) of the crack bridging mechanism.³⁰

Functionalizing CNT with amido-amine groups has also been shown to enhance the epoxy's resistance to fatigue crack propagation by initiating craze formation (Figure 2b) in the epoxy.¹⁴ The origin of the crazing behavior was traced to a significant amount of unreacted epoxy that was kinetically trapped in the crosslinked matrix structure that is formed at the CNT/epoxy interface. Such local heterogeneity in the curing may be caused by a variety of factors such as, for example, the fact that the chemistry may be modified locally due to the presence of amido-amine groups. Epoxy chain alignment, which is known to influence the cross-linking density, may also be modified locally due to the presence of these functional groups. Heterogeneous cross-linking results in localized pockets of enhanced molecular mobility;¹⁴ the correlated evolution of such contiguous mobile regions under mechanical loading leads to crazing which substantially boosts the toughness and the resistance to fatigue crack propagation of the baseline epoxy.

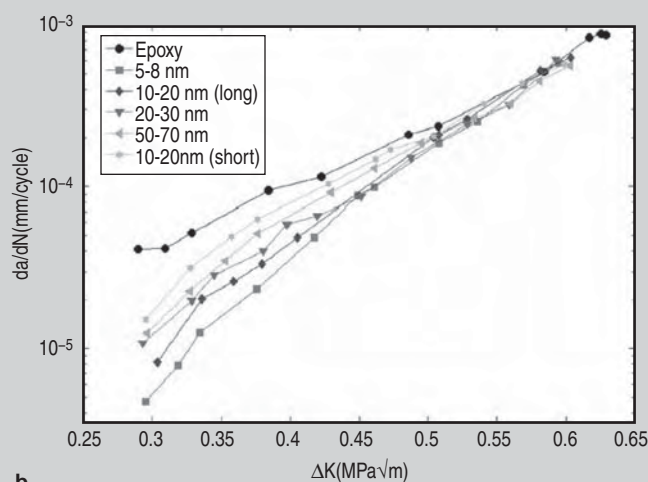
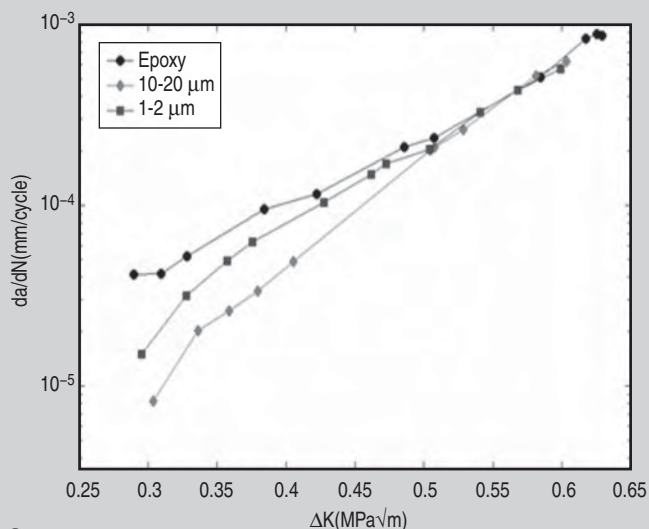


Figure B. (a) Effect of nanotube diameter on fatigue suppression performance; (b) effect of nanotube length on fatigue suppression performance.³⁰

CONCLUSION

Fatigue life improvements in epoxy composites have been studied and re-

searched for a wide variety of second-phase particles. Different kinds of fillers have different ways of obstructing FCP. Particulate fibers obstruct the fa-

tigue crack by crack deflection, crack pinning, debonding, and plastic void growth whereas short fibers undergo crack bridging and crack trapping.

Rubber composites degrade the original stiffness of the epoxy matrix whereas inorganic particles are not as efficient as rubber in enhancing the toughness of the composite. High-aspect-ratio fibers such as carbon nanotubes are able to significantly enhance the epoxy's fatigue crack propagation resistance at relatively low weight fractions (below 0.5%), but they lose their effectiveness at high stress intensity factor amplitudes. Graphene is another emerging nano-material and shows promise to enhance fracture and fatigue properties of polymers¹¹⁴ at low loading fractions due to its high specific surface area, two-dimensional sheet geometry, strong filler-matrix adhesion, and the outstanding mechanical properties of the sp^2 carbon bonding network in graphene.¹¹⁵ Due to the increasing interest of researchers in graphene composites, in-depth study of the fracture and fatigue properties of graphene-based composite materials is clearly warranted.

In addition, theoretical/computational modeling of fracture and fatigue in nanocomposites is still in its infancy. Improved models for toughness in nanocomposites and validation with experimental data are essential for development of nanocomposite polymers with optimized strength, stiffness, fracture, and fatigue properties.

ACKNOWLEDGEMENTS

N.K. acknowledges the funding support from the U.S. Office of Naval Research (Award Number: N000140910928) and the U.S. National Science Foundation (Award Number: 0900188).

References

1. S. Suresh, *Fatigue of Materials*, 2 (Cambridge University Press, 1998).
2. L.A. Pilato and M.J. Michno, *Advanced Composite Materials*, 1 (Berlin, Germany: Springer, 1994).
3. P.M. Ajayan et al., *Nanocomposite Science and Technology*, 1 (Weinheim, Germany: Wiley-VCH, 2003).
4. D. Hull and T. Clyne, *An Introduction to Composite Materials*, 2 (Cambridge, U.K.: Cambridge Univ. Press, 1996).
5. I.S. Lipatov et al., *Polymer Reinforcement*, 1 (Ontario, Canada: ChemTec Publishing, 1995).
6. V. Altstadt, "Fatigue of Polymeric Materials," *Encyclopedia of Materials: Science and Technology* (Amster-

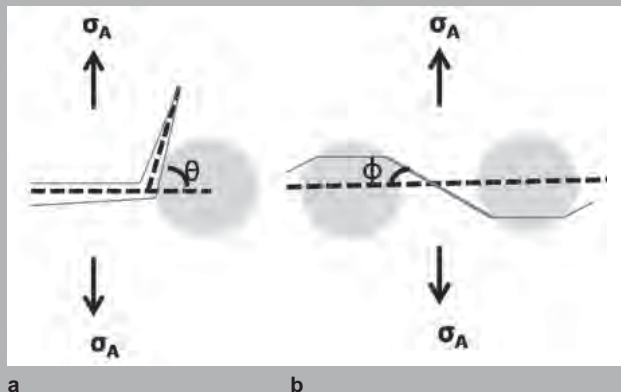


Figure 6. A schematic of crack front undergoing (a) tilt and (b) twist under mixed mode on encountering second phase particles,⁸⁴ (c) and (d) scanning electron micrograph comparing the surface roughness of neat and Al_2O_3 modified epoxy.⁸⁵

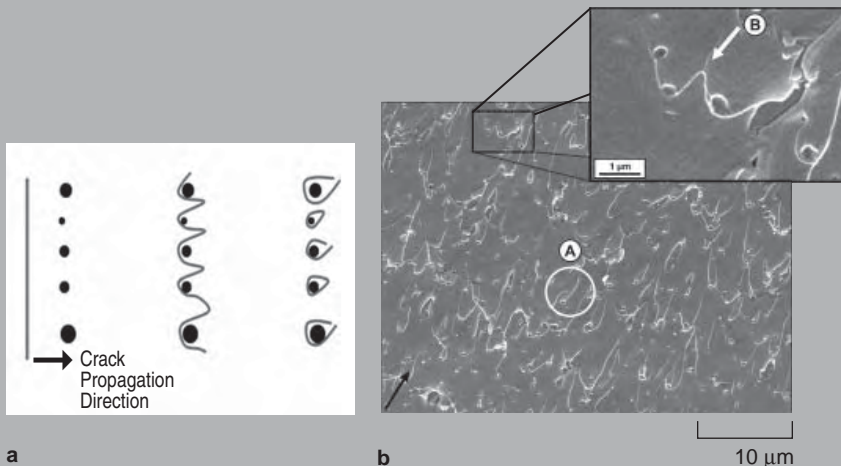
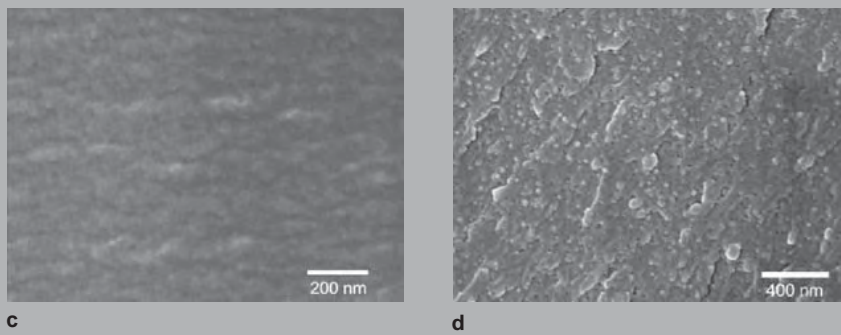


Figure 7. (a) A schematic of second phase particles pinning the crack front, leaving behind tail-like structure.⁴¹ (b) Scanning electron micrograph illustrating the fracture surface of epoxy reinforced with TiO_2 nanoparticles, demonstrating the tail-like structures.⁷⁵

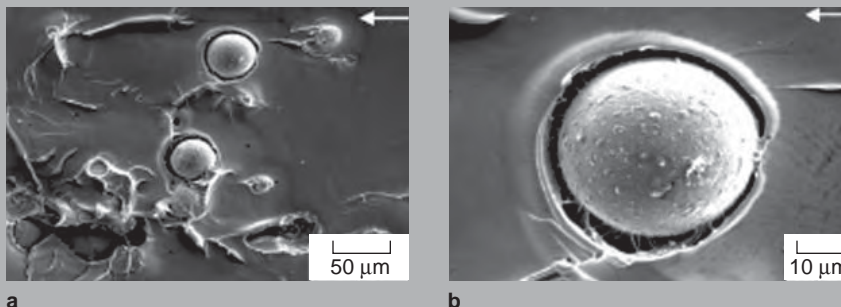


Figure 8. (a) and (b) Scanning electron micrographs illustrating the fracture surface of glass-particle epoxy matrix after debonding.¹⁶

- dam, NY: Elsevier Science Ltd, 2001), pp. 2972–2978.
7. P.C. Paris et al., *The Trend in Engineering*, 13 (1961), p. 6.
 8. Y.W. Mai and J.G. Williams, *J. Materials Science*, 14 (8) (1979), pp. 1933–1940.
 9. E. Urbaczewski-Espuche et al., *J. Applied Polymer Science*, 47 (6) (2003), pp. 991–1002.
 10. B. Blackman et al., *J. Materials Science*, 42 (16) (2007), pp. 7049–7051.
 11. W.J. Plumbridge, *J. Materials Science*, 7 (8) (1972), pp. 939–962.
 12. M.J. Salkind, *Composite Materials Testing and Design (2nd Conf)*. ASTM STP 497 (Baltimore, MD: Amer. Soc. for Testing and Materials, 1972).
 13. W. Bascom et al., *J. Materials Science*, 16 (10) (1981), pp. 2657–2664.
 14. W. Zhang et al., *Small*, 5 (12) (2009), pp. 1403–1407.
 15. T. Johannesson et al., *J. Materials Science*, 19 (4) (1984), pp. 1171–1177.
 16. T. Kawaguchi and R.A. Pearson, *Polymer*, 44 (15) (2003), pp. 4239–4247.
 17. J. Scheirs, *Compositional and Failure Analysis of Polymers* (Chichester, NY: Wiley, 2000).
 18. A.C. Garg and Y.-W. Mai, *Composites Science and Technology*, 31 (3) (1988), pp. 179–223.
 19. N.J. Johnston, "Synthesis and Toughness Properties of Resins and Composites" (Presentation at the ACEE Composite Struct. Technol. Program, Seattle, WA, 1984).
 20. A.S. Argon and R.E. Cohen, *Polymer*, 44 (19) (2003), pp. 6013–6032.
 21. S.C. Kunz and P.W.R. Beaumont, *J. Materials Science*, 16 (11) (1981), pp. 3141–3152.
 22. A.J. Kinloch et al., *Polymer*, 24 (10) (1983), pp. 1355–1363.
 23. C.B. Bucknall and I.K. Partridge, *British Polymer Journal*, 15 (1) (1983), pp. 71–75.
 24. C.B. Bucknall and A.H. Gilbert, *Polymer*, 30 (2) (1989), pp. 213–217.
 25. R.A. Pearson and A.F. Yee, *Polymer*, 34 (17) (1993), pp. 3658–3670.
 26. T. Kyu and J.-H. Lee, *Physical Review Letters*, 76 (20) (1996), pp. 3746–3749.
 27. J. Spanoudakis and R.J. Young, *J. Materials Science*, 19 (2) (1984), pp. 473–486.
 28. E. Urbaczewski et al., *Die Makromolekulare Chemie*, 191 (4) (1990), pp. 943–953.
 29. W. Zhang et al., *Applied Physics Letters*, 91 (19) (2007), pp. 193109–193113.
 30. W. Zhang et al., *Nanotechnology*, 19 (28) (2008), pp. 1–5.
 31. N.L. Harrison, *Fibre Science and Technology*, 4 (2) (1971), pp. 101–114.
 32. H.J. Konish, Jr. et al., *AIAA Journal*, 11 (1) (1973), pp. 40–43.
 33. S.S. Ray and M. Okamoto, *Progress in Polymer Science*, 28 (3) (1995), pp. 1539–1641.
 34. M. Alexandre and P. Dubois, *Materials Science and Engineering R: Reports*, 28 (1) (2000), pp. 1–63.
 35. Y.P. Wu et al., *Composites Science and Technology*, 65 (7–8) (2005), pp. 1195–1202.
 36. S.T. Kim et al., *J. Materials Science*, 31 (13) (1996), pp. 3523–3533.
 37. L.E. Nielsen and R.F. Landel, *Mechanical Properties of Polymers and Composites*, 2 (New York: CRC Press, 1994).
 38. S.Y. Fu and B. Lauke, *J. Materials Science and Technology*, 13 (5) (1997), pp. 389–396.
 39. N. Amdouni et al., *J. Applied Polymer Science*, 46 (10) (1992), pp. 1723–1735.
 40. J. Moczo and B. Pukánszky, *J. Industrial and Engineering Chemistry*, 14 (5) (2008), pp. 535–563.
 41. A.J. Kinloch and R.J. Young, *Fracture Behaviour of Polymers* (London: Elsevier Applied Science, 1983).
 42. C. Becker et al., *Organic-Inorganic Hybrid Materials for Photonics*, ed. L.G. Hubert-Pfalzgraf and S. Iraj Najafi (Bellingham, WA: SPIE, 1998), pp. 88–98.
 43. J. Menczel and J. Varga, *J. Thermal Analysis*, 28 (1) (1983), pp. 161–174.
 44. M. Fujiyama and T. Wakino, *J. Applied Polymer Science*, 42 (10) (1991), pp. 2739–2747.
 45. R.N. Rothman, *Particulate Fillers for Polymers*, 1 (Shawbury, U.K.: Rapra Technology Ltd., 2001).
 46. J.M. Felix and P. Gatenholm, *J. Applied Polymer Science*, 42 (3) (1991), pp. 609–620.
 47. S. Zhao et al., *Composites Science and Technology*, 68 (14) (2008), pp. 2965–2975.
 48. S. Zhao et al., *Composites Science and Technology*, 68 (14) (2008), pp. 2976–2982.
 49. Y. Wang et al., *Carbon*, 41 (15) (2003), pp. 2939–2948.
 50. D.R. Paul and L.M. Robeson, *Polymer*, 49 (15) (2008), pp. 3187–3204.
 51. H.S. Katz and J.V. Milewski, *Handbook of Fillers for Plastics* (New York: Van Nostrand Reinhold, 1987).
 52. K. Tamura et al., *Chemistry of Materials*, 20 (6) (2008), pp. 2242–2246.
 53. C. Henrist et al., *J. European Ceramic Society*, 27 (2–3) (2007), pp. 1023–1027.
 54. S. Iijima, *Nature*, 354 (6348) (1991), pp. 56–58.
 55. J.N. Sultan et al., *Applied Polymer Symposium*, 16 (1971), pp. 127–136.
 56. J.N. Sultan and F.J. McGarry, *Polymer and Engineering Science*, 13 (1) (1973), pp. 29–34.
 57. M.E. Roylance et al., *Am. Chem. Soc. Div. Org. Coatings Plast. Chem.*, 34 (2) (1974), pp. 294–299.
 58. F.J. McGarry, *Polymeric Materials Science and Engineering, Proceedings of the ACS Division of Polymeric Material*, 49 (1983), p. 223.
 59. A.J. Kinloch et al., *Polymer*, 24 (10) (1983), pp. 1341–1354.
 60. R.A. Pearson and A.F. Yee, *J. Materials Science*, 26 (14) (1991), pp. 3828–3844.
 61. C.B. Bucknall and I.K. Partridge, *Polymer Engineering & Science*, 26 (1) (1986), pp. 54–62.
 62. S. Sankaran and M. Chanda, *J. Applied Polymer Science*, 39 (8) (1990), pp. 1635–1647.
 63. S.C. Kunz et al., *Polymer*, 23 (13) (1982), pp. 1897–1906.
 64. G. Levita et al., *Polymer*, 26 (7) (1985), pp. 1110–1116.
 65. O. Gryshchuk et al., *Polymer*, 43 (17) (2002), pp. 4763–4768.
 66. E.J. Robinette et al., *Polymer*, 45 (18) (2004), pp. 6143–6154.
 67. J.-F. Hwang et al., *Polymer Engineering and Science*, 29 (20) (1989), pp. 1477–1487.
 68. E. Dreerman et al., *J. Applied Polymer Science*, 72 (5) (1999), pp. 647–657.
 69. G.-T. Wang et al., *Engineering Failure Analysis*, 16 (8) (2009), pp. 2635–2645.
 70. T. Okamoto et al., *J. Adhesion Science and Technology*, 12 (8) (1998), pp. 813–830.
 71. J. Wang et al., *J. Applied Polymer Science*, 60 (9) (1996), pp. 1425–1437.
 72. E. Sipahi-Saglam et al., *Polymer Engineering and Science*, 41 (3) (2001), pp. 514–521.
 73. D. Peretz and A.T. DiBenedetto, *Engineering Fracture Mechanics*, 4 (4) (1972), pp. 979–984.
 74. H.R. Azimi et al., *J. Materials Science*, 31 (14) (1996), pp. 3777–3789.
 75. B. Wetzel et al., *Engineering Fracture Mechanics*, 73 (16) (2006), pp. 2375–2398.
 76. T.A. Morelli and M.T. Takemori, *J. Materials Science*, 18 (6) (1983), pp. 1836–1844.
 77. S. Kunz-Douglass et al., *J. Materials Science*, 15 (5) (1980), pp. 1109–1123.
 78. J. Spanoudakis and R.J. Young, *J. Materials Science*, 19 (2) (1984), pp. 487–496.
 79. A. Kinloch et al., *J. Materials Science*, 40 (18) (2005), pp. 5083–5086.
 80. Y. Nakamura et al., *Polymer*, 32 (12) (1991), pp. 2221–2229.
 81. R.J. Young and P.W.R. Beaumont, *J. Materials Science*, 10 (8) (1975), pp. 1343–1350.
 82. F.F. Lange and K.C. Radford, *J. Materials Science*, 6 (9) (1971), pp. 1197–1203.
 83. L.E. Nielsen, *J. Composite Materials*, 9 (2) (1975), pp. 149–156.
 84. K.T. Faber and A.G. Evans, *Acta Metallurgica*, 31 (4) (1983), pp. 565–576.
 85. B.B. Johnsen et al., *Polymer*, 48 (2) (2007), pp. 530–541.
 86. D. Hull, *J. Materials Science*, 31 (17) (1996), pp. 4483–4492.
 87. K.T. Faber and A.G. Evans, *Acta Metallurgica*, 31 (4) (1983), pp. 577–584.
 88. F.F. Lange, *Philosophical Magazine*, 22 (179) (1970), pp. 983–992.
 89. X. Fu and S. Qutubuddin, *Polymer*, 42 (2) (2001), pp. 807–813.
 90. S.C. Tjong et al., *Chemistry of Materials*, 14 (1) (2002), pp. 44–51.
 91. Z. Wang and T.J. Pinnavaia, *Chemistry of Materials*, 10 (7) (1998), pp. 1820–1826.
 92. K.E. Strawhecker and E. Manias, *Chemistry of Materials*, 12 (10) (2000), pp. 2943–2949.
 93. P.C. LeBaron and T.J. Pinnavaia, *Chemistry of Materials*, 13 (10) (2001), pp. 3760–3765.
 94. Y. Zhou et al., *Materials Science and Engineering A*, 402 (1–2) (2005), pp. 109–117.
 95. O. Becker et al., *Polymer*, 43 (16) (2002), pp. 4365–4373.
 96. S.C. Tjong, *Materials Science and Engineering: R: Reports*, 53 (3–4) (2006), pp. 73–197.
 97. S.R. Ha et al., *J. Nanoscience and Nanotechnology*, 7 (11) (2007), pp. 4210–4213.
 98. M. Battistella et al., *Composites Part A: Applied Science and Manufacturing*, 39 (12) (2008), pp. 1851–1858.
 99. V.Z. Mordkovich, *Theoretical Foundations of Chemical Engineering*, 37 (5) (2003), pp. 429–438.
 100. O.M. Teyssier et al., *Macromolecular Materials and Engineering*, 291 (12) (2006), pp. 1547–1555.
 101. M.L. Shofner et al., *Composites Part A: Applied Science and Manufacturing*, 34 (12) (2003), pp. 1207–1217.
 102. T. Takahashi et al., *Chemical Physics Letters*, 436 (4–6) (2007), pp. 378–382.
 103. H. Miyagawa and L.T. Drzal, *Composites Part A: Applied Science and Manufacturing*, 36 (10) (2005), pp. 1440–1448.
 104. Y. Zhou et al., *J. Materials Science*, 42 (17) (2007), pp. 7544–7553.
 105. L. Tong et al., *3D Fibre Reinforced Polymer Composites*, 1 (Oxford, U.K.: Elsevier Science, 2002).
 106. A.P. Mouritz, *Proceedings of the Institution of Mechanical Engineers, Part L: Journal of Materials: Design and Applications*, 218 (2) (2004), pp. 87–93.
 107. A.P. Mouritz, *Composites Science and Technology*, 68 (12) (2008), pp. 2503–2510.
 108. V.P. Veedu et al., *Nat. Mater.*, 5 (6) (2006), pp. 457–462.
 109. M.F. De Riccardis et al., *Carbon*, 44 (4) (2006), pp. 671–674.
 110. S. Zhu et al., *Diamond and Related Materials*, 12 (10–11) (2003), pp. 1825–1828.
 111. I. Srivastava et al., *J. Nanoscience and Nanotechnology*, 10 (2) (2010), pp. 1025–1029.
 112. J. Qiu et al., *Nanotechnology*, 18 (27) (2007), pp. 1–11.
 113. R. Andrews and M.C. Weisenberger, *Current Opinion in Solid State and Materials Science*, 8 (1) (2004), pp. 31–37.
 114. M.A. Rafiee et al., *Small* (2009), doi 10.1002/sml.200901480.
 115. A.K. Geim, *Science*, 324 (5934) (2009), pp. 1530–1534.

I. Srivastava, research assistant with the Department of Materials Science and Engineering, and N. Koratkar, professor with the Department of Mechanical, Aerospace and Nuclear Engineering, are with Rensselaer Polytechnic Institute, 110 8th Street, Troy, NY 12180. Ms. Srivastava can be reached at srivai@rpi.edu.

The Current Activated Pressure Assisted Densification Technique for Producing Nanocrystalline Materials

J.E. Alaniz, J.R. Morales, and J.E. Garay

The harnessing of length-scale-dependent material properties has been an area of intense research in the past two decades. Retention of nanocrystalline features in fully dense bulk materials has been particularly elusive. Recently the current activated pressure assisted densification (CAPAD) technique has emerged as one of the most successful methods for the production of functional and structural nanocrystalline materials with large sizes. In this article we review some ongoing efforts in using the CAPAD technique for producing single component and nanocomposite systems from nanocrystalline powders. The properties of these nanocrystalline materials include improved light transmittance and magnetic properties caused by interfacial coupling of anti-ferromagnetic/ferrimagnetic phases.

INTRODUCTION

Current activated pressure assisted densification (CAPAD), often referred to as spark plasma sintering (SPS) or field assisted sintering (FAST), uses high heating rates (via Joule heating from an applied current) combined with simultaneous pressure application to densify materials. The densification is believed to be aided by high current flux which influences diffusion controlled mass transport as well as phase growth in the reaction process.^{1,2} Often, as in the case of bulk nanocrystalline materials, CAPAD is capable of producing materials unobtainable through traditional powder densification methods. High heating rates and short processing times on the order of minutes allow a high degree of densification while minimizing grain growth. This allows high grain and phase boundary densities to be maintained, allowing the properties of these boundaries/interfaces to play a

larger role in the overall properties of the bulk materials. Several oxide materials have been produced using this unique process with grain sizes <100 nm and even <20 nm.³⁻⁶

This paper will highlight some of our group's ongoing work with the overarching theme of tailoring properties using the nanocrystalline structure. See

the sidebar for a description of CAPAD processing.

MAGNETIC PROPERTIES OF IRON OXIDE NANOCOMPOSITES

Recently we have been exploring CAPAD as an efficient method for processing bulk magnetic nanocomposites that display length-scale dependent magnetic properties.^{8,9} Because magnetic domain behavior and interactions of magnetic moments occur in true nanoscale dimensions (<100 nm), materials for both hard and soft magnetic applications can be significantly affected by careful control of both composition and nanoscale grain structure. Conventional reaction sintering can achieve precise control of magnetic phase composition in bulk materials, but it requires long processing times that come at the expense of nano-structure. The strategy for making bulk nanocomposites is two-fold: We rely on phase transformations so that the materials "self-assemble" into nanocomposites, and we densify materials quickly to prevent exaggerated grain growth. CAPAD is excellent for taking advantage of both the metastable nature of iron oxide phases and the high densification rates necessary to maintain the nano-scale grain sizes of the starting powder.

Commercial single-phase $\gamma\text{-Fe}_2\text{O}_3$ nanopowders (Alfa Aesar, USA) with average crystallite diameters of 8 nm and 40 nm were used. Figure 1 shows a typical sample after CAPAD processing, next to a coin for size comparison. SEM images of samples derived from 8 nm and 40 nm powders are shown in Figure 2a and b. These samples were densified at 650°C. For all processing temperatures, the average final grain size of material from the 8 nm powder

How would you...

...describe the overall significance of this paper?

This article outlines the benefits of the Current Activated Pressured Assisted Densification (CAPAD) technique for producing bulk nanocrystalline materials from nanopowders. The CAPAD technique is not only efficient, but it also offers a higher degree of control than the better known and widely used methods of powder densification.

...describe this work to a materials science and engineering professional with no experience in your technical specialty?

Retention of nanocrystallinity is difficult since densification at high temperature is accompanied by thermally activated grain growth. However, the CAPAD technique's unique combination of simultaneously applied electric current and pressure allow the production of non-porous bulk materials with nanometric microstructure. At nano-length scales, interactions between grains are different than their microstructured counterparts. Two examples of this nanoscale related phenomenon are shown here.

...describe this work to a layperson?

Large sized nanocrystalline materials are exciting because they behave in very different ways allowing for new applications. In this paper we present a method that can produce bulk nano-materials for optical and magnetic applications.

is smaller (~3 times) than that from the 40 nm-derived powder. XRD analysis reveals that the samples are composed of multiple iron oxide phases (i.e., they are composites). Figure 3 shows prominent peaks representing a hexagonal lattice structure (α - Fe_2O_3) which gradually diminish as the processing temperature is increased to 900°C. Inversely, peaks consistent with a cubic lattice structure (Fe_3O_4) increase in amplitude as the temperature is increased until they are the only peaks present at 900°C.

Table I summarizes density, average grain size, and compositional information for both 8 nm and 40 nm samples at all of the processing temperatures. It is seen that 40 nm samples reach >0.90 density by 650°C, whereas 8 nm samples reach this density between 700°C and 800°C. Quantitative analysis of XRD data shown in the third column of Table I reflects the total phase transformation of α - Fe_2O_3 (hexagonal) to Fe_3O_4 (cubic) mentioned earlier.

The magnetic data for the 8 nm samples zero-field cooled (ZFC'ed) at 100 Oe are shown in Figure 4. In samples processed below 750°C, the most significant increase in magnetization occurs at ~265 K. Samples processed above 650°C show three separate in-

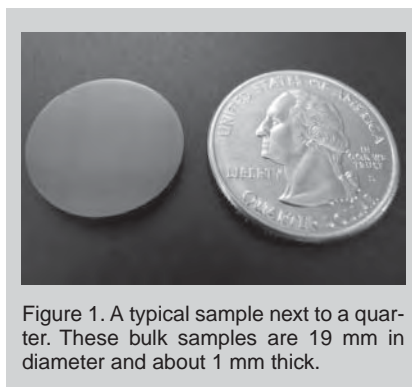


Figure 1. A typical sample next to a quarter. These bulk samples are 19 mm in diameter and about 1 mm thick.

creases at ~20 K, ~110 K, and 265 K. The sample processed at 900°C demonstrates the highest step height at ~110 K as well as the highest net magnetization. Figure 5 shows data for the 40 nm samples ZFC'ed at 100 Oe, and processed between 300 and 800°C. Clear step-like increases in magnetization appear at two temperatures, 120 K and 260 K. In samples processed below 650°C the step heights at both temperatures are similar in proportion as is the magnitude of magnetization. In samples processed above 600°C, the increase at 120 K is distinctly prominent over the diminutive step at 260 K. The largest change in step height as well as net magnetization occurs in the sample processed at the highest temperature, 800°C.

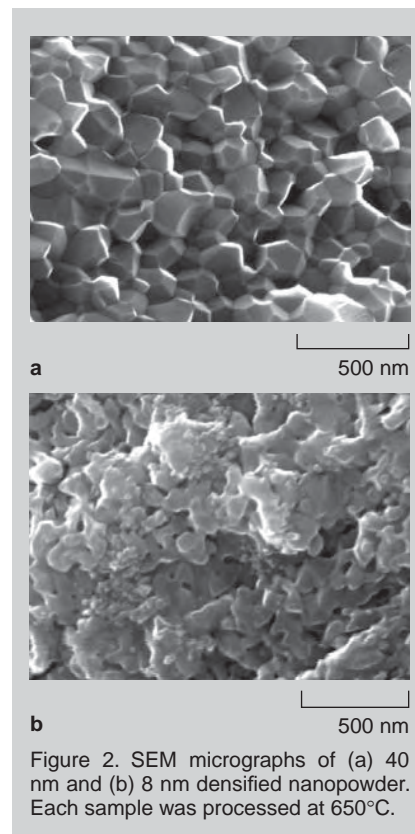


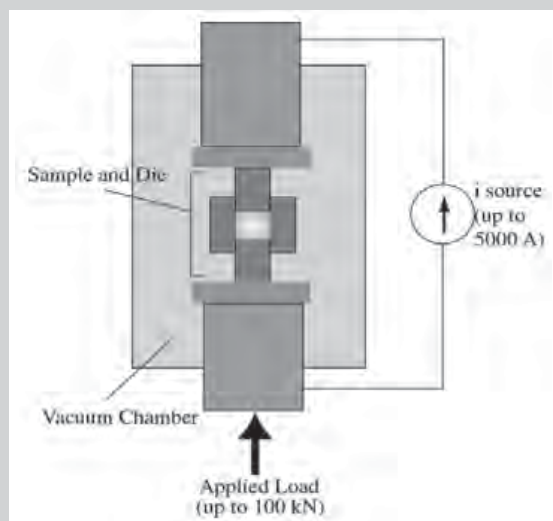
Figure 2. SEM micrographs of (a) 40 nm and (b) 8 nm densified nanopowder. Each sample was processed at 650°C.

Coercivity measurements (Figure 6) show different behavior between the 8 nm and 40 nm samples. 8 nm samples show a steep decrease in coercivity around 20 K and a small change at ~110 K with the exception of the 900°C sample. In contrast, the change in coercivity is unmistakable at 120 K for the 40 nm samples. In the 900°C sample, both the coercive value as well as the change in coercivity is less than it is for samples processed at lower temperatures such as 550°C and 675°C.

Ferrimagnetic γ - Fe_2O_3 (FM) undergoes a phase transformation to antiferromagnetic α - Fe_2O_3 (AFM) at temperatures higher than 300°C. A second phase transformation occurs between α - Fe_2O_3 (AFM) and Fe_3O_4 (FM) due to oxygen reduction during processing. Both α - Fe_2O_3 (AFM) and Fe_3O_4 (FM) are subject to changes in magnetic behavior due to temperature dependent magnetic ordering. For example, in α - Fe_2O_3 (AFM), the Morin transition coincides with a change of antiparallel magnetic moment alignment parallel to the c axis below $T_M = 265$ K. Above 265 K, the magnetic moment alignment flips to point parallel to the basal plane. The reorientation is associated with a small canting of the moments which results in a bulk weak ferromagnetic property. Evidence

CAPAD PROCESSING

Important components of a CAPAD system include a vacuum chamber and electrodes for delivering large electric currents and mechanical loads. We use a custom built CAPAD apparatus. Within the chamber, two water cooled copper electrodes are used to apply a load of up to 150 kN from a Universal test frame (Instron 5584, Instron Inc., Canada) to a graphite die and plunger system that contains the powder to be densified. These electrodes are capable of supplying a 4800 A current from programmable power supplies (Xantrex Inc., Canada) while the temperature of the sample is measured and controlled using a type-



k thermocouple placed in the die. Figure A shows a simple schematic of this system.

Commercial nanocrystalline powders were used in all of the work discussed here. Typical processing involves placing 1–2 g of the nanopowder between graphite dies of 19 mm diameter. We use a pressure of 100–140 MPa. For a detailed review of the CAPAD process, please see Reference 7.

Figure A. Schematic of the device used to perform the CAPAD technique in the studies presented in this paper.

and is higher in composites with smaller grain sizes.⁹

OPTICAL PROPERTIES OF NANOCRYSTALLINE CUBIC ZIRCONIA

There has been increasing interest in coupling the optical properties of single crystal ceramics with polycrystalline materials in order to make them more versatile.^{13,14} The CAPAD technique has been used to make several transparent bulk polycrystalline ceramics. This article will discuss how it was used to make polycrystalline 8 mol.% yttria stabilized zirconia (8YSZ) transparent¹⁵ and how these optical properties were characterized.¹⁶

Aside from having excellent mechanical properties, polycrystalline 8YSZ is widely used as a thermal barrier coating (such as for gas turbine components, etc.)¹⁷ and as an ionic conductor (such as used in oxygen sensors). However, by capturing the optical properties found in single-crystal zirconia, this material could potentially be used in a much

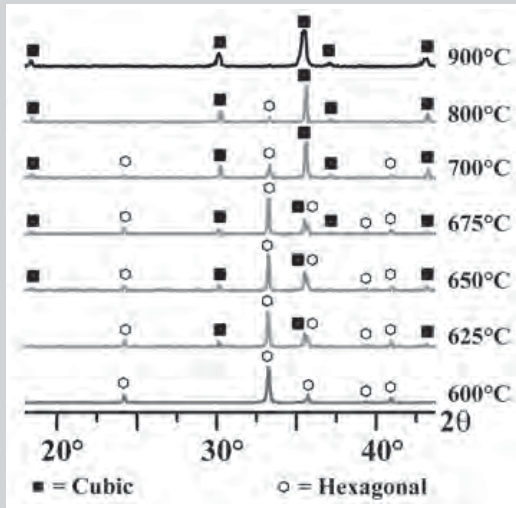


Figure 3. XRD data for samples prepared over a range of temperatures. A gradual temperature dependent phase transformation between 600°C and 900°C is seen as hexagonal peaks visible at 600°C eventually disappear and cubic peaks gradually increase until they are the only peaks present in the 900°C sample.

of the reorientation can be detected through small increases in magnetization values.^{11,12} In the case of $\text{Fe}_3\text{O}_{4(\text{FM})}$, the change in the easy axes of magnetization coincides with a structural lattice change. Below the Verwey transition ($T_V = 125 \text{ K}$), the monoclinic easy direction is $\langle 100 \rangle$. Above the T_V , the crystal structure changes to FCC with easy directions of magnetization in the $\langle 111 \rangle$ directions.^{11,12} This change produces a decrease in coercivity at the T_V which is not seen in $\gamma\text{-Fe}_2\text{O}_{3(\text{FM})}$.

In the 8 nm samples, the 265 K increase in ZFC magnetization is due to the Morin transition of $\alpha\text{-Fe}_2\text{O}_{3(\text{AFM})}$. The strongest increase in magnetization at $\sim 110 \text{ K}$ for the 8 nm 900°C sample can be linked to the lower temperature ($\sim 110 \text{ K}$) decrease of coercivity. This suggests that a low-temperature Verwey transition is responsible for both changes in magnetization and coerciv-

ity. Similar to the correlation between temperature and coercivity, there is a strong correlation between temperature and magnetization in the 40 nm samples (i.e., the changes in magnetization at $T_V = 120 \text{ K}$ and $T_M = 265 \text{ K}$). Interestingly, our nanocomposites display exchange bias caused by magnetic coupling at interfaces. The magnitude of the exchange field is composition dependent

Table I. Comparison of Experimental Parameters (Temperature and Avg. Crystallite Size of Nanopowder) and the Resulting Bulk Material Properties (Density, Avg. Grain Size, and Composition)

Temp.	Powder (nm)	Density	Avg. GS (nm)	% Comp. Hex:Cubic
600°C	8	0.69	—	95:5
	40	0.83	—	100:0
650°C	8	0.71	58	80:20
	40	0.99	180	76:24
700°C	8	0.78	77	62:38
	40	0.97	191	32:68
800°C	8	0.93	91	1:99
	40	0.97	372	15:85
900°C	8	0.94	173	0:100
	40	0.97	558	0:100

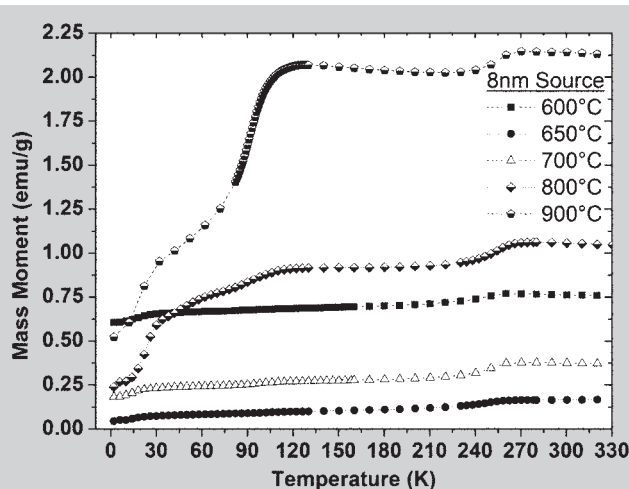


Figure 4. Mass moment (measured in ZFC (100 Oe)) data for the samples prepared from the 8 nm powder.

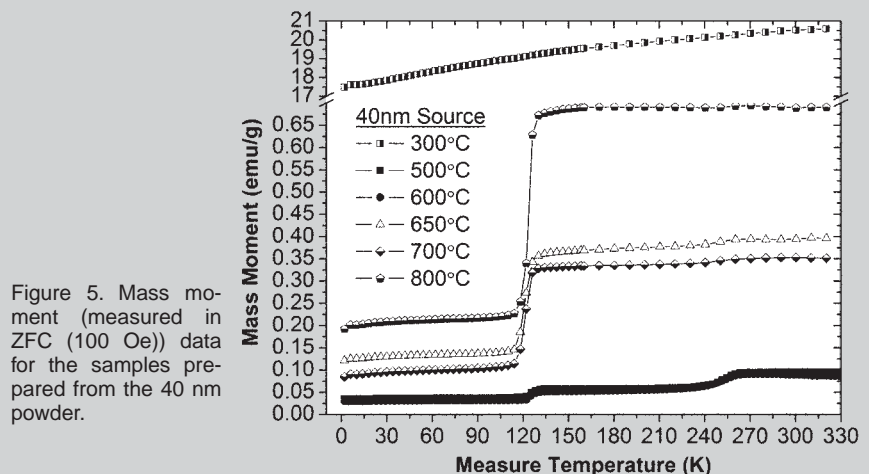


Figure 5. Mass moment (measured in ZFC (100 Oe)) data for the samples prepared from the 40 nm powder.

wider variety of applications such as furnace and cryogenic devices.

Each of the zirconia samples discussed in this paper were processed under vacuum ($<4 \times 10^{-4}$ torr) and contained 1.5 g of cold pressed (71 MPa for 1 min.) 8YSZ powder (Tosoh Corporation, Tokyo, Japan) with a reported crystal size of 50 nm. Two different processes were used to create these samples. The two-step load process consisted of an initial load ramp at 10 kN min^{-1} up to a pressure of 106 MPa (30 kN load). The samples were then heated to $1,200^\circ\text{C}$ at a rate of $200^\circ\text{C min}^{-1}$ after which the pressure was then raised to 141 MPa (40 kN load). These samples were then held at temperature and pressure for varying amounts of time (10, 11, and 12 min.). The one-step process simply consisted of the initial load increase to either 30 or 40 kN, the heating process, and the final hold. For comparison, the hold in the one-step process was adjusted to match the overall experiment time of a two-step process with a 10 min. hold (17 min. from start to finish). For an in-depth discussion of these processes see Reference 15.

Each of the two-step samples as well as the one-step 40 kN sample were found to be $>99.9\%$ dense through the Archimedes method. These samples showed transparency and translucency, respectively. The one step 30 kN sample was found to be 99.5% dense and was observed to be opaque. This difference in optical properties is most likely due to porosity as this has been shown to be the dominant mechanism in light interaction with ceramics.^{18,19} Each sample was a cylinder 19 mm in diameter and

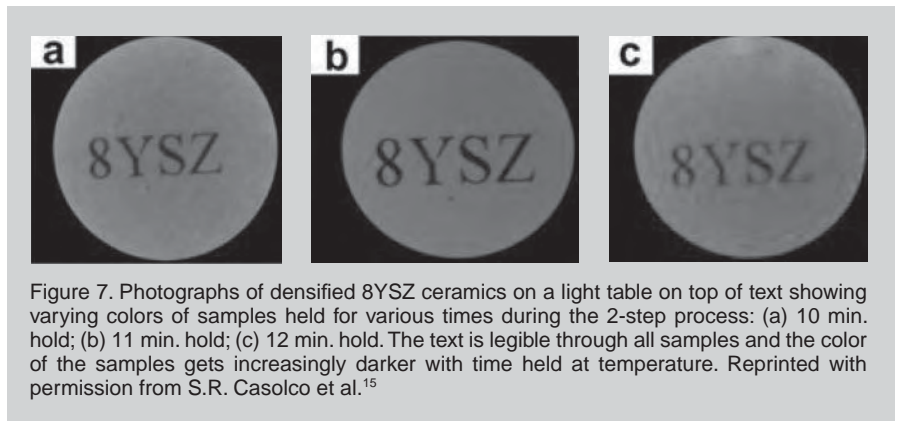


Figure 7. Photographs of densified 8YSZ ceramics on a light table on top of text showing varying colors of samples held for various times during the 2-step process: (a) 10 min. hold; (b) 11 min. hold; (c) 12 min. hold. The text is legible through all samples and the color of the samples gets increasingly darker with time held at temperature. Reprinted with permission from S.R. Casolco et al.¹⁵

approximately 1 mm thick. The two-step samples showed different characteristics as the final hold time was changed (Figure 7). As each of these samples were created with the same temperatures and pressures, it is reasonable to expect a different light interaction mechanism than porosity is causing these differences.

Scanning electron microscopy results show that the final grain sizes of these samples are 55 nm on average (Figure 8a,b). This is a clear example of how the beneficial characteristics of CAPAD can lead to fully dense samples with little to no grain growth, based on a reported starting crystal size of 50 nm.

To quantitatively characterize the two-step samples, the total transmission and reflection were measured. Figure 9 shows how the absorption coefficients increase dramatically as the final hold time is increased and decrease as wavelength. To determine whether oxygen vacancies or their associated defects—caused by the reducing atmosphere of the CAPAD—are responsible for the observed change in absorption a sample was annealed in air at 750°C for 2, 4, 8, 16, and 24 hour periods. Transmission,

reflection, and absorption data were taken for this sample using light of 633 nm wavelength. As seen in Figure 10, the absorption decreases dramatically with increased annealing time, indicating that free electrons (due to oxygen vacancies and their associated defect structures) are indeed responsible for light absorption in the zirconia samples. Detailed data and characterization explanations are available in Reference 16.

When comparing the absorption data of the reduced polycrystalline sample (as processed) with that of a reduced single crystal, the data is strikingly similar (Figure 11). Likewise, when the

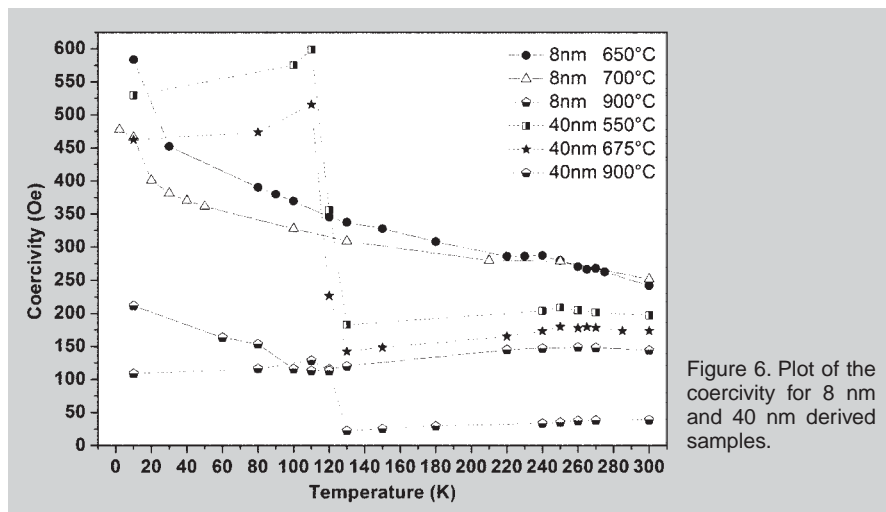


Figure 6. Plot of the coercivity for 8 nm and 40 nm derived samples.

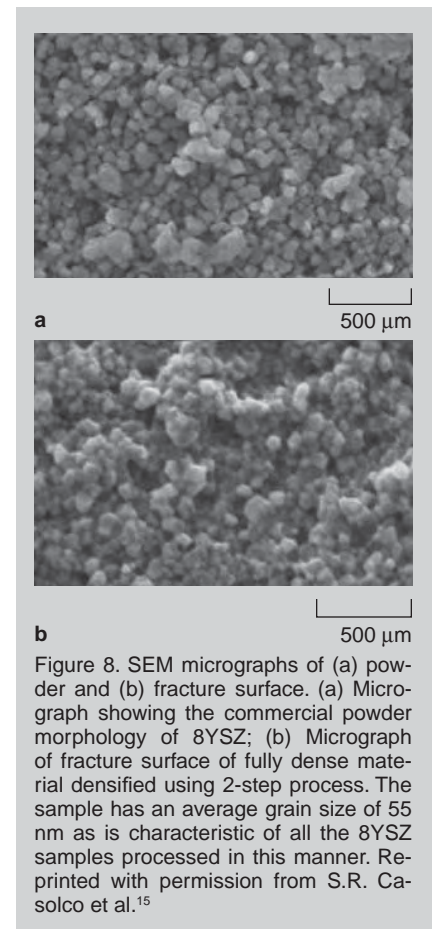


Figure 8. SEM micrographs of (a) powder and (b) fracture surface. (a) Micrograph showing the commercial powder morphology of 8YSZ; (b) Micrograph of fracture surface of fully dense material densified using 2-step process. The sample has an average grain size of 55 nm as is characteristic of all the 8YSZ samples processed in this manner. Reprinted with permission from S.R. Casolco et al.¹⁵

non-reduced polycrystalline sample is compared to the non-reduced single crystal sample,²⁰ the data is still in good agreement.

CONCLUSION

The CAPAD technique is capable of consolidating powders to very high densities through simultaneous application of both pressure and current and imparting new properties onto traditional materials by controlling the nanostructure of the bulk material. The control of both nanostructure and composition in iron oxide nanocomposites opens the door to further advances in magnetic materials. The studies of

materials like transparent polycrystalline 8YSZ and alumina²¹ suggest that many other wide band gap materials that have functional polycrystalline characteristics may have the potential to be made transparent. The strategies shown here can potentially be used to tailor other material properties. Thermal²² and electrical behavior²³ can be dramatically affected by either grain size or grain boundary stoichiometry. In addition, the electrical environment of grain boundaries can affect important characteristics like ionic mobility and stoichiometric homogeneity²⁴ of the bulk materials. The effects of the fundamental components involved in

this process are still not fully understood, which means the full versatility of the CAPAD process has yet to be realized. Property studies like the ones presented here are excellent indicators of the potential of this process.

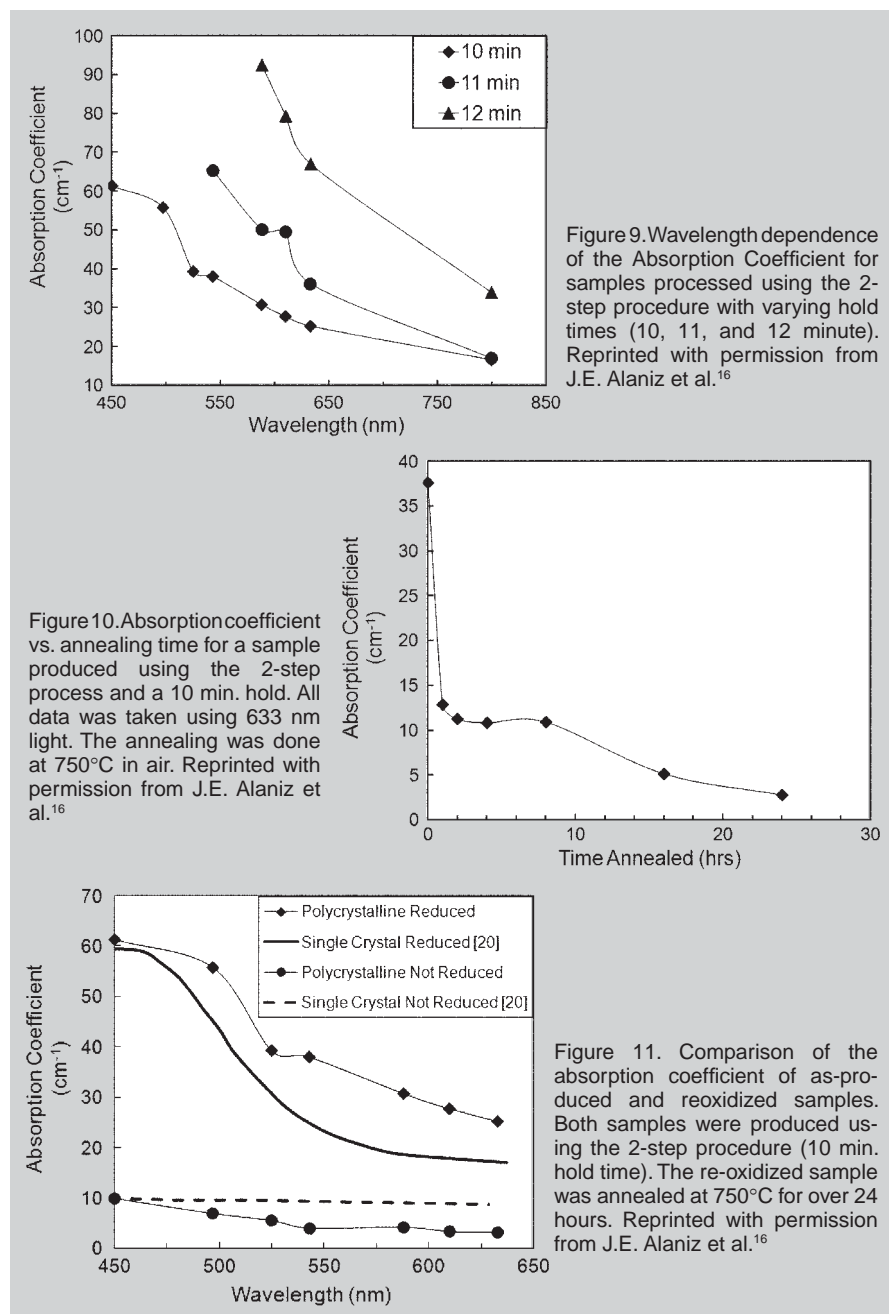
ACKNOWLEDGEMENTS

Support of this work by the Army Research Office and the Air Force Office of Scientific Research is gratefully acknowledged.

References

1. U. Anselmi-Tamburini, J.E. Garay, and Z.A. Munir, *Mater. Sci. Eng. A*, 407 (2005), p. 24.
2. J.E. Garay, U. Anselmi-Tamburini, and Z.A. Munir, *Acta Mater.*, 51 (2003), p. 4487.
3. U. Anselmi-Tamburini et al., *J. Mater. Res.*, 19 (2004), p. 3255.
4. G. Zhan et al., *J. Am. Ceram. Soc.*, 86 (2003), p. 200.
5. L. Mitoseriu et al., *Appl. Phys. Lett.*, 84 (2004), p. 84.
6. U. Anselmi-Tamburini, J.E. Garay, and Z.A. Munir, *Scripta Mater.*, 54 (2006), p. 823.
7. J.E. Garay, *Annual Reviews of Material Research* (to be published 2010).
8. J.R. Morales et al., *Appl. Phys. Lett.*, 93 (2008), 02254.
9. J.R. Morales et al., *Appl. Phys. Lett.*, 96 (2010) 013102.
10. U. Schwertmann and R.M. Cornell, *The Iron Oxides: Structure, Properties, Occurrences, and Uses*. 2nd ed. (Weinheim, Germany and New York: VCH, 1991), p. 26.
11. D.J. Dunlop and Ö. Özdemir, *Rock Magnetism: Fundamentals and Frontiers. Cambridge Studies in Magnetism* (Cambridge, U.K. and New York: Cambridge University Press, 1997).
12. F. Walz, *J. Physics-Condensed Matter*, 14 (12) (2002), pp. R285–R340.
13. L. Ji-Guang et al., *J. Am. Ceram. Soc.*, 83 (2000), p. 961.
14. X. Su et al., *J. Mater. Sci.*, 39 (2004), p. 6257.
15. S.R. Casolco, J. Xu, and J.E. Garay, *Scripta Mater.*, 58 (2008), pp. 516–519.
16. J.E. Alaniz et al., *Opt. Mater.* (2009), doi:10.1016/j.optmat.2009.06.004
17. C.G. Levi, *Curr. Opin. Solid Stat. Mater. Sci.*, 8 (2004), p. 77.
18. R. Apetz and M.P.B. van Bruggen, *J. American Ceramic Society*, 86 (2003), p. 480.
19. U. Anselmi-Tamburini, J.N. Woolman, and Z.A. Munir, *Advanced Functional Materials*, 17 (2007), p. 3267.
20. B. Savioni et al., *Physical Review B*, 57 (1998), p. 13439.
21. R.L. Coble, U.S. patent, 3,026,210 (20 March 1962).
22. R. Berman, *Proceedings of the Physical Society, A* 65 (1952), p. 1029.
23. V.I. Barbashov et al., *Physics of the Solid State*, 50 (2008), pp. 2261–2262.
24. Gianguido Baldinozzi et al., *Mater. Res. Soc. Symp. Proc. Vol. 1122* (Warrendale, PA: Materials Research Society, 2009).

J.E. Alaniz, J.R. Morales, and J.E. Garay are with the Department of Mechanical Engineering, Materials Science and Engineering Program, University of California, Riverside. Prof. Garay can be reached at jegaray@engr.ucr.edu.



Nanostructured Metal Composites Reinforced with Fullerenes

Francisco C. Robles-Hernández and H.A. Calderon

This work presents the results of the characterization of nanostructured Al or Fe matrix composites reinforced with fullerenes. The fullerene used is a mix of 15 wt.%C₆₀, 5 wt.%C₇₀, and 80 wt.% soot that is the product of the primary synthesis of C₆₀. The composites were produced by mechanical alloying and sintered by spark plasma sintering (SPS). It was found that in both composites, C₆₀ withstands mechanical alloying, and acts as a control agent, reducing the agglomeration of the particles. In both composite systems the as-mechanically alloyed powders as well as the SPS sintered products are nanostructured. During the SPS process the effect of the metal (Al or Fe) matrix with the fullerene is different for each composite. For instance, Al reacts with all the carbon in the fullerene mix and forms Al₄C₃; on the contrary, in the Fe-fullerene composite, Fe sponsors the synthesis of C₆₀ during the SPS process. The synthesis of the C₆₀ is presumably assisted by the catalytic nature of Fe and the electric field generated during the SPS sintering process.

INTRODUCTION

The successful synthesis of fullerenes and carbon nanotubes (CNT) is possible by different methods and has resulted in diverse structures.¹⁻⁴ The most common structures (buckyballs) are C₆₀ and C₇₀ that are composed of atomic arrangements of carbon with pentagons and hexagons and heptagons.^{2,5} Conventionally, the fullerenes are synthesized and enriched by the Krätschmer method,⁶ and fullerenes have been widely used as reinforcements for composites.^{7,8} The dispersion of carbides (e.g., Al₄C₃) in Al matrices is challenging, some attempts to increase the homogeneity and cohesion among the matrix and the reinforcements has been conducted by

means of: reaction milling, thixocasting, rheocasting, metal infiltration, and electromagnetic stirring.⁹⁻¹² The use of metallic matrices and carbon nanoparticles to produce composites is controver-

sial;^{1,13-18} some authors argue that when using Al the carbon nanoparticles tend to form carbides, but when CNT are added in small amounts (<2%) they act as effective reinforcements with limited to no interaction with the metallic matrix. For instance, it has been observed that mechanical properties improve with the formation of carbides (e.g., Al₄C₃) in metallic matrix composites; unfortunately this decreases electrical conductivity.

Mechanical alloying is a method that was originally proposed by Gilman and Benjamin in the 1960s to manufacture high-temperature nanostructured materials at room temperature.^{11,12} Using mechanical alloying it is possible to prevent or promote chemical reactions by controlling temperature, intensity, and time and in all cases the final product is usually highly homogeneous and nanostructured.¹⁹ The ideal conditions to preserve the nanostructured nature of mechanically alloyed powders include low temperature and short times, which are the typical operating conditions of spark plasma sintering (SPS).⁸

In the present work mechanical alloying and SPS are combined to produce nanostructured composites of Al, Fe, and fullerene. The characterization is conducted by means of scanning electron microscopy (SEM), x-ray diffraction (XRD), and transmission electron microscopy (TEM). In addition, hardness and density measurements have been performed on the sintered composites. Results are reported and discussed accordingly.

See the sidebar for experimental procedures.

RESULTS

Figure 1 shows SEM micrographs of the original and mechanically al-

How would you...

...describe the overall significance of this paper?

Mechanical alloying and spark plasma sintering (SPS) are ideal methods to produce nanostructured Al and Fe matrix composites reinforced with carbon nanoparticles. Al and Fe metallic matrices have different effects on carbon nanoparticles. For instance, Al sponsors the formation of carbides while Fe promotes an in-situ synthesis of C₆₀. The synthesis of the C₆₀ is presumably assisted by the catalytic nature of Fe and the electric field generated during the SPS sintering process.

...describe this work to a materials science and engineering professional with no experience in your technical specialty?

This work describes conventional methodologies to produce advanced metal matrix composites for various applications. For instance, mechanical alloying is a well known method and widely used and SPS offers the potential to sinterize powders at low temperatures and pressures in relatively short times, preserving the nanostructured nature of the composites. The main novelty in our work is the in-situ synthesis of C₆₀ during the SPS process.

...describe this work to a layperson?

In this paper we present a new method to sinterize fullerene (C₆₀) in-situ during sintering (SPS). This is a novel approach to produce nanostructured composites with nanoparticles of C₆₀ embedded as reinforcements. Furthermore, the use of Al or Fe has different effects with C₆₀ during the SPS process.

EXPERIMENTAL PROCEDURES

Commercial powders of iron (Fe; 99.9% purity and a particle size $<100\ \mu\text{m}$), aluminum (Al, 99.9 at.% purity and a particle size $<180\ \mu\text{m}$), and fullerene mix (15.5at.% C_{60} + 4.5at.% C_{70} + 80at.% C_{soot}) are used as starting materials. The nominal composition of the composite is Al or Fe and 15.7at.%C. The C_{60} present in the fullerene mix is approximately 2.35 at.%C that is equivalent to or 0.04 mol.% C_{60} .

Mechanical alloying has been conducted at different times up to and including 100 h, but only the results of 100 h of mechanical alloying are presented here. The powder-to-ball ratio used in the mechanical alloying process is 100:1 without additions of any control agents. The manipulation of the powders is conducted under controlled atmosphere (Ar). The milled powders are sintered by SPS at 773 K under 100 MPa for 600 s at a heating rate of 3.3 K/s. The SPS sintered samples are 13 mm in diameter and 5 mm in thickness.

X-ray diffraction (XRD) is conducted on a SIEMENS D5000 apparatus using a Cu tube with a characteristic K_{α} wavelength of 0.15406 nm. The scanning electron microscopy (SEM) observations are carried out on a JEOL JSFM35CF microscope operated at 20 kV. The SEM samples in powder form are prepared by dispersing the powders onto a graphite tape. Transmission electron microscopy (TEM) is conducted on a JEOL JEM200FXII operated at 200 kV. For TEM, the samples are prepared by dispersing the powders on ethanol to form a dilute suspension from which an aliquot is taken and is deposited on a Cu-graphite 300 mesh. The as sintered products are surface polished for SEM, and electropolished on a double jet electropolisher for TEM. The electropolishing is conducted at 230 K using an electrolyte solution of 25 vol.% HNO_3 + 75 vol.%. The density measurements are conducted by the Archimedes method and the rule of mixes. The density of fullerene is as per recommended by the manufacturer. The Vickers microhardness is conducted following the ASTM E92-82 standard procedures for a load of 25 g and a time of 10 s.

loyed powders. Figure 1a and b shows the typical spray cast structure of the original powders, and Figure 1c shows the fullerene powders synthesized by evaporation methods with its typical “fluffy-like” appearance. Figure 1d and e presents the mechanically alloyed powders for the Al-fullerene and Fe-fullerene composites, respectively. The mechanical alloying of the Al-fullerene and Fe-fullerene original mixes results in the production of nanostructured

particles with a normal particle size distribution and irregular shapes. The limited agglomeration of the alloyed powders is attributed to the control agent effect of fullerene.

Figure 2a shows the XRD pattern for the as-synthesized fullerene showing the presence of C_{60} and C_{70} . As per the relative intensity of the reflections it is clear that C_{60} is more abundant than C_{70} . The arrow in the XRD pattern indicates the presence of another fuller-

ene phase that has been previously reported as tetragonal C_{60} .¹³ In Figure 2b a dark field of a fullerene particle is presented which shows that the C_{60} in the fullerene mix has a face-centered cubic structure and the nanostructured nature of C_{60} . The calculated lattice parameters for C_{60} are: 1.44 Å and 1.43 Å as per the results of XRD and TEM, respectively. The XRD calculated lattice parameter for C_{70} is 1.92 Å. These values are within 1% different from the theoretical lattice parameters.

Figure 3a and b presents the XRD patterns for the mixes (before mechanical milling) of fullerene with the respective metallic (Al or Fe). Figure 3c and d shows the XRD matrix spectra after mechanical alloying. The limited amount of C_{60} present in the original fullerene mix makes its identification, by XRD, challenging; for this reason, the intensity of the Al-fullerene systems (before and after mechanical milling) is presented in logarithmic scale. The logarithmic scale helps reduce the contrast among the reflections between Al and C_{60} and enhances the C_{60} reflections, allowing its identification. Unfortunately, this process increases the level of noise in the XRD pattern. The logarithmic scale treatment is not possible for the Fe-fullerene system due to the relatively high amount of noise in the background complicating the identification of the C_{60} reflections in this system (Figure 3b and d).

Figure 4 shows XRD results for the mechanically alloyed powders and SPS

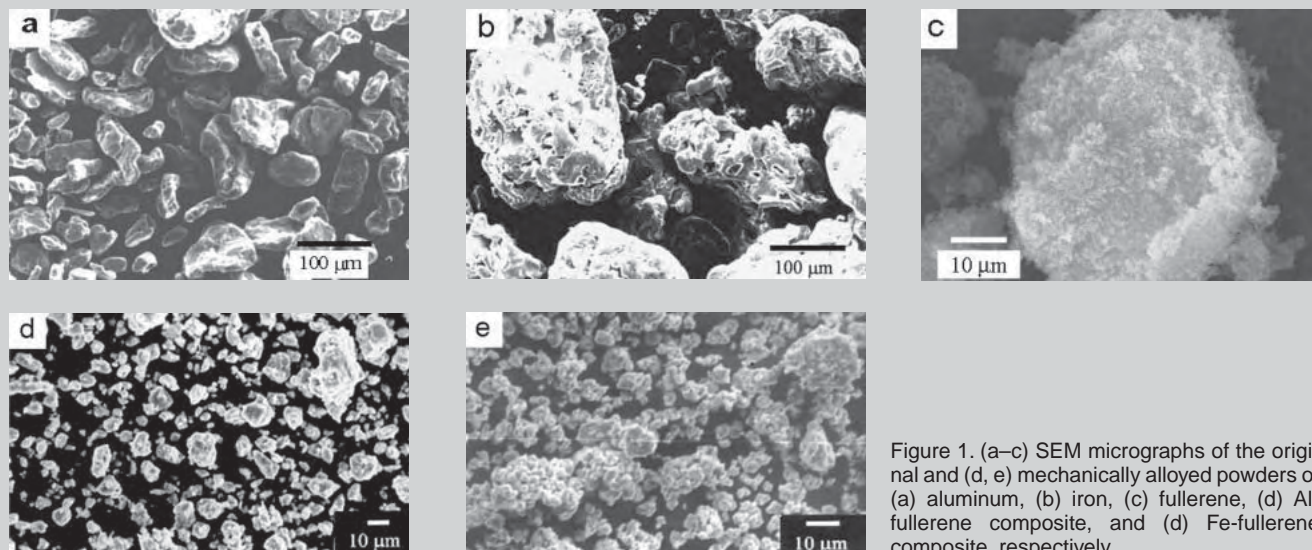


Figure 1. (a–c) SEM micrographs of the original and (d, e) mechanically alloyed powders of (a) aluminum, (b) iron, (c) fullerene, (d) Al-fullerene composite, and (e) Fe-fullerene composite, respectively.

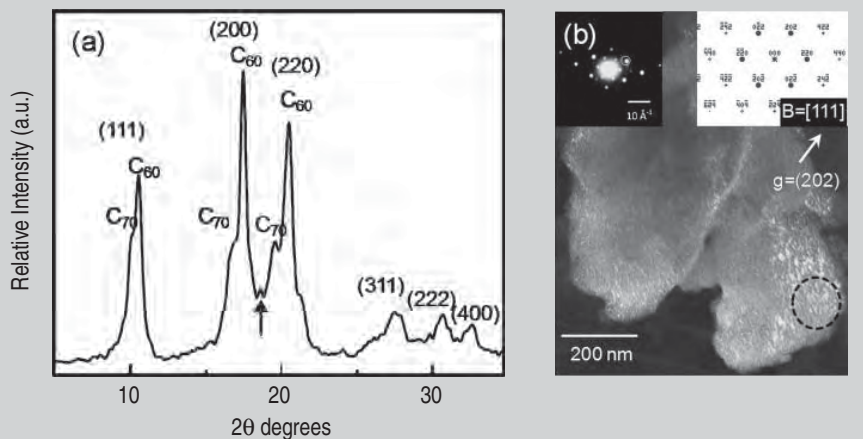


Figure 2. (a) X-ray diffraction pattern of the as synthesized fullerene (arrow identifying a reflection of tetragonal fullerene), and (b) TEM dark field and respective micro-diffraction selected area diffraction pattern (SADP), and simulated pattern. Location, plane and direction (g) for the SADP are indicated.

sintered samples. Comparing Figure 3 and Figure 4 it can be concluded that the XRD results show no evidence of chemical reactions among the metallic matrices and the reinforcement induced

by mechanical alloying. Nonetheless, in the case of the Al-fullerene composite the Al reflections become wider and proportionally smaller indicating a potential reduction in the crystal size

of the aluminum matrix. On the other hand, the iron matrix in the Fe-fullerene composite does not seem to be affected by mechanical alloying (Figure 3).

Figure 4 shows the different effects of the metal (Al or Fe) matrices reacting with the fullerene mix during the SPS sintering. For example, in the Al matrix composite all the carbon present in the fullerene mix reacts with Al to form Al_4C_3 . On the other hand, the intensity of the $(111)_{C_{60}}$ reflection is intensified considerably during SPS of the Fe-fullerene composite. This result indicates that C_{60} is synthesized in-situ during the SPS sintering process. Using the XRD results from Figures 3b and 4b it is determined that the amount of carbon in the form of C_{60} is approximately 8.2 at.%C that is equivalent to 0.14 mol.% C_{60} . The above indicates that the amount of C_{60} present in the

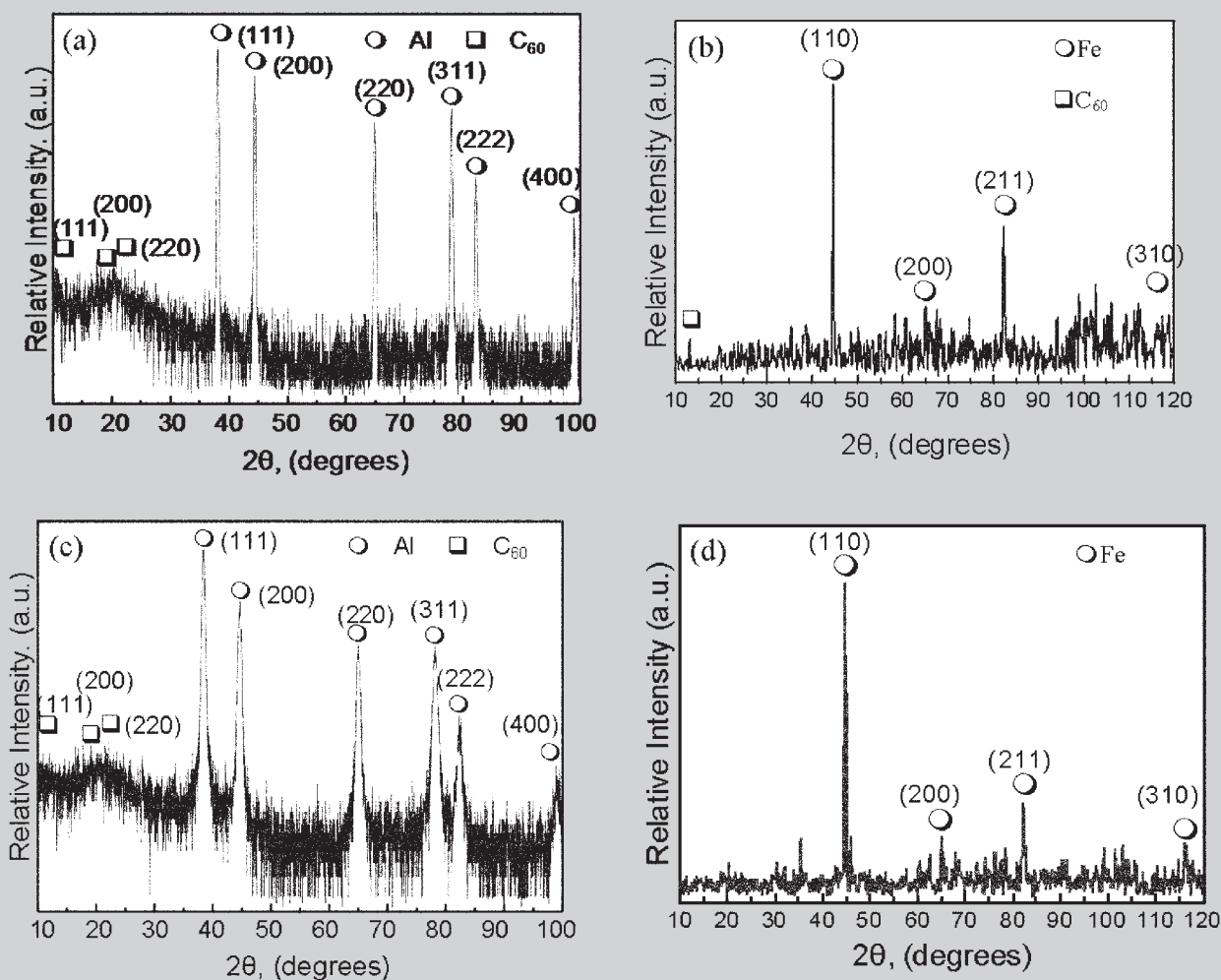


Figure 3. X-ray diffraction patterns for the (a) Al-fullerene and (b) Fe-fullerene systems, the mechanically alloyed (c) Al-fullerene and (d) Fe-fullerene composites. Note the absence of the C_{60} reflections in the Fe-fullerene system that is attributed to the low amount of C_{60} in the original mixes as well as the low amount of C_{60} present in the fullerene mix.

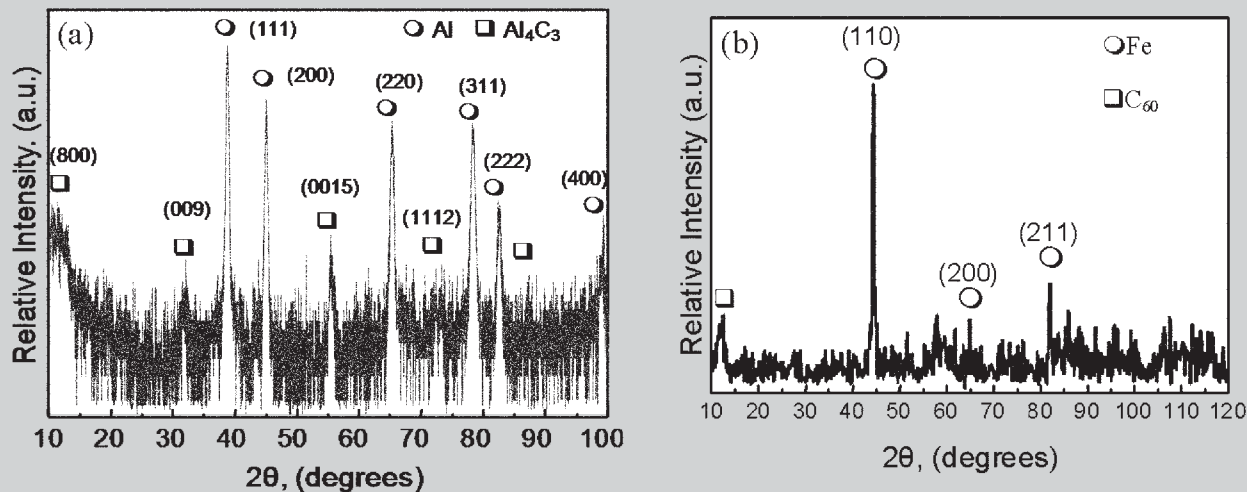


Figure 4. XRD diffractograms of the sintered products for the (a) Al-fullerene and (b) Fe-fullerene systems.

sintered Fe-fullerene sample is approximately 3.5 times larger than in the original samples (2.35 at.%C or 0.04 mol.%C₆₀) before SPS.

Figure 5 shows TEM dark field images and selected area diffraction patterns (SADP) of the mechanically alloyed powders of Al-fullerene and Fe-fullerene composites. The “g” identifies the corresponding reflecting planes utilized to produce the dark fields. In the TEM micrographs, it can be observed a high level of homogeneity for both metal (Al or Fe) matrix composites. This demonstrates that mechanical alloying has the ability to produce homogeneous and nanostructured Al and Fe matrix composites reinforced with fullerene. The bright zones on the TEM dark fields (Figure 5) are crystals of C₆₀ identified in either the Al-fullerene or the Fe-fullerene composites. It is of interest that the grain size of C₆₀

present in the Fe-fullerene composite is smaller than the ones present in the Al-fullerene composite.

The complete reaction of the carbon and Al forming the Al₄C₃ carbide indicates that the high affinity of carbon for Al during SPS process is not limited to C₆₀ or C₇₀, but it also includes the carbon in the soot (graphene-like arrangements). Tentatively, the affinity of carbon in the soot for Al is due to the large surface area characteristics of the graphene-like structures present in the carbon soot allowing a rapid reaction between carbon and Al and leading to the complete transformation of carbon into Al₄C₃ at high homologous temperature ($T/T_m \approx 0.8$). Figure 6 shows TEM images of the sintered products for both composites. It is important to notice that for the Al-fullerene composite some particles are pure Al and other particles are pure Al₄C₃ as seen

in Figure 6a and b. The composition of the Al₄C₃ particles has been verified by means of SEM-EDS and the results are presented in Figure 7.

Measurements of Vickers micro-hardness show that the hardness of the Al-fullerene composite increases to 291 μHV_{25} that is approximately 6 times the micro-hardness of pure aluminum (50 μHV_{25}). The Fe-fullerene composite micro-hardness increases to 722 μHV_{25} which represents an increase of more than 700% when compared to pure Fe (100 μHV_{25}). The increments in Vickers micro-hardness for the Al-fullerene composite are attributed to the presence of Al₄C₃. The results of densification conducted on the as-SPS sintered samples indicate that both composites reach an approximate density of 82% with respect to their corresponding theoretical values of 2.58 g/cm³ and 6.91 g/cm³ for the Al-fullerene and Fe-

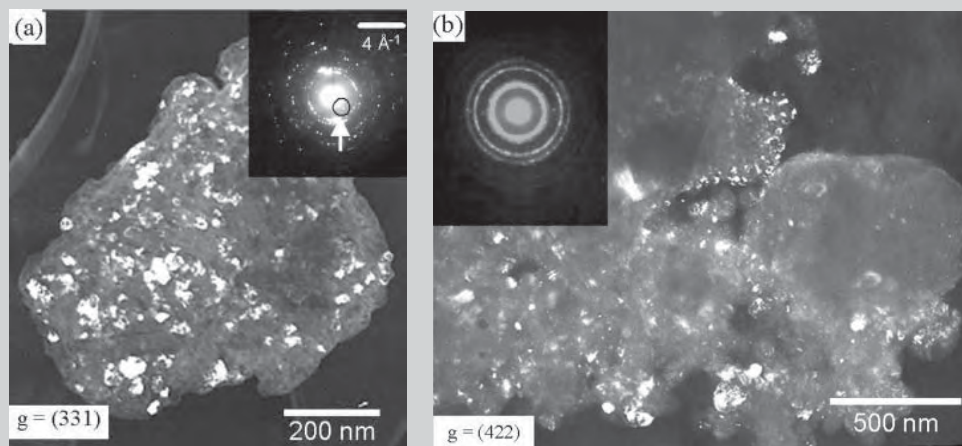


Figure 5. TEM dark field micrographs and their respective SADP after mechanical alloying for 100 h for the (a) Al-fullerene and (b) Fe-fullerene composites, “g” indicates the crystallographic plane used to produce the respective dark fields; the bright zones in the dark fields are crystallites of C₆₀.

fullerene composites, respectively. The calculated density for the Al-fullerene composite is 2.12 g/cm³ and 5.66 g/cm³ for the Fe-fullerene composite. This densification seems smaller when compared to values reported by other authors for composites sintered by SPS;^{14–16} relatively short densification times were chosen for the current work, since the intention was to prevent coarsening, and preserve the nanoscale microstructural features. Further work will be necessary to ascertain the optimum processing conditions (temperature, pressure, time) for achieving maximum density whilst preserving the beneficial nanoscale features.

DISCUSSION

Mechanical alloying effects on the constituents of the Al-fullerene and Fe-fullerene composites are almost negligible. No conclusions can be drawn from the XRD results regarding the effects of mechanical alloying on fullerenes for the Fe-fullerene composite (i.e., compare Figure 3b and d). However, by observing the respective TEM dark field for the Al-fullerene and Fe-

fullerene composites, it is evident that the crystallites of C₆₀ are smaller in the Fe-fullerene (Figure 5a and b). In addition, this clearly demonstrates that mechanical alloying is a promising method to produce a nanostructured composite for both Al-fullerene and Fe-fullerene systems.

The most important result in the present work is the interaction of the different metallic matrices when used in their respective composites with the fullerene mix. It is evident that in the Al-fullerene composite during the SPS process the chemical reaction between Al and the carbon present in the fullerene mix gives rise to the formation of Al₄C₃. On the other hand, in the Fe-fullerene composite we have identified an increase in the intensity of the C₆₀ reflection. The intensity of the peak is approximately 3.5 times higher, and represents an increase from 0.06 mol.% C₆₀ to 0.14 mol.% C₆₀ in the amount of C₆₀ present in the sintered product.

The increase in the intensity of the C₆₀ reflection (111)_{C60} can be an indication of the in-situ synthesis of C₆₀ during the SPS process. The in-situ synthesis is

further confirmed by TEM means. This type of synthesis is attributed to the presence of the electric field generated by the SPS and the catalytic nature of Fe to synthesize carbon nanoparticles such as C₆₀ or nanotubes.^{21–24} The sintering temperature, 773 K, is relatively low for the Fe-fullerene composite ($T/T_m \approx 0.42$) which results in a lower affinity for carbon when compared to Al at the same temperature. The amount of Fe₃C formed during the SPS process is relatively small which makes XRD phase identification difficult, but the Fe₃C is clearly identified by TEM.

The measured densification, with respect to the theoretical is relatively low; however, this is due to the temperature, pressure, and time used during the SPS sintering process. The conditions used during the SPS were intended to prevent grain coarsening. In addition, these conditions slow down reactions between Fe and the carbon present in the fullerene mix, thereby promoting the nucleation and growth of C₆₀ during the SPS process without excessive coarsening. The low homologous temperature may also be contributing to the

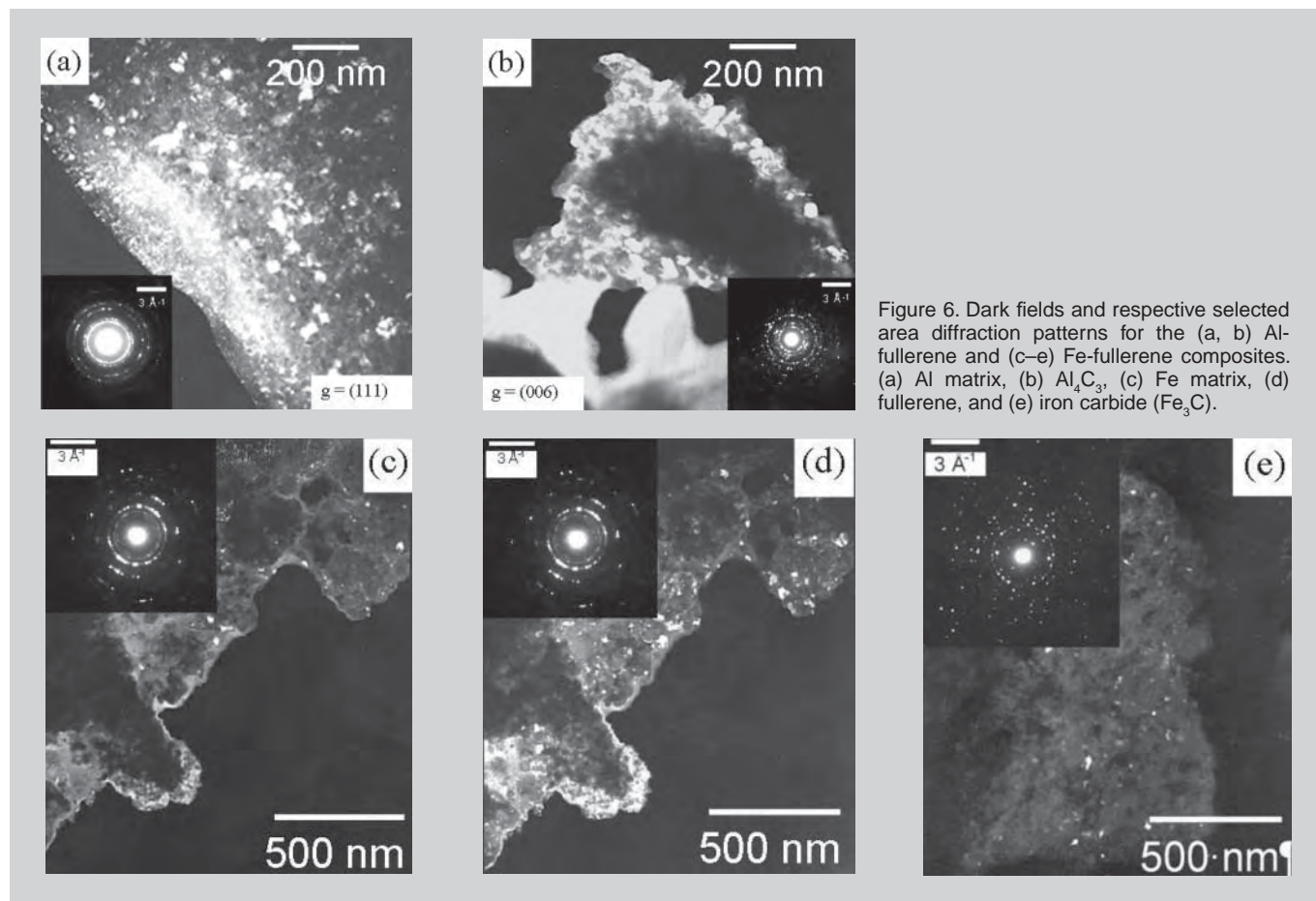


Figure 6. Dark fields and respective selected area diffraction patterns for the (a, b) Al-fullerene and (c–e) Fe-fullerene composites. (a) Al matrix, (b) Al₄C₃, (c) Fe matrix, (d) fullerene, and (e) iron carbide (Fe₃C).

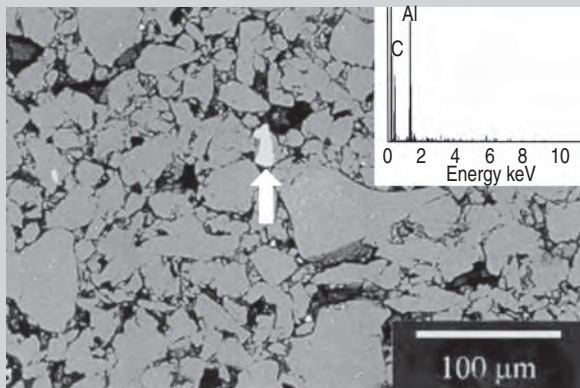


Figure 7. SEM micrograph of the Al-fullerene composite after the SPS sintering and respective EDX spectrum from the Al_4C_3 particle indicated with the arrow.

lower reactivity between fullerene and the Fe matrix. Therefore, using higher temperatures and/or longer times may lead to higher densification, but will likely result in coarsening of the grain and for the Fe-fullerene composite this may even preclude the desirable in-situ synthesis of C_{60} .

CONCLUSIONS

In the Al-fullerene composite, the high affinity of Al for carbon together with the SPS sintering temperature promoted their complete reaction and their transformation into Al_4C_3 . Alternatively, the combined effect of the electric field, relatively low SPS sintering temperature, and catalytic nature of Fe resulted in the in-situ synthesis of C_{60} which is a quite unique finding. The level of reactivity of the various constituents of the fullerene mix used in this work is uncertain, as is the type of carbon (C_{60} , C_{70} , or soot) that reacts with Fe and forms Fe_3C . However, it is conjectured that the C_{60} that has been synthesized in-situ during the SPS sintering process is obtained from the soot (i.e., graphene-like structures) present in the fullerene mix.

ACKNOWLEDGEMENTS

FCRH would like to express his gratitude to the University of Houston and the government of Texas for the start-up package funding. The authors would like to thank Drs. M. Umemoto and V. Garibay Febles for their outstanding support with mechanical alloying and spark plasma sintering methods. CONACYT and SIP-COFAA-IPN are acknowledged for financial support through grants 45887-Y, 28952U, 58133 (both authors), and SIP-20080337.

References

- P.J.F. Harris, *Carbon Nanotubes and Related Structures* (Cambridge; Cambridge University Press, 1999).
- H.W. Kroto et al., *Nature*, 318 (1985), p. 162.
- S. Iijima, *Nature*, 354 (1991), pp. 56–58.
- D. Ugarte, *Nature*, 359 (1992), pp. 707–709.
- H. Terrones and M. Terrones, *J. Phys. Chem. Solids*, 58 (1997), pp. 1789–1796.
- W. Krätschmer et al., *Nature*, 347 (1990), pp. 354–358.
- F.C. Robles Hernández (M.Sc. thesis, Instituto Politécnico Nacional, Mexico, 1999).
- V. Garibay-Febles et al., *Mater. and Manuf. Processes*, 15 (2000), p. 547.
- F. Adams and C. Vivès, *Netherlands Society for Materials Science*, 1 (1997), p. 337.
- D.M. Hulbert et al., *Mater. Sci. and Eng. A*, 488 (2008), pp. 333–338.

- J.S. Benjamin, *New Materials by Mechanical Alloying Techniques*, ed. E. Arzt and L. Schultz (Oberursel, Germany: DGM Informationgesellschaft, 1989), pp. 3–18.
- C. Suryanarayana, *Prog. in Mater. Sci.*, 46 (2001), pp. 1–184.
- M. Umemoto et al., *Mater. Sci. Forum*, 312-314 (1999), pp. 93–102.
- I. Wei Chen and X.H. Wang, *Nature*, 404 (2000), pp. 168–171.
- R.L. Coble, *J. Appl. Phys.*, 32 (1961), pp. 787–799.
- R.L. Coble and J.E. Burke, *Progress in Ceramic Science*, 3rd edition, ed. J.E. Burke (New York: Wiley-American Ceramic Society, 1963), pp. 197–251.
- R. Pérez-Bustamante et al., *Mater. Sci. and Eng. A*, 502 (2009), pp. 159–163.
- M. Oda et al., "Influence of Dispersed Carbon Nano-Fibers/Carbon Nano-Tubes in Al Matrix Composite" (Paper presented at the TMS 2009 Annual Meeting and Exhibition, San Francisco, CA, 15–19 February 2009).
- J. Guerrero-Paz et al., *Mater. Sci. Forum*, 360-362 (2001), pp. 317–322.
- T. Kuzumaki et al., *J. Mater. Res.*, 13 (1998), pp. 2445–2449.
- J.H. Hafner, *Chem. Phys. Lett.*, 296 (1998), pp. 195–202.
- H. Dai et al., *Chem. Phys. Lett.*, 260 (1996), p. 471.
- T. Gou et al., *Chem. Phys. Lett.*, 243 (1995), p. 49.
- W. Zhou et al., *Chem. Phys. Lett.*, 350 (2001), p. 6.

Francisco C. Robles-Hernández is assistant professor at the University of Houston, 304 Technology Building, Houston, TX 77057; H.A. Calderon, professor, is with the Departamento de Ciencia de Materiales, ESFM-IPN, Mexico DF 07738. Prof. Robles-Hernández can be reached at fcrbles@uh.edu, and Prof. Calderon can be reached at hcalder@esfm.ipn.mx.



**TMS KNOWLEDGE
RESOURCE CENTER**

Your Materials Books
and More e-Store!
<http://knowledge.tms.org>

Visit the Knowledge Resource Center to reserve your copy today!

Modeling of Casting, Welding, and Advanced Solidification Processes XII (MCWASP XII)

by Steve L. Cockcroft and Daan M. Maijer



These proceedings encapsulate the progress made in modeling casting processes and liquid-solid phase transformations over the years. The papers presented provide a clear picture of the modeling activities for processes involving solidification, covering continuous casting, welding, remelting, semi-solid, and shape and ingot casting processes. Other topics related to casting technologies, such as liquid metal treatment and casting tools (e.g., mold manufacturing and life time), are also examined. These proceedings bring together leading academic research that brings up to date information from the industry. Classical studies of structure and segregation formed upon solidification as well as new in-situ observation techniques are addressed.

A collection of papers from the 12th International Conference held in Vancouver, British Columbia June 7th-14th, 2009.

TMS Member price \$169; Non-member price \$244;
TMS Student Member price \$135

To order these or related publications, contact TMS:
E-mail publications@tms.org • Phone (724) 776-9000, ext. 256 • Fax (724) 776-3770

Bulk Metallic Glasses: Overcoming the Challenges to Widespread Applications

Peter K. Liaw, Gongyao Wang, and Judy Schneider

Since an amorphous solid was first synthesized by rapidly quenching with cooling rates up to 10^6 K/s,¹ the formation, structure, and property studies of metallic glasses have attracted increasing attention because of their fundamental scientific importance and engineering application potentials. New multicomponent glassy-alloy systems with lower critical cooling rates, such as Zr-Cu-Ni, Zr-Cu-Ni-Al, and Zr-Ti-Cu-Ni-Be were discovered in the 1990s.²⁻⁴ Now amorphous alloys can be fabricated into bulk forms ranging from several millimeters to several centimeters in thickness. Therefore, "bulk metallic glasses" (BMGs) is the name commonly used for these glassy metals. In addition, BMG composites were developed by introducing specific crystalline phases in an amorphous matrix to improve plasticity and toughness, which could broaden BMG applications.^{5,6}

In general, BMGs exhibit many desirable properties: high strength, high hardness, excellent elasticity, low coefficients of friction, near-net-shape casting, and almost perfect as-cast surfaces.⁴ As excellent candidates for structural materials, BMGs have been applied to new industrial products requiring high performance, such as microgears, casings for electronic products, and golf-club heads.⁴ To apply BMGs extensively, critical issues need to be solved.

First, BMGs usually lack ductility. The deformation and fracture behaviors of BMGs at room temperature are controlled by the initiation and propagation of shear bands, which result in the limited global deformation of about 2%, particularly under tensile deformations.⁷ It is important to understand the relationship between the ductility and atomic microstructure in BMGs.

Second, size effects in BMGs are interesting.⁹ The mechanical behaviors of metallic glasses during bending, compression, tensile, impact, and fatigue exhibit variations with the specimen geometry.^{10,11} Thus, the constraint of shear-band formation and deformation processes is critical to elucidate these phenomena. Third, understanding of the fatigue behavior of BMGs is limited.¹²⁻¹⁴ BMGs can exhibit a wide range of fatigue properties. Moreover, the characteristic for the formation of shear bands is unknown during cyclic deformation of metallic glasses, which raises additional questions: When and how will shear bands form? How does the fatigue crack initiate and propagate in metallic glasses? Another challenge is the fabrication of high-quality and large-size samples. Some good glass-forming alloys involve the use of elements that are either expensive or difficult to handle safely (such as beryllium³). However, with the development of alloys that are based on less expensive elements and more tolerant of impurities, the cost of BMGs will continue to decline relative to other high-performance alloys,⁴ and high-quality and large-size samples will become available. Finally, applications of BMGs are very few. Thus, how to find new applications for BMGs is pertinent for continued research activities of BMGs.

This *JOM* topic on BMGs presents discussions and developments related to the above questions. Due to the extent of the information available, four articles will be presented in this issue; another three will be published in April. The following papers are in this issue.

"Understanding the Properties and Structure of Metallic Glasses at the Atomic Level" by T. Egami reviews the behavior of glasses and liquids at

the atomic level and the microscopic mechanisms that control the properties of metallic glasses.

In "Mechanical Response of Metallic Glasses: Insights from In-situ High Energy X-ray Diffraction," Mihai Stoica et al. review the use of the synchrotron radiation to evaluate the elastic-plastic response of BMGs.

"Amorphous Metals for Hard-tissue Prosthesis" by Marios D. Demetriou et al. reviews the performance of amorphous alloys relevant to hard-tissue prosthesis.

"Metallic Glasses: Gaining Plasticity for Microsystems" by Yong Yang et al. summarizes the experimental findings related to size effects on plasticity in metallic glasses.

References

1. W. Klement, R. H. Willens, and P. Duwez, *Nature*, 187 (1960), p. 869.
2. A. Inoue, *Acta Mater.*, 48 (2000), p. 279.
3. A. Peker and W.L. Johnson, *Applied Physics Letters*, 63 (1993), p. 2342.
4. M.K. Miller and P.K. Liaw, editors, *Bulk Metallic Glasses* (New York: Springer, 2007).
5. D.C. Hofmann et al., *Nature*, 451 (2008), p. 1085.
6. J.W. Qiao et al., *Applied Physics Letters*, 94 (2009), 151905.
7. W.J. Wright, R. Saha, and W.D. Nix, *Mater. Trans.*, 42 (2001), p. 642.
8. J. Schroers and W.L. Johnson, *Phys. Rev. Lett.*, 93 (2004), 255506.
9. R.D. Conner et al., *Acta Materialia*, 52 (2004), p. 2429.
10. F.X. Liu et al., *Intermetallics*, 14 (2006), p. 1014.
11. H. Guo et al., *Nature Materials*, 6 (2007), p. 735.
12. C.J. Gilbert, V. Schroeder, and R.O. Ritchie, *Metallurgical and Materials Transactions A*, 30A (1999), p. 1739.
13. B.C. Menzel and R.H. Dauskardt, *Acta Mater.*, 54 (2006), p. 935.
14. G.Y. Wang et al., *Mater. Sci. and Eng.*, 494 (2008), p. 314.

Peter K. Liaw and Gongyao Wang are with the Department of Materials Science and Engineering, The University of Tennessee, Knoxville, TN 37996; and Judy Schneider is with the Mechanical Engineering Department, Mississippi State University, MS. Dr. Schneider is the *JOM* advisor from the Mechanical Behavior of Materials Committee of the TMS Structural Materials Division.

Understanding the Properties and Structure of Metallic Glasses at the Atomic Level

T. Egami

Liquids and glasses have been well known to human kind for millennia. And yet major mysteries remain in the behavior of glasses and liquids at the atomic level, and identifying the microscopic mechanisms that control the properties of glasses is one of the most challenging unsolved problems in physical sciences. For this reason, applying simplistic approaches to explain the behavior of metallic glasses can lead to serious errors. On the other hand because metallic glasses are atomic glasses with relatively simple structure, they may offer better opportunities to advance our fundamental understanding on the nature of the glass. The difficulties inherent to the problem and some recent advances are reviewed here.

INTRODUCTION

Elucidating the properties of materials in terms of the atomic, mesoscopic, and microscopic structure is one of the primary purposes of materials science. But if we try to proceed with such an effort for glasses and liquids we run into a major roadblock right away. Because glasses and liquids do not have the lattice periodicity it is not easy to characterize their structure and dynamics at the atomic level with sufficient accuracy. Consequently it is difficult to construct a realistic and meaningful model. In the absence of effective approaches many researchers resort to either computer simulations or phenomenological models such as the free-volume theory. However, both of these approaches suffer from severe drawbacks. In fact the nature of glass and glass transition is always listed among the most difficult unsolved problems in theoretical physics.^{1,2} Unfortunately the seriousness of the problem appears to be less than

How would you...

...describe the overall significance of this paper?

This paper provides a "big picture" of the science of metallic glasses at the atomic level. It points out that the structure and properties of metallic glasses are discussed often implicitly assuming a hard-sphere model, even though real atoms are far from hard-spheres. It then discusses serious problems associated with such an approach, and suggests a more balanced approach based on local structural fluctuations.

...describe this work to a materials science and engineering professional with no experience in your technical specialty?

Today the structure and properties of crystalline solids can be understood from the first-principles calculations with impressive accuracy. In comparison the science of glasses and liquids is in a much more primitive stage, because even describing the atomic structure accurately is a challenging task. However, because it is so challenging it is a very attractive field for creative and imaginative researchers. Unfortunately at present, simple, intuitive approaches are all too popular among the experimentalists in the field. This paper discusses the problems with such approaches and suggests alternative ways to make progress.

...describe this work to a layperson?

Major mysteries remain in the behavior of glasses and liquids at the atomic level. In general the science of non-crystalline materials, including macromolecules such as proteins, is less advanced than the science of crystalline materials. The main reason is that we have not developed effective theoretical methods to deal with extensively disordered systems with strong correlation. This paper discusses the pitfalls of simple and intuitive approaches, and suggests alternative approaches.

fully appreciated by the materials community. This article discusses why this problem is so difficult, and introduces alternative approaches that may hopefully lead to better understanding.

DIFFICULTIES

Computer Simulation

Today, first-principles calculations based upon quantum mechanics and the density functional theory (DFT) are so advanced that many properties of crystalline materials are well understood at a most fundamental level, and it is even possible to design new materials using theoretical calculations.³ When the DFT calculation is combined with the molecular dynamics (MD) technique it is possible to study liquids. However, there is a major problem of time-scale when the first-principles MD method is applied to supercooled liquid or glasses. As is widely known, MD simulation uses finite time steps to describe the temporal evolution. Because the typical frequency of atomic vibration in solids and liquids is 10^{12-13} 1/sec, to faithfully describe such dynamics the time step has to be of the order of a femto-second (10^{-15} sec). So even when one runs the MD simulation for a million steps, the time scale is only a nano-second (10^{-9} sec). On the other hand the glass transition is defined by the viscosity becoming 10^{13} poise, which corresponds to the time scale of 10^3 seconds. Thus we have a gap in the time scale by a factor of 10^{12} . Even when we use the model interatomic potential instead of the first-principles calculation, the gap in the time scale can be improved only by two orders of magnitude or so, leaving a gap of 10^{10} .

The consequence of this huge gap in time scale is that the models created by MD simulation, either by the first-

Table I. Factors that Indicate the Hardness of the Potential, for the Hard-sphere (HS) Potential, the Lennard-Jones (L-J) Potential, and the Johnson Potential (see text for definitions)

	γ	R	R'
HS	—	—	0
L-J	2.5	36	0.109
Johnson	0.874	27.8	0.153

principles calculation or with model potentials, are seriously under-relaxed because they are effectively quenched with extremely high cooling rates from high temperatures. Thus the short-range order in the model reflects that of a high-temperature liquid, not necessarily that of a glass. The glass transition observed by simulation corresponds to viscosity reaching only 10^2 to 10^3 poise rather than 10^{13} poise. Consequently the glass transition temperature determined by MD simulation is considerably higher than the real glass transition temperature. We still can learn from such simulations, but we should remember to use many grains of salt in interpreting such results. It is simply naïve to believe that the MD models describe the true state of the glasses.

Free-volume Theory

Another approach frequently adopted by researchers in the field of metallic glasses is the free-volume theory.⁴⁻⁶ One of the great mysteries of glasses and liquids is that viscosity changes as much as 15 orders of magnitude over a relatively small temperature range just above the glass transition temperature, T_g . The free-volume theory explains this mystery beautifully, by assuming that the excess free-volume in the liquid increases linearly with temperature above T_g . However the free-volume theory itself does not explain why the free-volume increases linearly with temperature. It is a phenomenological theory based upon the experimental observations.

Another, more serious problem for the metallic glass community is that the free-volume theory in its original form does not work well for metals. This is clearly stated in the original paper by Cohen and Turnbull.⁴ However, unfortunately many young researchers today apparently do not read such an old

paper, even though they may use this model. The most important parameter in the free-volume theory is the ratio of the critical value of the free-volume to accept an atom, v^* , to the atomic volume, v_a , v^*/v_a . This value is about 0.8 for van der Waals liquids, and the theory assumes this value to be close to unity. For metallic liquids this value is much less than unity, and is close to 0.1 (see Table II of Reference 4).

The validity of the free-volume concept is obvious for systems of hard-spheres (HS). For a hard sphere to move in a close-packed structure there must be extra space between the spheres, otherwise they are trapped in the cage made by neighbors and cannot move. The Lennard-Jones (L-J) potential that describes van der Waals solids is a hard potential as discussed below. For this reason the free-volume theory is successful for organic molecular liquids and glasses for which the intermolecular interaction can be modeled well by the L-J potential.

However, if atoms are soft and squeezable they may be able to move without free space, simply by squeezing in. Thus the relevance of the free-volume concept is less obvious for systems with softer interatomic potentials, such as metals. That metals are far from the HS systems can be clearly demonstrated by the density change upon melting. The volume fraction occupied by spheres in the dense-random-

Table II. Ratio of the Heat Released (ΔH) over the Change in Volume (ΔV) during Structural Relaxation

	$\Delta H/\Delta V$ (eV/Å)	$\Delta H/\Delta V$ (eV/atom)	Ref.
Zr ₅₅ Cu ₃₀ Al ₁₀ Ni ₅	0.416	7.61	22
Zr ₄₄ Ti ₁₁ Cu ₁₀ Ni ₁₀ Be ₂₅	0.461	7.70	23
Pt ₆₀ Ni ₁₅ P ₂₅	0.460	8.48	24

packed (DRP) HS system is $\rho_{DRP-HS} = 0.63$.⁷ On the other hand the volume density of the crystalline close packed system, face-centered cubic (f.c.c.) or hexagonal close packed (h.c.p.) is $\rho_{CP} = 0.74$. Thus the volume of the HS system increases by as much as 17% at melting. Indeed the volume expansion at melting is about 15% for argon that can be described well by the L-J potential. However, as shown in Figure 1 the volume expansion upon melting, $\Delta V/V$, is much smaller for metals and semimetals, ranging from 0 to 6%, with some of them being negative.⁸ The density of metallic liquids is much higher than $\rho_{DRP-HS} = 0.63$, because atoms can be closer than the average distance that defines the atomic size. For instance the density of the DRP model with the Johnson potential for iron⁹ is 0.74, virtually identical to ρ_{CP} .¹⁰ These results show that the HS model is unrealistic for metals.

Hardness of the Potential

In order to make this point even clearer let us discuss how to evaluate the hardness of the interatomic potential. Any pair-wise interatomic potential $V(r)$ can be expanded around the potential minimum at $r = r_0$ (see Equation 1 in the table).

For most of the potentials $A > 0$, $B < 0$. Hardness of the potential may be described by the ratio, $-B/A$. This ratio is related to the Grüneisen constant of anharmonicity, as given in Equation 2, where ν is the phonon frequency, which is proportional to \sqrt{A} .¹¹ When the value of γ is high the potential is strongly asymmetric at the bottom of the potential, and repulsion is much stronger than attraction. The value of γ for the HS potential is infinite. The values of γ for the L-J potential and the Johnson potential are shown in Table I. Another indicator of the hardness of the poten-

Equations

$$V(r) = V(r_0) + A \left(\frac{r}{r_0} - 1 \right)^2 + B \left(\frac{r}{r_0} - 1 \right)^3 + \dots \quad (1)$$

$$\gamma = - \frac{\partial \ln \nu}{\partial \ln V} = - \frac{B}{2A} \quad (2)$$

$$\sigma^{\alpha\beta}(i) = \frac{1}{\Omega_i} \sum_j f_{ij}^{\alpha} r_{ij}^{\beta} \quad (3)$$

$$\sigma^{\alpha\beta}(i) = \frac{2A}{\Omega_i} \sum_j \left(\frac{r_{ij}}{r_0} - 1 \right) r_{ij}^{\alpha} r_{ij}^{\beta} \quad (4)$$

$$E_p = \frac{\langle p^2 \rangle}{2B} = \frac{kT}{4} \quad (5)$$

$$kT_g = \frac{2\langle B \rangle \langle V \rangle}{K_\alpha} (\epsilon_v^T)^2, \quad K_\alpha = \frac{3(1-\nu)}{2(1-2\nu)} \quad (6)$$

tial is the curvature to the depth ratio, $R = A/V(r_0)$, and the ratio between the distance at which the potential crosses over zero, $V(r_c) = 0$ and r_0 , relative to unity, $R' = 1 - r_c/r_0$. These two factors are closely related. When R is large or R' is small the potential energy quickly rises as r decreases below r_0 , so that the atom cannot be squeezed much. These values for the HS potential, the L-J potential and the Johnson potential are also shown in Table I.

Now the depth of the potential is related to the cohesive energy and the boiling temperature T_b , and the curvature A is related to the phonon frequency and the melting temperature, T_m . Therefore the parameter $R2$ is related to the ratio of T_m/T_b . As shown in Figure 2, this ratio is close to unity for van der Waals systems such as radon (other rare gases do not show melting under 1 atm.), but much lower for metals and semimetals, ranging from 0.3 to 0.6.¹² These results again show that van der Waals liquids and solids are more difficult to squeeze and behave like hard-spheres, whereas metals are unlike hard-spheres and are much more squeezable and harmonic.

Experimental Evidence against the Simple Free-volume Concept

One of the examples of experimental data Cohen and Turnbull used in cautioning against the use of the free-volume theory for metals is the observation by Nachtrieb and Petit¹³ that the pressure dependence of diffusivity is much less than expected for the free-volume theory. Because pressure would squeeze out free-volume and make the atomic motion more restrict-

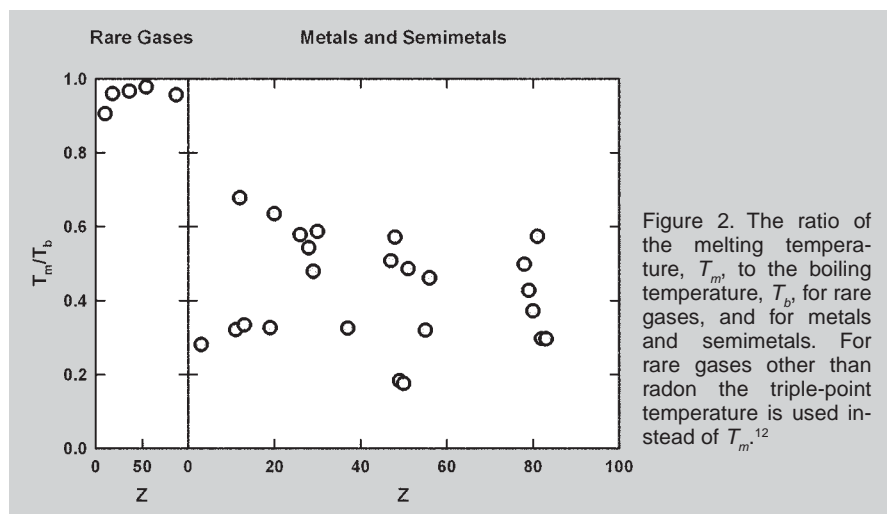


Figure 2. The ratio of the melting temperature, T_m , to the boiling temperature, T_b , for rare gases, and for metals and semimetals. For rare gases other than radon the triple-point temperature is used instead of T_m .¹²

ed it should exert a major effect on diffusivity, whereas the observed effect is much less dramatic.¹⁴ A more recent measurement by Klugkist et al.¹⁵ underscores this point. This, again, is because the free-volume in metals is much smaller than atoms.

When the metallic glass is annealed at a temperature below T_g the structure relaxes toward a more stable state. This phenomenon is commonly observed in all kinds of glasses, and is known as structural relaxation.¹⁶ It is possible to observe what is happening to the structure by diffraction measurement.¹⁷ Figure 3 shows recent data on the change in the x-ray atomic pair-density function (PDF).¹⁸ It is clear that both long and short bonds are eliminated as a result of relaxation. Because the interatomic potentials of metals are more harmonic, when the structure is rapidly cooled some bonds remain too short or too long, and these bonds are relaxed out by annealing. Long bonds may

characterize “free-volume,” or negative (n -type) density fluctuations, but then short bonds could describe “anti-free-volume,” or positive (p -type) density fluctuations, regions of high density, as shown in Figure 4.^{19–21} Recombination of these two types of local density fluctuations can explain the structural relaxation.

During the structural relaxation heat is released as the structure relaxes to a more stable state. The amount of heat released, ΔH , and the volume change, ΔV , during the relaxation were measured by various researchers.^{22–24} The values of $E_a = \Delta H/\Delta V$ are shown in Table II, in the units of eV/Å³, and eV/atom. Usually the vacancy formation energy is about 2 eV/atom, but the values shown here are significantly larger, by a factor of four. The value of E_a should also be comparable to the activation enthalpy for diffusion, which is also 2–3 eV.¹⁴ This disagreement can be resolved if we assume that during the structural relaxation not only free-volumes (n -type defects) are eliminated, decreasing the volume, but also “anti-free-volumes” (p -type defects) are eliminated, increasing the volume. Thus the total change in volume represents the small difference after cancellation of the bulk of the positive and negative changes.^{20,24} Thus the use of the total volume change in evaluating $\Delta H/\Delta V$ results in overestimate.

Another very interesting observation is that irradiating a metallic glass with high energy particles does not seem to result in void formation easily.^{25,26} It is well known that irradiating crystalline materials with electrons

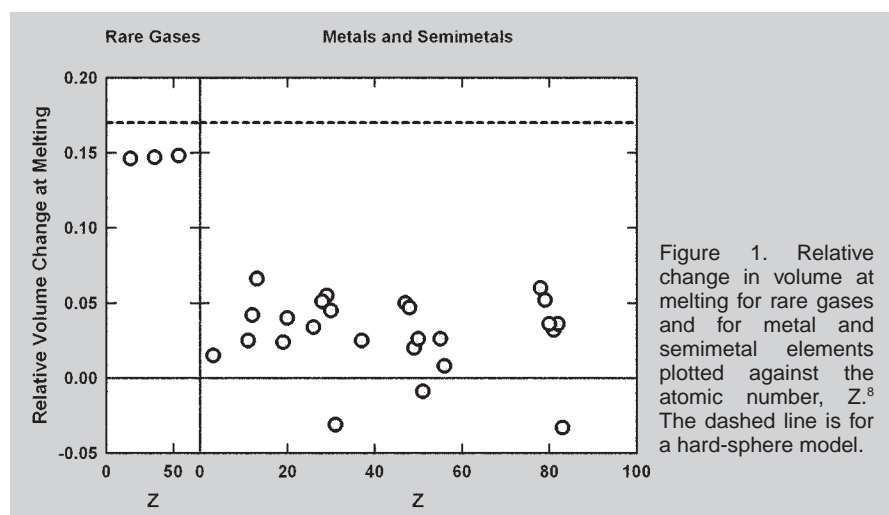


Figure 1. Relative change in volume at melting for rare gases and for metal and semimetal elements plotted against the atomic number, Z .⁸ The dashed line is for a hard-sphere model.

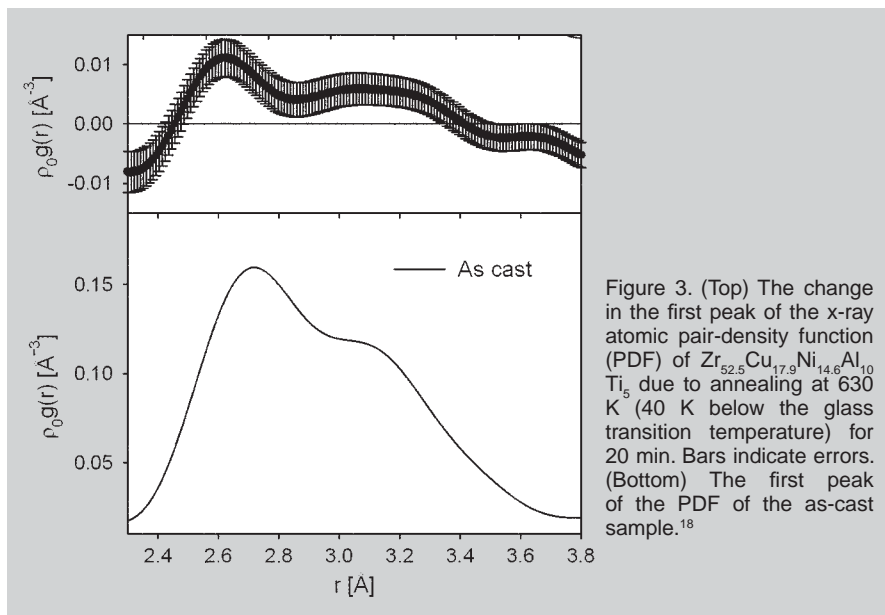


Figure 3. (Top) The change in the first peak of the x-ray atomic pair-density function (PDF) of $Zr_{52.5}Cu_{17.9}Ni_{14.6}Al_{10}Ti_5$ due to annealing at 630 K (40 K below the glass transition temperature) for 20 min. Bars indicate errors. (Bottom) The first peak of the PDF of the as-cast sample.¹⁸

or neutrons produces voids and leads to swelling. If the defects in metallic glasses were free-volumes that are similar to vacancies, after irradiation they may accumulate and coagulate as voids. Apparently that is not the case. Irradiation may produce both positive and negative local density fluctuations, but they will soon recombine without leaving much trace. For this reason metallic glasses are likely to be quite radiation resistant.

These results demonstrate that in metals the critical value of free-volume, v^* , is much smaller than the atomic volume, and free-volumes are accompanied by their mirror state, anti-free-volumes. A more balanced description of the state of liquids and glasses requires both negative as well as positive local density fluctuations.

ALTERNATIVE APPROACHES

Jamming Theory

In spite of the problems with using the HS models for metals, the HS potential has many attractive features. It is the simplest potential, with only one parameter. Because there is no energy scale in this potential, all the problems are reduced to those of geometry and mathematics rather than physics. Thus definite answers for various well-defined problems can be obtained, and these answers can serve as the yardstick for real materials, even though the HS potential may not be realistic for many

materials. Furthermore, it is the right potential for granular materials, such as sands. For these reasons the models with the HS potential have been studied extensively.

A notable recent achievement is the development of the jamming theory, which is closely related to the free-volume theory. At low densities the system of hard spheres are fluid, but fluidity is reduced as the density is reduced and free-volume is removed from the system. At a critical density the system becomes jammed, as hard spheres are interlocked with each other, just as in the traffic jam caused by gridlock. As noted above the density of the HS-DRP system is $\rho_{DRP} = 0.63$. Jamming occurs, however, already at a slightly lower density of $\rho_j = 0.53$,²⁷ because the movement of spheres becomes very much restricted even before the system

is completely frozen. We now have a better understanding of the behavior of the system in the vicinity of this critical density, for instance in terms of various scaling laws.^{28,29} Thus the properties of the system can now be semi-quantitatively predicted.

Theories of Local Density Fluctuation

However, the HS system is a very artificial model, and is pathological in many ways. First, because there is no attraction, the system has to be kept together by an external pressure, or the boundary condition. Its potential energy is indeterminate because during the collision of hard spheres the infinite potential is experienced for zero time. Thus we cannot even talk about the virial theorem. As is well known the lattice dynamics of crystalline solids is very well described in terms of phonons. But in the HS solids there are no phonons unless the system is slightly expanded, and even in such a case phonons are strongly attenuated and do not propagate well. We have already discussed how poor this model is to describe the metallic systems realistically. Perhaps the HS model is too far away from the reality of the metallic systems, and to use this model as a starting point to develop the theory of metallic glasses may be ill-advised after all. There may be a better way to start the effort.

The lattice dynamics theory of a solid starts with the harmonic approximation.³⁰ Then it should be possible to start the theory of liquids in a similar way. For instance, in the HS system the

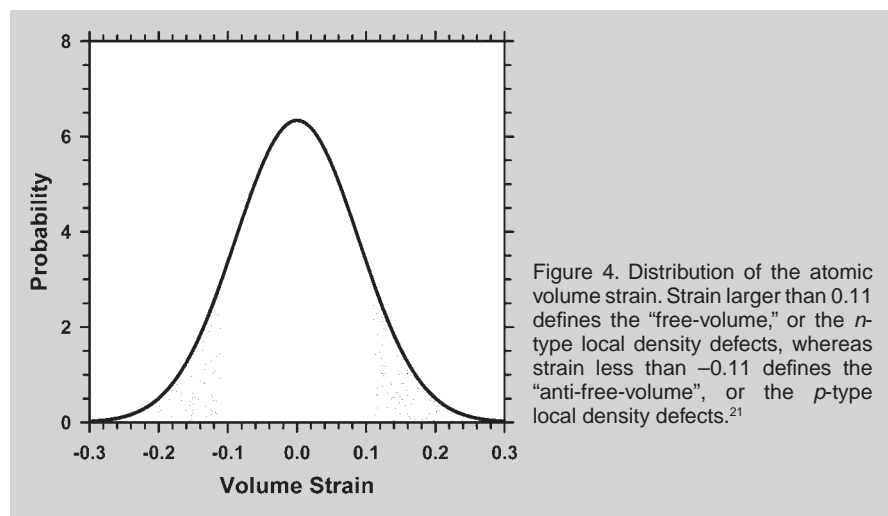
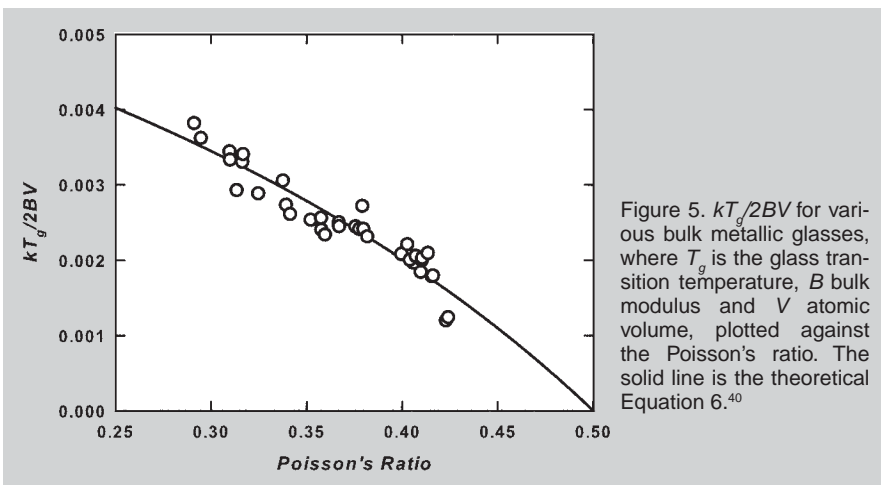


Figure 4. Distribution of the atomic volume strain. Strain larger than 0.11 defines the "free-volume," or the n -type local density defects, whereas strain less than -0.11 defines the "anti-free-volume", or the p -type local density defects.²¹



local volume cannot be contracted, but can only be expanded. In an harmonic system, however, the local volume can be contracted or expanded at the equal cost in energy. Thus the local density fluctuations are equally negative and positive. Then the local density fluctuation may be a good starting point for the theory of liquids. Indeed a large body of literature on hydrodynamic theories exists that starts with the local density fluctuations, both negative and positive.³¹ The mode-coupling theory^{32,33} was developed by extending the linear hydrodynamic theory by introducing non-linear coupling. It has been quite successful in describing the dynamic behavior of liquids from high temperature down to the supercooled liquid region. However, it is questionable if it can be extended down to the temperature range for the glassy state.³⁴

Theory of Atomic Level Stresses

In the local density fluctuation theories liquids are regarded as a continuum body with locally varying density, and atomic discreteness does not enter the theory directly. It is only obliquely reflected in the non-linear coupling of density-density correlations.³³ On the other hand the concept of the atomic-level stress was introduced in order to describe the atomic environment realistically.³⁵ The starting point is the realization that in liquids and glasses the atoms are not ideally packed as in the closed packed structures, and consequently the atomic environment of each atom is severely distorted. This is similar to the situation in human society. We do not live in an ideal world. The aspiration and desire of each indi-

vidual is too often not consistent with reality, which results in mental stresses. Stresses can either destroy a weak person or let a strong person grow, but in turn, we may be able to characterize the society by the level of the stress. In a similar way the structure of a glass or a liquid may be characterized by the atomic level stresses.

At the atomic level the stress can be defined by Equation 3,³⁵ where α and β are Cartesian coordinates, f_{ij}^α is the α component of the two-body force between atoms i and j , and r_{ij}^β is the β component of the distance vector between atoms i and j . In a system of atoms interacting by a pair-wise harmonic potential ($B = 0$ in Equation 1), the force is proportional to the deviation from the ideal distance, r_0 . Then, from Equation 1 we can derive Equation 4. Thus the atomic level stress describes the distortion of the environment of each atom away from the ideal state, where all neighbors are at $r_{ij} = r_0$, which never occurs in reality. The stress is a 3×3 tensor, with six independent components. The trace corresponds to the pressure, p , whereas the deviatoric components describe the five components of shear stresses.³⁵

This theory was initially introduced for the purpose of defining the elusive defects in the glassy structure, but it was found to have much wider utility. It was successfully used in calculating the composition limit of glass formation in binary glasses.³⁶ It was also found that the elastic self-energy of the pressure is proportional to temperature at high temperatures, see Equation 5, where B is the bulk modulus, and other five shear components also follow the same

virial, or equipartition, theorem.^{37,38} This relationship thus forms the basis for the statistical mechanical theory of liquids.

Equation 5 extrapolates to zero at $T = 0$. However, such a state, the ideal state, cannot be achieved, because the system becomes jammed and immobile at some temperature where $\langle p^2 \rangle$ becomes small enough. The minimum value of the volume strain, $\epsilon_v = p/B$, was found to be ± 0.06 for homogeneous strain and ± 0.11 for local strain (Figure 4), from the topological instability condition.^{21,40} The derivation of these critical values is too lengthy for this article, and the readers are referred to References 21, 39, and 40. From this condition Equation 6 describes the glass transition temperature, where v is Poisson's ratio, was deduced. This equation fits the experimental data with impressive accuracy as shown in Figure 5.⁴⁰ This is probably the first time that the glass transition temperature was calculated from the first principles virtually without a fitting parameter. Currently the theory is being extended to account for the mechanical deformation and the effects of stresses on the flow properties in terms of the intrinsic local fluctuations in shear stresses, rather than defects.

CONCLUSION

Although the science of crystals is at a very advanced stage, the science of glasses and liquids is still languishing at the level of infancy. The primary reason for this is the lack of effective methods of describing the structure and dynamics at the atomic level. Many researchers working on metallic glasses still describe the structure-property relationship only in terms of free-volumes, even though the creators of the theory cautioned against using this concept for metallic liquids without due modifications. In metallic systems the critical value of free-volume is much smaller in volume than atoms, and is only about 10% of the atomic volume. The state of a metallic glass is better described in terms of local density fluctuations, not only negative fluctuations (free-volume), but also positive fluctuations (anti-free-volume). In addition the local shear distortion plays a major role, for instance, in deformation. It is

about time for us to evolve gradually out of indiscriminate use of the free-volume concept, and develop more realistic and accurate microscopic and atomistic description of metallic glasses based on local structural fluctuations.

ACKNOWLEDGEMENT

The author is grateful to his collaborators for valuable input, T. Nagase in particular for his comments and information regarding radiation damage in metallic glasses. This work has been sponsored by the Division of Materials Sciences and Engineering, Office of Basic Energy Sciences, U.S. Department of Energy.

References

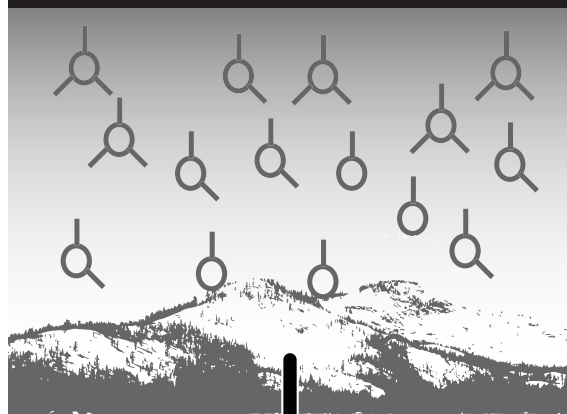
1. P.W. Anderson, *Science*, 267 (1995), p. 1615.
2. J.S. Langer, *Physics Today* (February 2007), pp. 8–9.
3. For example, R.M. Martin, *Electronic Structure: Basic Theory and Practical Methods* (Cambridge, U.K.: Cambridge University Press, 2004).
4. M.H. Cohen and D. Turnbull, *J. Chem. Phys.*, 31 (1959), pp. 1164–1169.
5. D. Turnbull and M.H. Cohen, *J. Chem. Phys.*, 34 (1961), pp. 120–125.
6. D. Turnbull and M.H. Cohen, *J. Chem. Phys.*, 52 (1970), pp. 3038–3041.
7. J.D. Bernal and J. Mason, *Nature*, 188 (1960), pp.

- 910–911.
8. D. Wallace, *Proc.: Math. Phys. Sci.*, 433 (1991), pp. 631–661.
9. A.R. Johnson, *Phys. Rev.*, 134 (1964), pp. A1329–1336.
10. K. Maeda and S. Takeuchi, *J. Phys. F: Met. Phys.*, 8 (1978), pp. L283–L288.
11. For example, L. A. Girifalco, *Statistical Physics of Materials* (New York: John Wiley & Sons, 1973).
12. D.R. Lide and W.M. Haynes, editors, *CRC Handbook of Chemistry and Physics*, 90th Edition (Oxford, U.K.: Taylor and Francis, 2009).
13. N.H. Nachtrieb and J. Petit, *J. Chem. Phys.*, 24 (1956), pp. 746–750.
14. F. Faupel et al., *Rev. Mod. Phys.*, 75 (2003), pp. 237–280.
15. P. Klugkist et al., *Phys. Rev. Lett.*, 80 (1998), pp. 3288–3291.
16. T. Egami, *Ann. N.Y. Acad. Sci.*, 37 (1981), pp. 238–251.
17. T. Egami, *J. Mat. Sci.*, 13 (1978), pp. 2587–2599.
18. W. Dmowski et al., *Mater. Sci. Eng. A*, 471 (2007), pp. 125–129.
19. D. Srolovitz, T. Egami, and V. Vitek, *Phys. Rev. B*, 24 (1981), pp. 6936–6944.
20. T. Egami et al., *J. de Phys.*, 41 (1980), pp. C8-272–274.
21. T. Egami, *Bulk Metallic Glasses*, ed. M. Miller and P. Liaw (Berlin: Springer-Verlag, 2008), pp. 27–56.
22. A. Slipenyuk and J. Eckert, *Scripta Mater.*, 50 (2004), pp. 39–44.
23. M.E. Launey et al., *Appl. Phys. Lett.*, 91 (2007), 051913.
24. M. Kohda et al., unpublished.
25. Y. Petrusenko et al., *Intermetallics*, 17 (2009), pp. 246–248.
26. T. Nagase, private communication.
27. For example, R.S. Farr, J.R. Melrose, and R.C.

- Ball, *Phys. Rev. E*, 55 (1997), pp. 7203–7211.
28. C.S. O'Hern et al., *Phys. Rev. Lett.*, 86 (2000), pp. 111–114.
29. P. Olsson and S. Teitel, *Phys. Rev. Lett.*, 99 (2007), 178001.
30. M. Born and K. Huang, *Dynamical Theory of Crystal Lattices* (Oxford: Clarendon Press, 1954).
31. For example, J.P. Hansen and J.R. McDonald, *Theory of Simple Liquids* (London: Academic Press, 1986).
32. S.P. Das, *Rev. Mod. Phys.*, 76 (2004), pp. 785–851.
33. W. Götzke, *Complex Dynamics of Glass-Forming Liquids: A Mode-Coupling Theory* (Oxford: Oxford University Press, 2009).
34. For example, V.N. Novikov and A.P. Sokolov, *Phys. Rev. E*, 67 (2003), 031507.
35. T. Egami, K. Maeda, and V. Vitek, *Phil. Mag. A*, 41 (1980), pp. 883–901.
36. T. Egami and Y. Waseda, *J. Non-Cryst. Solids*, 64 (1984), pp. 113–134.
37. S.-P. Chen, T. Egami and V. Vitek, *Phys. Rev. B*, 37 (1988), pp. 2440–2449.
38. V.A. Levashov et al., *Phys. Rev. B*, 78 (2008), 064205.
39. T. Egami, *Mater. Sci. Eng.*, A226-228 (1997), pp. 261–267.
40. T. Egami et al., *Phys. Rev. B*, 76 (2007), 024203.

T. Egami, University of Tennessee-Oak Ridge National Laboratory distinguished scientist and professor, is with the Joint Institute for Neutron Sciences, Department of Materials Science and Engineering, and Department of Physics and Astronomy, University of Tennessee, Knoxville, TN 37996, and Oak Ridge National Laboratory, Oak Ridge, TN 37831. Prof. Egami can be reached at egami@utk.edu.

**For the latest advances in all aspects of MOVPE Technology...
It's where you belong...**



**ICMOVPE
XV**

**15th International Conference
on Metal Organic
Vapor Phase Epitaxy**

**May 23 – 28, 2010
Hyatt Regency Lake Tahoe
Incline Village, Nevada, USA**

**Registration is
Now Available!**

<http://www.tms.org/Meetings/Specialty/icmovpe-xv/home.aspx>



Mechanical Response of Metallic Glasses: Insights from In-situ High Energy X-ray Diffraction

Mihai Stoica, Jayanta Das, Jozef Bednarčík, Gang Wang, Gavin Vaughan, Wei Hua Wang, Jürgen Eckert

The term “metallic glass” usually refers to a metallic alloy rapidly quenched in order to “freeze” its structure from the liquid state. A metallic glass is a metastable alloy, which lacks the symmetry typical for crystalline materials and at room temperature shows an amorphous liquid-like structure. Bulk metallic glasses (BMGs) represent a class of amorphous alloys. The most notable property of BMGs is their ultrahigh (near theoretical) strength and hardness. Because the known BMGs usually miss tensile plasticity and thus exhibit catastrophic failure upon tension it is important to understand deformation mechanisms involved and thus improve their performance. This article analyzes the use of synchrotron radiation for evaluating the elastic-plastic response of such materials.

INTRODUCTION

Due to the lack of crystalline structure, bulk metallic glasses (BMGs) may achieve interesting properties, including high strength and high hardness, excellent corrosion resistance, high wear resistance, very good soft magnetic properties, and, depending on composition, biocompatibility.^{1,2} The high strength of BMGs is sometimes accompanied by plastic deformation and their deformation and fracture mechanisms are quite different from crystalline materials.³⁻⁷ Bulk metallic glasses have strengths approaching the theoretical limit,⁸ but their plasticity at room temperature is typically very low. In uniaxial tension, the plastic strain is almost zero.⁹ For most of the known BMGs, plastic strain at room temperature is limited, less than 2%, even under compression, resulting from pronounced shear localization and work softening. The lack of plasticity makes BMGs prone to catastrophic failure in

load-bearing conditions and restricts their application. This also hinders the precise study of some fundamental issues in glasses, such as the deformation mechanism and the dynamics of plastic deformation, in which large plasticity is needed for detailed analysis.⁹ Plastic deformation of metallic glasses at room temperature occurs through the formation and evolution of shear bands and is localized in thin shear bands.¹⁰ Therefore, brittleness is regarded as an intrinsic defect of metallic glasses.

Many methods have been developed and employed to rule out the de-

formation mechanisms characteristic to BMGs.¹¹ Recently, characterization of amorphous materials by diffraction methods for the purpose of strain scanning was established.¹² Several glasses were investigated since then, using different synchrotron sources: HASYLAB at Deutsches Elektronen-Synchrotron (DESY) Hamburg, Germany; European Synchrotron Radiation Facilities (ESRF) Grenoble, France; or Advanced Photon Source (APS) at Argonne National Laboratory, USA. Monochromatic hard x-rays with energies at 80–100 keV were used for these experiments.

Ex-situ compression tests are usually performed to study the mechanical behavior of BMGs. This method is relatively simple and suitable for small samples. Tensile tests have technical limitations. First, for such tests a dog-bone shaped plate or rod sample is necessary, with a length of a few centimeters. This requires a BMG sample with quite large geometrical dimensions, which cannot be achieved by a poor glass former. The sample should be homogeneous, but in practice some small voids (as pores or oxides inclusions) may be present upon casting. Another limitation comes from the device used for tests—it is quite difficult to create a proper clamping system. Due to the difference in hardness between BMGs and the hardened steel used for tools, the BMG sample tends to slide from the grips.

See the sidebar for experimental details.

DATA TREATMENT AND THEORETICAL BACKGROUND

The elastic scattering intensity $I(Q)$ is measured as a function of the scattering vector (or wave vector) Q , which is defined as $4\pi \sin \theta / \lambda$, where θ is half of

How would you...

...describe the overall significance of this paper?

This article analyzes the use of the synchrotron radiation for evaluating the elastic-plastic response of bulk metallic glasses (BMGs). BMGs are a new class of materials and their properties make them very attractive for applications. Here we show some results obtained upon in-situ x-ray diffraction using synchrotron beam.

...describe this work to a materials science and engineering professional with no experience in your technical specialty?

Due to the absence of a crystalline network, the BMGs may achieve high strength and elasticity, together with good wear and corrosion resistance. It is of great importance to understand deformation mechanisms involved and thus to improve their performance. Time resolved in-situ x-ray diffraction experiments may give crucial insights about the mechanical behavior up to atomic level.

...describe this work to a layperson?

Bulk metallic glasses, novel materials with amorphous structure, have outstanding mechanical properties. The emergence of such properties can be studied by analyzing the x-ray diffraction patterns upon in-situ experiments.

the scattering angle (see Figure B) and λ the wave length of the radiation. The structure factor can be written as:

$$S(Q) = \frac{I(Q)}{N \langle f(Q) \rangle^2} \quad (1)$$

where N is the number of atoms, $f(Q)$ is the atomic scattering factor for x-rays, and the angular brackets indicate averaging over the composition of the material.¹⁸ The real-space structural information available from $S(Q)$ is the pair distribution function $g(r)$, (PDF), in which r is the distance from an average atom located at the origin. Without entering too much in details—the entire mathematic background can be found in several other works^{12–18}—one should mention that the pair distribution function is related to $S(Q)$ by a Fourier transform. It is also common to write the real-space structural information in terms of the radial distribution function (RDF), which is defined as $4 \pi r^2 g(r)$. With this definition, the coordination number of a particular atomic shell of interest can be obtained by integrating the RDF over a suitably chosen range of r .

When an amorphous material is subjected to forces that create a macroscopic stress, both $S(Q)$ and $g(r)$ will be affected. For uniaxial loading, the changes in real space can be easy to anticipate. The tensile stress will tend to move atoms apart in the loading direction, and thus a peak in $g(r)$ for that direction will move to larger values of r . For a compressive stress, the opposite should happen. In the reciprocal space, Q , it is expected to shift toward lower values in the case of tensile stress and higher values when the sample is compressed. By analogy with the simple definition of engineering strain, the tensile strain for an applied stress σ can be defined as:

$$\varepsilon_i(\phi, \sigma) = \frac{Q(\phi, 0) - Q(\phi, \sigma)}{Q(\phi, \sigma)} \quad (2)$$

which is angular dependent. In the transverse direction, one expects a strain of the opposite sign due to the Poisson effect. A typical diffraction image of an amorphous sample is illustrated in Figure 1a. The amorphicity is proved by the absence of any clear ring. Then the image is integrated upon the polar coordinates (s, ϕ). The integration is done by dividing the entire circle into 36 sections of 10° each. The data were inte-

grated with the help of the FIT2D software¹⁹ and after integration the intensity curves were corrected for background, polarization, and inelastic Compton scattering. A typical diffraction pattern after integrating the diffraction image is presented in Figure 1b. The diffracted

intensity I as a function of wave vector Q can then be transformed into the structure factor $S(Q)$. The index i in Equation 2 takes the discrete values from 1 to 18 (due to the 36 section used for integration). Once the tensile load is applied, the round concentric halos from Figure

EXPERIMENTAL SET-UP AND MEASURED BMGs

The requirements for in-situ tensile tests under synchrotron radiation are: proper sample, proper testing device, access at the hard x-ray source, and proper geometric set-up. In our case, the samples used for testing were cast as amorphous plates which further were machined by the spark erosion method in order to obtain a dog-bone shaped specimen with $10 \text{ mm} \times 2 \times 1 \text{ mm}^2$ reduced section (Figure A). The dog-bone shaped specimen was strained using a tensile module from Kammrath and Weiss GmbH, which can achieve a maximum load of 5 kN. The room temperature in-situ x-ray diffraction experiments were performed on the wiggler beamline BW5 at the DORIS positron storage ring (HASYLAB at DESY, Hamburg, Germany) using monochromatic synchrotron radiation of 103.8 keV ($\lambda = 0.0119 \text{ nm}$). The layout of the experimental setup is shown in Figure B. The measured samples were exposed for 10 s to the well collimated incident beam having a cross section of $1 \times 1 \text{ mm}^2$. Two dimensional (2-D) ($2,300 \times 2,300$ pixels, $150 \times 150 \mu\text{m}^2$ pixel size) x-ray diffraction (XRD) patterns were collected using a MAR 345 2-D image plate detector carefully mounted orthogonally to the x-ray beam. The diffraction pattern from LaB_6 was used to calibrate the sample-to-detector distance D and tilting of the image plate detector with respect to the beam axis.

The BMGs studied using this set-up were of the composition $\text{Zr}_{64.13}\text{Cu}_{15.75}\text{Ni}_{10.12}\text{Al}_{10}$.^{13,14} At the same location, BW5 beamline, and with the same geometrical set-up, Wang et al.¹⁵ measured $\text{Zr}_{62}\text{Al}_8\text{Ni}_{13}\text{Cu}_{17}$ and $\text{La}_{62}\text{Al}_{14}(\text{Cu}_{5/6}\text{Ag}_{1/6})_{14}\text{Co}_5\text{Ni}_5$ BMGs using x-ray radiation with $\lambda = 0.012389 \text{ nm}$. In-situ tensile tests at BW5 were also reported by Mattern et al.¹⁶ Their samples were amorphous ribbons with the compositions $\text{Cu}_{50}\text{Zr}_{50}$ and $\text{Cu}_{65}\text{Zr}_{35}$ and the radiation had $\lambda = 0.01265 \text{ nm}$. Prior to these experiments, few others were performed in compression. At ESRF Grenoble, Poulsen et al.¹² investigated the $\text{Mg}_{60}\text{Cu}_{30}\text{Y}_{10}$ BMGs and Das et al.¹⁷ $\text{Cu}_{47.5}\text{Zr}_{47.5}\text{Al}_5$ and $\text{Zr}_{35}\text{Cu}_{20}\text{Ni}_{10}\text{Al}_{10}\text{Ti}_5$ BMGs. The wave length of the radiation used for these experiments was $\lambda = 0.01412 \text{ nm}$ for Mg-based glasses and $\lambda = 0.0155 \text{ nm}$ for Zr-based glasses. Other BMGs, $\text{Zr}_{57}\text{Ti}_5\text{Cu}_{20}\text{Ni}_8\text{Al}_{10}$, were tested in uniaxial compressive load using a 0.0154 nm radiation at Advanced Photon Source at Argonne National Laboratory by Hufnagel, Ott, and Almer.¹⁸ For further comparisons between measured data it is important to point out that for almost all mentioned experiments, the diffraction



Figure A. A dog-bone shaped sample used for tensile tests.

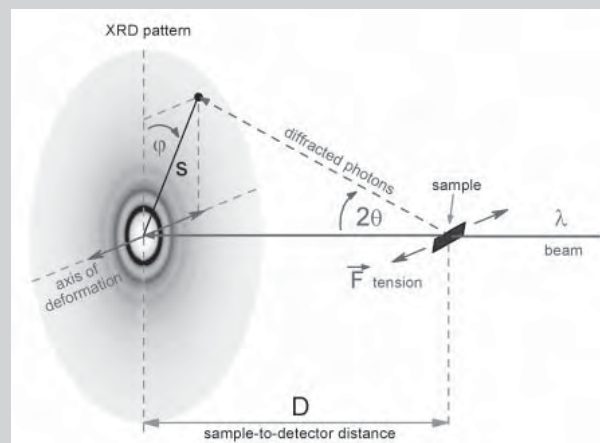


Figure B. A sketch of a typical in-situ tensile experiment.

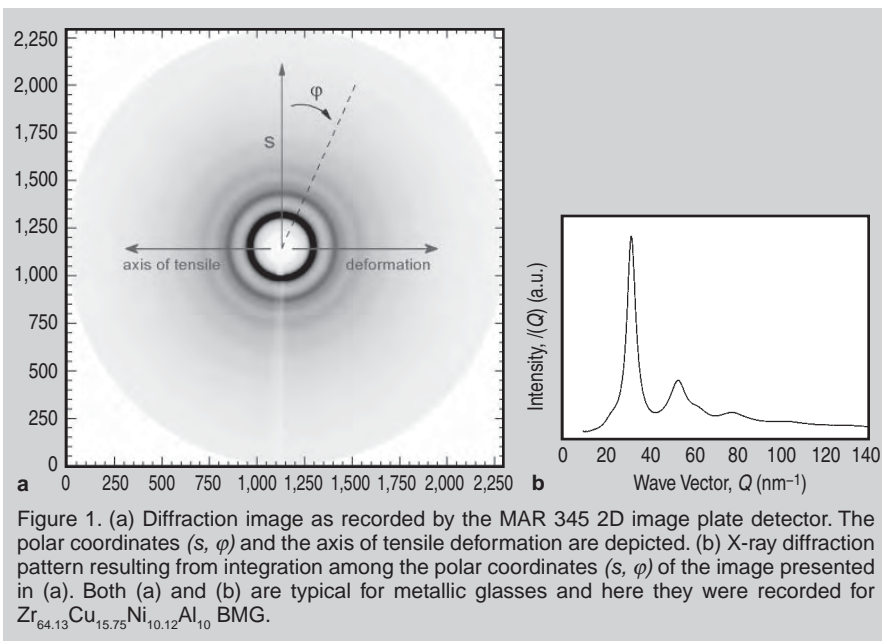


Figure 1. (a) Diffraction image as recorded by the MAR 345 2D image plate detector. The polar coordinates (s , φ) and the axis of tensile deformation are depicted. (b) X-ray diffraction pattern resulting from integration along the polar coordinates (s , φ) of the image presented in (a). Both (a) and (b) are typical for metallic glasses and here they were recorded for $Zr_{64.13}Cu_{15.75}Ni_{10.12}Al_{10}$ BMG.

la become elliptical and the asymmetry is higher as the load increases. Then the angular variation of the strain can be fitted with:¹³

$$\varepsilon(\varphi, \sigma) = \varepsilon_{11} \sin^2 \varphi + \varepsilon_{12} \sin \varphi \cos \varphi + \varepsilon_{22} \cos^2 \varphi \quad (3)$$

As a result, the strain tensor can be determined, and the axial ε_{11} , tangential ε_{22} , and in-plane shear component ε_{12} can be derived. Taking into account the set-up presented in Figure B, $\varphi = 90^\circ$ corresponds to the axial stress and $\varphi = 0^\circ$ to the tangential stress. Components not in the plane perpendicular to the incoming beam can be determined by rotating the specimen around an axis perpendicular to the incoming beam. In the more general case of a multiaxial stress state, the complete strain tensor can be determined from measurement of the strain in various directions.^{14,18}

The same analysis can be done in the real space. However, experimentally a good correlation was observed between the two sets of data. Dmowski and Egami²⁰ pointed out that in the presence of structural anisotropy, it is necessary to expand the PDF into spherical harmonics, otherwise systematic errors may occur especially in the first neighborhood.

STRAIN ANALYSIS

Tensile Tests and Reciprocal Space

The 2-D diffraction pattern of as-cast $Zr_{64.13}Cu_{15.75}Ni_{10.12}Al_{10}$ exhibits the diffuse scattering pattern typical for me-

talic glasses and confirms the presence of glassy structure without any hint of crystalline inclusions (see Figure 1). The symmetric circular diffraction pattern is characteristic for the samples prior to applying tensile stress. With increasing tensile load it becomes elliptical. The changes are most pronounced for the first and strongest diffuse ring (halo) appearing in the 2-D XRD pattern. To describe such changes more quantitatively one has to construct the set of symmetrized intensity distributions as described previously and trace the change in the first peak position as a function of azimuth angle, φ , and tensile stress, σ . It should be noted here that no changes were observed between seven diffraction patterns, independently acquired along the length of the sample (in 1 mm steps), when holding the load at a fixed value of external stress. The experimental scatter of the measured strain values at each different stress level for seven independent locations along the gauge length is shown as error bars in Figures 2 and 3. From Figure 2 it is evident that the asymmetry of the first diffuse maximum increases with increasing load. The decrease in the peak position with increasing tensile stress (the curve corresponding to $\varphi = 90^\circ$ Figure 1) reflects the fact that atoms move apart along the tensile direction. An opposite behavior is seen in transversal direction (the curve corresponding to $\varphi = 0^\circ$ in Figure 1). Figure 2 shows the angular variation of the strain at a given stress σ as calculated from the el-

ative change in the position of the first peak using Equation 2. The fit of the experimental data to Equation 3 yields two components of the strain tensor, ε_{11} and ε_{22} (the axial and tangential components, respectively). The stress-strain curves as observed for different strain tensor components are plotted in Figure 4. Within the experimental error all of them show a linear behavior, indicating the elastic regime of the tensile deformation for the investigated specimens. The samples fractured at a stress of about 1,500 MPa with no sign of yielding, despite the fact that the compressive yield strength of this BMG was reported to be 1,690–1,851 MPa,²¹ indicating a significant strength asymmetry for this BMG. The maximum axial strain (ε_{11}) is $1.50 \pm 0.01\%$. The elastic modulus determined in tensile mode is $E_{11} = 94 \pm 1$ GPa and the experimentally determined Poisson's ratio $\nu = -\varepsilon_{22} / \varepsilon_{11}$ is 0.325 ± 0.01 .

Using the diffraction data by in-situ high-energy XRD, the tensile modulus and Poisson's ratio can be accurately evaluated in the case of $Zr_{62}Al_8Ni_{13}Cu_{17}$ and $La_{62}Al_{14}(Cu_{5/6}Ag_{1/6})_{14}Co_5Ni_5$ BMGs.¹⁵ As in the case of $Zr_{64.13}Cu_{15.75}Ni_{10.12}Al_{10}$, no tensile plasticity was observed, despite the fact that both Zr-glasses are rather deformable in compression.^{15,21} The strains determined from the diffraction data of tensile/transverse directions for the $Zr_{62}Al_8Ni_{13}Cu_{17}$ and $La_{62}Al_{14}(Cu_{5/6}Ag_{1/6})_{14}Co_5Ni_5$ BMGs are presented in Figure 5. There one can see the good linear behavior and basically no sign of yielding. By linearly fitting the points and calculating the ratio of strains between the transverse and tensile directions for each alloy, the tensile elastic modulus and Poisson's ratio were obtained, about 83 GPa and 0.37 for $Zr_{62}Al_8Ni_{13}Cu_{17}$ BMG and 34 GPa and 0.36 for $La_{62}Al_{14}(Cu_{5/6}Ag_{1/6})_{14}Co_5Ni_5$ BMG, respectively.

Using the same method, Mattern et al.¹⁶ measured upon tensile loading amorphous ribbons with the compositions $Cu_{50}Zr_{50}$ and $Cu_{65}Zr_{35}$. The corresponding data for $Cu_{50}Zr_{50}$ are presented in Figure 6. There one can see again a good linear behavior up to the highest value before fracture of the strain with applied stress and no sign of plastic deformation. The Young's modulus $E = 63$ GPa and the Poisson's ratio $\nu = 0.31$ were calculated directly from the slopes

of the axial and tangential components ϵ_{11} and ϵ_{22} vs. stress. The other glass, $\text{Cu}_{65}\text{Zr}_{35}$, behaves similarly.

Compression Tests and Reciprocal Space

The evaluation of the elastic tensor by synchrotron radiation was established by Poulsen et al.¹² At ESRF, they measured several $\text{Mg}_{60}\text{Cu}_{30}\text{Y}_{10}$ BMGs under compressive load. A good linear dependence of the strain as a function of the applied stress was also found.¹² This BMG was known to be brittle,²² and, as a consequence, the samples failed at the end of the elastic regime. Hufnagel, Ott, and Almer¹⁸ measured, at APS, $\text{Zr}_{57}\text{Ti}_5\text{Cu}_{20}\text{Ni}_8\text{Al}_{10}$ BMGs loaded in uniaxial compression. They used the structure factor $S(Q)$ recorded for the loading direction from many x-ray scattering patterns taken at various stresses during incremental loading from 0 MPa to 1,080 MPa (approximately 60% of the yield stress for this alloy¹⁸) and back to zero. As the compressive stress increases, the largest peak in $S(Q)$ shifts to larger Q in the loading direction. The opposite trend was observed for $S(Q)$ in the transverse direction. As a result, the axial component ϵ_{11} of the strain tensor became negative and the tangential component ϵ_{22} became positive.

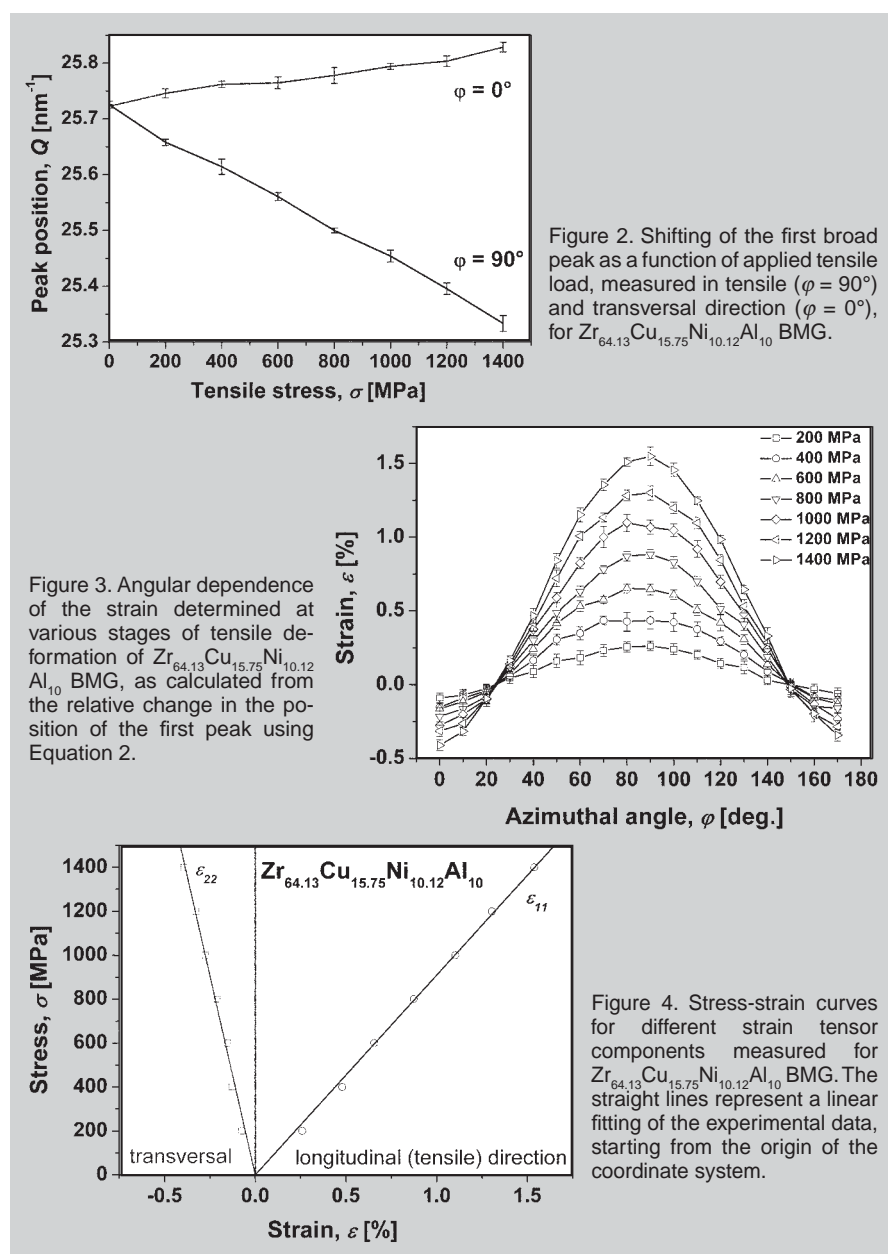
The results indicated that the strain increases linearly with increasing compressive stress. A straight-line fit to the data yields an elastic modulus of $E = 87 \pm 2$ GPa, in good agreement with values for E determined by macroscopic measurements on closely related amorphous alloys.¹⁸ Data for the transverse direction are also in a linear dependence with the applied stress and from both directions one can obtain the value for Poisson's ratio of $\nu = 0.34 \pm 0.01$, also in reasonable agreement with the macroscopic measurements.¹⁸

Strain scanning by x-ray diffraction beyond the Hookean limit, in order to investigate the plastic yielding phenomena of two different BMGs at higher resolution, was done by Das et al.¹⁷ The alloys are "plastic" $\text{Cu}_{47.5}\text{Zr}_{47.5}\text{Al}_5$ and macroscopically "brittle" $\text{Zr}_{55}\text{Cu}_{20}\text{Ni}_{10}\text{Al}_{10}\text{Ti}_5$ BMGs. The experiments have been performed at ESRF Grenoble, France, and the detailed experimental setup is described elsewhere.¹⁷ The diffraction patterns showed the elliptical nature of the

ring after loading compared to a circular feature of the unloaded state, indicating a decrease of the atomic spacing of the nearest neighbors along the loading axis. The data analysis has been performed by the Q -space method in reciprocal space, as described earlier. In the case of each integrated intensity $I(Q)$, the shift of the first halo was determined with respect to the unloaded condition.

Figure 7a and b, taken from Reference 17, shows the evolution of the different atomic-scale strain components (ϵ_{11} , ϵ_{22} and $\gamma_{12} = \epsilon_{12}$) with applied stress for $\text{Zr}_{55}\text{Cu}_{20}\text{Ni}_{10}\text{Al}_{10}\text{Ti}_5$ and $\text{Cu}_{47.5}\text{Zr}_{47.5}\text{Al}_5$, respectively. In the case of $\text{Zr}_{55}\text{Cu}_{20}\text{Ni}_{10}\text{Al}_{10}\text{Ti}_5$, the strain components in the loading direction (ϵ_{11}) and transverse direction (ϵ_{22}) increase.

However, the shear component γ_{12} values remain close to zero. The increment of ϵ_{11} and ϵ_{22} strains slightly deviates from linearity after 1,400 MPa (a dotted line has been drawn to show the linearity of the elastic stress-strain relationship), and the sample broke at 1,740 MPa with an axial strain $\epsilon_{11} = -0.0174$ and a transverse strain ϵ_{22} of $+0.00675$. This strength value is similar to the macroscopic yielding (MY) of this alloy at 1,727 MPa, as observed earlier.²⁴ $\text{Cu}_{47.5}\text{Zr}_{47.5}\text{Al}_5$ shows (Figure 7b) a very similar stress-strain relationship. However, the nonlinear stress-strain behavior starts at around 1,200 MPa and, finally, the elastic strain saturates at a stress of 1,506 MPa with an axial strain $\epsilon_{11} = -0.0150$ and a transverse strain



$\epsilon_{22} = +0.0056$ without alteration of the shear component γ_{12} , which is close to 0. The test was stopped at 1,700 MPa at a plastic strain of about 0.6%–0.7%. Note that the microscopic yield stress has been measured to be 1,547 MPa for $\text{Cu}_{47.5}\text{Zr}_{47.5}\text{Al}_5$, as reported earlier.²³ Therefore, the stress required for mac-

roscopic yielding under compression and the saturation of the elastic strain at the atomic scale is consistent for both the investigated alloys.

Strain Analysis from the Real Space

The strain analysis can be done using

the data from the real space. For that, one has to calculate the structure factor $S(Q)$ or pair correlation function $g(r)$ as described earlier. An example is given in Figure 8, which represents $g(r)$ of $\text{Zr}_{64.13}\text{Cu}_{15.75}\text{Ni}_{10.12}\text{Al}_{10}$ BMG at different stages of deformation. The first peak in $g(r)$ (see the inset) shifts to larger r with increasing load, as expected, and the transverse data (not shown) show the opposite trend. According to different authors,^{18,20} the peak positions in $g(r)$ are difficult to determine accurately because the peaks at low r are asymmetric while those at larger r are rather broad, which leads to significant scatter in the measured strain. A more robust technique proposed by Hufnagel, Ott, and Almer¹⁸ is to focus not on the tops of the peaks, but on the places where $g(r) = 1$. These crossing points are less sensitive to the effects of asymmetry and can be accurately determined even for peaks at large r . Although no dependence of strain on r was observed, it is interesting that the strain determined from the lowest value of r at which $g(r) = 1$ is consistently smaller in magnitude than the strains determined at larger values of r .¹⁸ This is related to the asymmetry of the peaks, due by the changes in the interatomic bonding lengths. More, the asymmetry becomes more pronounced when the applied stress is increasing. To investigate this further, one has to move to RDF and try to deconvolute the first peak which corresponds to the first coordination shell. We cannot unambiguously identify the atomic pairs contributing to the first peak in the RDF, but we can make some reasonable approximations for this $\text{Zr}_{64.13}\text{Cu}_{15.75}\text{Ni}_{10.12}\text{Al}_{10}$ alloy. First, because the contribution of each atomic pair to the RDF is weighted by the atomic scattering factors of the elements and by their concentration, we can neglect the influence of Al, because it has a low atomic number and is present at relatively low concentration. Second, the separation of the atoms in each pair is related to the sum of their atomic radii; since Cu and Ni are nearly the same size (1.28 and 1.25 Å, respectively),²⁵ their contributions are indistinguishable. It is almost clear that Zr–Zr, Zr–Cu, and Zr–Ni are the dominant atomic pairs which constitute the first coordination shell of the PDFs, so only two partials [Zr–(Cu,Ni) and

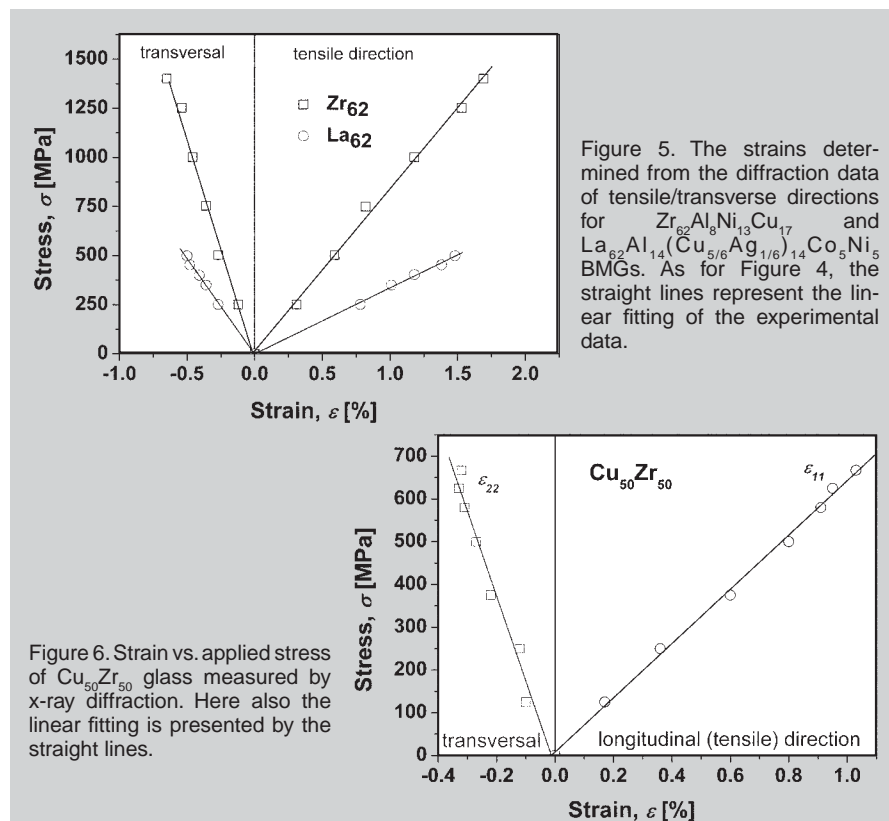


Figure 5. The strains determined from the diffraction data of tensile/transverse directions for $\text{Zr}_{62}\text{Al}_8\text{Ni}_{13}\text{Cu}_{17}$ and $\text{La}_{62}\text{Al}_{14}(\text{Cu}_{5/6}\text{Ag}_{1/6})_{14}\text{Co}_5\text{Ni}_5$ BMGs. As for Figure 4, the straight lines represent the linear fitting of the experimental data.

Figure 6. Strain vs. applied stress of $\text{Cu}_{50}\text{Zr}_{50}$ glass measured by x-ray diffraction. Here also the linear fitting is presented by the straight lines.

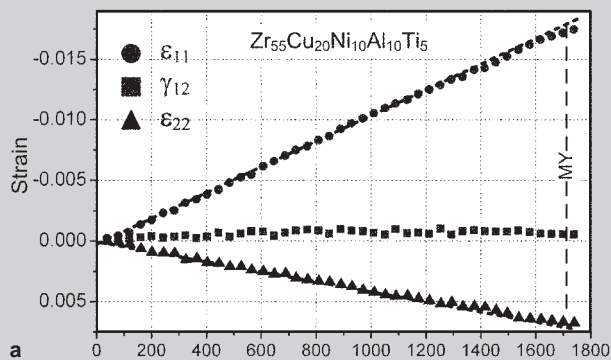
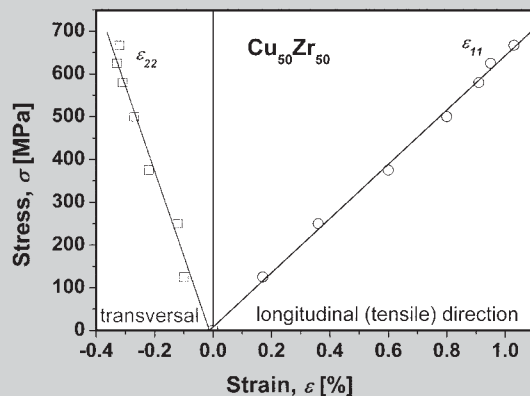
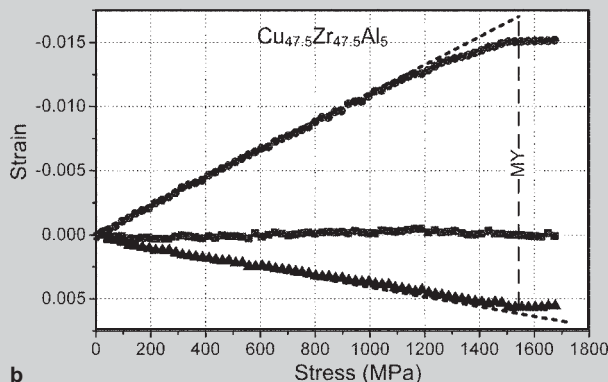


Figure 7. Evolution of elastic strain components of (a) $\text{Zr}_{55}\text{Cu}_{20}\text{Ni}_{10}\text{Al}_{10}\text{Ti}_5$ and (b) $\text{Cu}_{47.5}\text{Zr}_{47.5}\text{Al}_5$ during compressive loading. The increment of ϵ_{11} and ϵ_{22} strains deviates from linearity on atomic scale before the onset of macroscopic yielding (MY). The figure is taken from Reference 17.



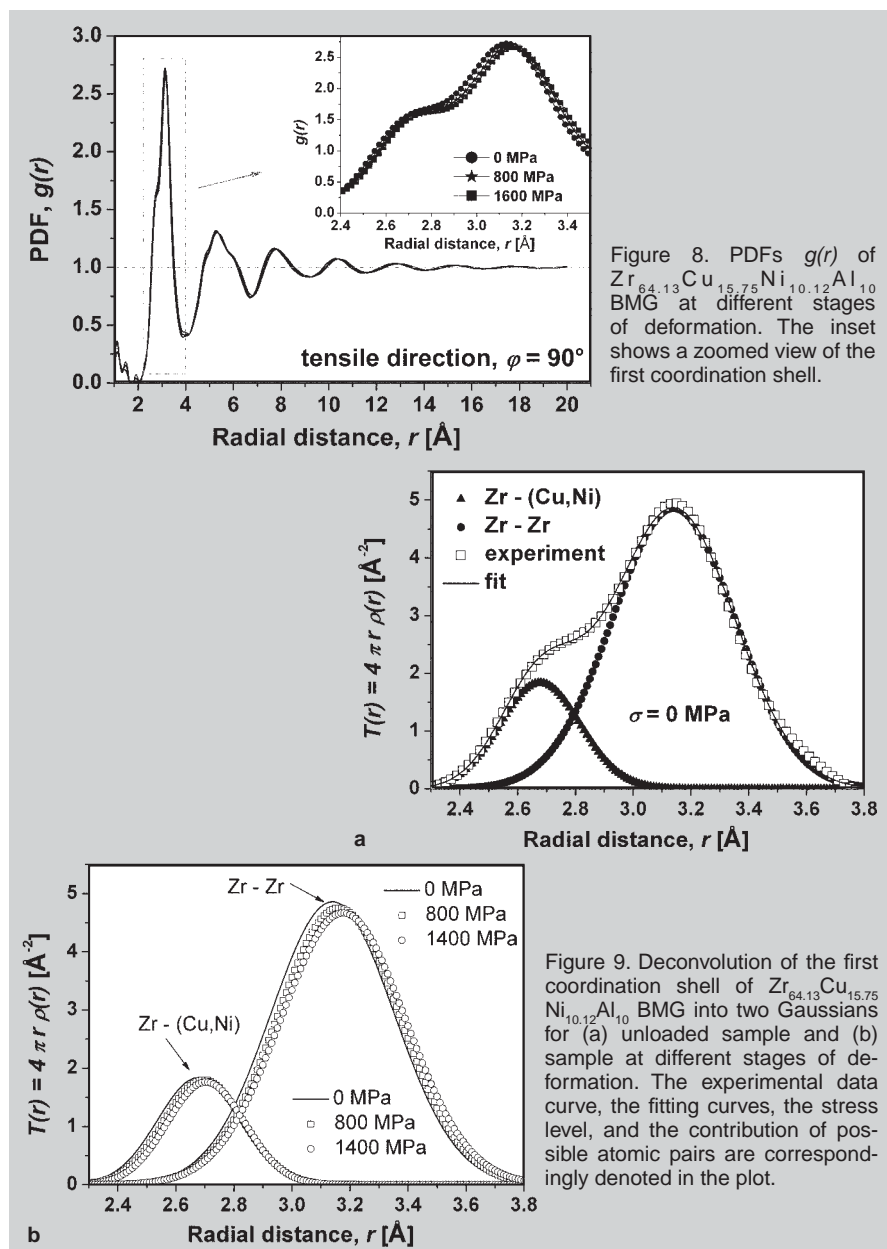
(Zr–Zr)] need to be resolved. Figure 9a shows the result of the deconvolution for the first shell of undeformed $Zr_{64.13}Cu_{15.75}Ni_{10.12}Al_{10}$. The center of the first peak was estimated to be at 2.68 Å corresponding to Zr–(Cu,Ni) atomic pairs. The major component centered at 3.14 Å originates from Zr–Zr atomic pairs. As can be seen from Figure 9b, an increase in tensile stress shifts both peaks toward higher r values. This proves that tensile stress increases the average atomic distances along the loading direction. Similar results were obtained in the case of the other metallic glasses discussed here; in the case of compressive loadings, the average atomic distances along the loading direction became smaller.¹⁸

DATA SUMMARY, COMPARISON, AND DISCUSSION

All of the above discussion assumes that the amorphous material is isotropic. This is often the case for amorphous alloys, but counterexamples can be found in thin films and in bulk alloys subjected to processing that renders them anisotropic. Even in these cases the deviation from isotropy is usually small and the scattering data are analyzed using the isotropic assumption. For the data presented here it was assumed that one can neglect the anisotropy induced by the small uniaxial elastic strain. Hufnagel, Ott and Almer mention¹⁸ that a full treatment would involve the application of cylindrical distribution functions to properly handle the symmetry.

Table I summarizes the values of Young's modulus E and Poisson's ratio ν for the metallic glasses analyzed here. Two types of data are presented: measured by XRD using synchrotron radiation and measured using ultrasound methods or macroscopic tensile/compression tests. Basically, there always are differences in the constants measured using the two methods.

For compressive loads, as mentioned also by Hufnagel, Ott, and Almer,¹⁸ Poulsen and co-workers¹² demonstrated for the first time that the theoretical considerations used in this work are essentially correct, by measuring elastic strain and strain distributions in $Mg_{60}Cu_{30}Y_{10}$ BMG. They showed that the strain measured in both reciprocal and real space



increased linearly with uniaxial stress. The strain measured from the position of the first peak in $I(Q)$ showed good agreement with strain calculated based on macroscopic measurements of Young's modulus E . However, the strain calculated from $g(r)$ showed a pronounced dependence on r , being the smaller for the first near neighbor peak and increasing with peaks at higher r to asymptotically approach the strain calculated from the $I(Q)$ peak position. The strain calculated from the third $g(r)$ peak was even 2.7 times as large as that from the first peak. Poulsen et al. attributed this observation to unspecified "structural rearrangements on the length scale of 4–10 Å."¹² Hufnagel and co-workers¹⁸ observed as well that the strain in the nearest-neighbor shell is

smaller than that at longer scales, the effect being smaller than that reported by Poulsen et al.¹² They propose that "the difference between the stiffness of the nearest-neighbor atomic environment and that over longer length scales can be attributed to the effect of topological rearrangements in the nearest-neighbor environments of a relatively small fraction of the atoms, without the need to invoke significant structural rearrangements over longer length scales."¹⁸

The differences in mechanical constants measured using different techniques are even higher when the samples were subjected to tensile loads (see Table I). Here the stiffness of the neighbor cells becomes more important. Basically, upon tensile tests no sign of plastic deformation was observed. In

Table I. The Values for Young's Modulus E and Poisson's Ratio ν for the Metallic Glasses Presented in this Paper

Composition	Experiment	E (GPa)	ν
$Zr_{64.13}Cu_{15.75}Ni_{10.12}Al_{10}$	Tensile, synchrotron ¹³	94	0.325
	Ultrasound ¹³	78	0.377
$Zr_{62}Al_8Ni_{13}Cu_{17}$	Tensile, synchrotron ¹⁵	83	0.37
	Ultrasound ¹⁵	80	0.38
$La_{62}Al_{14}(Cu_{5/6}Ag_{1/6})_{14}Co_5Ni_5$	Tensile, synchrotron ¹⁵	34	0.36
	Ultrasound ¹⁵	35	0.36
$Cu_{50}Zr_{50}$	Tensile, synchrotron ¹⁶	63	0.31
	Ultrasound ²⁶	83	0.384
$Cu_{65}Zr_{35}$	Tensile, synchrotron ¹⁶	97	0.33
	Ultrasound ²⁶	92	0.352
$Mg_{60}Cu_{30}Y_{10}$	Compression, synchrotron ¹²	64.1	0.373
	Ultrasound ²²	51.5	N/A
$Zr_{57}Ti_5Cu_{20}Ni_8Al_{10}$	Compression, synchrotron ¹⁸	87	0.34
	Macroscopic compression ²⁷	82	0.362
$Cu_{47.5}Zr_{47.5}Al_5$	Compression, synchrotron ¹⁷	99.2	0.34
	Ultrasound ¹⁷	90.1	0.365
$Zr_{55}Cu_{20}Ni_{10}Al_{10}Ti_5$	Compression, synchrotron ¹⁷	91.1	0.38
	Ultrasound ¹⁷	85.5	0.378

fact¹³ we considered that here one can deal with two types of glasses: intrinsically brittle and plastic deformable in compression. Judging from the trend of the values of the elastic constants summarized in Table I, as measured by ultrasonic methods and as calculated from the strain tensor measured by diffraction experiments, it is very clear that in the case of "nondeformable" or intrinsically brittle BMGs, the bulk elastic constants as derived from ultrasound measurements and the ones obtained from the strain tensor analysis are almost similar, indicating a similar elastic behavior of each atomic shell. In the case of plastically deformable BMGs each atomic shell has a different stiffness, as revealed from the large differences of the elastic constants from ultrasonic and tensor analysis. Most likely, such local fluctuations of the elastic properties in the glassy structure can rather easily induce local shear transformation and, thus, the BMG exhibits macroscopic plasticity.¹³ However, in a glassy material a range of local atomic environments of the atoms exists. As a consequence of the disorder, fluctuation of inter-atomic distances may occur, which leads to variations of the atomic-level stress.¹⁶ The analysis of the first neighborhood, done by Mattern et al.¹⁶ for their CuZr binary glasses, confirms the anelastic changes of the short-range order under tensile stress well below the yield strength. The

response of the nearest neighborhood upon loading leads toward the directional changes in the chemical short-range order. All together may explain the differences in mechanical behavior observed at the microscopic level (x-ray diffraction) when compared with the averaged macroscopical behavior.

CONCLUSIONS

In-situ x-ray synchrotron diffraction enables the atomic level elastic strain of metallic glasses under uniaxial tensile or compressive stress to be characterized. The elastic moduli can be estimated not only considering the shift of the first maximum of the scattering curve in reciprocal space but also from the shift of the larger inter-atomic distances in the PDF in real space. The analysis of the short-range order of several metallic glasses vs. stress confirms the structural changes in the elastic regime. The anelastic deformations are accompanied by bond reorientation leading to direction dependent changes in chemical short-range order. The elastic constants calculated from the strain tensor are different from those measured by macroscopic techniques. These differences are supposed to arise because the ultrasound techniques average the elastic constants of different atomic shells and measure the bulk properties of the material, while the diffraction measurements may detect differences in stiffness of

the first, second, third, and consecutive atomic shells.

ACKNOWLEDGEMENTS

The authors thank N. Mattern and S. Pauly for stimulating discussions. We thank also the beamline staff from BW5, Hasylab Hamburg, Germany and from ID11, ESRF Grenoble, France, for their help during diffraction measurements. The authors are grateful for the financial support provided by the European Union within the framework of the Research Training Network on "Ductile BMG composites" (MRTN-CT-2003-504692). The Alexander von Humboldt Foundation is acknowledged for financial support of G. Wang.

References

- W.L. Johnson, *MRS Bull.*, 24 (1999), p. 42.
- A. Inoue, *Acta Mater.*, 48 (2000), p. 279.
- H. Chen et al., *Nature*, 367 (1994), p. 541.
- S. Venkataraman et al., *Scripta Mat.*, 54 (2006), p. 835.
- M. Stoica et al., *Intermetallics*, 13 (2005), p. 764.
- U. Kühn et al., *Appl. Phys. Lett.*, 77 (2000), p. 3176.
- J. Eckert, *Mat. Sci. Eng. A*, 226 (1997), p. 364.
- A.L. Greer, *Science*, 267 (1995), p. 1947.
- L.Q. Xing et al., *Phys. Rev. B*, 64 (2001), 180201.
- J.J. Lewandowski and A.L. Greer, *Nat. Mater.*, 5 (2006), p. 15.
- D.M. Dimiduk et al., *Science*, 312 (2006), p. 1188.
- H.F. Poulsen et al., *Nat. Mater.*, 4 (2005), p. 33.
- M. Stoica et al., *J. Appl. Phys.*, 104 (2008), 013522.
- J. Bednarčik and H. Franz, *J. Phys.: Conf. Series*, 144 (2009), 012058.
- X.D. Wang et al., *Appl. Phys. Lett.*, 91 (2007), 081913.
- N. Mattern et al., *Acta Mat.*, 57 (2009), p. 4133.
- J. Das et al., *Phys. Rev. B*, 76 (2007), 092203.
- T.C. Hufnagel, R.T. Ott, and J. Almer, *Phys. Rev. B*, 73 (2006), 064204.
- A.P. Hammersley et al., *High Press. Res.*, 14 (1996), p. 235.
- W. Dmowski and T. Egami, *J. Mater. Res.*, 22 (2007), p. 412.
- Y.H. Liu et al., *Science*, 315 (2007), p. 1385.
- A. Castellero et al., *J. Alloys and Comp.*, 434-435 (2007), p. 48.
- J. Das et al., *Phys. Rev. Lett.*, 94 (2005), 205501.
- K. Hajlaoui et al., *J. Non-Cryst. Solids*, 353 (2007), p. 327.
- ASM Handbook: Volume 1.2 Metals Handbook* (Materials Park, OH: ASM International, 1992).
- G. Duan et al., *Scripta Mater.*, 58 (2008), p. 159.
- J.J. Lewandowski, W.H. Wang, and A.L. Greer, *Philos. Mag. Lett.*, 85 (2005), p. 77.

Mihai Stoica and Gang Wang, researchers, and Jürgen Eckert, director, are with the Institute for Complex Materials, Helmholtzstr. 20, Dresden, 01069, Germany; Jayanta Das, senior research fellow, is with IIT Kharagpur, Department of Metallurgical and Materials Engineering, Kharagpur, India; Jozef Bednarčik, scientist, is with DESY, Hamburg, Germany; Gavin Vaughan, scientist, is with ESRF, Grenoble, France; and Wei Hua Wang, professor, is with the Institute of Physics, Chinese Academy of Sciences, Beijing, China. Dr. Stoica can be reached at m.stoica@ifw-dresden.de.

Amorphous Metals for Hard-tissue Prosthesis

Marios D. Demetriou, Aaron Wiest, Douglas C. Hofmann, William L. Johnson, Bo Han, Nikolaj Wolfson, Gongyao Wang, and Peter K. Liaw

Owing to a unique atomic structure lacking microstructural defects, glassy metals demonstrate certain universal properties that are attractive for load-bearing biomedical-implant applications. These include a superb strength, which gives rise to very high hardness and a potential for minimizing wear and associated adverse biological reactions, and a relatively low modulus, which enables high elasticity and holds a promise for mitigating stress shielding. There are, however, other non-universal properties specific to particular amorphous metal alloys that are inferior to presently used biometals and may be below acceptable limits for hard-tissue prosthesis. In this article, features of the performance of amorphous metals relevant to hard-tissue prosthesis are surveyed and contrasted to those of the current state of the art, and guidelines for development of new biocompatible amorphous metal alloys suitable for hard-tissue prosthesis are proposed.

INTRODUCTION

Medical use of metals as prosthetic replacements or fracture fixation devices for human bone has become widespread over the past two decades with millions of hard-tissue replacement and repair surgeries carried out annually in the United States. Despite medical statistics showing high rates of success, there remain serious problems. For example, the rate of revision surgeries for orthopedic implants is approximately 7% after 10 years of service.¹ With an aging population and surgeries on younger patients due to trauma or sports injuries, the rate of revision procedures is growing at an accelerated rate of approximately 60%.¹ Improvements in the biocompatibility,

How would you...

...describe the overall significance of this paper?

This article surveys a range of features of the performance of amorphous metals relevant to hard-tissue prosthesis, compares these features to those of the current state of the art, and proposes guidelines for development of new biocompatible amorphous metal alloys suitable for load-bearing implant applications.

...describe this work to a materials science and engineering professional with no experience in your technical specialty?

Amorphous metals differ fundamentally from conventional crystalline metals in their atomic structure and fundamental thermodynamic state. Specifically, an amorphous metal is a configurationally-frozen non-equilibrium metallic liquid that fails to form a stable crystalline state, and consequently reveals no long-range atomic order. The distinctive structural state of amorphous metals gives rise to unique corrosion characteristics, mechanical performance, and processing capabilities that render amorphous metals attractive for load-bearing biomedical implant applications.

...describe this work to a layperson?

Tens of thousands of hard-tissue replacement surgeries are carried out annually in the United States. Despite medical statistics showing high rates of success, there remain serious problems, particularly with respect to tissue compatibility as well as from the perspective of patient comfort, mobility, and functionality. Improvements in the biological compatibility, durability, and functionality of orthopedic implants will be of widespread benefit to implant recipients. Amorphous metals with unique mechanical and chemical characteristics are highly promising candidate materials for achieving these goals.

durability, and longevity of orthopedic implants as well as optimization of orthopedic hardware from the perspective of patient comfort, mobility, and functionality will be of widespread benefit to implant recipients.

Manufacturers of orthopedic hardware have active research programs aimed at developing materials with improved biocompatibility, which entails environmental stability in living tissue, mechanical performance, and ability to match, functionally replace, and integrate with various types of living tissue. Amorphous metals with unique mechanical and chemical properties and attractive processing capabilities are promising candidate materials for achieving these goals. This article surveys a range of features of the performance of amorphous metals and assesses their suitability for hard-tissue prosthesis.

See the sidebar on page 86 for background on biocompatibility of currently-used materials.

AMORPHOUS METALS AS PROSPECTIVE BIOMATERIALS

Bulk amorphous metals are a relatively new class of engineering materials developed over the past two decades. Unlike traditional engineering metals which are structurally crystalline, amorphous metals are configurationally frozen liquids which fail to crystallize during solidification from the molten state. While they are electronically and optically metallic like ordinary metals, the absence of crystals and associated extended defects such as vacancies, dislocations, or grain boundaries gives rise to physical, chemical, and mechanical properties that differ fundamentally from conventional metals. For example,

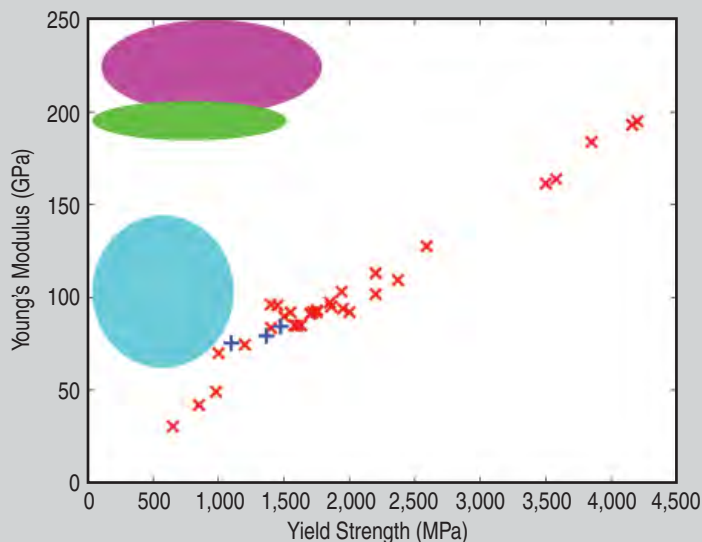


Figure 1. Young's modulus vs. yield strength data for amorphous metals [x]¹¹ and ductile-phase reinforced amorphous metals [+]¹² shown together with data for stainless steels [■]², Co-Cr-based [■]² and Ti-based alloys [■]².

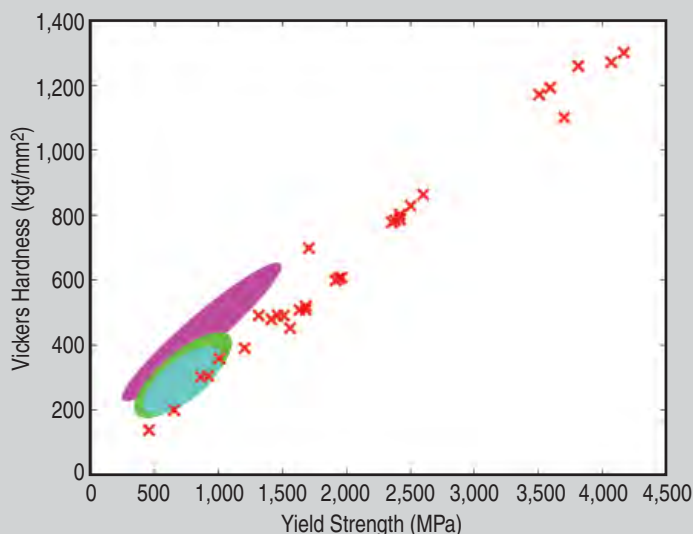


Figure 2. Vickers hardness vs. yield strength data for amorphous metals [x]¹⁶ shown together with data for stainless steels [■]², Co-Cr-based [■]² and Ti-based alloys [■]².

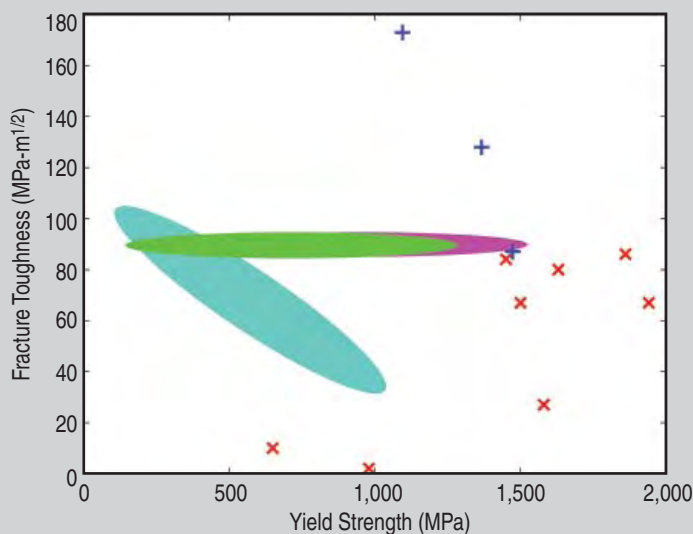


Figure 3. Fracture toughness vs. yield strength data for amorphous metals [x]¹⁸ and ductile-phase reinforced amorphous metals [+]¹² shown together with data for stainless steels [■]¹⁹, Co-Cr-based [■]¹⁹ and Ti-based alloys [■]¹⁹.

amorphous metals typically exhibit very high strength, hardness, and elasticity compared with conventional metals. Unlike silicate glasses, they tend to be tough and have fracture toughness that is often comparable to ordinary metals. The absence of microstructural defects influences their chemical behavior as well, often resulting in improved resistance to corrosion and chemical attack. Lastly, their ability to soften and flow upon relaxation at the glass transition gives rise to a viscoplastic-flow behavior which opens the possibility of “thermoplastic” forming processes similar to those employed for processing plastics. The above features have stimulated broad interest in metallic-glass engineering applications.

The aspects of the performance of amorphous metals that are most attractive for hard-tissue prosthesis are their high strength and hardness, which suggest good load-bearing capability and high wear resistance; their low modulus, which implies better load transfer to the surrounding bone and a potential for mitigating stress-shielding; and their good corrosion resistance. Their unique processing capabilities represent another attractive feature of these materials, as they can potentially simplify the currently complex fabrication procedures and bring down fabrication costs. The attractive advantages presented by the thermoplastic and micro-forming capabilities of these materials as they relate to biomedical applications are emphasized in a recent article by Schroers and co-workers.¹⁰

MECHANICAL PERFORMANCE OF AMORPHOUS METALS

Elasticity

Owing to a liquid-like atomic structure associated with structural length scales on the order of few hundred atoms, amorphous metals offer an unusual combination of very high strength and low elastic modulus.¹¹ Low elastic modulus is highly desirable in hard-tissue prosthesis, as it would minimize the modulus mismatch between bone and biomaterial, facilitate load transfer to the surrounding bone, and potentially mitigate stress shielding. As demonstrated in Figure 1, for a given strength require-

ment an amorphous metal exhibits a significantly lower modulus than any of the conventional crystalline metallic biomaterials. The recently developed ductile-phase-reinforced amorphous metals also present this advantage,^{12,13} as their overall elastic behavior appears to resemble that of the monolithic amorphous metal. Consider for example a 1-GPa strength requirement. An amorphous metal combines such strength with a modulus that is 75% the modulus of a titanium-based alloy, 25% the modulus of a stainless steel alloy, or 20% the modulus of a Co-Cr-based alloy. Essentially, a low modulus for a given strength implies a high elastic limit. Hard tissue (cortical bone) exhibits an elastic strain limit that ranges from 1 to 1.5%, depending on the degree of mineral content.¹⁴ Crystalline metals exhibit elastic strain limits that typically range between 0.1% and 0.5%.¹⁵ Amorphous metals, on the other hand, exhibit elastic strain limits that range from 1.5 to 2%,¹⁵ and thus more closely match the elasticity of natural tissue. This unique combination of high strength and elasticity renders amorphous metals attractive load-bearing biomaterials that could potentially mitigate stress shielding.

Hardness

Hardness is the mechanical property that mostly influences the wear resistance capabilities of a material. Since hardness is understood to be a measure of flow stress, it correlates linearly with the material yield strength. Specifically, the Vickers hardness is expected to scale linearly with the material yield strength ($H_v \sim 3\sigma_y$). Owing to their superb yield strength, amorphous metals demonstrate an advantage over crystalline metals in terms of hardness. The hardness of amorphous metals as a function of yield strength is plotted in Figure 2,¹⁶ along with data for conventional crystalline metallic biomaterials.² As expected, the hardness of all metallic materials, whether amorphous or crystalline, is shown to obey a tight universal relation with strength. By correlating the abrasive and sliding wear resistance of various amorphous metal alloys to their microhardness values, Greer and Myung¹⁷ demonstrated a one-to-one correspondence between wear resistance and hardness. Moreover, the

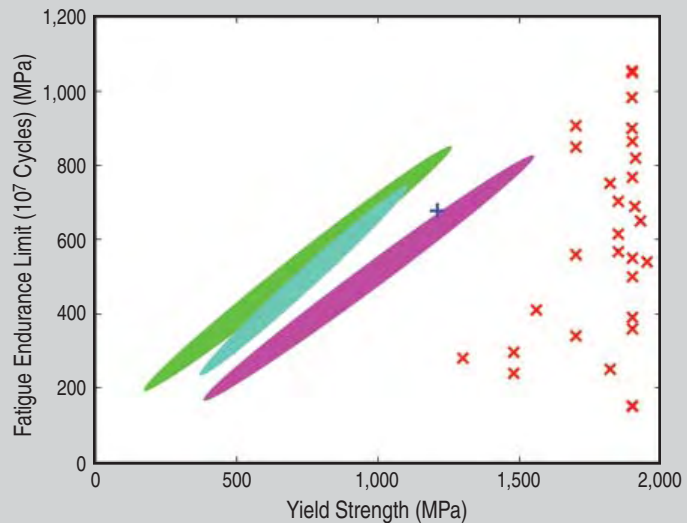


Figure 4. Fatigue endurance limit (stress-range based) vs. yield strength data for amorphous metals [x]²¹ and ductile-phase reinforced amorphous metals [+],²³ shown together with data for stainless steels [■],²³ Co-Cr-based [■],²³ and Ti-based alloys [■].²³

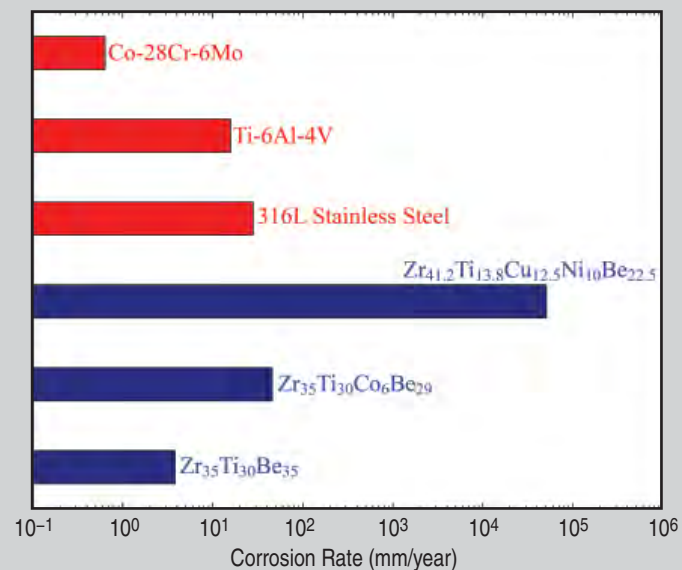


Figure 5. Corrosion rates of various amorphous Zr-based alloys compared with surgical-grade Co-Cr-based, Ti-based, and stainless steel in 12 M HCl solution.²⁹

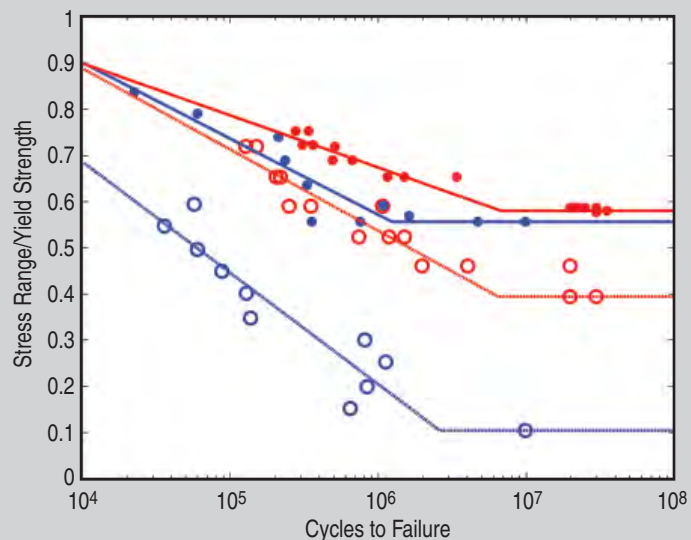


Figure 6. Stress-life curves for cyclic uniaxial loading of glassy Zr-Ti-Co-Be in air (●) and 0.6 M NaCl (○)³³ and for 316 stainless steel in air (●) and 0.5 M NaCl (○).³⁴

wear resistance of amorphous metals was found to exceed that of ceramics at the same hardness, which suggests that the mechanism of wear deformation in amorphous metals does not involve brittle fracture. The high wear resistance of amorphous metals implied by their high hardness could be of great benefit in load-bearing biomedical implant applications, as it presents a potential for reducing wear and mitigating the associated adverse biological effects.

Toughness

Fracture toughness is a measure of the load-bearing capacity of a mate-

rial before fracture, and is a critical property determining the overall mechanical performance of a load-bearing implant. Despite their excellent biological compatibility and high wear resistance, ceramics are not the materials of choice in hard-tissue prosthesis because of their low fracture toughness ($K_{IC} < 10 \text{ MPa m}^{1/2}$). Instead, the preferred materials for such applications are metals, because despite an inferior biological compatibility, metallic biomaterials exhibit very high toughness ($K_{IC} \sim 100 \text{ MPa m}^{1/2}$). The atomic structure of an amorphous metal lacks microstructural mechanisms for arresting

propagating plastic-flow bands (shear bands) prior to turning into opening cracks, and consequently their fracture toughness is generally lower than values typical of structural crystalline metals. Some amorphous metal alloys, however, tend to generate highly dense shear band networks upon yielding that are able to self-arrest in a manner that leads to a higher toughness, approaching values characteristic of structural crystalline metals. Amorphous metals therefore exhibit toughness values that vary from as low as the values characteristic of brittle ceramics to as high as the values characteristic of engineering metals.¹⁵ The fracture toughness of certain amorphous metals is plotted in Figure 3 against their respective yield strengths,¹⁸ together with data for conventional crystalline metallic biomaterials.¹⁹ It should be noted that many of the toughness data for amorphous metals shown in Figure 3 do not represent actual K_{IC} values (because of sample sizes insufficient to warrant plane-strain conditions or lack of pre-existing flaws), and are thus not directly comparable to those of crystalline biomaterials. Nevertheless, some amorphous metal systems appear to exhibit fracture toughness that can be adequate for load-bearing biomedical implant applications. Interestingly, reinforcement of the glassy structure with a ductile dendritic crystalline phase provides a unique microstructural mechanism for arresting propagating shear bands that leads to superb fracture toughness.^{12,13} As presented in Figure 3, the fracture-toughness values of the highly toughened ductile-phase-reinforced amorphous metals,¹² which were determined to roughly represent actual K_{IC} values,²⁰ clearly surpass those of crystalline metals. The very high strength and toughness of these materials is an attractive combination that could lead to superior biomechanical performance.

Fatigue

Fatigue endurance is perhaps the single most important property that dictates the overall service life of a load-bearing implant. It is estimated that the average non-active person imposes several millions of cycles of stress on the hip joint per year.¹⁹ Over a period of 20–30 years, this rate cor-

BIOCOMPATIBILITY AND CURRENT STATE OF THE ART

Biocompatibility is regarded as the ability of a biomaterial to perform with an appropriate biological response.² The aspects that define biocompatibility are the “host response” and the “material response.” The “host response” is defined as the local and systemic response (other than the intended therapeutic response) of the living systems to the material, while the “material response” is the response of the material to the living system.² The most basic material responses encountered in load-bearing implant applications include corrosion or dissolution due to chemical attack, friction and wear, and mechanical failure due to plastic deformation, fracture, or fatigue. Typical host responses include tissue adaptation, which can be either positive (e.g., osseointegration) or negative (e.g., stress shielding), inflammation, allergic response, and carcinogenesis.

Owing to their high strength and hardness and superior fracture and fatigue resistance, metallic materials demonstrate a much more favorable mechanical response to biological systems than polymeric or ceramic materials, and are presently regarded as the materials of choice for load-bearing implant applications. The most common metallic biomaterials used traditionally in load-bearing implant applications are stainless steels, Co-Cr-based alloys, and Ti-based alloys, while recently certain Zr-based and Ta-based alloys have been introduced.¹ Despite demonstrating an overall favorable mechanical performance, metallic orthopedic biomaterials have been associated with certain adverse local and remote tissue responses. For example, the stiffness of these materials, particularly of Co-Cr alloys and stainless steels, is very high compared to that of hard tissue (Young’s modulus of Co-Cr-based alloys is 200–250 GPa vs. 10–20 GPa for cortical bone). Consequently, the modulus mismatch and uneven load sharing between implant and bone, known as stress shielding, can lead to bone resorption and eventual loosening of the implant.³ Another issue critical to the long-term performance and longevity of the joint replacement prosthesis is the degradation products of these biomaterials and the subsequent tissue reactions to these products. The degradation processes most frequently associated with adverse biological reactions and implant failures are wear and corrosion. Particulate debris generated by metal-on-metal wear is known to induce inflammatory responses that often lead to clinical failures. For example, foreign-body granulation tissue response to wear debris has the ability to invade the bone-implant interface and initiate a progressive local bone loss (wear-debris-induced osteolysis) that can threaten the fixation of the device and limit the longevity of the total joint prosthesis.⁴ Electrochemical corrosion occurring at metal-implant surfaces can have two main adverse effects: the degradation process may reduce the structural integrity of the device, and the degradation products (e.g., metal ions) may remotely or systemically affect the biological host. Structural failure mechanisms related to corrosion include stress-corrosion cracking, corrosion fatigue, and fretting corrosion.⁵ Metal ions that have been associated with adverse biological reactions include Ni (contained in relatively high fractions in certain stainless steels), Al (common in Ti-based alloys), Co (the base metal of Co-Cr-based alloys), and Cr (contained in relatively high fractions in stainless steels and Co-Cr-based alloys). Hypersensitivity to Ni is the most common (affects approximately 14% of the population), followed by Co and Cr.⁶ Nickel, Co, and Cr are known carcinogens in pure form,⁷ while Ni and Cr form certain compounds that are found to be carcinogenic.⁸ Aluminum has been linked to several neurodegenerative diseases such as Parkinsonism dementia and Alzheimer’s disease.⁹

responds to approximately 10^8 loading cycles. Therefore, the resistance of a material to cyclic loading is critical in ensuring longevity of the device. The fatigue performance of amorphous metals has not been broadly investigated. Most investigations were performed on Zr-based glasses. The fatigue endurance limit for this class of amorphous metals at 10^7 cycles is plotted in Figure 4 against the corresponding yield strengths.²¹ The data includes results from uniaxial, bending, and rotating fatigue experiments. Data for conventional crystalline biomaterials are also presented on the same plot.²² The ratio of the fatigue endurance limit to the material yield strength is known as the fatigue ratio. Unlike crystalline biomaterials which exhibit rather consistent endurance limits and high fatigue ratios, the endurance limits of Zr-based glasses are shown to be highly scattered and the fatigue ratios ranging from very small (~ 0.1) to rather high (~ 0.5). The origin of such high scatter in the endurance limit of Zr-based glasses is not yet clear. Extrinsic factors such as variations in loading geometry and loading frequency or intrinsic factors such as variations in alloy composition, defect concentration, or glass temperature history are possible causes of the apparent inconsistency. Since fatigue data for families other than the Zr-based family (e.g., Fe-based or Pd-based) are rather scarce, no definitive conclusions can be drawn for the overall fatigue behavior of amorphous metals. It can be firmly stated, however, that unless the amorphous metal alloy demonstrates a fatigue-endurance limit that is reliable and reproducible and represents a significant fraction of its yield strength, its use as load-bearing implant material would be severely hindered. Interestingly, the highly toughened ductile-phase-reinforced amorphous metals (data also plotted in Figure 4) appear to perform substantially better than monolithic amorphous metals in terms of fatigue endurance exhibiting a fatigue ratio comparable to crystalline biomaterials.²³ The high and consistent endurance limit of ductile-phase-reinforced metallic glasses is attributed to the same "microstructural arrest" mechanism that controls the toughness of these alloys.²³

CORROSION BEHAVIOR OF AMORPHOUS METALS

Static Corrosion

The chemically homogeneous structure of amorphous metals lacking microstructural defects such as dislocations, grain boundaries, and precipitates/segregates is thought to promote the formation of uniform passive layers without weak points that can provide enhanced protection against corrosion or chemical attack. From an electrochemical standpoint, amorphous metal alloy families can be grouped into early-transition-metal based (e.g., Zr-based), ferrous-metal based (e.g., Fe-based), and noble-metal based (e.g., Pd-based). Zirconium-based and Fe-based amorphous metals are the most extensively studied in corrosion. The nature of corrosion resistance of these glasses is directly related to the formation of a passive surface layer.²⁴ Noble-metal based amorphous metals have not been extensively studied, and the key mechanism controlling their corrosion behavior is unknown.

In chloride environments, Zr-based glasses (both Be-bearing and Al-bearing) exhibit a rather low resistance to pit initiation and growth and a rather weak repassivation ability.^{25,26} The corrosion resistance of Zr-based glasses relies on the formation of barrier-type protective layers several nanometers thick, consisting mainly of Zr oxides and often small fractions of Al or Be oxides. Other late transition metals often included in the composition of these alloys (e.g., Ni and Cu) are enriched around sub-surface layers, as a result of selective surface oxidation.²⁷ Wiest²⁸ recently demonstrated that by properly selecting these late transition metals and optimizing their atomic fractions, the overall corrosion resistance of these alloys in chloride environments can be dramatically enhanced. As shown in Figure 5, the corrosion resistance of Zr-based Be-bearing glasses in an acidified chloride solution is drastically enhanced when late-transition-metals Ni and Cu are replaced by Co and the overall concentration is reduced. With the aid of x-ray photoelectron spectroscopy, Wiest observed more chemically-uniform passive layers on systems with low fractions of late-transition metals. Compared to the cor-

rosion rate of surgical-grade 316L stainless steel, Ti-6Al-4V, and Co-Cr-Mo in the same solution, the corrosion rate of Be-bearing Zr-based glasses varies from a much higher value in the case of Zr-Ti-Ni-Cu-Be to a low comparable value in the case of Zr-Ti-Be.²⁸ In phosphate-buffered saline, Al-bearing Zr-based glasses were also found to exhibit corrosion rates comparable to conventional biomaterials.²⁹

Several amorphous Fe-based alloys are known to exhibit superb resistance to corrosion.³⁰ For example, Fe-Cr-P-C glasses are found to exhibit corrosion rates in acidified chloride solutions many orders of magnitude lower than conventional (crystalline) stainless-steel alloys.³¹ These Fe-based glasses appear to resist pitting when anodically polarized. Their high corrosion resistance is attributed to their ability to passivate spontaneously upon immersion, forming thick, uniform, and chemically homogeneous passive layers enriched with corrosion-resistant elements. Owing to their exceptionally high corrosion resistance, these amorphous Fe-based alloys may be attractive alternatives to conventional stainless-steel biomaterials.

Stress/Fatigue Corrosion

Stress corrosion and fatigue corrosion failures occur as a consequence of the combined interaction of electrochemical reactions and mechanical damage. Resistance to such failure is an important attribute of a load-bearing biomedical implant. Studies of stress and fatigue corrosion for amorphous metals are limited to mostly Zr-based and Fe-based. Zirconium-based glasses (both Be-bearing and Al-bearing) are found to exhibit substantially lower fatigue ratios in saline solutions compared to their values in air, a consequence of considerably higher (2–3 orders of magnitude) fatigue-crack growth rates realized in saline compared to air.^{32,33} In Figure 6 the stress-life curves for glassy Zr-Ti-Co-Be in air and saline solution³⁴ are contrasted to the respective curves for 316 stainless steel.³⁵ The two materials exhibit comparable fatigue ratios in air (~ 0.55). In saline, however, glassy Zr-Ti-Co-Be exhibits a much lower fatigue ratio (~ 0.1) than stainless steel (~ 0.4). The mechanism governing the corrosion fatigue behavior of these glasses was

BIOLOGICAL COMPATIBILITY OF AMORPHOUS METALS

A set of testing procedures is required to study the biological compatibility of a biomaterial. National and international standards organizations provide assistance in the design of biomaterials, including the American Society for Testing Materials (ASTM) and the International Standards Organization (ISO). Biocompatibility tests can typically be grouped into in-vitro and in-vivo. In-vitro evaluations typically include cytotoxicity and cellular adhesion tests. In-vivo tests involve tissue compatibility assessments, and include evaluation of (i) sensitization, irritation, and reactivity, (ii) systemic, subchronic, and chronic toxicity, (iii) genotoxicity, (iv) carcinogenicity, (v) hemocompatibility, and (vi) immune responses.³⁹

In-vitro Investigations

A standard in-vitro biocompatibility test (ISO protocol 10993 part 5: Test for cytotoxicity – in vitro methods) was conducted by NAMS on Zr-Ti-Co-Be and Pd-Ag-P-Si amorphous alloys. In the test, a single extract of the metallic-glass test article was prepared using single-strength Minimum Essential Medium supplemented with 5 vol.% serum and 2 vol.% antibiotics. The test extract was placed onto three monolayers of L-929 mouse fibroblast cells incubated at 37°C in a 5% CO₂ atmosphere for 48 hours. Following incubation, the cultures were examined microscopically to evaluate the cellular characteristics and percent lysis. The test extracts for both amorphous metal alloys showed no evidence of causing toxicity. Specifically, the performance of both materials received the grade of zero, which corresponds to no reactivity, no cell lysis, and all cultures appear as discrete intracytoplasmic granules. In another 7-day in vitro cellular adhesion test where amorphous Zr-Ti-Co-Be discs were immersed into a fibroblast-enriched environment, the material demonstrated a favorable biological performance as cell adherence and proliferation were observed to

be adequate and compatible (Figure A). In vitro cytotoxicity and cellular-adhesion investigations for other amorphous metal alloys have been reported,^{10,40-44} most of which yielded mostly favorable results.

In-vivo Investigations

A standard in-vivo biocompatibility test (ISO protocol 10993 part 6: Tests for local effects after implantation) was conducted by NAMS on Zr-Ti-Co-Be and Pd-Ag-P-Si amorphous alloys. In the test, sterilized metallic-glass test samples were implanted in the muscle tissue of three male New Zealand White rabbits. After administering buprenorphine and a general anesthetic to each animal, one incision was made on each side of the back through the skin and parallel to the lumbar region of the vertebral column. Four metallic-glass test article sections and four high-density polyethylene negative control sections were implanted in the right and left paravertebral muscle of each rabbit. The skin incisions were closed with tissue glue. The rabbits were euthanized two weeks later, muscle tissues were excised and the implant sites were examined microscopically and macroscopically. No significant macroscopic reactions were detected for either material compared to the negative control implant material. The tissue responses to the Zr-Ti-Co-Be articles observed microscopically were similar to those for the negative control, while those for Pd-Ag-P-Si were slightly more favorable. Both materials were classified as non-irritant. A follow-up study involving amorphous Pd-Ag-P-Si rods implanted subcutaneously in rats for 28 days verified the superb biological performance of this material, as no tissue reaction was detected over the 28-day period of the experiment (Figure B). In vivo tissue compatibility investigations for other amorphous metal alloys have been reported,^{10,44} most of which yielded mostly favorable results.

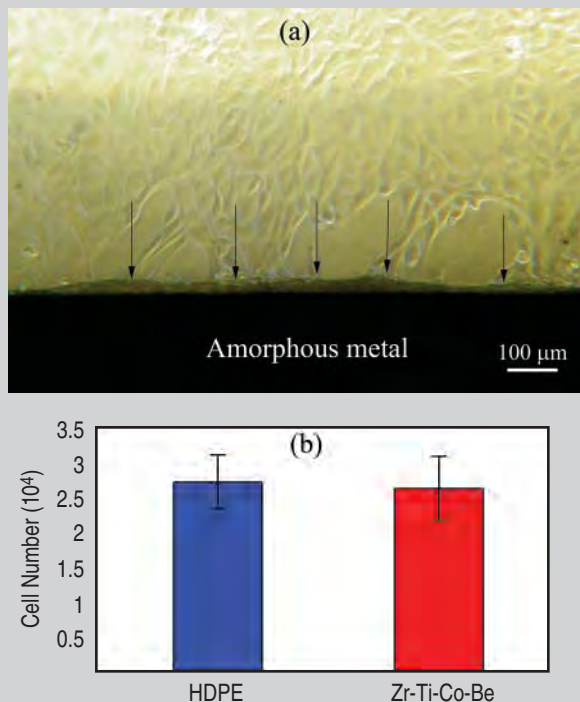


Figure A. Fibroblast cell attachment on amorphous Zr-Ti-Co-Be and high-density polyethylene (HDPE) discs. (a) Micrograph of the amorphous metal surface after 7 days (arrows point to cell-layer buildup at the interface). (b) Cell proliferation on the amorphous metal and plastic surfaces.

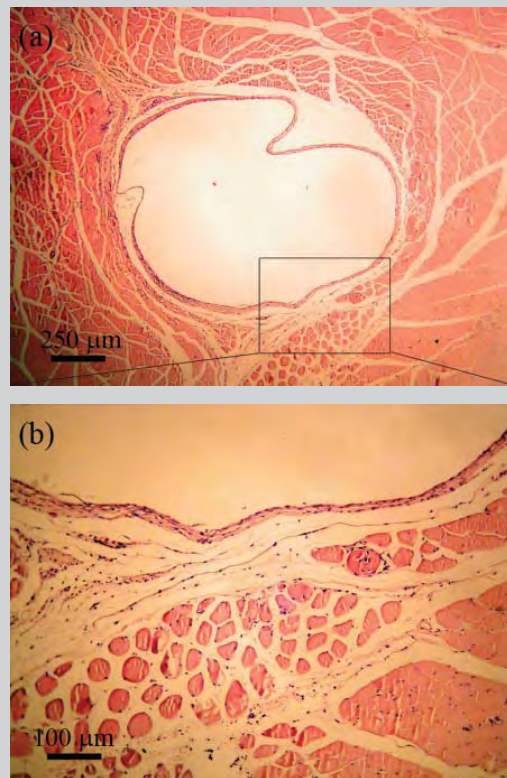


Figure B. Micrographs of the tissue surrounding a Pd-Ag-P-Si rod (circular region in the center of the image) implanted intramuscularly in rat for 28 days: (a) 40× magnification, (b) 100× magnification.

identified to be stress-corrosion cracking involving stress-assisted anodic dissolution at the crack tip.^{33,36} Overall, the poor corrosion-fatigue performance of Zr-based glasses in saline environments has been attributed primarily to their electrochemistry, which yields passive layers that lack the ability to rapidly repassivate in solution thereby providing only limited protective effect at the crack tip against chloride attack.³⁶

By contrast, certain Fe-based glasses known to be immune to pitting corrosion demonstrate rapid repassivation ability in chloride solutions. In passive film damage/reformation experiments, the repassivation of glassy Fe-Ni-Cr-P-C in an acidified chloride solution was measured to be more rapid than conventional (crystalline) stainless-steel alloys.³⁷ Owing to their ability to re-passivate rapidly at a crack tip, these alloys exhibit good stress-corrosion characteristics. For example, amorphous Fe-Cr-Ni-P-C is found to exhibit very limited stress-corrosion cracking and embrittlement in tensile tests performed in neutral sodium chloride solutions or in acidic solutions with low chlorine concentration.³⁸ Such features are highly desirable in load-bearing biomedical implant applications.

See the sidebar on page 88 for details on the biological compatibility of amorphous metals.

POROUS AMORPHOUS METALS

Porosity is thought to be a form of surface irregularity, and its importance in bioprosthesis in guiding cells and aiding tissue repair is increasingly growing. Interconnected-pore architectures with pore sizes in the range of 75–250 μm are thought to be optimal for tissue ingrowth.⁴⁵ In addition to eliciting cell attachment and tissue ingrowth, porosity functions to reduce the structural properties of monolithic bulk materials (e.g., strength and stiffness) to values closer to those of natural bone.

Owing to their high strength combined with relatively low moduli, amorphous metals can be thought as attractive base materials for developing strong highly-elastic porous solids capable of matching the mechanical properties of cancellous bone. Methods for developing porous amorphous metals with ei-

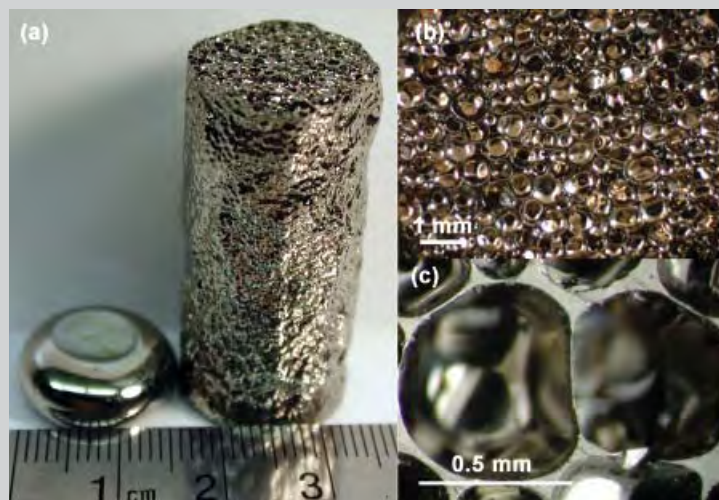


Figure 7. (a) Amorphous Pd-Ni-Cu-P foam (88% porosity).⁵¹ (b) and (c) Micrographs of the cellular structure at high magnifications.

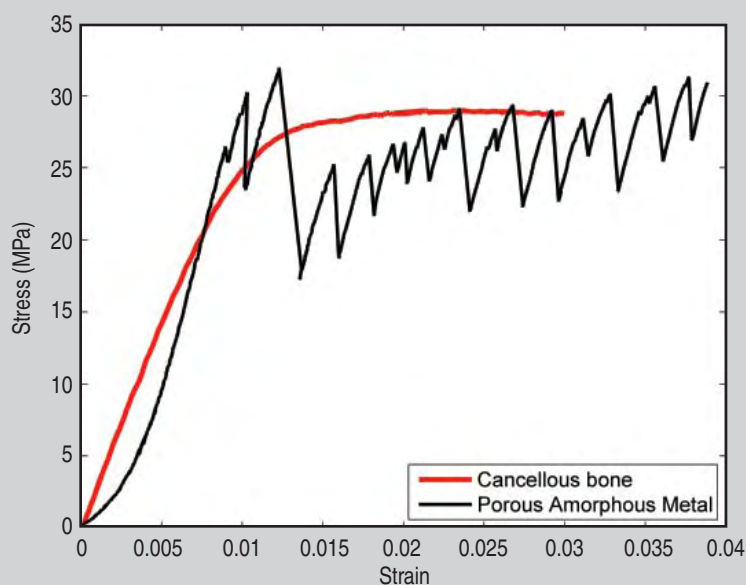


Figure 8. Compressive loading responses of amorphous Pd-Ni-Cu-P foam⁵¹ and cancellous bone.⁵²

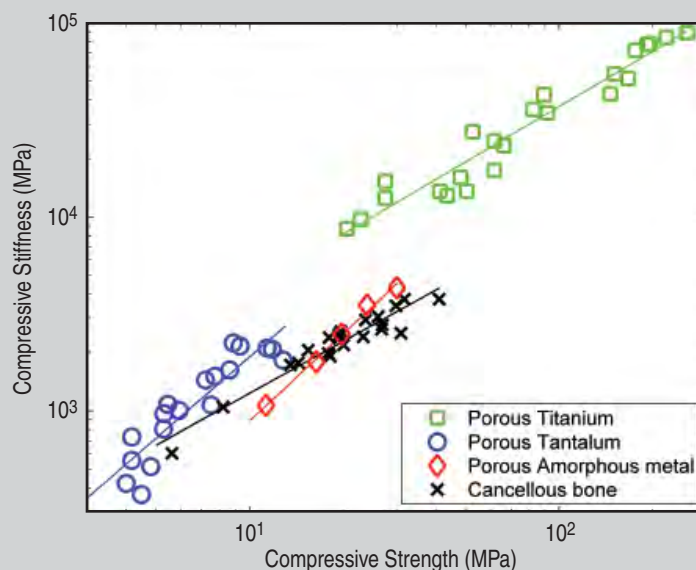


Figure 9. Compressive stiffness vs. strength data for amorphous Pd-Ni-Cu-P foam⁵¹ shown together with data for porous Ti,⁵³ porous Ta,⁵⁴ and cancellous bone.⁵²

ther open- or closed-pore architectures and porosities exceeding 90% have been reported over the past five years (Figure 7).⁴⁶⁻⁴⁹ At a specific porosity level, these cellular structures exhibit a modulus that roughly reflects the low modulus of the amorphous metal. Their strength, however, varies according to the mechanism accommodating failure, and does not always reflect the high strength of the amorphous metal.⁵⁰ It has recently been demonstrated that by matching the characteristic length scales controlling structural failure, the porous amorphous metal can inherit the high strength of the monolithic amorphous metal over a broad range of porosity, and thus emerge as one of the strongest porous solids of any kind.⁵¹ As shown in Figure 8, a strong highly-elastic porous amorphous metal is able to replicate the mechanical response of cancellous bone, roughly matching its stiffness, strength, and plastic deformability. More importantly, as shown in Figure 9, porous amorphous metals of varying porosity match the strength and modulus of cancellous bone over a broad range. Conventional porous metals such as porous Ti and Ta, on the other hand, which exhibit moduli and strengths that reflect the high modulus and low strength of their base metals, are not able to match the range of stiffness and strength of cancellous bone by varying porosity (Figure 9). Porous amorphous metals can hence be thought as attractive scaffold materials for bone-growth applications.

DESIGN CRITERIA FOR BIOCOMPATIBLE AMORPHOUS METALS

Based on the discussion in the preceding sections, amorphous metals exhibit certain universal properties that could be attractive for load-bearing biomedical-implant applications. These include a very high strength, which gives rise to high hardness and a potential for improving wear resistance over existing hard-tissue prosthesis metals, and a relatively low modulus, which gives rise to high elasticity and holds a promise for mitigating stress shielding. There are also non-universal properties specific to particular amorphous metal alloy systems that are below acceptable limits for hard-tissue prosthesis and could hinder their use in such applica-

tion. These include a low toughness for some Fe-based glasses that could limit their overall mechanical performance, an inconsistent fatigue-endurance limit for Zr-based glasses that could render their fatigue performance unreliable, and a low pitting-corrosion resistance and poor stress/fatigue corrosion performance for Zr-based glasses that could limit their use in biological solutions. Another critical aspect is the chemical composition of these alloys. Almost all known amorphous metal alloy compositions contain elements that are known to cause adverse biological reactions. For example, most known compositions contain Ni and/or Cu. Both elements are highly allergenic and toxic while Ni is possibly carcinogenic, and should be avoided in long-term implantations that involve wear and corrosion reactions. All bulk-glass-forming Zr-based compositions contain either Al or Be. Aluminum is a known neurodegenerative toxin linked to Alzheimer's disease and is highly undesirable even in small quantities. Beryllium is a known respiratory toxin causing chronic lung disease when inhaled, and despite the lack of conclusive evidence of Be toxicity in the bloodstream, Be remains biologically controversial. Lastly, cost is another critical issue. Several noble-metal-based (Pd, Pt, and Au) glasses are known, which exhibit rather high toughness. Even though no extensive corrosion studies have been reported to date, their corrosion resistance is expected to be rather high as well. Owing to their high cost, however, their extensive use in hard-tissue prosthesis would be hindered and may be limited to dental applications.

Recognizing the above deficiencies, a set of criteria for designing new biocompatible amorphous alloys can be laid out. The "structural" amorphous metals can be grouped into three major alloy families: early-transition-metal based (e.g., Zr-based), ferrous-metal based (e.g., Fe-based), and noble-metal based (e.g., Pd-based).

Zirconium-based systems free of Ni and Cu have been developed;⁵⁵ however, no Al or Be free bulk-glass-forming compositions have been reported. Aluminum and Be were proven to be vital elements that critically facilitate glass formation in those systems, hence their

substitution may not be easy. A Zr-based glass should also be adequately tough and have high and consistent fatigue endurance, a criterion that could be met through careful alloying and proper testing. Lastly, the resistance to pitting corrosion and stress-corrosion cracking of these alloys should be high. The poor resistance to these reactions has been attributed to the overall electrochemical character of these glasses,³⁶ therefore overcoming this deficiency may not be easy. Nevertheless, the value in developing a biocompatible Zr-based glass will be enormous, as it would represent a high-hardness low-modulus alternative to biomaterials of comparable cost such as surgical Ti-based and Zr-based alloys.

Interestingly, many of the deficiencies of Zr-based glasses can be overcome by reinforcing the glassy phase with a ductile dendritic crystalline phase. Ductile-phase reinforced Zr-based glasses were found to exhibit superb toughness^{12,13,20} and a high and consistent fatigue-endurance limit.²³ It is not obvious how the ductile-phase reinforcement affects their corrosion behavior and stress/fatigue corrosion performance, as no corrosion investigations have been performed to date. Also, the highly toughened compositions reported to date contain Be (albeit in small concentrations), which may be problematic in terms of long-term biocompatibility. Nonetheless, a corrosion-resistant ductile-phase reinforced Zr-based glass (preferably Be free) will represent a superior load-bearing implant material with structural properties that cannot be matched by any other known biomaterial.

Iron-based glasses bearing Cr are known to exhibit superb corrosion resistance³¹ as well as good stress-corrosion-cracking resistance.³⁸ Bulk-glass-forming Fe-based compositions exhibit very high strength and hardness but unfortunately tend to be brittle. Recently a series of amorphous Fe-based compositions has been reported⁵⁶ which exhibit a level of toughness that may be adequate for load-bearing implant applications. Some of these compositions are very low cost, are free of undesirable elements such as Ni, and bear Cr which is highly desirable for good corrosion and stress/fatigue corrosion behavior. These Fe-based glasses may be attractive ultra-hard low-modulus alternatives

to existing stainless-steel biomaterials. The ferromagnetic characteristics exhibited by many Fe-based compositions however may render their biomedical use problematic.

Lastly, a tough corrosion-resistant bulk-glass-forming Pd-based alloy free of Ni and Cu would be desirable for dental applications. Noble-metal glasses are generally tough and are expected to be highly corrosion resistant. Also, since their glass-forming ability is controlled mostly by metal/metalloid interactions, substitution of Ni and Cu (which are present in all known compositions) with other less harmful late-transition-metals may be easily attainable. Such Pd-based glass will represent an attractive high-hardness low-modulus alternative to existing dental Pd-based alloys.

A notable recent advance in the design of biocompatible amorphous metal alloys is the development of biodegradable Mg-Zn-Ca glass.⁵⁷ Owing to the liquid-like atomic structure of the glassy metal allowing broad solubility of alloying elements, a glass-forming composition was designed with corrosion characteristics in biological solutions (e.g. degradation rate and hydrogen evolution rate) optimal for a biodegradable implant. Although glassy Mg-based alloys are generally not considered “structurally advanced” ($\sigma_y < 1$ GPa; $K_{IC} < 10$ MPa),^{11,18} their strength and elasticity far surpass those of conventional (crystalline) biodegradable Mg-based alloys, and are thus thought of as attractive alternatives for biodegradable implant applications.

CONCLUSION

The lack of long-range crystalline order in the atomic structure of amorphous metals and the absence of associated microstructural defects give rise to certain universal properties, such as high strength, hardness, and elasticity that are considered very attractive for load-bearing biomedical implant applications. In addition to these desirable universal properties, amorphous metal alloys demonstrate certain composition-specific properties that make them less appealing for such applications. Some amorphous metal alloys have toughness and fatigue-endurance limits that are low compared to ordinary crystalline metals, others demonstrate low re-

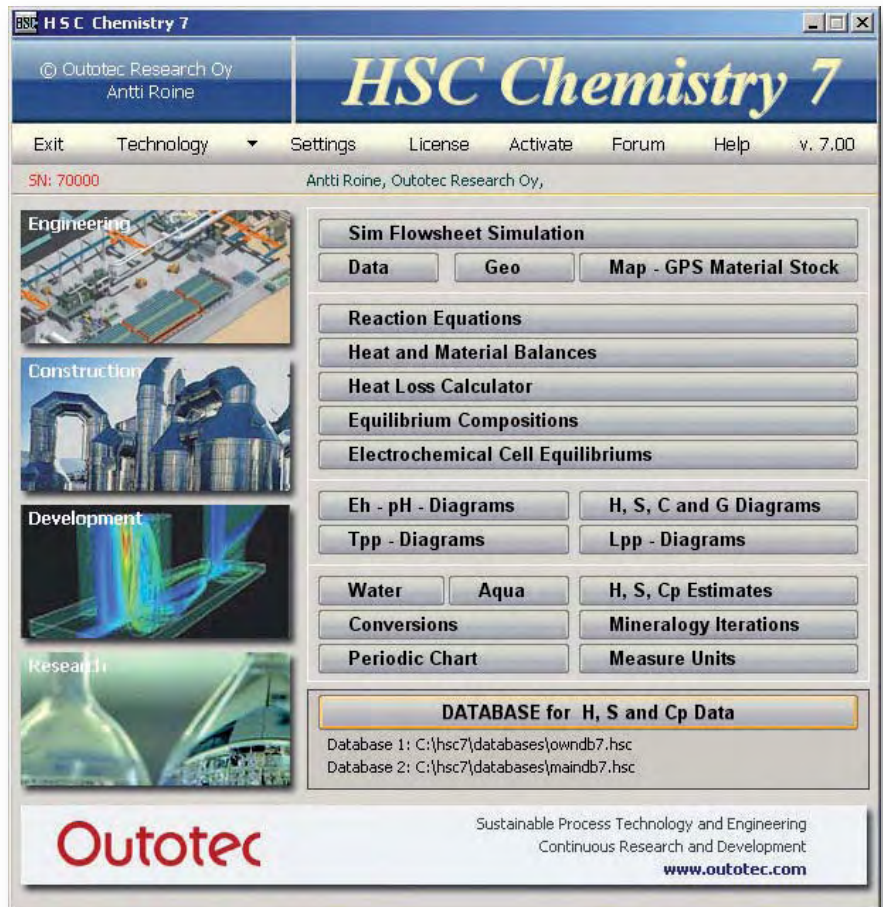
sistance to corrosion and stress/fatigue corrosion, while most contain elements that have been associated with adverse biological reactions. It appears that none of the presently known compositions collectively exhibits the entire set of biocompatibility requirements vital for hard-tissue prosthesis. Nevertheless, the ability of various amorphous metal alloys to compete or rival the present state of the art in various biocompatibility areas suggests that development of a highly biocompatible amorphous-metal implant material may be within reach.

References

1. N.J. Hallab, J.J. Jacobs, and J.L. Katz, *Biomaterials Science, An Introduction to Materials in Medicine*, 2nd ed., ed. B.D. Ratner et al. (Amsterdam: Elsevier Academic Press, 2004), pp. 526–555.
2. J. Black, *Biological Performance of Materials: Fundamentals of Biocompatibility* (Boca Raton, FL: CRC Press, 2006).
3. R. Huiskes, H. Weinans, and B. Vanrietbergen, *Clinical Orthopaedics and Related Research*, 274 (1992), pp. 124–134.
4. J.J. Jacobs et al., *J. American Academy of Orthopedic Surgeons*, 2 (1994), pp. 212–220.
5. K.J. Bundy, C.J. Williams, and R.E. Luedemann, *Biomaterials*, 12 (1991), pp. 627–639.
6. D.A. Basketter et al., *Contact Dermatitis*, 28 (1993), pp. 15–25.
7. D. Beyersmann, *Toxicology Letters*, 72 (1994), pp. 333–338.
8. A. Hartwig, *Toxicology Letters*, 102–103 (1998), pp. 235–239.
9. M. Kawahara, *J. Alzheimers Disease*, 8 (2) (2005), pp. 171–182.
10. J. Schroers et al., *JOM*, 61 (9) (2009), pp. 21–29.
11. W.L. Johnson and K. Samwer, *Physical Review Letters*, 95 (2006), 195501.
12. D.C. Hofmann et al., *Nature*, 451 (2008), 1085–U3.
13. D.C. Hofmann et al., *Proceedings of the National Academy of Sciences of the United States of America*, 105 (2008), pp. 20136–20140.
14. S.W. Yu et al., *J. Bone and Joint Surgery-American*, 57 (1975), pp. 692–695.
15. M.F. Ashby and A.L. Greer, *Scripta Materialia*, 54 (2006), pp. 321–326.
16. W.L. Johnson, unpublished data collection (2005).
17. A.L. Greer and W.N. Myung, *Supercooled Liquid, Bulk Glassy and Nanocrystalline States of Alloys, MRS 2000 Fall Meeting Proceeding*, ed. A. Inoue et al., 644 (2000), L10.4.
18. J.J. Lewandowski, W.H. Wang, and A.L. Greer, *Philosophical Magazine Letters*, 85 (2005), pp. 77–87.
19. J.R. Davis, *Handbook of Materials for Medical Devices* (Materials Park, OH: ASM International, 2003).
20. M.E. Launey et al., *Applied Physics Letters*, 94 (2009), 241910.
21. G.Y. Wang, P.K. Liaw, and M.L. Morrison, *Intermetallics*, 17 (2009), pp. 579–590.
22. J.B. Brunski, *Biomaterials Science, An Introduction to Materials in Medicine*, 2nd edition, ed. B.D. Ratner et al. (Amsterdam: Elsevier Academic Press, 2004), pp. 137–153.
23. M.E. Launey et al., *Proceedings of the National Academy of Sciences of the United States of America*, 106 (2009), pp. 4986–4991.
24. J.R. Scully, A. Gebert, and J.H. Payer, *J. Materials Research*, 22 (2007), pp. 302–313.
25. W. H. Peter et al., *Intermetallics*, 10 (2002), pp. 1157–1162.

26. M.L. Morrison et al., *Intermetallics*, 12 (2004), pp. 1177–1181.
27. A. Gebert et al., *Materials Science and Engineering, A* 267 (1999), pp. 294–300.
28. A. Wiest (Ph.D. thesis dissertation, California Institute of Technology, 2009).
29. M.L. Morrison et al., *J. Biomedical Materials Research, Part A*, 74A (2005), pp. 430–438.
30. Y. Waseda and K.T. Aust, *J. Materials Science*, 16 (1981), pp. 2337–2359.
31. K. Hashimoto, *Corrosion*, 58 (2002), pp. 715–722.
32. V. Schroeder, C.J. Gilbert, and R.O. Ritchie, *Scripta Materialia*, 40 (1999), pp. 1057–1061.
33. M.L. Morrison et al., *Materials Science and Engineering, A* 467 (2007), pp. 198–206.
34. A. Wiest et al., *Scripta Materialia* (in press).
35. Y.R. Qian and J. R. Cahoon, *Corrosion Science*, 53 (1997), pp. 129–135.
36. V. Schroeder and R.O. Ritchie, *Acta Materialia*, 54 (2006), pp. 1785–1804.
37. R.B. Diegle, *Corrosion*, 35 (1975), pp. 250–258.
38. A. Kawashima, K. Hashimoto, and T. Masumoto, *Corrosion Science*, 16 (1976), pp. 935.
39. J.M. Anderson and F.J. Schoen, *Biomaterials Science, An Introduction to Materials in Medicine*, 2nd edition, ed. B.D. Ratner et al. (Amsterdam: Elsevier Academic Press, 2004), pp. 360–367.
40. S. Buzzi et al., *Intermetallics*, 14 (2006), pp. 729–734.
41. C.L. Qiu et al., *Scripta Materialia*, 55 (2006), pp. 605–608.
42. L. Liu et al., *Scripta Materialia*, 58 (2008), pp. 231–234.
43. L. Liu et al., *J. Biomedical Materials Research Part A*, 86A (2008), pp. 160–169.
44. L. Liu et al., *Intermetallics*, 17 (2009), pp. 235–240.
45. R.M. Pillar, *J. Biomedical Materials Research*, 21 (1987), pp. 1–33.
46. J. Schroers et al., *J. Applied Physics*, 96 (2004), pp. 7723–7730.
47. A.H. Brothers, R. Scheunemann, and D.C. Dunand, *Scripta Materialia*, 52 (2005), pp. 335–339.
48. T. Wada and A. Inoue, *Materials Transactions*, 45 (2004), pp. 2761–2765.
49. M.D. Demetriou et al., *Applied Physics Letters*, 91 (2007), 161903.
50. M.D. Demetriou et al., *Advanced Materials*, 19 (2007), pp. 1957–1962.
51. M.D. Demetriou et al., *Physical Review Letters*, 101 (2008), 145702.
52. T.M. Keaveny et al., *J. Biomechanics*, 27 (1994), pp. 1137–1146.
53. I.-H. Oh et al., *Scripta Materialia*, 49 (2003), pp. 1197–1202.
54. D.A. Shimko et al., *J. Biomedical Materials Research Part B*, 73B (2005), pp. 315–324.
55. A. Wiest et al., *Acta Materialia*, 56 (2008), pp. 2625–2630.
56. M.D. Demetriou et al., *Applied Physics Letters*, 95 (2009), 041907.
57. B. Zberg, P. J. Uggowitzer, and J. F. Löffler, *Nature Materials*, 8 (2009), pp. 887–891.

Marios D. Demetriou, senior research fellow, Aaron Wiest, civilian scientist with the Department of the Navy, Douglas C. Hofmann, visiting scientist, and William L. Johnson, professor of engineering and applied science, are with California Institute of Technology, 1200 E. California Blvd., Pasadena, CA 91125; Bo Han, assistant professor of research, is with the University of Southern California, Los Angeles, CA; Nikolaj Wolfson, orthopedic surgeon, is with Mills-Peninsula Health Services, and the California Pacific Medical Center, San Francisco, CA; and Gongyao Wang, research associate, and Peter K. Liaw, professor of materials science and engineering, are with the University of Tennessee, Knoxville, TN. Dr. Demetriou can be reached at marios@caltech.edu.



HSC Chemistry[®] 7

Outotec's new innovative process calculation software contains an updated flowsheet simulation module and a thermochemical database expanded to over 25,000 species. With 22 calculation modules and 12 databases at your fingertips, HSC 7 is an invaluable tool for any process engineer or scientist because one laboratory experiment may cost much more than a single HSC license.

Once the compass gave us a competitive edge when navigating in foggy waters. Today modeling and simulation give us a similar advantage when we navigate oceans of data with hundreds of variables. This is the only way to utilize the current massive information overload. The new HSC 7 provides us with an easy simulation tool to steer process development and research.

Ask for the 32 page "What's new in HSC 7" paper from:

Outotec Research Oy

Email: hsc@outotec.com, Tel: +358-20-529 211



Outotec
www.outotec.com/hsc

Metallic Glasses: Gaining Plasticity for Microsystems

Yong Yang, Jianchao Ye, Jian Lu, Yanfei Gao, and Peter K. Liaw

Since the 1960s, metallic glasses (MGs) have attracted tremendous research interest in materials science and engineering, given their unique combination of mechanical properties. However, the industrial applications of MGs have been hindered due to their lack of ductility in bulk form at room temperature. In contrast, it was observed that MGs could exhibit excellent plasticity at the small size scale. In this article, we summarize the related experimental findings having been reported so far together with the possible origins of such a size effect in MGs. The enhanced plasticity of MGs in small volumes, together with their high mechanical strengths and remarkable thermoplastic formability, strongly implies that MGs are the promising materials for fabricating the next generation of micro- and nano-devices.

INTRODUCTION

Metallic glasses (MGs) emerged as a newcomer to the family of amorphous solids in the 1960s and were first synthesized through the rapid quenching of supercooled liquids.¹ Compared with metallic crystals, MGs exhibit much higher mechanical strengths and better corrosion resistance for the absence of crystalline defects, which renders MGs promising for structural applications.²⁻⁴ Since the advent of the first Au-based MG, tremendous research efforts have been stimulated with a gigantic amount of research works archived in the literature.¹⁻²⁷ Different strategies are seen to have been practiced in the synthesis and characterization of a variety of MGs aiming to find the recipe that produces the metallic-glassy system with optimized mechanical properties and a critical dimension as large as possible.^{5,27} Despite the dedicated re-

search efforts over the past years, MGs of bulk form usually show brittle-like fracture in uniaxial tensile or compres-

sive experiments at room temperature (RT) due to the catastrophic shear-band propagation upon yielding. The lack of RT ductility in MGs remains as the longstanding issue to be solved and the major hurdle hindering the deployment of MGs in various structural applications.²⁸

Unlike metallic crystals, the atomic structure of MGs lacks long-range order because of the overall random packing of atoms. In some regions, the atoms are loosely packed, forming atomic clusters, called the 'shear transformation zones' (STZs),⁷ which are a few nanometers in size¹⁶ and prone to shear transformations upon mechanical loading. In the others, the atoms are closely packed, forming the elastic media that surround the STZs. Upon the application of external stresses, the STZs behave in a liquid-like manner on an individual basis to initiate plastic flows in MGs through shear transformations.²⁶ On the other hand, the elastic media, consisting of all sorts of solid-like clusters in an amorphous structure, offer the essential resistance to such an inelastic deformation process.²⁶ When the applied shear strain reaches the critical value of about ~2% at room temperature,^{11,12} the shear transformation events occurring on the individual STZs percolate and result in the local breakdown of the elastic media, which, then, gives rise to the formation of a shear band, namely, a 10-nm thick planar defect on which severe strain concentration occurs.²⁰

If unhindered, the propagation of the shear band is catastrophic and detrimental to the overall ductility of bulk metallic glasses (BMGs). During the shear-band propagation, the viscosity of materials plunges^{6,7} within the shear band and is accompanied by a

How would you...

...describe the overall significance of this paper?

This article provides an overview of the recent studies on the size effect in metallic glasses at room temperature. The experimental and theoretical results indicate that metallic glasses, although brittle in bulk forms, can display extensive plastic flows at the microscopic scale without sacrifice of their mechanical strengths. The combined superb strength and high ductility indicate that metallic glasses are promising for the fabrication of microsystems of next generation.

...describe this work to a materials science and engineering professional with no experience in your technical specialty?

Unlike crystalline metals, metallic glasses deform plastically via shear banding at room temperature. In bulk forms, metallic glasses exhibit brittle fracture, suffering from the catastrophic growth of shear bands. In sharp contrast, metallic-glass micro-specimens can withstand extensive plastic deformation without shear fracture. The transition from brittle to plastic deformation originates from the shear-banding dynamics, which entails the shear-induced materials softening and subsequent structural relaxation in metallic glasses.

...describe this work to a layperson?

Despite brittleness in bulk forms at room temperature, metallic glasses, an emerging material for future microsystems, exhibit good plasticity and high strength when machined into small volumes. Such a size effect in metallic glasses implies that metallic glasses are a good candidate for structural applications in the area of micro-electro-mechanical systems (MEMS).

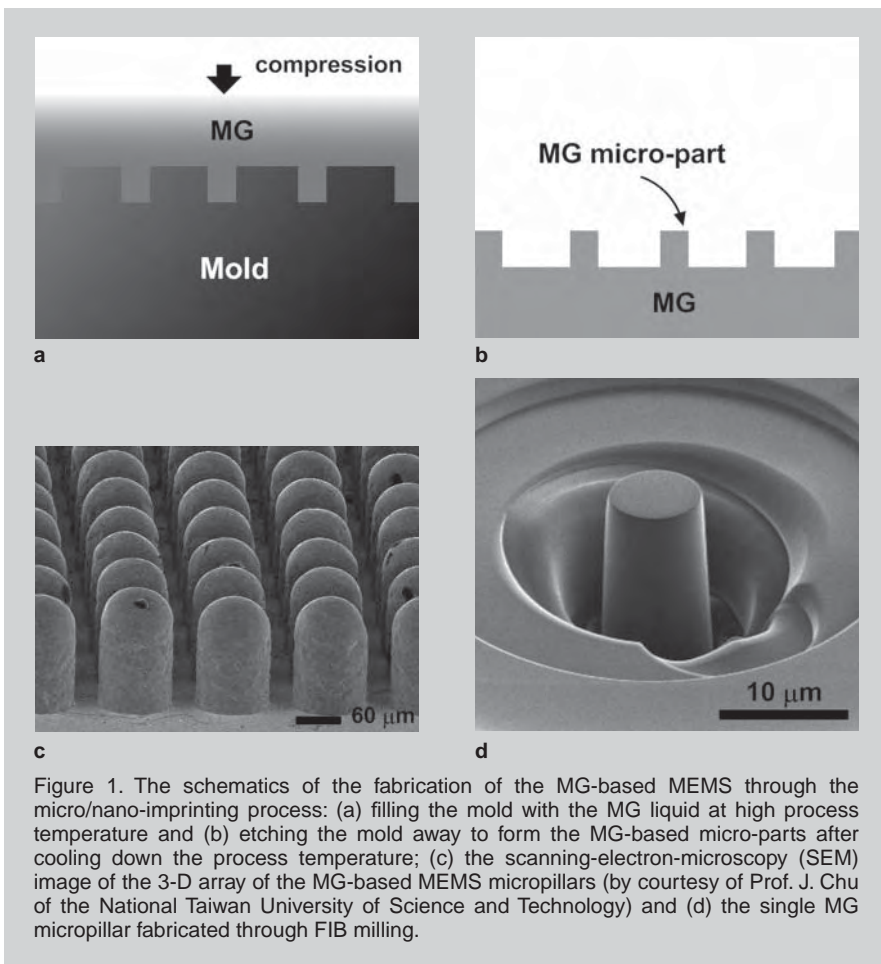


Figure 1. The schematics of the fabrication of the MG-based MEMS through the micro/nano-imprinting process: (a) filling the mold with the MG liquid at high process temperature and (b) etching the mold away to form the MG-based micro-parts after cooling down the process temperature; (c) the scanning-electron-microscopy (SEM) image of the 3-D array of the MG-based MEMS micropillars (by courtesy of Prof. J. Chu of the National Taiwan University of Science and Technology) and (d) the single MG micropillar fabricated through FIB milling.

temperature surge,^{9,19} which accompanies severe materials softening therein and subsequent brittle-like fracture. Through various numerical simulations, it has been shown that the stress-induced dilatation triggers the materials-softening process at the early stage of the shear-band propagation, whereas the temperature rise is mainly responsible for the final fracture in BMGs.^{9,13} As a consequence, the coupled effect of these two materials softening mechanisms renders BMGs vulnerable to the shear-band propagation with little RT ductility shown at the macroscopic scale.^{17,21}

In contrast, the shear-banding process is much less threatening in MG micro-samples than in MG bulk samples at room temperature. It was observed that shear bands propagated in a sluggish manner in the compression tests of MG micropillars^{29–36} and also in the tension tests of MG submicrometer-sized strips.³⁷ Unlike classic nanoindentation tests in which the propagation of shear bands is constrained,³⁸ the micro-compression/tension tests

allow for the free gliding of shear bands across the lateral dimension of a micro-sample. The stable shear-band propagation, as already witnessed in the micro-compression/tension tests, thus implies an enhanced RT plasticity in MGs at the microscopic scale.

The experimental results reported for the micromechanical behavior of MGs are encouraging to the future applications of MG-based micro-electromechanical systems (MEMS), which emerged recently as a new area in micro- and nanotechnology.^{39–41} By exploiting the thermoplastic formability of MGs, a variety of MG-based micro- and nano-devices have been successfully fabricated through the micro- and nano-imprinting technique. This fabrication process involves the compression of an amorphous MG material into a mold at the processing temperature higher than the glass-transition point, T_g , but below the melting point, T_x of the corresponding MG material (Figure 1a). After cooling down the whole system, the amorphous MG material settles in the mold and forms the

shape of the desired micro-part after removing the mold material via chemical etching (Figure 1b). Figure 1c presents the three-dimensional (3-D) array of the Pd-based MG micropillars fabricated using the micro-imprinting technique. As a comparison, Figure 1d shows the MG micropillar fabricated through focused-ion-beam (FIB) milling, whose geometry has been widely adopted in the prior micro-compression experiments.^{29,31–35} It is evident that the present micro-imprinting technique results in significant surface roughening and tip rounding in the MG-based MEMS micropillars, which contrasts the smoothness and sharpness of the FIB-milled micropillars. Until now, research efforts have mainly focused on the characterization of the mechanical properties of the FIB-milled micropillars whereas reports on the mechanical properties of MEMS micropillars are still scarce.

MICROMECHANICAL STUDY OF METALLIC GLASSES

Since the pioneering work of Uchic et al.,⁴² who used the FIB-milled micropillars to study the size effect in single crystals, the FIB-based micro-compression method has been widely employed in the study of the mechanical behavior of a variety of materials in small volumes⁴³ and, in the meantime, the method itself has also received considerable investigations.^{44–46} Although it is still debated whether or not the size effect witnessed in the micro-compression of single crystals is caused by the FIB-induced damage,^{44–47} it is generally believed that, for amorphous metals that are radiation tolerant, the FIB-induced surface damage is not severe, only occupying a 3–4 nm thick region in the vicinity of the sample surface if an appropriate FIB milling procedure is followed.^{29,33} In such a case, the major concern about the validity of the measured MG micropillars' yield strengths is the micropillar's tapering, which arises due to the ion-beam divergence and becomes unavoidable for the submicrometer-sized FIB-milled micropillars.³¹

To address the taper effect, we recently extended the shear-plane criterion proposed by Packard et al.¹⁰ to the case of micro-compression. Pro-

vided that the Mohr–Coulomb law is satisfied on the whole shear plane at the yielding point, the taper effect on the micropillar’s yield strength can be quantified.³⁶ In principle, the theoretical calculation shows that the intrinsic yield strength of a micropillar, as dictated by the Mohr–Coulomb’s law, can be accurately extracted if the MG’s normal stress coefficient, the pillar’s taper angle, and the distance from the shear band to the pillar’s central axis are known. (The yielding of BMGs obeys the Mohr–Coulomb’s law, which can be written as: $\tau_o = \tau_n + \mu \sigma_n$, in which τ_o denotes the intrinsic shear strength; τ_n and σ_n denote the shear and normal stress acting on the shear plane with the unit normal of n , respectively; and μ is the normal stress coefficient. In uniaxial compression experiments, μ is related to the shear angle θ through $\mu = 1/\tan(2\theta)$.) In practice, the first two factors can be determined prior to the micro-compression testing, whereas the last factor can hardly be measured in a precise manner. However, it can be shown that, in a 3°-tapered micropillar, it only introduces a maximum measurement uncertainty of 5% by assuming that shear bands always nucleate at the pillar’s edge, which, on the other hand, simplifies the measurement of the yield strengths of the MG micropillars.

Figure 2a presents the yield strengths, σ_y , obtained from the Cu-, Zr-, Mg-, and Fe-based MG micropillars as a function of the pillar’s top diameter. Evidently, the yield strengths of all the MG micropillars exhibit the trend of a modest size effect. The yield strengths increase slightly with the decreasing pillar’s diameter. In the literature, such a size effect in MGs is attributed to the Weibull statistics,^{31–33,36} which indicates that the size shrinkage in MGs contributes to the strength elevation mainly by reducing the contents of the defects of lowest strengths (also called the weakest links). In doing so, the pillar’s Young’s modulus is also elevated through the reduction of the weakest-link content.^{34,36} As a result, the ratios of σ_y/E extracted from the micro-compression experiments largely overlap with those reported for bulk samples,¹¹ as shown in Figure 2b.

Although the normalized yield

strength of MGs can be regarded as a size-independent mechanical property on average (Figure 2b), the plasticity of MGs shows the strong size dependence. As mentioned above, there are numerous reports on the plasticity enhancement seen in the miniaturized MG samples, which span a wide spectrum of MG alloys available to date.^{29,30,32,33,35–37} For instance, the Fe-based MG appears extremely brittle in a bulk form, shattered into many pieces upon yielding (Figure 3a,b). However, significant plastic flows were observed in the Fe-based MG micropillars due to the stable shear-banding process at the microscopic scale (Figure 3c–e). Such sharp contrast in the plastic deformation behavior across a large length scale for a wide range of MG compositions implies that the size effect should be a characteristic of the MG plasticity, which needs to be considered in the design of the future MG-based micro- /nano-devices.

ORIGIN OF SIZE EFFECT IN METALLIC GLASSES

From the mechanistic perspective, a fundamental understanding of the shear-banding behavior in metallic glasses can be attained by considering the material instability in rate-dependent plastic solids, which is manifested by the spectral growth of the strain field,⁴⁸ as opposed to the instantaneous instability in rate-independent plastic solids (such as soils and clays) for which the necessary condition of strain localization corresponds to the loss of ellipticity of the equations governing the incremental equilibrium.⁴⁹ When materials display rate dependence, starting from initial imperfections or small spatial fluctuations, the strain field will gradually grow into the localized mode, and this strain-localization process can be significantly delayed by the material-rate sensitivity. The amount of the delay in the onset of lo-

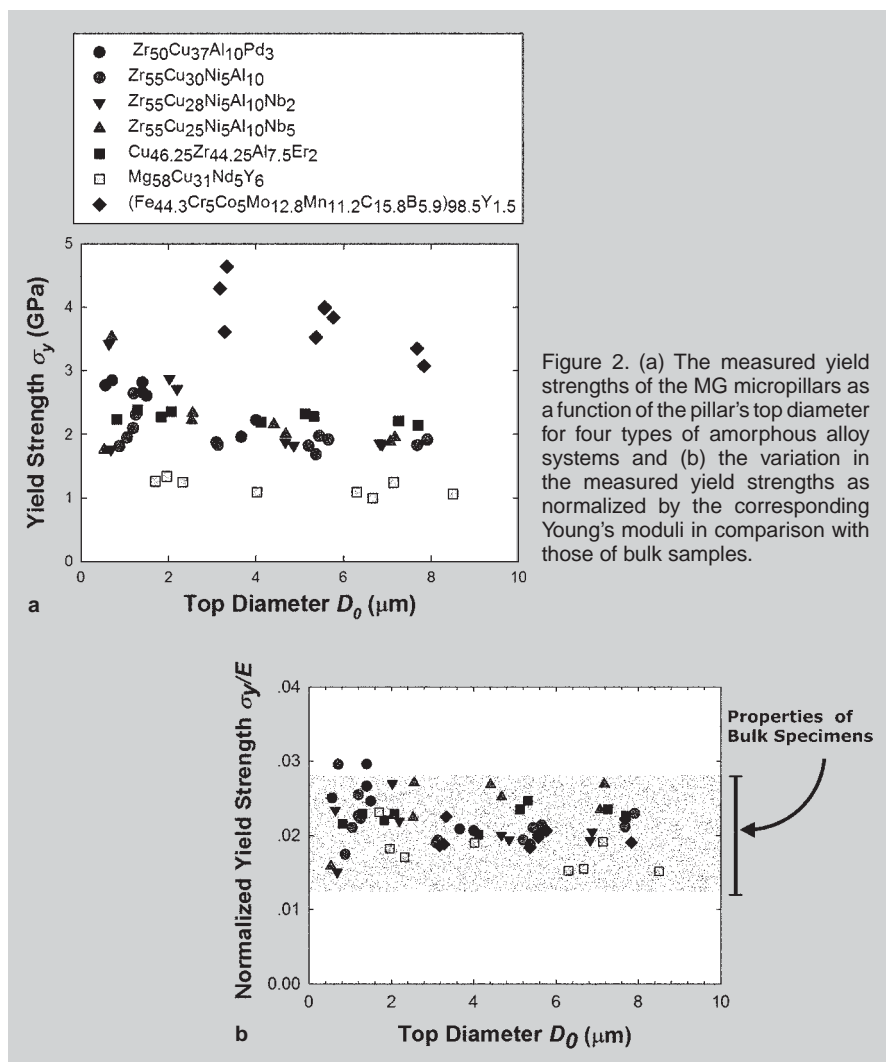


Figure 2. (a) The measured yield strengths of the MG micropillars as a function of the pillar’s top diameter for four types of amorphous alloy systems and (b) the variation in the measured yield strengths as normalized by the corresponding Young’s moduli in comparison with those of bulk samples.

calization depends on the kinetics of strain softening, structural relaxation, and strain-rate hardening, as well as on the imperfections.

In macroscopic tests, the plastic strain in unconstrained shear bands can be arbitrarily large so that the catastrophic failure will quickly follow the initiation of shear bands. With geometrical constraints, enhanced plasticity can be achieved by blocking the propagation of shear bands so that multiple shear bands take place to accommodate the applied strain field. Therefore, the plastic strain will be distributed over many shear bands, and the onset of fracture can be delayed and noticeable macroscopic plastic strains may be realized. In these cases, rate effects are usually weak unless the rate approaches the kinetic limit of shear-band initiation.

In contrast to the observations in large specimens where unstable shear-band propagation usually leads to catastrophic fracture, in small specimens the shear bands propagate in a sluggish, and sometimes stable, manner so that extensive plastic deformation can be achieved. When a smoothly varying

strain field evolves into narrow bands inside which the strain fields localize and outside of which the materials experience elastic unloading, the equilibrium deformation pathway corresponds to an elastic snap-back instability. In micromechanical tests, the release rate of the elastic energy in micro-pillars are far less than those in the bulk samples, and the magnitude of the elastic spring back can be decreased.^{29,35,50,51} Consequently, the resulting shear-banding behavior in samples of reduced dimensions will be in a stable manner even under unconstrained conditions, and various kinetic processes involved in the evolution of strain fluctuation can be observed in this extended delay.

The above argument does not need a detailed picture of the atomistic deformation mechanisms. If the elastic unloading outside of shear bands results in a negligible spring back (as in small specimens), and the material has a rate-dependent strain-softening mechanism, be it the stress-assisted evolution of free volumes or STZs, the strain localization process will become non-catastrophic and sluggish in time.

Consequently, the stable shear-banding process manifests itself as the plastic flow serrations on a load-displacement curve as shown in Figure 3e.

On the other hand, our understanding of the shear-banding mechanism in MGs has advanced greatly over the past decades.^{6,7,11,19,23,25,52,53} The recent rate-jump experiments on MGs at different temperatures clearly indicate that structural relaxation plays an important role during the propagation of a shear band.⁵³ The effect of structural relaxation is to mitigate or even completely cancel out the softening effect brought about by the shear-induced dilation. As a rate-dependent diffusion process, the effect of the shear-induced structural relaxation depends on the waiting time between two successive atom migration events and, thus, the kinetic energy acquired by atoms at the onset of shear banding, which scales with the released elastic energy.³⁵ In quasi-static mechanical experiments, because of the dimensional misfit between the elastic energy release (from a volume) and plastic energy dissipation (on a plane), a size effect naturally arises. In small samples, the elastic energy release rate becomes inadequate to drive a shear band into a runaway defect as in large samples, and the shear band is arrested before a complete load drop occurs, which, then, gives rise to the serrated plastic flows as seen in microcompression experiments.³⁵

In the literature, a variety of constitutive models have been proposed by different researchers targeting at the size effect.^{9,37,42,50,54} Shimizu et al. conjectured that, once atoms are displaced from their original positions in a shear-banding region, they can still form a new stable structure with their new neighbors for a small shear displacement; complete shear fracture occurs only after a large shear displacement occurs.⁹ Likewise, Wu et al. proposed a similar concept, termed as the critical shear offset, to rationalize the size effect reported in the literature.⁵⁴ They argued that each type of MG possesses a critical shear offset and stable shear banding takes place when the actual shear offset is less than the critical value. However, based on the above-mentioned shear-banding kinetics,^{35,52,53} the so-called critical shear offset, as left by

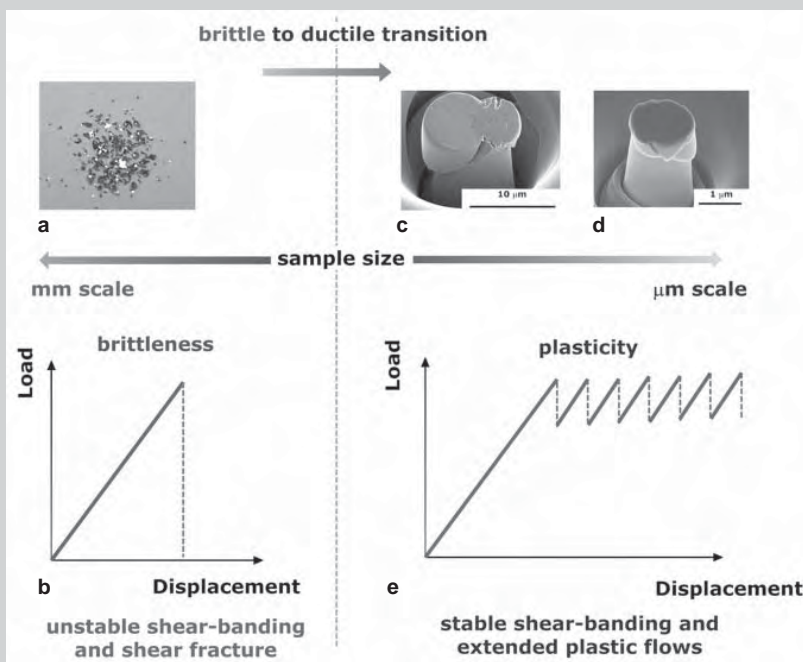


Figure 3. The brittle-to-ductile transition in the Fe-based MG as the sample size decreases from the macroscopic to microscopic scale: (a) the fragmentation fracture of the Fe-based BMG bulk sample indicating the RT brittleness at the macroscopic scale (by courtesy of Prof. Z.P. Lu of the University of Science and Technology, Beijing); (b) the sketch of the typical load-displacement curve for brittle fracture in a Fe-based BMG bulk sample; (c) the stable single shear-banding in the Fe-based BMG micropillar with the diameter of $\sim 8 \mu\text{m}$; (d) the stable multiple shear-banding in the Fe-based BMG micropillar with the diameter of $\sim 1 \mu\text{m}$; and (e) the sketch of the typical load-displacement curve for stable shear-banding in a Fe-based BMG micropillar.

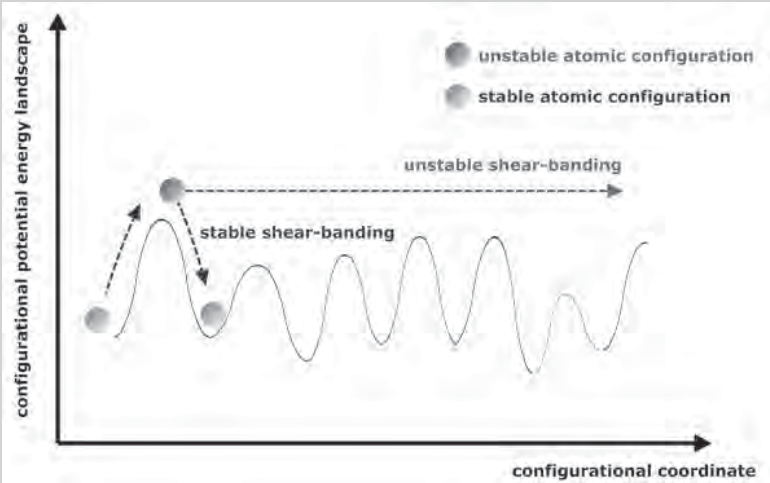


Figure 4. The schematic illustration of shear banding through an irreversible energy barrier crossing event on the configurational potential energy landscape of a metallic glass (the dashed black arrow indicates a stable shear-banding process whilst the dashed gray arrow indicates an unstable one).

a shear band on a sample surface before shear-banding instability, is just a reflection of the competition between the shear-induced materials softening and subsequent structural relaxation, which is expected to be rate- and temperature dependent rather than a materials constant. On the other hand, through energy balance, it can be shown that the instantaneous shear offset, Δs , of a propagating shear band scales with the dimension of a sample as following:³⁴

$$\Delta s \propto H + \alpha D_0 \quad (1)$$

where H and D_0 denote the height and diameter of an MG sample, respectively, and the pre-factor α accounts for the elastic energy transfer into the sample from its surroundings and depends on the elastic and size mismatch between the sample and its elastic supports. When an MG sample is compressed between two ideally rigid supports, such an elastic transfer is prohibited and $\alpha = 0$. In other cases, the pre-factor α is of a finite value and the size effect manifests itself essentially as a geometry effect on the plasticity of MGs.

A rather intriguing point made by Harmon et al. through their study on the anelastic to plastic transition in metallic glass-forming liquids is that irreversible deformation occurs via interbasin hopping events on a configurational potential energy landscape.¹² The similar yielding mechanism is expected for metallic glasses according to the cooperative shear model (CSM) proposed

by Johnson et al.¹¹ As the strain in MGs reaches a critical value, the shear transformation occurring on the individual STZs percolates, which then leads to the nucleation of a shear band. From the perspective of CSM, this strain-controlled shear-band nucleation process corresponds to the elevation of the system's internal energy from a basin point to its nearest saddle point on the potential energy landscape (Figure 4). After passing through the saddle point, the whole system can step down to a new basin point by dissipating away the accumulated mechanical energy, which is the case for MG micropillars. Such balanced energy dissipation is achieved through the irreversible structural relaxation process (α -relaxation) as in the metallic glass-forming liquids.¹² In contrast, if unbalanced energy dissipation occurs, the whole system is unable to find any basin point to rest on the energy potential landscape because of the excessive elastic energy released during the energy-barrier crossing event and, thus, a shear catastrophe occurs.

Mechanistically, the material rate dependence introduces a length scale through the initial imperfections. Smaller specimens will have fewer imperfections for strain localization to initiate a plastic flow, which is similar to the explanations based on the Weibull distribution.^{32,33} On the other hand, length scales can be introduced into the constitutive relationship of the material, such as the heat conduction

length^{21,22} or the diffusional length.⁵⁵ Starting from randomly distributed free volumes or STZs, the strain fields will evolve from these initial imperfections into mature shear bands, and the spatial spectrum of the growth rate will be determined by the kinetic processes and these material-dependent length scales. Here, these material-dependent length scales correspond to the nucleation lengths of shear bands. Specimens with sizes comparable to these scales will exhibit a scale dependence of the deformation modes. However, most up-to-date micro-compressions show stable, but still inhomogeneous, deformation mode. To probe the homogeneous plastic deformation mode in MGs, a sample size much smaller than those of the current micropillars is demanded.

CONCLUSIONS

Based on the above discussions, it is evident that the transition of plasticity to brittleness is intrinsic to the shear-band mediated plastic deformation mode in metallic glasses. With the reduction in the sample size, a metallic glass tends to exhibit plasticity rather than brittleness because of the time delay in the localization process, or, in other words, because of the recovery effect of structural relaxation. However, such a physical picture for the size effect relies on the operation of shear bands. In this regard, a question that naturally arises is whether a fundamental change in the plastic deformation mode can be experimentally probed by shrinking the sample size to the level where shear bands cannot nucleate, as already witnessed in atomistic simulations.^{56,57}

Such a small sample size, which is close to the shear-band nucleation (or process zone) length, has not been accessed in the micropillar tests. In the literature, it was argued that shear bands could not nucleate as the sample size was reduced below the shear-band thickness at nucleation,¹⁵ which was estimated as ~ 10 nm for MGs.^{20,58} However, the analysis of such a shear-band thickness was based on the scenario of shear-band nucleation in a bulk material and it can be anticipated that the boundary conditions, such as free surfaces, could affect the nucleation of

shear bands at the very small scale.⁵⁷ To fully understand the size effect in MGs, the nanomechanical testing technique, which targets the MG-based nanostructures, such as the recently synthesized MG nanowires,⁵⁹ is still needed.

ACKNOWLEDGEMENTS

Y.Y. acknowledges the internal research fund (Grant # 1-ZV4J), provided for newly recruited staff, by the Hong Kong Polytechnic University for conducting the current research. J. Lu is grateful for the financial support from GRF, the Hong Kong Government, with the grant number of PolyU 5203/08E. P.K.L. would like to greatly acknowledge the support of the National Science Foundation International Materials Institutes (IMI) Program (DMR-0231320). Y.F.G. acknowledges support from the National Science Foundation (DMR 0909037). The authors appreciate the provision of testing materials by Prof. C.T. Liu, Prof. J.S.C. Jang, Prof. Y. Yokoyama, and Dr. G. Wang.

References

1. K. Klement, R.H. Willens, and P. Duwez, *Nature*, 187 (1960), pp. 869–870.
2. A.L. Greer, *Science*, 267 (1995), pp. 1947–1953.
3. M.F. Ashby and A.L. Greer, *Scripta Mater.*, 54 (2006), pp. 321–326.
4. W.H. Peter et al., *Intermetallics*, 10 (2002), pp. 1157–1162.
5. A. Inoue, *Acta Mater.*, 48 (2000), pp. 279–306.
6. F. Spaepen, *Acta Metall.*, 23 (1977), pp. 407–415.
7. A.S. Argon, *Acta Metall.*, 27 (1979), pp. 47–58.
8. D.B. Miracle, *Nature*, 3 (2004), pp. 697–712.
9. F. Shimizu, S. Ogata, and J. Li, *Acta Mater.*, 54 (2006), pp. 4293–4298.
10. C.E. Packard and C. Schuh, *Acta Mater.*, 55 (2007), pp. 5348–5358.
11. W.L. Johnson and K. Samwer, *Phys. Rev. Lett.*, 95 (2005), 195501.
12. J.S. Harmon et al., *Phys. Rev. Lett.*, 99 (2007), 135502.
13. C.A. Schuh, T.C. Hufnagel, and U. Ramamurty, *Acta Mater.*, 55 (2007), pp. 4067–4109.
14. C.A. Schuh and A.C. Lund, *Nature Mater.*, 2 (2003), pp. 449–452.
15. C.A. Schuh, A.C. Lund, and T.G. Nieh, *Acta Mater.*, 52 (2004), pp. 5879–5891.
16. D. Pan et al., *Proc. Natl. Acad. Sci.*, 105 (39) (2008), pp. 14769–14772.
17. H. Zhang, S. Maiti, and G. Subhash, *J. Mech. Phys. Solids*, 56 (6) (2008), pp. 2171–2187.
18. B. Yang, C.T. Liu, and T.G. Nieh, *Appl. Phys. Lett.*, 88 (2006), 221911.
19. J.J. Lewandowski and A.L. Greer, *Nature Mater.*, 5 (2006), pp. 15–18.
20. Y. Zhang and A.L. Greer, *Appl. Phys. Lett.*, 89 (2006), 071907.
21. M.Q. Jiang and L.H. Dai, *J. Mech. Phys. Solids*, 57 (2009), pp. 1267–1292.
22. Y.F. Gao, B. Yang, and T.G. Nieh, *Acta Mater.*, 55 (2007), pp. 2319–2327.
23. M.W. Chen, *Annu. Rev. Mater. Res.*, 38 (2008), pp. 445–469.
24. A. Furukawa and H. Tanaka, *Nature Mater.*, 8 (2009), pp. 601–609.
25. H.W. Sheng et al., *Nature Mater.*, 6 (2007), pp. 192–197.
26. Y.Q. Cheng, A.J. Cao, and E. Ma, *Acta Mater.*, 57 (2009), pp. 3253–3267.
27. A.L. Greer and E. Ma, *MRS Bulletin*, 32 (2007), pp. 611–615.
28. A.L. Greer, *Materials Today*, 12 (1-2) (2009), pp. 14–22.
29. C.A. Volkert, A. Donohue, and F. Spaepen, *J. Appl. Phys.*, 103 (2008), 083539.
30. Z.W. Shan et al., *Physical Review B*, 77 (2008), 155419.
31. B.E. Schuster et al., *Acta Mater.*, 56 (2008), pp. 5091–5100.
32. C.J. Lee, J.C. Huang, and T.G. Nieh, *Appl. Phys. Lett.*, 91 (2007), 161913.
33. Y.H. Lai et al., *Scripta Mater.*, 58 (2008), pp. 890–893.
34. Y. Yang et al., *Acta Mater.*, 57 (2009), pp. 1613–1623.
35. J.C. Ye et al., *Acta Mater.*, 57 (2009), pp. 6037–6046.
36. J.C. Ye et al., *Intermetallics* (2009), doi:10.1016/j.intermet.2009.1008.1011.
37. H. Guo et al., *Nature Mater.*, 6 (2007), pp. 735–739.
38. U. Ramamurty et al., *Acta Mater.*, 53 (2005), pp. 705–717.
39. J. Schroers, Q. Pham, and A. Desai, *J. Microelectromechanical Sys.*, 16 (2) (2007), pp. 240–247.
40. G. Kumar, H.X. Tang, and J. Schroers, *Nature*, 457 (2009), pp. 868–872.
41. J.S. Jang et al., *Adv. Eng. Mater.*, 10 (11) (2008), pp. 1048–1052.
42. M.D. Uchic et al., *Science*, 305 (2004), pp. 986–989.
43. R. Dou and B. Derby, *Scripta Mater.*, 61 (2009), pp. 524–527.
44. H. Bei et al., *Appl. Phys. Lett.*, 91 (2007), 111915.
45. R. Maab et al., *Appl. Phys. Lett.*, 91 (2007), 131909.
46. R. Maab et al., *Appl. Phys. Lett.*, 89 (2006), 151905.
47. D. Kiener et al., *Mater. Sci. Eng. A*, 459 (2007), pp. 262–272.
48. A. Needleman, *Comput. Method Appl. Mech. Eng.*, 67 (1988), pp. 69–85.
49. J.R. Rice, *Theoretical and Applied Mechanics*, ed. W.T. Koiter (Amsterdam: North-Holland, 1977), pp. 207–220.
50. S. Xie and E.P. George, *Intermetallics*, 16 (2008), pp. 485–489.
51. Y.F. Gao and A.F. Bower, *Modell. Simul. Mater. Sci. Eng.*, 12 (2004), pp. 453–463.
52. F.H. Dalla Torre et al., *Acta Mater.*, 56 (2008), pp. 4635–4646.
53. A. Dubach, F.H. Dalla Torre, and J.F. Löffler, *Acta Mater.*, 57 (2009), pp. 881–892.
54. F.F. Wu, Z.F. Zhang, and S.X. Mao, *Acta Mater.*, 57 (2009), pp. 257–266.
55. Y. Shi et al., *Phys. Rev. Lett.*, 98 (2007), 185505.
56. Y.Q. Cheng et al., *Acta Mater.*, 56 (2008), pp. 5263–5275.
57. F. Delogu, *Phys. Rev. B*, 79 (2009), 184109.
58. M.Q. Jiang, W.H. Wang, and L.H. Dai, *Scripta Mater.*, 60 (2009), pp. 1004–1007.
59. K.S. Nakayama et al., *Adv. Mater.*, 21 (2009), pp. 1–4.

Yong Yang, Jianchao Ye, and Jian Lu are with the Department of Mechanical Engineering, The Hong Kong Polytechnic University, Hong Kong, China; Yanfei Gao and Peter K. Liaw are with the Department of Materials Science and Engineering, The University of Tennessee, Knoxville, TN. Yanfei Gao also holds a joint position in the Computer Science and Mathematics Division, Oak Ridge National Laboratory, Oak Ridge, TN. Dr. Yang can be reached at mmyyang@polyu.edu.hk.



Kn
KNOWLEDGE


**TMS KNOWLEDGE
RESOURCE CENTER**

**Your Materials Books
and More e-Store!**
<http://knowledge.tms.org>

These proceedings are from *The International Symposium on Liquid Metal Processing and Casting, held on September 20-23 at the El Dorado Hotel in Santa Fe, New Mexico, USA.*

The International Symposium on Liquid Metal Processing proceedings cover the following areas:

- Primary and secondary melt processing including VIM, VAR, ESR, EBCHR and PAM
- Physical property measurements of liquid metals
- Refining, evaporation and gas/metal reactions
- Casting and solidification of ingots, and mechanisms for defect formations during the casting and solidification process
- Modeling of metallurgical processes, including heat/mass flow modeling of liquid metal and solidifications
- Ceramic, slag and refractory reactions with liquid metals
- Fundamentals of reactions involving liquid metals in production processes
- Direct forming of parts from liquid metals



**International Symposium
on Liquid Metal
Processing and Casting**

Edited by
Peter D. Lee, Alec Mitchell, and Rod Williamson

A Publication of
TMS

**TMS
Member price \$109**

**TMS Student
Member price \$84**

To order these or related publications, contact TMS:

E-mail publications@tms.org • Phone (724) 776-9000, ext. 256 • Fax (724) 776-3770

Symposia Proposals and Abstract Submissions: For TMS-sponsored meetings, symposia proposals and abstracts must be submitted through ProgramMaster, the on-line TMS conference and proceedings management system. The system can be accessed at www.tms.org. Using the Meetings & Events pulldown menu, select the Upcoming TMS Meeting for which you wish to submit a symposia proposal or an abstract, and follow the on-line instructions. The society especially encourages the submission of "hot-topic" symposia or special-session proposals on timely or developing subjects. To advance an idea, use the symposium creation form in ProgramMaster. Additional information can be acquired from the TMS Technical Support Services Department, 184 Thorn Hill Road, Warrendale, PA 15086; (724) 776-9000, ext. 212; fax (724) 776-3770.

Offshore Technology Conference 2010

May 3–6, 2010
Houston, Texas

The Offshore Technology Conference (OTC) is the world's foremost event for the development of offshore resources in the fields of drilling, exploration, production, and environmental protection. OTC also offers case studies and updates on the latest deepwater projects from majors, independents, national oil companies, and service companies. Technical topics to be addressed at OTC 10 include alternative energy (such as offshore wind energy, ocean wave energy, ocean thermal energy conversion, and hydrates), drilling technology, facilities and production operations, enhanced oil recovery, facilities and production operations, financial aspects, field development concepts, marine geoscience and geohazards, materials technology, ocean engineering resources, offshore pipelines, public policy, regulatory issues, and more. **Contact:** Offshore Technology Conference, 222 Palisades Creek Drive, Richardson, Texas 75080; (972) 952-9494; e-mail service@otcnet.org; www.otcnet.org/2010/index.html.

15th International Conference on Metal Organic Vapor Phase Epitaxy (ICMOVPE 2010)

May 23–28, 2010
Lake Tahoe, Nevada

The objectives are to provide a forum for the latest advances in science, technology, and applications of MOVPE and to bring together researchers from around the world to discuss and share experiences in the growth, characterization, and device applications of metal organic vapor phase epitaxy. Technical topics will include: basic growth studies; nitrides; arsenides, phosphides, antimonides and dilute nitrides; low bandgap materials;

II-VI materials and devices; oxides (TCO, dielectrics); novel materials; heteroepitaxy; nanostructures; patterned growth and selective area; epitaxy; devices; atomic layer deposition and epitaxy; virtual substrates and epitaxial lift-off; in-situ monitoring and process control; in-situ etching; characterization; growth of devices; energy technology (solid state lighting, PV, thermoelectrics, etc.); equipment, safety, environmental and production issues. **Contact:** TMS Meeting Services, 184 Thorn Hill Road, Warrendale, PA 15086; (724) 776-9000, ext. 243; email: mtgserv@tms.org; www.tms.org/Meetings/Specialty/icmovpe-xv/home.aspx/.

Copper 2010

June 6–10, 2010
Hamburg, Germany

The theme of Copper 2010 is Copper—Indicator of the Progress of Civilization. Copper 2010 is an important technical event for engineers, scientists, fabricators, and users of copper. Recently copper has become an important factor in the developing economies of East Asian countries and can be seen as an indicator of the progress of civilization in each country. All relevant areas of copper production and application and their surroundings like energy savings, process optimization, health and safety issues, cost and commerce, recycling, and new developments will be presented in a series of parallel sessions. The program will include such topics as economics; downstream fabrication, applications and new products; mineral processing; pyrometallurgy; hydrometallurgy; electrowinning, electro-metallurgy and refining; process control, automatization and optimization; recycling, and sustainable development/health, safety and environmental control; as well as plenary sessions of general interest. The conference will be followed by post-conference tours and field trips to local industry productions.

Contact: Mickael Kopke, Norddeutsche Affinerie AG; Hoverstrasse 50, 20539 Hamburg, Germany; +49-10-78-83-38-01; e-mail: cu2010@gdmb.de; www.cu2010.gdmb.de/.

Electronic Materials Conference 2010 (EMC 2010)

June 23–26, 2010
Notre Dame, Indiana

Electronic materials are defined as relating to, produced, or operated by the controlled flow of electrons through a semiconductor, gas, or free space along with those relating to devices, systems, or circuits that employ components such as vacuum tubes, integrated circuits, or transistors in their design. The TMS Electronic Materials Conference is the premier annual forum on the preparation and characterization of electronic materials. Held in conjunction with the Device Research Conference, this conference presents both invited and contributed oral presentations, an exhibition, and related activities. Technical symposia topics include: chemical and biological sensors; materials, interfaces, and integration; dilute nitride semiconductors; epitaxy; flexible and printed thin film electronics; nanotubes and nanowires; organic-inorganic hybrid photovoltaics; solar cell materials and devices; thermoelectrics and thermionics; and several others. **Contact:** TMS Meeting Services, 184 Thorn Hill Road, Warrendale, PA 15086; (724) 776-9000, ext. 243; email: mtgserv@tms.org; www.tms.org/Meetings/Specialty/EMC10/home.aspx.

1st TMS-ABM International Materials Congress

July 26–30, 2010
Rio de Janeiro, Brazil

Held in conjunction with 65th Annual Congress of ABM (Brazilian Metallurgical,

Materials and Mining Association) and the 18th International Federation for Heat Treatment and Surface Engineering Congress, this inaugural congress will feature seven proposed symposia covering important contemporary issues in materials science and engineering. This congress builds on the TMS Alliance of the Americas initiative to work together with Society partners in South America and Canada. Technical symposia themes include: Characterization and Application of Biomaterials; Dynamic Behavior of Materials; Composite Materials; Light Weight Materials for Transportation: Processing and Properties; Materials and Society; Mechanical Properties of Materials with Emphasis on Grain-size Effects; and Computational Modeling and Advanced Characterization. There will be a CD-only proceedings published. **Contact:** Meeting Services, TMS, 184 Thorn Hill Road, Warrendale, PA 15086; (724) 776-9000, ext. 243; e-mail: mtgserv@tms.org; www.tms.org/meetings/specialty/ABM-TMS/home.aspx.

7th Pacific Rim International Conference on Advanced Materials and Processing —PRICM 7

August 1–5, 2010
Cairns, Australia

This international conference is the 7th in a series devoted to advanced materials and processing. The conference, which is held every three years, is jointly sponsored by the Chinese Society for Metals (CSM), The Japan Institute of Metals (JIM), The Korean Institute of Metals and Materials (KIM), Materials Australia (MA), and The Minerals, Metals & Materials Society (TMS) and is organized in rotation. The purpose of PRICM is to provide an attractive forum for the exchange of scientific and technological information on materials and processing. The symposia will cover such topics as advanced steels and processing, advanced high temperature structural materials, light metals and alloys, bulk metallic glasses and nanomaterials, advanced ceramics, energy generation harvesting and storage materials, and others. **Contact:** Ms. Helen Woodall, Materials Australia, Suite 205, 21 Bedford Street, North Melbourne, VIC 3111, Australia; +61-9326-7266; e-mail: helen@materialsaustralia.com.au; www.materialsaustralia.com.au/scripts/cgiip.exe/WService=MA/ccms.r?PageID=19070.

Third International Conference on Uranium—U2010

August 15–18, 2010
Saskatoon, Saskatchewan, Canada

The plenary session will discuss: The Next Generation of Nuclear Power; Uranium Resources – Exploration and New Mines; Uranium Processing – Milling, Refining, Conversion and Enrichment; and Regulatory and Public Issues. The technical sessions will include papers on mining, uranium processing, refining/conversion/fuel fabrication, reactor designs and decommissioning, radiation safety and advances, and various other topics. **Contact:** Brigitte Farah, Metallurgical Society of CIM, 3400 de Maisonneuve West, Suite 855, Montreal, Quebec, Canada H3Z 3B8; (514) 939-2710, ext. 1317; e-mail: bfarah@cim.org; www.metsoc.org/u2010.

10th International Conference on Steel Rolling—ICSR

September 15–17, 2010
Beijing, China

The theme of the 10th ICSR is “Rolling the Future: Process, Products, and Environment,” with the aim of showing the progress and development in the field of steel rolling (technology, process, and products) in the past four years. The sessions will examine new process, technology, and facilities for flat products, long products, and pipes; special rolling technology and products; equipment and maintenance; clean rolling; mathematical modeling, simulation, automatization and intelligentization; advanced products development and application; measurements and control technology for rolling and products; etc. A plant tour of a rolling mill in China is being organized as well. **Contact:** Bin Gao, Chinese Society for Metals, 46 Dongsixi Dajie, Beijing 100711, China; +86-10-65133925; e-mail: icsr10@csm.org.cn; hy.csm.org.cn/.

Lead-Zinc 2010 [in conjunction with Conference of Metallurgists (COM 2010)]

October 3–6, 2010
Vancouver, BC, Canada

Lead-Zinc 2010 is the fifth decennial symposium by the Minerals, Metals & Materials Society (TMS) that is devoted to the theory and practice of the extractive metallurgy of Lead and Zinc. This meeting is held

in conjunction with the 2010 Conference of Metallurgists, the premier annual event of the Metallurgical Society of the Canadian Institute of Mining, Metallurgy and Petroleum (MetSoc) from October 3–6, 2010 in Vancouver, British Columbia. The Lead-Zinc 2010 symposium will provide an international forum for the lead and zinc processing industries to exchange information about current processing technologies for primary and secondary lead and zinc, as well as emerging technologies for both metals. The symposium scope extends from process fundamentals to operational practices, and also includes the important aspect of environmental issues. At the operations level, comprehensive reviews of the major applications of both metals will be outlined. Emphasis will be placed on recent commercial developments with less energy-intensive technologies; the better understanding of existing technologies and the development of new processing concepts; environmental concerns; a series of plenary lectures by industry leaders. A short course on lead and zinc processing and industrial tours are also planned. **Contact:** Brigitte Farah; Metallurgical Society of CIM; 3400 de Maisonneuve West, Suite 855, Montreal, Quebec, Canada H3Z 3B8; (514) 939-2710, ext. 1317; e-mail: metsoc@cim.org; www.metsoc.org/com2010/tp_lead_zinc.asp.

7th International Symposium on Alloy 718 & Derivatives

October 10–13, 2010
Pittsburgh, Pennsylvania

This symposium will address recent innovations in material processing and understanding of superalloys, including alloy 718 and related compositions. Specific topics will include: raw material developments and trends; ingot metallurgy and melt process advances; supply chain expansion and new capability; casting technology and developments; fabrication technology and developments; novel product forms technology and applications; field applications and trends (energy, aero, chemical, etc.); microstructure, properties, and advanced characterization; and corrosion, coatings, and environmental effects. **Contact:** TMS Meeting Services; 184 Thorn Hill Road, Warrendale, PA 15086; (724) 776-9000, ext. 243; e-mail: mtgserv@tms.org; www.tms.org/Meetings/Specialty/superalloys2010/home.aspx.



**TRACE
ELEMENT ANALYSIS**

5 Day Turnaround

- High Purity Metals & Alloys
- Ceramics
- Glasses
- Semiconductors
- Thick Films
- Carbon, Graphite
- High Temperature Alloys

Utilizing State of the Art Techniques

- Glow Discharge Mass Spectrometry (GDMS)
- Inductively Coupled Plasma Mass Spectrometry (ICPMS)
- Inductively Coupled Plasma Optical Emission Spectrometry (ICP-OES)
- Spark Source Mass Spectrometry (SSMS)
- Combustion and Inert Gas Fusion Methods (LECO)

Northern Analytical Laboratory

13 Delta Drive Unit #4
Londonderry, NH 03053

Tel: 603-434-8400 • Fax: 603-434-8500
E-Mail: NALABS@northernanalytical.com
Website: www.northernanalytical.com

A C T Aluminum Casting Technology, LLC

Professional Consulting Services; Project, Metallurgy, Field Service, Engineering of Casting Equipment & upstream/downstream Operations

Contact: JOHN V. GRIFFIN, P.E.

7 Lone Cedar Way Office: (1) 201-767-9044
Old Tappan, New Jersey 07675 Fax : (1)201-750-2279
United States E-mail : johnvj@optonline.net

James E. Hoffmann and Associates Co.
P.O. Box 420545
Houston, Texas USA 77242-0545

JAMES E. HOFFMANN, FIMM. P.E.

CONSULTING EXTRACTIVE METALLURGICAL ENGINEER
NON FERROUS, RARE, AND PRECIOUS METALS

BUS (281) 493-9441 E-MAIL: jehentp@aol.com
FAX (713) 780-0761

ISO-9001 and ISO-17025 Certified

Analytical Services & Reference Standards
SEM/X-ray, Electron Microprobe, Surface Analysis (Auger) Metallography, Particle Size Counting & Surface Roughness

Quantitative analysis of small amounts of material in concentrations to 10 ppm, surface oxides, stains & cleanliness, corrosion, diffusion, reverse engineering, elemental mapping, diffusion gradients (carbon, nitrogen, etc.) Get your data by e-mail. Digital micrographs and elemental maps. We manufacture traceable standards for magnification (SEM, OM, etc.) and over 240 pure elements, alloys, glasses and compounds for micro-analysis.

Put our years of experience to work on your specimens!



**GELLER
MICROANALYTICAL
LABORATORY**

426e Boston St. (Rt. 1), Topsfield, MA 01983-1216
978 887-7000 fax: 887-6671 www.gellermicro.com

**Thermophysical
Properties Instruments
& Testing Services**

- Thermal Expansion
- Thermal Conductivity
- Thermal Diffusivity
- Specific Heat Capacity
- -180°C to 2800°C Range

Anter Corporation 1700 Universal Road Pittsburgh, Pa 15235-3998
Tel: 412.795.6410 Fax: 412.795.8225 E-mail: sales@anter.com

ISO9001:2000 Certified
www.anter.com/jom



micron inc.

ANALYTICAL SERVICES

3815 LANCASTER PIKE
WILMINGTON, DE 19805
302-998-1184, FAX 302-998-1836

micronanalytical@compuserve.com
WWW.MICRONANALYTICAL.COM



*Worldwide experience in
technology development*

FLOGEN Technologies

6 Non-Ferrous and Ferrous Metallurgy, Inorganic and Organic Chemistry, Environment and InfoTechnology etc
6 Thermodynamic and kinetic quantification of slags, mattes, metals, etc., smelting, converting and refining process development and optimization, modeling and simulation, Atomic Absorption Spectrometry, minor and trace element analysis, electroanalytical techniques (biosensors), heavy metal pollution analysis, analytical quality assurance, mercury speciation, etc.

www.flogen.com

5757 Decelles Ave., Suite 511 Tel: (514) 344-8786
Montreal, Quebec Fax: (514) 344-0361
Canada H3S 2C3 Email: secretary@FLOGEN.COM

TMS

**Your Professional Partner
for Career Advancement**

www.tms.org

**Read by thousands
of the field's leading
professionals and
decision-makers,
JOM can deliver an
impressive international
audience, both in print
and online.**

**The new TMS
Media Kit
is now available.**

**To request your copy,
contact ads@tms.org**

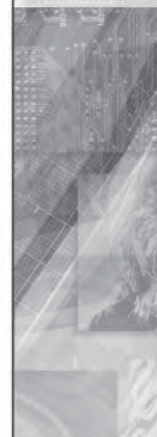


**Check out the TMS media kit at
<http://www.tms.org/pubs/journals/JOM/ads.html>**

**MATERIALS
SCIENCE**

**Materials & Metallurgical
Testing, Analysis & Consulting**

TEM, SEM, EDX, XRD, WDXRF, AES,
NIR, m-FTIR, PLM/PCM, AA, ICP, GC/MS



- Materials Characterization
- Metallurgical Analysis
- XRD Phase Analysis
- Failure Analysis
- Product Comparison
- Contamination Analysis
- Surface Analysis
- Forensic Analysis
- Chemical Analysis
- Mechanical Testing
- R&D Support and Consulting
- 20 Years Of Experience

**www.EMSL.com
800.220.3675**



THE SCIENCE: Air Quality, Environmental Microbiology,
Industrial Hygiene, Lead, Mercury, Forensic, Environmental Chemistry

**CORPORATE LABORATORY
107 HADDON AVENUE
WESTMONT, NJ**



POSTDOCTORAL RESEARCH ASSOCIATE IN NEUTRON SCATTERING

Neutron Scattering Sciences Division
Oak Ridge National Laboratory
Oak Ridge, Tennessee - ORNL10-34-NSSD

The Powder Diffraction Group the Neutron Scattering Sciences Division (NSSD) of Oak Ridge National Laboratory (ORNL) (<http://www.ornl.gov>) has several opportunities for postdoctoral research. Specific areas of interest include the following:

- Phase transformation and deformation behavior in high-strength steel
- Structure, thermal stability, and deformation of nano structured ferritic alloys
- Texture and dynamic recrystallization of Mg alloys
- In-situ neutron scattering measurement of transient phenomena

Each candidate will be part of an interdisciplinary research team involving scientists in several divisions at ORNL, primarily Materials Science and Technology Division and Computer Science and Mathematics Division. The research will utilize the VULCAN diffractometer at the Spallation Neutron Source as a primary research tool, although there will be complementary experiments involving synchrotron scattering and microscopy. In commissioning as of summer 2009, VULCAN is a world-class engineering diffractometer designed to tackle a broad range of problems in materials science and engineering, including stress mapping in structural components, in-situ deformation studies, transient behaviors during synthesis and processing, and the kinetics of multi-length scale phase transformations.

QUALIFICATIONS: A Ph.D. in materials science, physics, mechanical engineering, or related fields is required. Preference will be given to candidates with experience in neutron or synchrotron scattering techniques (e.g., diffraction or small angle scattering). Strong written and oral communications skills are desirable. The candidate must be willing to work in a team environment on technically and scientifically challenging problems. Applicants cannot have received the most recent degree more than five years prior to the date of application appointment and must complete all degree requirements before starting their appointment.



HOW TO APPLY: Qualified applicants must apply online at https://www2.ornl.gov/ORNL_POST/. Technical questions regarding the position can be directed to Dr. Xun-Li Wang at wangxl@ornl.gov. Please include the requisition number and title when corresponding. This appointment is offered through the ORNL Postgraduate Research Participation Program and is administered by the Oak Ridge Institute for Science and Education (ORISE).

Multiscale Modeling The University of North Texas

The University of North Texas invites applications for a tenured Full Professor in multiscale modeling. This hire in the Materials Modeling Research Cluster (MMRC) is part of a multi-year, \$25 M investment by UNT in multi-disciplinary research collaborations. The successful candidate will have an established international reputation with an active, externally funded research program. An earned doctorate in Materials Science, Engineering, Chemistry, Mechanical Engineering, Physics or a related field is also required. The area of specialization is broadly defined, but preference will be given to candidates who complement existing MMRC strengths (<http://mmrc.unt.edu>). Please visit: <http://facultyjobs.unt.edu/applicants/Central?quickFind=50513> for additional information, qualifications and to apply. Review of applicants will begin immediately and continue until the search is closed. The University of North Texas is undergoing significant expansion in research personnel and capabilities: the new hire will join an exceptionally productive and collaborative cluster of researchers – 13 faculty, >50 researchers – encompassing computational chemistry, material science, physics and engineering. UNT is a Class I – Doctorate Granting Institution located in Dallas-Fort Worth (DFW), 30 minutes from the DFW International Airport. DFW is an area of more than six million people, with significant economic growth, low cost of living, numerous industrial establishments, and excellent school districts. This area and the university provide excellent cultural and educational opportunities as well as exceptional employment opportunities for spouses. UNT is the fourth largest university in Texas with over 36,000 students. UNT is an EOE/ADA/AA institution.

Another TMS Member Benefit:

Materials Technology@TMS

www.materialstechnology.tms.org/TECpage.asp

*Your resource for
technology overviews,
news stories, downloadable
resources, and links.*

FREE WEB PLACEMENT OF EVERY CONSULTANTS DIRECTORY AD

JOM's Consultants Directory ads reach experienced professionals who look to JOM for technical and professional guidance. It is also the first place to which the staff directs readers with technical questions.

For as long as the consultant's ad appears in the print version of the journal, the ad also appears in the on-line version of the directory at no additional cost. If a web address is available, the ad will link to that site as well.

**To check it out, visit
<http://www.tms.org/consultants.html>**

I'VE SPECIALIZED FOR 30 YEARS

in the placement of Metallurgical, Materials, and Welding Engineers in the areas of R&D, Q.C. Production, Sales & Marketing, nationwide. My background as a Met. Eng. can help you! Salaries to \$190K. Fees paid by Co. Call/Send/E-mail Resume:

Michael Heineman, Meta-Find, Inc.; P.O. Box 610525, Bayside, NY, 11361; Phone (212) 867-8100; E-mail mikeh@meta-findny.com; Web: www.meta-findny.com

If you have a key position to fill, JOM Classified Advertising can help you track down that special individual with the right qualifications and background to match your needs.

Products and Services

The Best Liquid Aluminum Quality Measurements

ABB Analytical Business Unit
Phone: +1 418-877-2944
metal@ca.abb.com
www.abb.com/analytical



Thermo-Calc Software Inc

Thermodynamic and Diffusion Modeling Software
Ask about our new software releases!
www.thermocalc.com Paul@thermocalc.com

HSC Chemistry® 7



www.outotec.com/hsc

SHIMADZU

Powerful Material Testers & X-ray Instrumentation

www.ssi.shimadzu.com
800-477-1227 • webmaster@shimadzu.com



FACULTY POSITION IN MATERIALS SCIENCE AND ENGINEERING

U. S. Steel Canada Endowed Position in Sustainable Steel Production

The Department of Materials Science and Engineering at McMaster University is seeking qualified applicants for a tenure-track US Steel Canada Endowed Position. The position may be filled at the Assistant, Associate or Full Professor rank, depending on the experience of the candidate. The successful applicant at the Associate or Full Professor rank will be an outstanding researcher with demonstrated expertise in sustainability issues related to primary production of steel, which will involve a strong background in process metallurgy, recycling and energy issues. The position at these ranks will be the U. S. Steel Canada Chair in Sustainable Steel Production. The successful applicant at the Assistant Professor rank will demonstrate outstanding potential in the same research area.

The position is associated with the McMaster Steel Research Centre that has attracted strong industrial interest and funding. The McMaster Steel Research Centre is part of a network of research institutes that provide stimulating interdisciplinary research opportunities, including the General Motors Canada Centre for Automotive Materials and Corrosion, the McMaster Manufacturing Research Institute, and the Brockhouse Institute for Materials Research.

The successful candidate will be expected to develop strong research activities that will attract external research funding, supervise graduate students and teach both undergraduate and graduate courses. Applicants must have a Ph.D. in Materials Engineering or a closely related discipline. Registration or eligibility for registration, by the Professional Engineers of Ontario will be considered an asset.

McMaster is strongly committed to employment equity within its community, and to recruiting a diverse faculty and staff. The University encourages applications from all qualified candidates, including women, members of visible minorities, Aboriginal persons, members of sexual minorities, and persons with disabilities. All other qualified candidates are encouraged to apply; however, Canadian citizens and permanent residents will be given priority. Salary is commensurate with qualifications and experience.

This position will start on July 1, 2010 or after. The review of applications will begin immediately and continue until the position is filled. Applications referencing the position and including a CV, a statement detailing research and teaching interests, and the names of three referees should be sent to:

Faculty Selection Committee
Department of Materials Science & Engineering
McMaster University, JHE 357
1280 Main Street West, Hamilton, ON L8S 4L7
email: malsci@mcmaster.ca
Reference: USSTEEL09
January 2010



FLSMIDTH

One Source, One Partner for all of your Mineral Processing Needs
www.FLSmidthMinerals.com

PERMATECH®

SHAPING THE FUTURE OF REFRACTORY TECHNOLOGY

Graham, NC • permatech.net • 336.578.7728

Outotec

www.outotec.com



Magnesium Elektron

SERVICE & INNOVATION IN MAGNESIUM

www.magnesium-elektron.com

Meetings and Workshops

FRAY INTERNATIONAL SYMPOSIUM

December 4-7, 2011 * Cancun, Mexico

- Incorporating three international symposia:
- Advanced Sustainable Iron and Steel Making
 - Sustainable Non-Ferrous Smelting in 21st Century
 - Molten Salts and Ionic Liquids 2011

Visit www.flogen.com/FraySymposium for additional details.

Global Innovations Symposium Flies High at TMS 2010

Lynne Robinson

Editor's Note: This is excerpted from an article that first appeared on MaterialsTechnology@TMS and is now archived in the Emerging Materials Community at <http://materialstechnology.tms.org/EMT/home.aspx>.

Floating on muslin wings and bound together with horsehide glue, the Wright Flyer launched powered air travel in four shuddering flights of less than a minute each in 1903. Its fragile wooden frame, ultimately reduced to splinters by a heavy gust of wind, stood in stark contrast to the powerful aircraft that now routinely soar above the clouds. What these two eras of flight have very much in common, however, is a drive for discovery and innovation. This pursuit of new technology to enable faster, safer, and more cost-efficient flight will be explored and celebrated during the TMS 2010 Annual Meeting at the 11th Materials Processing & Manufacturing Division (MPMD) Global Innovations Symposium: Global Innovations in Manufacturing of Aerospace Materials.

Chosen, in part, for the meeting's location in the aerospace center of Seattle, the symposium's topic will highlight key advances in the manufacturing of aerospace materials across a wide spectrum of technologies. Said Deborah D. Whitis, section manager,

Materials Applications Engineering for GE Aviation and symposium organizer, "The symposium has been split into several sessions to highlight different trends across various manufacturing processes such as casting, forming/forging, and machining/joining, as well as alloy systems, including titanium, superalloys, and intermetallics. One exciting trend to be examined will be additive manufacturing, which has recently seen a resurgence due to advances in powder manufacturing methods."

Computational materials engineering will also be highlighted, because, said Whitis, "An overarching challenge and opportunity for our community is to better incorporate modeling and simulation into metals processing in order to develop new alloys and processes more quickly and with fewer iterations."

According to Whitis, this year's symposium provides a balanced perspective with a number of invited speakers from industry, academia, and government. Kicking off the symposium on February 15 will be "Future Materials and Process Needs for Commercial Jet Transports: the 21st Century Challenge," a keynote presentation by Alan Miller, director of 787 Technology In-

tegration for Boeing.

As a member of both the MPMD's Shaping and Forming Committee and the Structural Materials Division's (SMD) High Temperature Alloys Committee, Whitis said she was pleased to have been able to integrate the interests and involvement of both groups in developing the symposium. Exchanging knowledge and ideas across disciplines to provide a more comprehensive view of trends and advancements has been the cornerstone of the Global Innovations Symposium since it was introduced a decade ago as a new concept in programming at the TMS Annual Meeting. In addition to organizing their own symposia, the MPMD's technical committees were asked to contribute to a division "super-symposium" that reflected the breadth of materials processing and manufacturing within an emerging technology or industry. "It was our desire to engage as many production organizations as possible to strengthen the technical breadth of our membership—both within the division and within the society," said John Smugeresky, technical staff member at Sandia National Labs and MPMD chair at the time that the symposium was established.

"The Global Innovations Symposium has historically featured high profile speakers to provide a foundation for focused topics where new innovation has been occurring," said Thomas R. Bieler, professor at Michigan State University and symposium co-organizer. "This year's event is no exception and will provide participants the opportunity to gain a high-level view of where the industry is heading in using new technologies to improve production of aerospace materials and parts."

Lynne Robinson is a news and feature writer for TMS.



Figure 1. Featuring state-of-the-art advanced materials technology, a Boeing 787 Dreamliner completes engine runs necessary for its flight test at Boeing's facility in Everett, Washington. (Photo courtesy of Boeing.)

A century of sophisticated solutions



Please visit us at booth 319 during
2010 TMS Annual Meeting.

Outotec is a worldwide technology leader in minerals and metals processing, providing innovative and environmentally sound solutions for a wide variety of customer needs in iron and steel, aluminum and non-ferrous metals industries. The Outotec share is listed on the OMX Nordic Exchange Helsinki. www.outotec.com

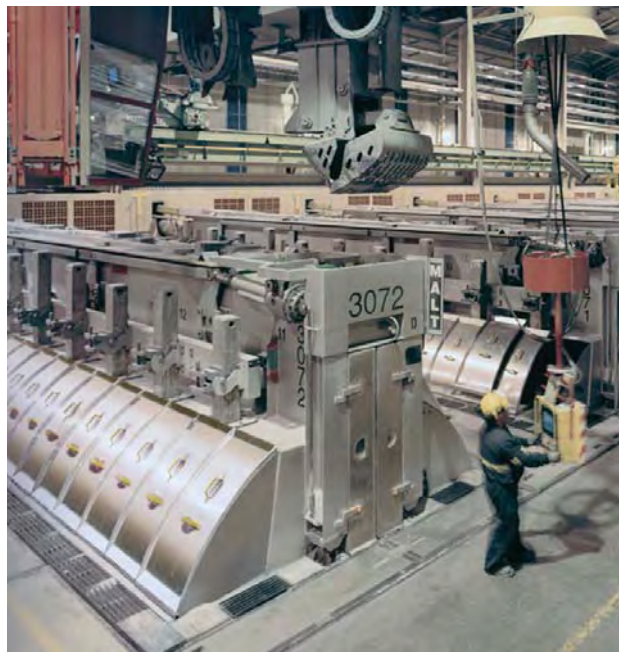
When it comes to minerals and metals processing technology, Outotec has been at the cutting edge of innovation for nearly a century. Its expertise in creating energy efficient, environmentally sustainable solutions is second to none. As well as being the market leader in alumina calcining technology, the majority of the world's iron ore pellets are made using Outotec processes. In addition to this, nearly half of all primary copper and a third of all nickel from sulphide ores is produced using its acclaimed flagship technology, Flash Smelting. Plants installed by Outotec professionals also account for more than a third of the world's sulfuric acid capacity.

With two in-house research centers, eight laboratories and four test plants, it's hardly surprising dozens of Outotec technologies have become industry standard. What's more, the European Union has rated many of these the greenest economically viable options on the market. If you're in the metals or minerals industry and need a partner with a proud tradition of providing sophisticated solutions, Outotec is always at hand to help.

Outotec
More out of ore

ABB's solutions help you increase your plant productivity and product quality

Molten Metal Quality Measurement

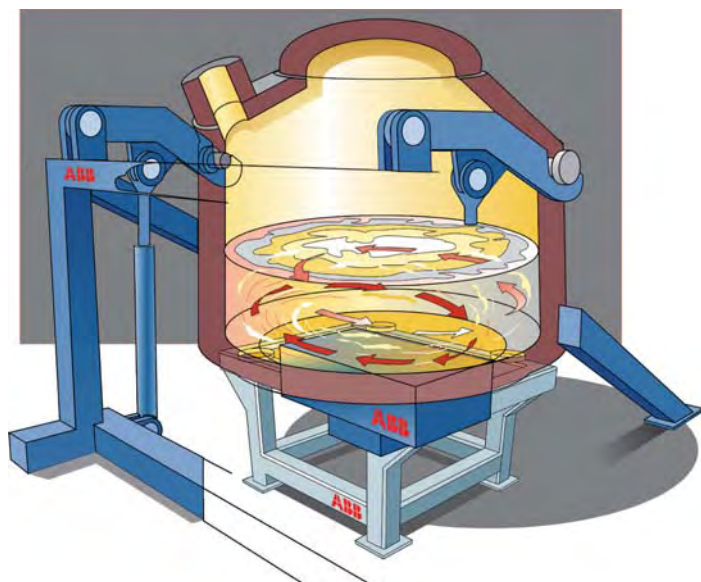


LiMCA CM Liquid Metal Cleanliness Analyzer

- Available to all Aluminum Plants
- Integrated to the Process and Plant Network
- In-Line Continuous Monitoring
- Automated Operation and Minimum Maintenance



Electromagnetic Stirring for State-of-the-Art Aluminum Treatment



ABB, the world's leading supplier of electromagnetic stirring systems for aluminum melting and holding furnaces of all types and sizes, announces that AL-EMS for ladles and crucible stirring is as equally reliable when it comes to temperature control and total melt homogenization.

As with furnace stirring, investment for this powerful new application is normally recovered in less than one year.

Stop by the ABB booth #513.

ABB
Analytical Business Unit
Quebec City, Qc, Canada
Phone: +1 418-877-2944
metal@ca.abb.com
www.abb.com/analytical

ABB Inc.
JME Division
Whitby, Ontario, Canada
Phone: +1 905-666-2251
info.metallurgy@se.abb.com
christer.k.carlsson@us.abb.com
www.abb.com/metals

